



8-2022

Structural Steel Connection Design For Tensile Rupture by Advanced Inelastic Analysis

Kaylaln H. Truman-Jarrell
University of Tennessee, Knoxville, ktrumanj@vols.utk.edu

Follow this and additional works at: https://trace.tennessee.edu/utk_gradthes



Part of the [Structural Engineering Commons](#)

Recommended Citation

Truman-Jarrell, Kaylaln H., "Structural Steel Connection Design For Tensile Rupture by Advanced Inelastic Analysis. " Master's Thesis, University of Tennessee, 2022.
https://trace.tennessee.edu/utk_gradthes/6452

This Thesis is brought to you for free and open access by the Graduate School at TRACE: Tennessee Research and Creative Exchange. It has been accepted for inclusion in Masters Theses by an authorized administrator of TRACE: Tennessee Research and Creative Exchange. For more information, please contact trace@utk.edu.

To the Graduate Council:

I am submitting herewith a thesis written by Kaylaln H. Truman-Jarrell entitled "Structural Steel Connection Design For Tensile Rupture by Advanced Inelastic Analysis." I have examined the final electronic copy of this thesis for form and content and recommend that it be accepted in partial fulfillment of the requirements for the degree of Master of Science, with a major in Civil Engineering.

Mark Denavit, Major Professor

We have read this thesis and recommend its acceptance:

Mark Denavit, Nicholas Wierschem, Hongyu Zhou

Accepted for the Council:

Dixie L. Thompson

Vice Provost and Dean of the Graduate School

(Original signatures are on file with official student records.)

**STRUCTURAL STEEL CONNECTION DESIGN
FOR TENSILE RUPTURE BY ADVANCED
INELASTIC ANALYSIS**

A Thesis Presented for the
Master of Science
Degree
The University of Tennessee, Knoxville

Kaylalyn Hope Truman-Jarrell
August 2022

ACKNOWLEDGEMENTS

First and foremost, I would like to express my sincere gratitude toward my research advisor Dr. Mark Denavit. His dedication to his students and their education is second to none. I am especially grateful for his wide range of knowledge and patience given to me throughout my education. I would like to extend a special thanks to IDEA StatiCa for funding this project and specifically Dr. Martin Vild for his continued support and advice with this project. Thank you to Dr. Nicholas Wierschem and Dr. Hongyu Zhou for serving on my committee. I am very grateful for the help of undergraduate research assistant Avery Burnham on this project. I would like to thank my parents, Steve and Leigh Truman, for teaching me the priceless value of hard work and for always supporting me. I would also like to thank Nathan Parkison for his patience, kindness, and unwavering love in every aspect of my life. Last, but certainly not least, I would like to thank my Lord and Savior for my countless undeserving blessings and opportunities throughout my life.

ABSTRACT

Connections are critical in structural steel buildings for transferring forces from member to member. Connections must be designed for safety and to ensure they serve their intended function. Many resources are available to engineers designing connections with common configurations and loads. But connection designers often encounter configurations and loading conditions for which there is little guidance. In these cases, design by advanced inelastic analysis can be advantageous. IDEA StatiCa is a steel connection design software for design by advanced inelastic analysis. In this software, some limit states are captured in the same manner as standard strength equations, while others are not. The net-section tensile rupture limit state is among the most basic limit states not captured using standard strength equations. It is not necessary to use standard strength equations in design by advanced inelastic analysis if the analysis provides a comparable or higher level of reliability. To date, no rigorous reliability analysis has been performed to show IDEA StatiCa, and the underlying component-based finite element method, provides a comparable or higher level of reliability than provided by the standard strength equations. Such a reliability analysis is performed in this work for the limit state of tensile rupture. Data from hundreds of previously published experimental results exhibiting tensile rupture in a variety of connection types were examined and analyzed. Strengths from both standard equations and IDEA StatiCa were compared to the experimentally obtained strengths and to each other. A reliability analysis based on Monte Carlo simulations was conducted using results from the strength comparisons. Additionally, the sensitivity of the IDEA StatiCa strength to mesh parameters and plastic strain limit was quantified. The results indicate that IDEA StatiCa does, in most cases, provide a comparable or higher level of reliability than the standard strength equations. Cases where it does not are identified and options for modifications are recommended. Documentation of the level of safety provided by IDEA StatiCa for the tensile rupture limit state presented in this work will bring confidence to the overall approach and enable the wider use of this helpful tool.

TABLE OF CONTENTS

CHAPTER 1	Introduction.....	1
CHAPTER 2	Experimental Database	4
CHAPTER 3	Methods.....	8
3.1	Experimental Results	8
3.2	AISC Specification	8
3.3	IDEA StatiCa	11
3.3.1	Typical Modeling Process.....	13
3.3.2	Member Model Type	14
3.3.3	Mesh Study	19
3.4	Reliability Analysis.....	21
CHAPTER 4	Welded Round HSS	27
4.1	Description of Connection	27
4.2	Comparison to Experimental Results.....	29
4.2.1	Description of Experimental Specimens.....	29
4.2.2	Results.....	35
4.3	Reliability Analysis.....	44
4.3.1	Description of Reliability Set.....	44
4.3.2	Results.....	48
CHAPTER 5	Welded Rectangular HSS	52
5.1	Description of Connection	52
5.2	Comparison to Experimental Results.....	54
5.2.1	Description of Experimental Specimens.....	54
5.2.2	Results.....	61
5.3	Reliability Analysis.....	74
5.3.1	Description of Reliability Set.....	74
5.3.2	Results.....	74
CHAPTER 6	Welded Angles.....	79
6.1	Description of Connection	79

6.2	Comparison to Experimental Results.....	82
6.2.1	Description of Experimental Specimens.....	82
6.2.2	Results.....	95
6.3	Reliability Analysis.....	111
6.3.1	Description of Reliability Set.....	111
6.3.2	Results.....	111
CHAPTER 7	Bolted Angles.....	116
7.1	Description of Connection	116
7.2	Comparison to Experimental Results.....	118
7.2.1	Description of Experimental Specimens.....	118
7.2.2	Results.....	125
7.3	Reliability Analysis.....	136
7.3.1	Description of Reliability Set.....	136
7.3.2	Results.....	140
CHAPTER 8	Welded Plates.....	143
8.1	Description of Connection	143
8.2	Comparison to Experimental Results.....	143
8.2.1	Description of Experimental Specimens.....	143
8.2.2	Results.....	150
8.3	Reliability Analysis.....	159
8.3.1	Description of Reliability Set.....	159
8.3.2	Results.....	162
CHAPTER 9	Bolted Plates	166
9.1	Description of Connection	166
9.2	Comparison to Experimental Results.....	166
9.2.1	Description of Experimental Specimens.....	166
9.2.2	Results.....	178
9.3	Reliability Analysis.....	191
9.3.1	Description of Reliability Set.....	191

9.3.2 Results.....	195
CHAPTER 10 Conclusions.....	198
List of References	201
Vita.....	206

LIST OF TABLES

Table 2.1: Specimen Enumeration by Reference.....	5
Table 2.2: Specimen Enumeration by Connection Type	6
Table 3.1: Mesh Parameter Set List.....	15
Table 3.2: Single Angle Bearing Member-End Condition Study.....	17
Table 3.3: End Condition Study.....	18
Table 3.4: Summary statistics for random variables used in the reliability analysis	26
Table 4.1: Round HSS Specimen Enumeration.....	30
Table 4.2: Round HSS Specimen Details	30
Table 4.3: Round HSS Specimen Weld Details.....	31
Table 4.4: Round HSS AISC Calculation Results	36
Table 4.5: Round HSS Results Summary	37
Table 4.6: Statistical Results for Round HSS	46
Table 4.7: Round HSS Reliability Analysis Parameters.....	47
Table 4.8: Round HSS Reliability Strength Results	49
Table 5.1: Rectangular HSS Specimen Enumeration	55
Table 5.2: Rectangular HSS Specimen Detail	56
Table 5.3: Rectangular HSS AISC Calculation Results	62
Table 5.4: Rectangular HSS Results Summary	64
Table 5.5: Statistical Results for Rectangular HSS	73
Table 5.6: Rectangular HSS Reliability Analysis Parameters	75
Table 5.7: Rectangular HSS Reliability Strength Results	76
Table 6.1: Welded Angle Specimen Enumeration.....	83
Table 6.2: Welded Angles Specimen Details	85
Table 6.3: Welded Angle Weld Details	89
Table 6.4: Welded Angle AISC Calculation Results.....	96
Table 6.5: Welded Angle Results Summary.....	100
Table 6.6: Statistical Results for Welded Angles	112
Table 6.7: Welded Angle Reliability Analysis Parameters	112

Table 6.8: Welded Angle Reliability Strength Results	113
Table 7.1: Bolted Angle Specimen Enumeration	119
Table 7.2: Bolted Angle Specimen Details.....	119
Table 7.3: Bolted Angle Fastener Details	121
Table 7.4: Bolted Angle AISC Calculation Results.....	126
Table 7.5: Bolted Angles Results Summary	128
Table 7.6: Statistical Results for Bolted Angles	137
Table 7.7: Bolted Angle Reliability Analysis Parameters	138
Table 7.8: Bolted Angle Reliability Analysis Spacing Parameters	139
Table 7.9: Bolted Angle Reliability Strength Results.....	141
Table 8.1: Welded Plate Specimen Enumeration	144
Table 8.2: Welded Plate Specimen Details.....	146
Table 8.3: Welded Plate Weld Details.....	147
Table 8.4: Welded Plates AISC Calculation Results	151
Table 8.5: Welded Plate Results Summary.....	152
Table 8.6: Statistical Results for Welded Plates	160
Table 8.7: Welded Plate Reliability Analysis Parameters	161
Table 8.8: Welded Plate Reliability Strength Results.....	163
Table 9.1: Bolted Plate Specimen Enumeration	167
Table 9.2: Bolted Plate Specimen Details.....	169
Table 9.3: Bolted Plate Fastener Details.....	172
Table 9.4: Bolted Plate AISC Calculation Results	179
Table 9.5: Bolted Plate Results Summary	182
Table 9.6: Statistical Results for Bolted Plates.....	192
Table 9.7: Bolted Plate Reliability Analysis Parameters	193
Table 9.8: Bolted Plate Reliability Analysis Bolt Spacing Parameters	194
Table 9.9: Bolted Plate Reliability Strength Results	196

LIST OF FIGURES

Figure 3.1: Load-deformation curve from Dhanuskar and Gupta (2021b).....	9
Figure 3.2: Load-deformation curve from Fang et al. (2013).....	9
Figure 3.3: Table D3.1 from the AISC <i>Specification</i> (AISC 2016).....	12
Figure 3.4: Local Axes on Bolted Angle	17
Figure 3.5: Deformed shapes of angle with end condition N-Vy-Mz	20
Figure 3.6: Deformed shapes of angle with end condition N-Vy-Vz	20
Figure 3.7: Mesh refinement for round and rectangular HSS.....	22
Figure 4.1: Welded Round HSS Schematic	28
Figure 4.2: Figure from AISC <i>Specification</i> (2022) defining parameters of round HSS .	28
Figure 4.3: Detail of welds for HSS members from Willibald et al. (2006).....	31
Figure 4.4: Typical Round HSS Model	33
Figure 4.5: Round HSS results: strength ratio vs. index.....	38
Figure 4.6: Round HSS results: normalized strength as a function of material ratio scatterplot.....	40
Figure 4.7: Round HSS results: IDEA StatiCa to experimental ratio as function of material ratio scatterplot	41
Figure 4.8: Round HSS results: strength ratio vs. index for varying plastic strain limits	42
Figure 4.9: Round HSS results: ratio of strength to IDEA StatiCa strength with 5% plastic strain limit plotted with index	43
Figure 4.10: Round HSS experimental set index 3 plastic stress concentration, deformation scale: 10.....	45
Figure 4.11: Round HSS results: ratio of varying mesh parameters sets to the default mesh settings plotted with index.....	46
Figure 4.12: Round HSS: Reliability index for IDEA StatiCa and AISC 2022	51
Figure 5.1: Welded Rectangular HSS Schematic	53
Figure 5.2: Figure from AISC <i>Specification</i> (2022) defining rectangular HSS parameters	55
Figure 5.3: Typical Rectangular HSS Model.....	59

Figure 5.4: Rectangular HSS results: strength ratio vs. index	67
Figure 5.5: Rectangular HSS: normalized strength as a function of material ratio scatterplot.....	68
Figure 5.6: Rectangular HSS: IDEA StatiCa to experimental ratio as function of material ratio scatterplot.....	70
Figure 5.7: Rectangular HSS results: strength ratio vs. index for varying plastic strain limits	71
Figure 5.8: Rectangular HSS results: ratio of strength to IDEA StatiCa strength with 5% plastic strain limit plotted with index.....	72
Figure 5.9: Rectangular HSS results: ratio of varying mesh parameters sets to the default mesh settings plotted with index.....	73
Figure 5.10: Rectangular HSS: Reliability index for IDEA StatiCa and AISC 2022.....	78
Figure 6.1: Weld Angle Schematic	80
Figure 6.2: Example and dimensions for case 2 and 4 of Table D3.2 from the AISC <i>Specification</i>	81
Figure 6.3: Typical Welded Angle Model	93
Figure 6.4: Welded angle results: strength ratio vs. index.....	104
Figure 6.5: Welded angle results: normalized strength as a function of material ratio scatterplot.....	106
Figure 6.6: Welded angle results: IDEA StatiCa to experimental ratio as function of material ratio scatterplot	107
Figure 6.7: Welded angle results: strength ratio vs. index for varying plastic strain limits	108
Figure 6.8: Welded angle results: ratio of strength to IDEA StatiCa strength with 5% plastic strain limit plotted with index.....	109
Figure 6.9: Welded angle results: ratio of varying mesh parameters sets to the default mesh settings plotted with index.....	110
Figure 6.10: Welded angles: Reliability index for IDEA StatiCa and AISC.....	115
Figure 7.1: Bolted Angle Schematic	117

Figure 7.2: Typical Bolted Angle Model.....	124
Figure 7.3: Bolted angles results: strength ratio vs. index.....	130
Figure 7.4: Bolted angle results: normalized strength as a function of material ratio scatterplot.....	132
Figure 7.5: Bolted angle results: IDEA StatiCa to experimental ratio as function of material ratio scatterplot	133
Figure 7.6: Bolted angles results: ratio of strength to IDEA StatiCa strength with 5% plastic strain limit plotted with index.....	134
Figure 7.7: Bolted angle results: ratio of strength to IDEA StatiCa strength with 5% plastic strain limit plotted with index.....	135
Figure 7.8: Bolted angle results: ratio of varying mesh parameters sets to the default mesh settings plotted with index	137
Figure 7.9: Bolted angles: Reliability index for IDEA StatiCa and AISC	142
Figure 8.1: Welded Plate Schematic.....	144
Figure 8.2: Typical Welded Plate Model.....	148
Figure 8.3: Welded plate results: strength ratio vs. index.....	153
Figure 8.4: Welded plate results: normalized strength as a function of material ratio scatterplot.....	155
Figure 8.5: Welded plate results: IDEA StatiCa to experimental ratio as function of material ratio scatterplot	156
Figure 8.6: Welded plate results: strength ratio vs. index for varying plastic strain limits	157
Figure 8.7: Welded plate results: ratio of strength to IDEA StatiCa strength with 5% plastic strain limit plotted with index.....	158
Figure 8.8: Welded plate results: ratio of varying mesh parameters sets to the default mesh settings plotted with index.....	160
Figure 8.9: Welded plates: Reliability index for IDEA StatiCa and AISC	165
Figure 9.1: Bolted Plate Schematic.....	167
Figure 9.2: Typical Bolted Plate Model.....	177

Figure 9.3: Bolted plate results: strength ratio vs. index	185
Figure 9.4: Bolted plate results: normalized strength as a function of material ratio scatterplot.....	187
Figure 9.5: Bolted plate results: IDEA StatiCa to experimental ratio as function of material ratio scatterplot	188
Figure 9.6: Bolted plate results: strength ratio vs. index for varying plastic strain limits	189
Figure 9.7: Bolted plate results: ratio of strength to IDEA StatiCa strength with 5% plastic strain limit plotted with index.....	190
Figure 9.8: Bolted plate results: ratio of varying mesh parameters sets to the default mesh settings plotted with index	192
Figure 9.9: Bolted plates: reliability index results	197

CHAPTER 1

INTRODUCTION

Structural connections are crucial to safely transfer load from member to member. Connections in structural steel buildings take many forms and are subject to many different loading conditions. For some common connection types, detailed design guidance has been developed based on experimental and analytical research. For example, part 10 of the AISC *Steel Construction Manual* (2017) contains design recommendations for single plate shear connections. Similarly, AISC Design Guide 1 (2006) provides guidance and recommendations on the design of base plates and anchor rods. However, connection designers often encounter configurations and loading conditions for which there is little design guidance.

In the United States, the design of structural steel connections for buildings is governed by the *Specification for Structural Steel Buildings* published by the American Institute of Steel Construction (AISC). The latest edition of this standard was published in 2016 (AISC 2016). The next edition, to be published in 2022 is nearly final and drafts have been available for public review (AISC 2022a).

Design per the AISC *Specification* (AISC 2016) involves identifying applicable limit states, computing required strengths, computing available strengths, and ensuring that the available strength is greater than or equal to the required strength for each limit state. This process applies to common and uncommon connections alike, typically with calculations that can be completed by hand. The challenge for uncommon connections is that computing required and available strengths often relies on the use of unproven behavioral assumptions.

An alternative approach, made possible by advances in computer hardware and software, is to build a model capable of simulating the relevant behavioral effects, perform an analysis, and ensure that certain limits are met. This approach is permitted by the AISC *Specification* (AISC 2016) in the provisions of Appendix 1. Any method that uses inelastic analysis to design connections is permitted so long as it meets the general requirements of Section 1.3.1 of the AISC *Specification*.

Design by advanced inelastic analysis requires suitable analysis software. IDEA StatiCa is a steel connection design software based on the component-based finite element method (CBFEM). Connecting elements (e.g., plates, rolled shapes, hollow structural sections) are modeled with nonlinear shell elements that capture yielding, bolts are modeled as nonlinear springs, and welds are modeled as special constraints.

Extensive verification and validation studies have been performed on IDEA StatiCa to ensure accuracy and safety. The studies have mostly been conducted in comparison to European standards (Wald et al. 2020) however, comparisons to US standards are ongoing (Denavit and Truman-Jarrell 2021; Kasapoglu et al. 2021; Mustafa 2021). This study furthers the verification of IDEA StatiCa for US practice by examining how well the limit state of net-section tensile rupture is captured by IDEA StatiCa and identifying when IDEA StatiCa provides a comparable or higher level of reliability than the provisions of the AISC *Specification*.

The tensile rupture limit state was selected for investigation because it is the most basic and widely understood limit state that IDEA StatiCa captures in a fundamentally different manner than as prescribed in the AISC *Specification* (AISC 2016). The tensile yielding strength per IDEA StatiCa will never appreciably exceed that from the available strength from the AISC *Specification* given the constitutive relations used in the IDEA StatiCa model. Additionally, the limit states of bolt shear rupture, bearing, and tearout are evaluated in IDEA StatiCa using the equations from the AISC *Specification*. Tensile rupture, on the other hand is not directly evaluated in IDEA StatiCa. It is captured with a plastic strain limit. The default plastic strain limit in IDEA StatiCa is 5%. In the AISC *Specification*, tensile rupture is calculated based on the tensile strength of the steel, F_u , and employs a resistance factor of $\phi = 0.75$, neither of which are considered in IDEA StatiCa. In IDEA StatiCa the steel yields at the yield stress of the steel, F_y , times the resistance factor typically used for yielding, $\phi = 0.9$. Without explicit verification, it is unclear that these tradeoffs result in safe and accurate results.

The objective of this work is to rigorously evaluate how effectively IDEA StatiCa captures the tensile rupture limit state and to identify when IDEA StatiCa provides

comparable or higher reliability when compared to the AISC *Specification* (AISC 2016) equations for tensile rupture. The work includes comparisons between previously published experimental results, results from design equations in the AISC *Specification*, and results from IDEA StatiCa.

This thesis is organized as follows. Chapter 2 describes the development of the database of previously published experimental data. Chapter 3 provides an overview of the methods used in the study. Specific connection types are evaluated in Chapters 4 through 9. Finally, the work is summarized and conclusions are presented in Chapter 10.

CHAPTER 2

EXPERIMENTAL DATABASE

To provide a trusted benchmark for comparing the results of various design approaches, a database of previously published well-documented results of physical experiments was compiled. An extensive review of the literature was performed to identify papers and reports that document tests relevant to the study, i.e., structural steel members loaded monotonically in tension to failure. Specimens were considered useful if they failed in tensile rupture or tensile yield. Specimens were not included if they were reported to have failed in the bolts, welds, tearout, block shear rupture, or any limit state other than tensile yield or tensile rupture.

The references used in the database are listed in Table 2.1 with the corresponding number of applicable specimens for the study. A total of 384 specimens were included in the database. The specimens were categorized into the following connection types: welded round HSS, welded rectangular HSS, bolted angles, welded angles, bolted plates, and welded plates. Table 2.2 provides the number of specimens found applicable for each connection type. It should be noted there were several experimental tests that were conducted using riveted connections. These connections were categorized as bolted specimens. Further discussion on these specimens is provided where necessary.

The information recorded in the database was dependent on the connection type. In general, the following parameters were documented for bolted connections: author(s), year, specimen name, cross-section name, measured dimensions, material grade, measured yield strength, measured ultimate strength, bolt material, bolt size, edge distances, bolt gage, bolt spacing, number of bolts per row, number of rows of bolts, experimental strength, and experimental failure mode. For welded specimens, the following information was typically recorded: author(s), year, specimen name, cross-section name, measured dimensions, material grade, measured yield strength, measured ultimate strength, weld strength, weld size, length of welds, experimental strength, and experimental failure mode.

Table 2.1: Specimen Enumeration by Reference

Reference	Specimen Count	Connection Type
Gonzalez (1989)	9	Welded Plates
Gonzalez (1989)	7	Welded Angles
Kulak and Wu (1997)	24	Bolted Angles
Zhu et al. (2009)	9	Welded Angles
Willibald et al. (2006)	4	Welded Round HSS
Zhao et al. (2008)	29	Welded Rectangular HSS
Korol (1996)	7	Welded Rectangular HSS
Epstein (1992)	6	Bolted Angles
Yeomans (1993)	10	Welded Rectangular HSS
Yeomans (1993)	6	Welded Round HSS
Ke et al.(2018)	9	Bolted Angles
Ke et al. (2018)	9	Welded Angles
Fang et al. (2013)	12	Welded Angles
Može and Beg (2010)	16	Bolted Plates
Munse (1959)	67	Riveted Plates
Schutz and Newmark (1952)	22	Riveted Plates
Regan and Salter (1984)	17	Welded Angles
Petretta (2000)	7	Welded Angles
Mannem (2002)	19	Welded Plates
Mannem (2002)	16	Welded Angles
Bauer and Benaddi (2002)	6	Welded Angles
Greiner (1897)	2	Riveted Angles
McKibben (1907)	15	Riveted Angles
Gibson and Wake (1942)	4	Welded Angles
Dhanuskar and Gupta (2021a)	18	Welded Angles
Dhanuskar and Gupta (2021b)	8	Welded Angles
Cheng et al. (1998)	9	Welded Round HSS
Uzoegbo (1998)	14	Welded Angles

Table 2.2: Specimen Enumeration by Connection Type

Connection Type	Specimen Count
Welded Round HSS	19
Welded Rectangular HSS	46
Welded Angles	126
Bolted Angles	56
Welded Plates	28
Bolted Plates	109
Total	384

Many specimens were reported in metric units. In these instances, all lengths and cross-section names were converted to inches and reported to three decimal places. All forces were converted to kips and stresses to ksi. These were both rounded and reported to one decimal place.

CHAPTER 3

METHODS

Strengths from three different sources, 1) physical experiments, 2) AISC *Specification* equations, and 3) IDEA StatiCa, are compared in this work. General information on each is presented in this chapter with details specific to each connection types presented in the chapter on that connection type. In the context of this thesis, each of these values will be referred to generically as “strength”, “connection strength”, or with the symbol ‘ P ’.

3.1 Experimental Results

The peak load recorded in the experiment, P_{EXP} , was taken as reported by the experimentalists for each specimen. As previously noted, the peak load recorded in the experimental and the observed failure mode were both included in the database for each specimen. Most experiments report the tensile rupture strength after significant yielding occurred and the load at which significant yielding occurred is not reported. An example of this is provided in Figure 3.1 from Dhanuskar and Gupta (2021b). Specimen 1-S1-250/90-B is represented by the solid black curve. The experimental strength was reported as 478.8 kN (107.6 kips), which is clearly beyond the point of yield. Another example is provided in Figure 3.2 with a plot from Fang et al. (2013) where the strengths extended beyond the linear portion of the load-deformation curve as well.

3.2 AISC Specification

The AISC *Specification for Structural Steel Buildings* (AISC 2016) governs the design of structural steel buildings in the United States. Strength design under the AISC *Specification* is performed using either the provisions for load and resistance factor design (LRFD) or the provisions for allowable strength design (ASD). This study focuses on LRFD exclusively. The governing strength equation for LRFD is

$$R_u \leq \phi R_n \quad (3-1)$$

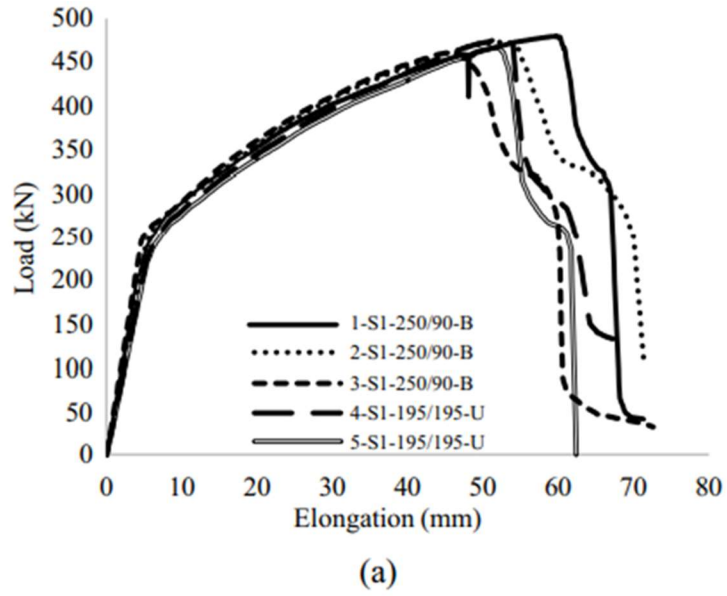


Figure 3.1: Load-deformation curve from Dhanuskar and Gupta (2021b)

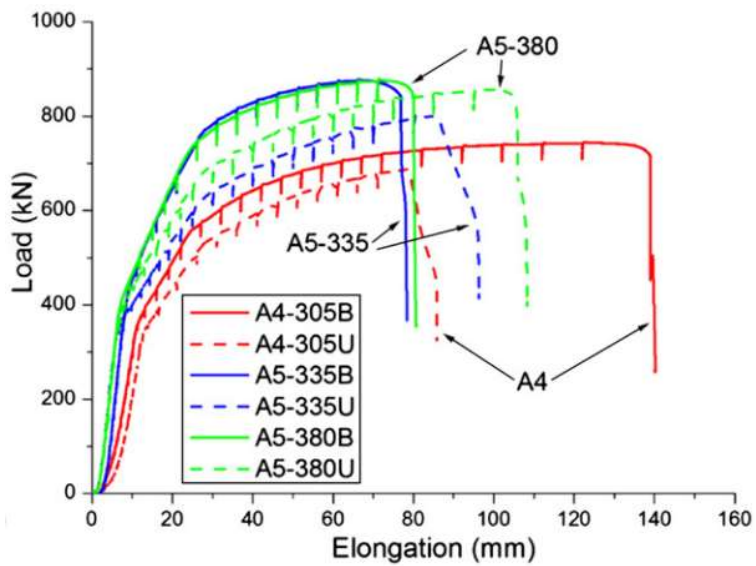


Figure 3.2: Load-deformation curve from Fang et al. (2013)

where, R_u is the required strength using LRFD load combinations, R_n is the nominal strength, ϕ is the resistance factor, and ϕR_n is the available or design strength.

The nominal strength is the expected strength of the structure or component whereas the design strength is reduced by the resistance factor to account for unavoidable deviations of the nominal strength from the actual strength and for the manner and consequences of failure. The *AISC Specification* (AISC 2016) includes equations for the nominal strength and lists resistance factors for each limit state.

This study focuses on two limit states: tensile yielding in the gross section and tensile rupture in the net section, both defined in Chapter D of the *AISC Specification* (AISC 2016). Other limit states were not evaluated because (1) if other limit states controlled the *AISC Specification* strength but did not fail in the physical experiments then their actual strengths were more sufficient than indicated by the *AISC Specification* equations, (2) if other limit states controlled the physical experiments the specimens were deemed irrelevant to the current study and consequently removed.

Unless otherwise noted, measured dimensions and material properties were used in the *AISC Specification* (2016) equations. The tensile yield equation is provided in Equation 3-2, with the tensile rupture equation to follow in Equation 3-3 and 3-4

$$P_{YIELD} = F_y A_g \quad (3-2)$$

$$P_{RUPTURE} = F_u A_e \quad (3-3)$$

$$A_e = A_n U \quad (3-4)$$

where F_y is the yield strength, A_g is the gross area of the member, F_u is the ultimate strength, A_e is the effective net area of the member, A_n is the net area of the member, and U is the shear lag factor.

The shear lag factor, U , accounts for the uneven distribution of stresses across the cross-section of a member in tension. This factor results in a reduction for tension members connected by only some of the cross-sectional elements. The length of the connection and the centroid are factors that can impact the magnitude of U . The shear lag factor was determined based on Table D3.1 in the *AISC Specification* (2016) and

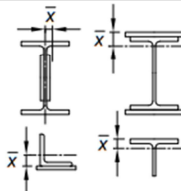
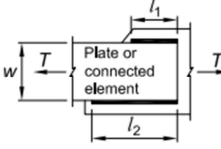

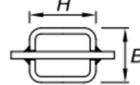
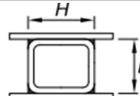
replicated here as Figure 3.3. Each chapter will describe in detail the cases used from this table for each connection type.

The overall strength of a specimen according to the AISC *Specification* is denoted as P_{AISC} . However, there are instances where it is appropriate to discuss only the tensile rupture strength. For these cases, the strength will be denoted as $P_{RUPTURE}$. On the contrary, the tensile yield strength is denoted as P_{YIELD} . Lastly, resistance factors were not implemented for the experimental specimens. However, the appropriate resistance factors were used for the reliability specimens where ϕ is 0.90 for tensile yield and 0.75 for tensile rupture.

3.3 IDEA StatiCa

IDEA StatiCa is a steel connection software that implements the CBFEM. Engineers using this software model a connection, apply loads obtained from a structural analysis of the overall structure (performed by hand or using other software), run an analysis of the connection, then review the results to determine the adequacy of the connection. The main results are the plastic strain in the members and connecting elements and the utilization ratios of the bolts and welds. The plate plastic strain limit is set to 5.0% by default, however the limit can be adjusted as desired. The bolt and weld utilization ratios are calculated such that a value of 100% or below is passing and a value exceeding 100% is failing. If the connection does not pass all checks, then the connection should be adjusted, and the analysis rerun. In other modes, IDEA StatiCa has the capability to perform capacity design, approximate the design resistance of the connection, and evaluate fatigue.

The graphical user interface of IDEA StatiCa allows modeling of connection far quicker than general finite element software packages. Members, loads, and operations (including connecting elements, bolts, and welds) are defined either using templates or from scratch. Meshing is done automatically. Members and plates are modeled with shell elements with a bilinear elastic-plastic constitutive relations. The yield stress is reduced

TABLE D3.1			
Shear Lag Factors for Connections to Tension Members			
Case	Description of Element	Shear Lag Factor, U	Example
1	All tension members where the tension load is transmitted directly to each of the cross-sectional elements by fasteners or welds (except as in Cases 4, 5 and 6).	$U = 1.0$	-
2	All tension members, except HSS, where the tension load is transmitted to some but not all of the cross-sectional elements by fasteners or by longitudinal welds in combination with transverse welds. Alternatively, Case 7 is permitted for W, M, S and HP shapes. (For angles, Case 8 is permitted to be used.)	$U = 1 - \frac{\bar{x}}{l}$	
3	All tension members where the tension load is transmitted only by transverse welds to some but not all of the cross-sectional elements.	$U = 1.0$ and $A_n = \text{area of the directly connected elements}$	-
4 ^[a]	Plates, angles, channels with welds at heels, tees, and W-shapes with connected elements, where the tension load is transmitted by longitudinal welds only. See Case 2 for definition of \bar{x} .	$U = \frac{3l^2}{3l^2 + w^2} \left(1 - \frac{\bar{x}}{l}\right)$	
5	Round HSS with a single concentric gusset plate through slots in the HSS.	$l \geq 1.3D, U = 1.0$ $D \leq l < 1.3D, U = 1 - \frac{\bar{x}}{l}$ $\bar{x} = \frac{D}{\pi}$	
6	Rectangular HSS.		
	with a single concentric gusset plate	$l \geq H, U = 1 - \frac{\bar{x}}{l}$ $\bar{x} = \frac{B^2 + 2BH}{4(B+H)}$	
	with two side gusset plates	$l \geq H, U = 1 - \frac{\bar{x}}{l}$ $\bar{x} = \frac{B^2}{4(B+H)}$	
7	W-, M-, S- or HP-shapes, or tees cut from these shapes. (If U is calculated per Case 2, the larger value is permitted to be used.)	with flange connected with three or more fasteners per line in the direction of loading	$b_f \geq \frac{2}{3}d, U = 0.90$ $b_f < \frac{2}{3}d, U = 0.85$
		with web connected with four or more fasteners per line in the direction of loading	$U = 0.70$
8	Single and double angles. (If U is calculated per Case 2, the larger value is permitted to be used.)	with four or more fasteners per line in the direction of loading	$U = 0.80$
		with three fasteners per line in the direction of loading (with fewer than three fasteners per line in the direction of loading, use Case 2)	$U = 0.60$

B = overall width of rectangular HSS member, measured 90° to the plane of the connection, in. (mm); D = outside diameter of round HSS, in. (mm); H = overall height of rectangular HSS member, measured in the plane of the connection, in. (mm); d = depth of section, in. (mm); for tees, d = depth of the section from which the tee was cut, in. (mm); l = length of connection, in. (mm); w = width of plate, in. (mm); \bar{x} = eccentricity of connection, in. (mm).

^[a] $l = \frac{l_1 + l_2}{2}$, where l_1 and l_2 shall not be less than 4 times the weld size.

Figure 3.3: Table D3.1 from the AISC Specification (AISC 2016)

by a resistance factor, taken as 0.9 for US-based design using LRFD. The hardening slope is taken as $E/1000$, where E is the modulus of elasticity. This is a minimal value, used only to avoid the numerical issues that would arise with zero post-yield stiffness, and does not produce any significant strain hardening. Bolts and anchors are analyzed as nonlinear springs and welds are modeled as special constraints.

3.3.1 Typical Modeling Process

For the purpose of this study, the maximum applied load that the program deems safe, referred to as P_{IDEA} , was of the most interest. To calculate P_{IDEA} , applied loads were adjusted and the analysis rerun in an iterative process until the connection was right at the limit. The typical modeling process was as follows:

1. In code setup, all LRFD resistance factors were set to:
 - a. for experimental specimens
 - b. Default values for reliability specimens
2. Materials representative of each specific specimen were created.
 - a. Inputting measured F_y , measured F_u , measured E (if given) for experimental specimens
 - b. Using nominal properties based on material grade for reliability specimens
3. Cross-sections representative of each specific specimen were created.
 - a. Inputting measured geometric dimensions including, but not limited to, heights, widths, thicknesses, fillets, etc. for experimental specimens
 - b. Using nominal cross sections already in IDEA StatiCa for reliability specimens
4. Models based on the specific connection type were created.
5. Analyses were performed, adjusting loading to determine P_{IDEA} .

For most analyses, the iterative determination of P_{IDEA} was performed using a script written in the Python programming language that communicated with IDEA StatiCa through its application programming interface (API). The tolerance for the plastic

strain limit was set as 0.0005. For example, if the target plastic strain is 5.0% (i.e., the default value), the script would perform analyses in succession, updating the magnitude of loading until the maximum plastic strain was between 0.0495 and 0.0500 (4.95% and 5.00%). When a result in this range was found, the applied load for that specific analysis was taken as P_{IDEA} . The results of approximately 20% of the specimens were manually checked in IDEA StatiCa. In addition to P_{IDEA} , the script records the connection name, mesh parameter set, plastic strain limit, plastic strain, bolt utilization, and weld utilization.

Automation of the analyses allowed investigation of varying plastic strain limits and mesh density. Four sets of mesh parameters were investigated as detailed in Table 3.1 where mesh parameter set ‘B’ represents the default parameters. Five plastic strain limits were evaluated: 1.0%, 2.5%, 5.0% (default), 7.5%, and 10%. For each specimen, there were 20 outputs (five plastic strain limits for each of the four mesh sets). Unless otherwise stated, the results throughout the entirety of this study are presented as mesh parameter set ‘B’ and 5% plastic strain limit.

3.3.2 Member Model Type

IDEA StatiCa is a connection design software and models only the connection. Therefore, it is necessary to place end conditions at the end of the member away from the connection. There are 6 degrees-of-freedom at each member end, and these can be set as either fixed or free. There are four options for end condition settings (model types) in IDEA StatiCa: N-Vy-Vz-Mz-My-Mz, N-Vz-My, N-Vy-Mz, and N-Vy-Vz. The inclusion of ‘Mx’, ‘My’, or ‘Mz’ in the mode name indicates that member end is free to rotate about the ‘x’, ‘y’, or ‘z’ axes, respectively. The axes are defined with respect to the member with the ‘x’ axis defined along the length of the member and the ‘y’ and ‘z’ axes defined perpendicular to the longitudinal axis of the member. The inclusion of ‘Vy’, or ‘Vz’ in the mode name indicates that the member end is free to translate in the ‘y’, or ‘z’ directions, respectively. ‘N’ is included in all model names, indicating that in all cases the member end is free to translate along the longitudinal axis of the member. The absence of

Table 3.1: Mesh Parameter Set List

Code Setup Parameters	Mesh Parameter Set			
	A	B*	C	D
Division of surface of the biggest circular hollow member	32	64	96	128
Division of arc of rectangular hollow member	3	3	6	12
Number of elements on biggest member web or flange	4	8	16	32
Number of elements on biggest web of RHS member	8	16	32	64
Minimal size of element	0.394" (10 mm)	0.394" (10 mm)	0.197" (5 mm)	0.098" (2.5 mm)
Maximal size of element	3.937" (100 mm)	1.969" (50 mm)	1.969" (50 mm)	0.984" (25 mm)

* default settings in IDEA StatiCa

a degree-of-freedom from the model name indicates that the degree-of-freedom is restrained (i.e., zero displacement or rotation).

Determining the end conditions that best represents physical behavior can be critical to the end results. A small study was conducted to determine the appropriate end conditions for the tension members investigated in this work. The following specimens were used in the study: bolted angle S1 from Kulak and Wu (1997), welded plate P-B-2 from Gonzalez (1989), and welded tee T-L-1a from Gonzalez (1989). The Gonzalez specimens are actually double plates and double tee specimens, however for this study only single tension members were used. These specimens were chosen to investigate the effect of end conditions on eccentricity in two directions (as exists for the angle), eccentricity in one direction (as exists for the tee), and minimal eccentricity (as exists for the plate). For clarity, all tension members presented in this study are oriented on the same local axes. As shown in Figure 3.4, the x -axis runs along the length of the tension member, the y -axis runs along the width of the gusset plate, and the z -axis is perpendicular to the plane of the gusset plate.

The end conditions and selection of bearing and nonbearing members were investigated in this study. In IDEA StatiCa, boundary conditions are applied to the end of the bearing member to restrict rigid body motion of the connection. There can only be one bearing member in IDEA StatiCa with all other members analyzed as nonbearing. The study presented below was conducted on the single angle tension member from Kulak and Wu (1997). The results are presented in Table 3.2. The failure mode in IDEA StatiCa was plate strain for all analyses, however the failing member did vary based on the bearing member selection. This is noted in the table under “Failure Detail”. Since the results do not change when the bearing member end conditions vary, it was concluded the end conditions of the bearing member do not impact the results. Therefore, the only significant end condition is that of the nonbearing member. Unless otherwise noted, all tension members are modeled as nonbearing members. Table 3.3 presents results from the remainder of the end condition study. The table contains results from the angle, tee, and plate tension member specimens. The gusset plate was set as the bearing

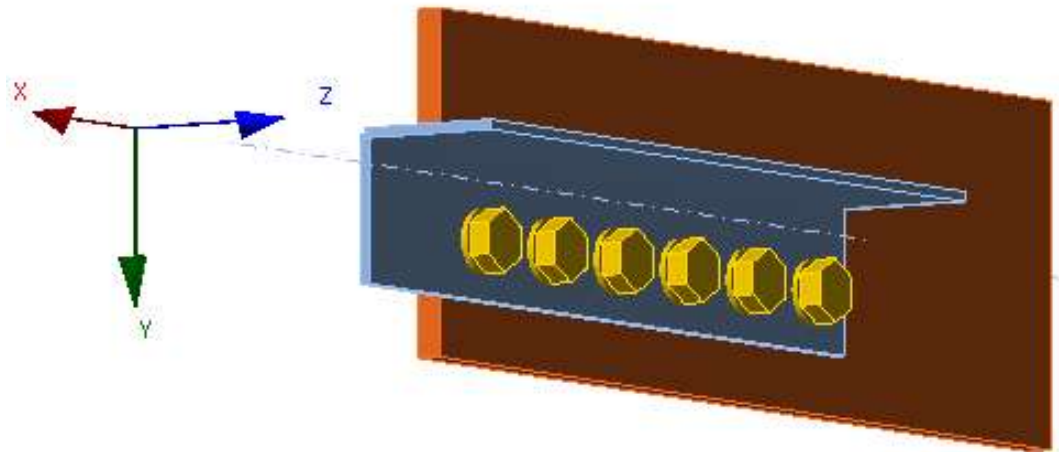


Figure 3.4: Local Axes on Bolted Angle

Table 3.2: Single Angle Bearing Member-End Condition Study

Index	Bearing Member	Model Type		IDEA StatiCa Results			
		Gusset Plate	Tension Member	Strength, kips	Plate Strain, %	Bolt/Weld Utiliz., %	Failure Detail
1	GP	[1]	[1]	27.3	4.8	46.2	GP
2	GP	[2]	[1]	27.3	4.8	46.2	GP
3	GP	[3]	[1]	27.3	4.8	46.2	GP
4	GP	[4]	[1]	27.3	4.8	46.2	GP
5	TM	[1]	[1]	46.4	4.9	27.6	TM
6	TM	[1]	[2]	46.4	4.9	27.6	TM
7	TM	[1]	[3]	46.4	4.9	27.6	TM
8	TM	[1]	[4]	46.4	4.9	27.6	TM

GP is gusset plate; TM is tension member; [1] is 'N-Vy-Vz-Mx- My-Mz'; [2] is N-Vz-My; [3] is N-Vy-Mz; [4] is N-Vy-Vz

Table 3.3: End Condition Study

Index	Tension Member Type	Tension Member Model Type	Strength, kips	Plate Strain, %	Bolt/Weld Utiliz., %	Failure Detail
1	Angle	[1]	27.3	4.8	46.2	GP
2	Angle	[2]	27.3	4.8	46.2	GP
3	Angle	[3]	63.4	4.9	46.3	TM
4	Angle	[4]	54.2	4.9	33.1	TM
5	Tee	[1]	17.4	5	87.6	TM
6	Tee	[2]	17.4	4.8	87.5	TM
7	Tee	[3]	65	5	85.9	TM
8	Tee	[4]	62	5	80.1	TM
9	Plate	[1]	41.3	4.6	79.6	TM
10	Plate	[2]	41.3	4.6	79.5	TM
11	Plate	[3]	41	4.5	79.7	TM
12	Plate	[4]	41.3	5	79.5	TM

GP is gusset plate; TM is tension member; [1] is 'N-Vy-Vz-Mx-My-Mz'; [2] is N-Vz-My; [3] is N-Vy-Mz; [4] is N-Vy-Vz

member for all analyses presented in the table. Plate strain controlled for all analyses as well.

The angle specimen has two directions of eccentricity, and the strength varies significantly for all model types. The tee specimen has one direction of eccentricity, and two model types result in similar strengths. The plate specimen has minimal eccentricity, and two model types produce the same results with the remaining being not far off. It is concluded that end conditions become less significant as the eccentricity approaches zero however, for specimens with multiple directions of eccentricity the end conditions are very significant. For the angle and tee analyses, the model type [2] produced unrealistically low strengths. The angle and tee specimens indicate end conditions [3] and [4], ‘N-Vy-Mz’ and ‘N-Vy-Vz’, respectively, are more realistic of the physical experiments than the other options. For context, deformed shapes of the angle specimen with end conditions [3] and [4] are provided below in Figure 3.5 and Figure 3.6. All deformed shapes are shown with a deformation scale set to 10. The deformed shape of the angle with end condition N-Vy-Mz shows significant bending in the plate and tension member. Whereas, Figure 3.6 does not show significant bending in the tension member or gusset plate. IDEA StatiCa recommends engineers to model braced members using the ‘N-Vy-Vz’ model type. Tension members are commonly used as braced members in trusses. Per the recommendation, the ‘N-Vy-Vz’ model type was chosen for all subsequent analyses in this study.

3.3.3 Mesh Study

A small study was conducted to better understand the sensitivity of the strength results to the mesh parameters in IDEA StatiCa. Similarly sized round and rectangular (square) HSS members were used for this study. The specimens included the following parameters: HSS6×6×1/4 square HSS and 6.000×0.250 round HSS, A500 Gr. C material ($F_y = 50$ ksi, $F_u = 62$ ksi), 0.375 in. weld size, 8 in. weld length, and plate thickness of 0.5 in. All analyses were conducted with 5.0% plastic strain limit. This study was conducted

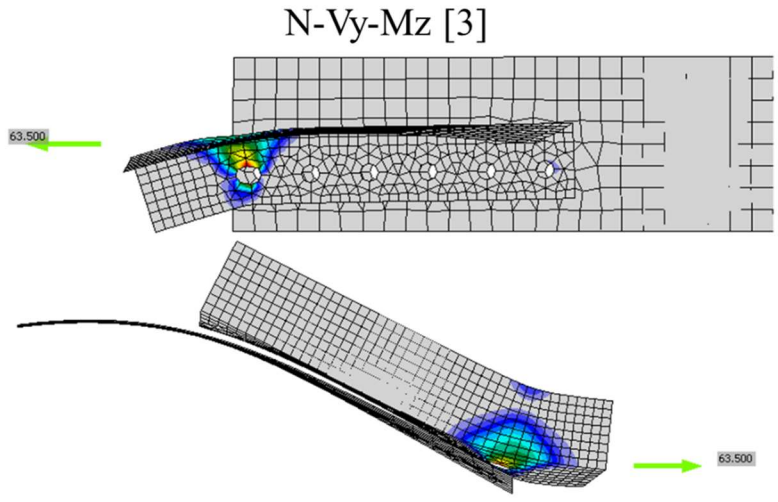


Figure 3.5: Deformed shapes of angle with end condition N-Vy-Mz

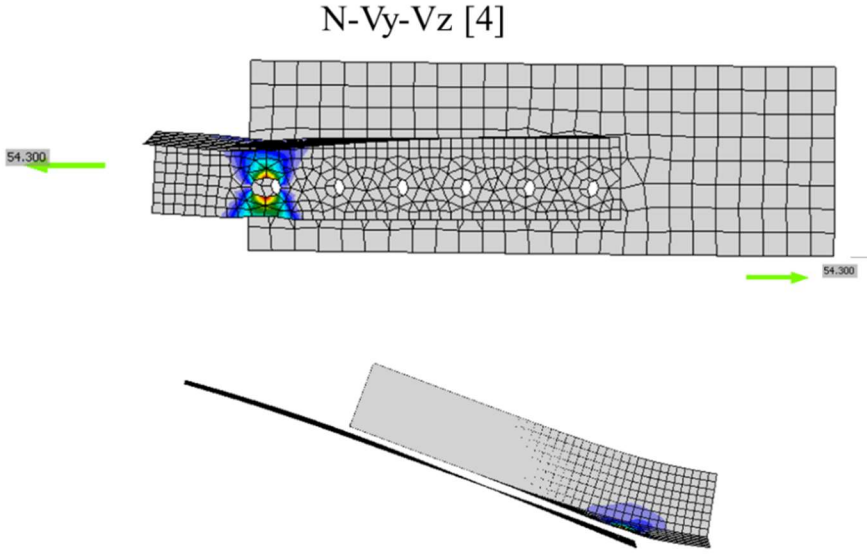


Figure 3.6: Deformed shapes of angle with end condition N-Vy-Vz

using more increments than the mesh parameters outlined in Table 3.1. The rectangular HSS mesh is defined by the parameters ‘number of elements on biggest web of RHS member’ and ‘division of arc of rectangular hollow member’, whereas the round HSS is defined only by the parameter ‘division of surface of the biggest circular hollow member’. Figure 3.7 provides the results of the study. The strengths are plotted against the number of elements around the perimeter of the HSS member. The results are provided for both the design strengths (including resistance factors) and the nominal strengths (not including resistance factors). The results show a decrease in strength with increasing number of elements, but no distinct convergence. Plateaus in the results were observed where a minimal change in strength is noted for two or more increments and followed by decreases in strength for the following increments. The runtime of the analyses increases dramatically with number of elements and occasionally results in analysis error; therefore, it was not determined if the results would eventually converge.

3.4 Reliability Analysis

As previously mentioned, the AISC *Specification* (AISC 2016) allows design by advanced inelastic analysis when the analysis provides a comparable or higher level of reliability. Thus, analyses are performed in this work to evaluate the reliability of connections designed per the AISC *Specification* in comparison to those designed using IDEA StatiCa. Structural reliability is commonly expressed in terms of the reliability index, β . The reliability index is a value that represents the probability of failure for a particular structural component. According to the Commentary of the AISC *Specification* (AISC 2016), current provisions provide a reliability index of approximately 4.0 for connections and 2.6 for members. For the development of the new provisions for rectangular HSS in the 2022 AISC *Specification*, Dowswell (2021) used a target reliability index of 4.0 for tensile rupture.

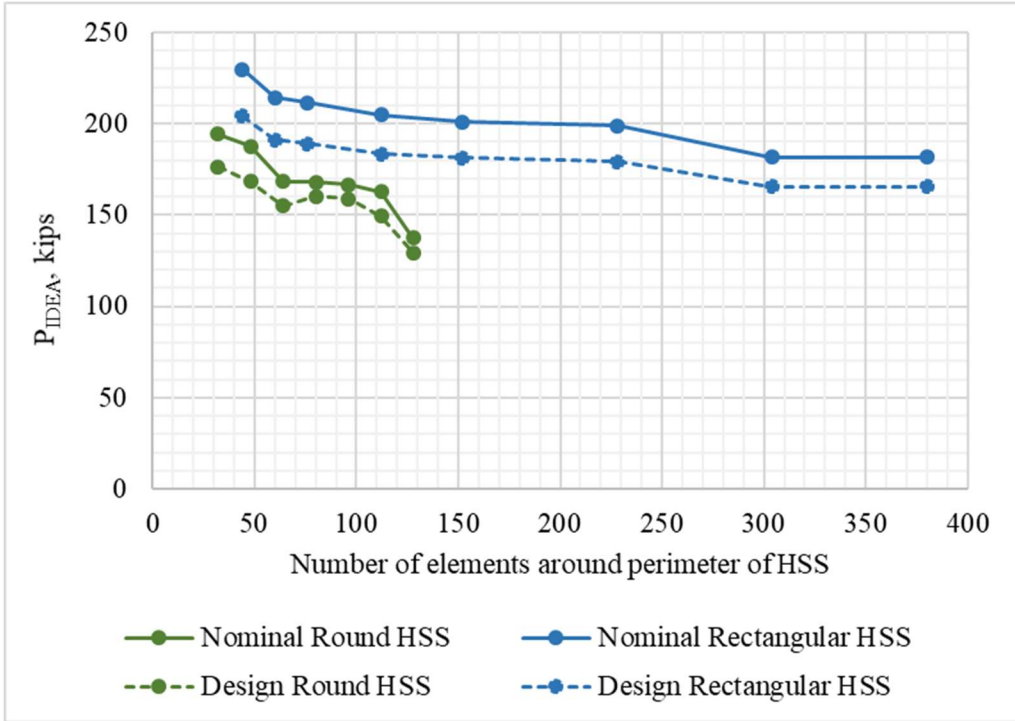


Figure 3.7: Mesh refinement for round and rectangular HSS

The methodology for the reliability analysis is outlined in the following discussion. To begin, a limit state function for tensile yield and tensile rupture can be represented by \tilde{g}_Y and \tilde{g}_R , respectively. These are expressed in the following equations.

$$\tilde{g}_Y = \tilde{R}_Y - \tilde{Q} \quad (3-5)$$

$$\tilde{g}_R = \tilde{R}_R - \tilde{Q} \quad (3-6)$$

where \tilde{R}_Y is a random variable representing the resistance for the tensile yield limit state, \tilde{R}_R is a random variable representing the resistance for the tensile rupture limit state, and \tilde{Q} is a random variable representing the demand on the connection.

The random variable for the resistance of the tensile yield limit state is a function of \tilde{A}_g and \tilde{F}_y , expressed as the following:

$$\tilde{R}_Y = \tilde{A}_g \tilde{F}_y \quad (3-7)$$

where \tilde{A}_g is a random variable representing actual gross area and \tilde{F}_y is a random variable representing the actual yield stress.

These two variables are expressed as such in the following equations:

$$\tilde{A}_g = \tilde{X}_A A_{gn} \quad (3-8)$$

$$\tilde{F}_y = \tilde{X}_{Fy} F_{yn} \quad (3-9)$$

where \tilde{X}_A is a random variable representing the ratio between actual and nominal gross area, A_{gn} is the nominal gross area, \tilde{X}_{Fy} is a random variable representing the ratio between actual and nominal yield stress, and F_{yn} is the nominal yield stress.

The random variable for the resistance of the tensile rupture limit state is a function of \tilde{X}_R , \tilde{A}_e , and \tilde{F}_u , more specifically expressed as the following:

$$\tilde{R}_R = \tilde{X}_R \tilde{A}_e \tilde{F}_u \quad (3-10)$$

where, \tilde{X}_R is a random variable representing the ratio of actual strength and calculated tensile rupture strength (also referred to as the professional factor). \tilde{A}_e is a random variable representing the actual effective net area. \tilde{F}_u is a random variable representing

the actual ultimate tensile strength. \tilde{A}_e and \tilde{F}_u are expressed like so in the following equations:

$$\tilde{A}_e = \tilde{X}_A A_{en} \quad (3-11)$$

$$\tilde{F}_u = \tilde{X}_{Fu} F_{un} \quad (3-12)$$

where \tilde{X}_A is a random variable representing the ratio of actual and nominal effective net area, A_{en} is the nominal effective net area, \tilde{X}_{Fu} is a random variable representing the ratio of actual to nominal ultimate tensile strength, and F_{un} is the nominal ultimate tensile strength.

The demand, \tilde{Q} , is the sum of the dead load and the live load and can be expressed as:

$$\tilde{Q} = \tilde{X}_D P_{Dn} + \tilde{X}_L P_{Ln} \quad (3-13)$$

where \tilde{X}_D is a random variable representing the ratio of the actual to nominal dead load, P_{Dn} is the nominal dead load, \tilde{X}_L is the random variable representing the ratio of the actual to nominal live load, and P_{Ln} is the nominal live load. \tilde{X}_D and \tilde{X}_L were taken from literature and are provided later in the section. However, P_{Dn} and P_{Ln} were calculated based on load combinations and a chosen live to dead load ratio (P_{Ln}/P_{Dn}). The load ratio was taken as one, and the applied loads were calculated the assuming the connection was designed at the exact capacity limit point for AISC and IDEA StatiCa respectively:

$$P_u = \max(1.4P_{Dn}, 1.2P_{Dn} + 1.6P_{Ln}) = \phi P_{n,AISC} = \min(0.9A_{gn}F_{yn}, 0.75A_{en}F_{un}) \quad (3-14)$$

$$P_u = \max(1.4P_{Dn}, 1.2P_{Dn} + 1.6P_{Ln}) = P_{IDEA} \quad (3-15)$$

where P_{Dn} and P_{Ln} are calculated based on the ratio chosen, $\phi P_{n,AISC}$ is the design strength according to the AISC *Specification* (AISC 2016), and P_{IDEA} is the strength determined by IDEA StatiCa for a given connection (with resistance factors applied).

Failure occurs when the demand exceeds the resistance, \tilde{R}_Y or \tilde{R}_R . Numerically, the probability of failure is expressed as the probability of either \tilde{g}_Y or \tilde{g}_R being less than zero:

$$P_f = P(\tilde{g}_Y < 0 \cup \tilde{g}_R < 0) \quad (3-16)$$

The probability of failure is converted into an index value, referred to as the reliability index. This is expressed as the following:

$$\beta = -F_x^{-1}(P_f) \quad (3-17)$$

where F_x^{-1} is the inverse normal cumulative distribution.

In general, the process included the following: (1) determine mean and coefficient of variation for certain test-to-predicted ratios for each connection type based on the experimental database, (2) determine properties of other random variables from the literature, (3) define set of controlled connections, (4) calculate strength of connections with nominal properties based on the AISC *Specification* (AISC 2016) equations, (5) model connection set in IDEA StatiCa using nominal properties and resistance factors and determine maximum applied load, P_{IDEA} , (5) calculate reliability indices, β , for AISC and IDEA StatiCa respectively using a Python script which implements the above equations to determine the reliability index using 1,000,000 Monte Carlo simulations.

Table 3.4 provides the values used in this analysis and their origin. \tilde{X}_R varies from connection type to connection type and is determined based off the results of each chapter in this report. The values used for this random variable are presented in later chapters where applicable.

Table 3.4: Summary statistics for random variables used in the reliability analysis

Variable	Mean	COV	Distribution	Source	
\tilde{X}_R	varies*	varies*	Normal	this study	
\tilde{X}_D	1.05	0.10	Normal	Ellingwood et al. (1980)	
\tilde{X}_L	1.00	0.25	Extreme Value Type I	Ellingwood et al. (1980)	
\tilde{X}_A	1.00	0.05	Normal	Ravindra and Galambos (1978)	
\tilde{X}_{Fu}	A36 (plate)	1.39	0.07	Bivariate Lognormal	Liu et al. (2007)
	A572 Gr. 50 (plate)	1.16	0.07	Bivariate Lognormal	Liu et al. (2007)
	A500 Gr. C	1.3	0.1**	Bivariate Lognormal	AISC 341-22 (2022)
	A53 Gr. B	1.59	0.11	Bivariate Lognormal	Liu et al. (2007)
	A36 (angle)	1.34	0.07	Bivariate Lognormal	Liu et al. (2007)
\tilde{X}_{Fy}	A36 (plate)	1.23	0.04	Bivariate Lognormal	Liu et al. (2007)
	A572 Gr. 50 (plate)	1.26	0.07	Bivariate Lognormal	Liu et al. (2007)
	A500 Gr. C	1.2	0.1**	Bivariate Lognormal	AISC 341-22 (2022)
	A53 Gr. B	1.16	0.06	Bivariate Lognormal	Liu et al. (2007)
	A36 (angle)	1.22	0.04	Bivariate Lognormal	Liu et al. (2007)

COV: coefficient of variation; *mean and COV of the professional factor were computed from test-to-predicted ratio for each connection type, **assumed value

CHAPTER 4

WELDED ROUND HSS

4.1 Description of Connection

Round HSS members that are welded to a gusset plate are evaluated in this chapter. A typical schematic of this connection is shown in Figure 4.1 with the relevant terminology consistent throughout this chapter. The typical connection includes a slotted round HSS welded to a gusset plate. It should be noted some connections in the experimental set include a notched plate where the round HSS is not slotted. The hidden line in Figure 4.1 indicating the edge of the gusset plate would not be representative of those specific specimens.

For this connection, the AISC *Specification* (2016, 2022a) calculations for the shear lag factor used in the evaluation of tensile rupture vary significantly from the 2016 edition to the 2022 edition based on the work of Martinez-Saucedo and Packer (2009). For this reason, the AISC *Specification* calculations are provided for both editions. The 2016 shear lag factor calculations include the use of Case 5 in Table D3.1 of the AISC *Specification* shown in Figure 3.3. The equation is as follows:

$$l \geq 1.3D, \quad U = 1.0 \quad (4-1)$$

$$D \leq l < 1.3, \quad U = 1 - \frac{\bar{x}}{l} \quad (4-2)$$

$$\text{and } \bar{x} = \frac{D}{\pi} \quad (4-3)$$

For the 2022 edition of the AISC *Specification*, the equation is as follows:

$$U = \left[1 + \left(\frac{\bar{x}}{l} \right)^{3.2} \right]^{-10} \quad (4-4)$$

$$\bar{x} = \frac{R \sin \theta}{\theta} - \frac{1}{2} t_p \quad (4-5)$$

where l is the length of the weld and θ (in radians), R , and t_p are defined in Figure 4.2. It should be noted, the specimens including a notched plate are not slotted, therefore the net area is equal to the gross area. Additionally, there are some connections with a weld

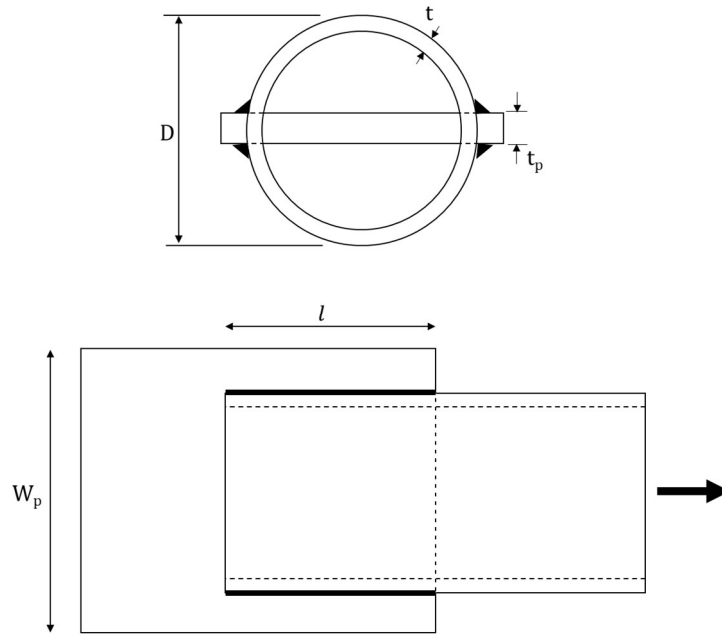


Figure 4.1: Welded Round HSS Schematic

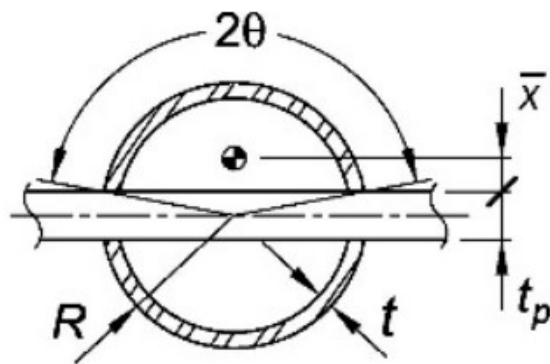


Figure 4.2: Figure from AISC *Specification* (2022) defining parameters of round HSS

across the thickness of the gusset plate (i.e., a weld return). The net area of specimens with a weld return was taken as the gross area. Whereas, the net area of specimens without a weld return was taken as the gross area minus the removed area for the slot on both sides. A more in-depth discussion of this weld is provided in a later section.

4.2 Comparison to Experimental Results

4.2.1 Description of Experimental Specimens

There were 19 total round HSS specimens found in the literature. The detailed enumeration for this connection is included in Table 4.1. It should be noted there were actually 8 round HSS specimens presented in Willibald et al. (2006). However, two specimens were excluded as they were subject to compression. An additional two specimens failed in block shear rupture and were consequently removed from the study.

A description of each specimen is provided in Table 4.2 and Table 4.3. This information was used to model the specimens in IDEA StatiCa and to calculate the strengths according to the AISC *Specification* for the 2016 edition and the 2022 edition. The material grades were not provided for every specimen, however measured tensile yield strengths and ultimate strengths were reported and used for all calculations and modeling. Additionally, the weld strength was rarely provided. Unless otherwise specified in the text, E70XX weld strength was always used. Willibald et al. (2006) indicated an E480XX weld strength in metric units, E70XX was determined as the equivalent weld strength. Yeomans (1993) did not provide the weld size but noted that welds were designed to never control. A weld size of 0.197 in. (5 mm) was used for the Yeomans specimens. For all round HSS specimens, the gross area was calculated based on the measured diameter and measured thicknesses. The column in the table labeled “Weld Return” refers to the indication of a weld around the edge of the plate, as shown in (B) of Figure 4.3.

Table 4.1: Round HSS Specimen Enumeration

Reference	Specimen Count
Cheng et al. (1998)	9
Willibald et al. (2006)	4
Yeomans (1993)	6
Total	19

Table 4.2: Round HSS Specimen Details

Index	Reference	Specimen	* F_y , ksi	* F_u , ksi	* D , in.	* t , in.
1	Willibald et al. (2006)	A2	72.2	78.3	6.572	0.191
2	Willibald et al. (2006)	B2	72.2	78.3	6.572	0.191
3	Willibald et al. (2006)	C1**	72.2	78.3	6.572	0.191
4	Willibald et al. (2006)	C2**	72.2	78.3	6.572	0.191
5	Yeomans (1993)	C-SEP-1	47.1	71.6	2.374	0.127
6	Yeomans (1993)	C-SEP-2	47.7	71.2	2.374	0.165
7	Yeomans (1993)	C-SEP-3	44.5	72.4	2.374	0.188
8	Yeomans (1993)	C-SEP-4	42.1	65.8	4.500	0.140
9	Yeomans (1993)	C-SEP-5	41.3	66.7	4.500	0.190
10	Yeomans (1993)	C-SEP-6	44.5	64.4	4.500	0.249
11	Cheng et al. (1998)	PWC1	57.0	65.1	3.962	0.246
12	Cheng et al. (1998)	PWC2	57.0	65.1	3.962	0.246
13	Cheng et al. (1998)	PWC3	57.0	65.1	3.962	0.246
14	Cheng et al. (1998)	PWC4	57.0	65.1	3.962	0.246
15	Cheng et al. (1998)	PWC5	54.4	65.4	3.967	0.177
16	Cheng et al. (1998)	PWC6	54.4	65.4	3.967	0.177
17	Cheng et al. (1998)	PWC7	54.4	65.4	3.967	0.177
18	Cheng et al. (1998)	SPEC1	50.5	62.5	8.568	0.291
19	Cheng et al. (1998)	SPEC2	50.5	62.5	8.568	0.291

*indicates measured value; **indicates specimen with notched plate, see (C) in Figure 4.3

Table 4.3: Round HSS Specimen Weld Details

Index	Weld Size, in.	l , in	Cut Width, in.	Weld Return
1	0.390	7.560	1.060	No
2	0.351	8.190	1.060	Yes
3	0.551	6.478	1.060	No
4	0.551	7.677	1.060	No
5	-	3.150	0.390	Yes
6	-	3.150	0.484	Yes
7	-	2.953	0.602	Yes
8	-	5.906	0.602	Yes
9	-	5.906	0.787	Yes
10	-	5.709	0.787	Yes
11	0.234	6.630	0.390	Yes
12	0.234	6.630	0.390	Yes
13	0.234	6.630	0.390	Yes
14	0.234	6.630	0.390	Yes
15	0.195	5.850	0.390	Yes
16	0.195	5.850	0.390	Yes
17	0.195	5.850	0.390	Yes
18	0.390	13.455	0.780	Yes
19	0.390	10.725	0.780	Yes

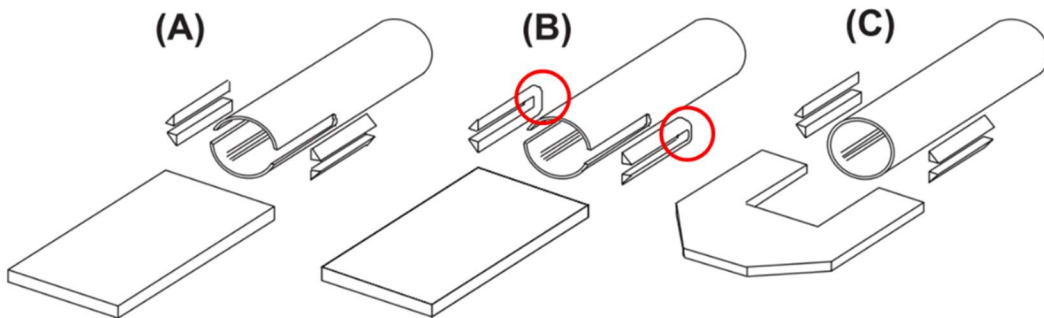


Figure 4.3: Detail of welds for HSS members from Willibald et al. (2006)

The modeling of the round HSS tension members is different from the majority of the other connection types in the study because the tension members are slotted. For most of the other connection types, specimens are modeled with a plate being considered a ‘member’ in IDEA StatiCa. However, the HSS required additional operations which did not allow this approach. Therefore, a rigid wide-flange member was created and the gusset plate was welded to this member and connected to the HSS on the other side as appropriate. An example for a typical round HSS is shown in Figure 4.4. The modeling of the specimens includes the following process:

1. Process outlined in Chapter 3.3
2. Create members:
 - a. Member 1: Rigid wide flange member
 - i. Geometrical Type set to “Continuous”
 - ii. Pitch of 90°
 - b. Member 2: Round HSS tension member
 - i. Geometrical Type set to “Ended”
 - ii. β set to 180°
3. Create Stiffening Plate operation
 - a. Select material based on specimen parameters
 - b. Select thickness based on specimen parameters
 - c. Input B1-width and B2-width based on specimen specific plate width
 - i. B1, B2 are equal to half the plate width
 - d. Input H1-height
 - i. Unless otherwise specific in the text, the distance between the column and the HSS was always taken as 3.937 in. (100 mm)
 - ii. H1 is calculated as (distance between the column and the HSS) + the weld length, l
 - e. Origin is set to member with the member being the rigid wide flange (member 1)
 - f. Plate set to “Top Flange 1”

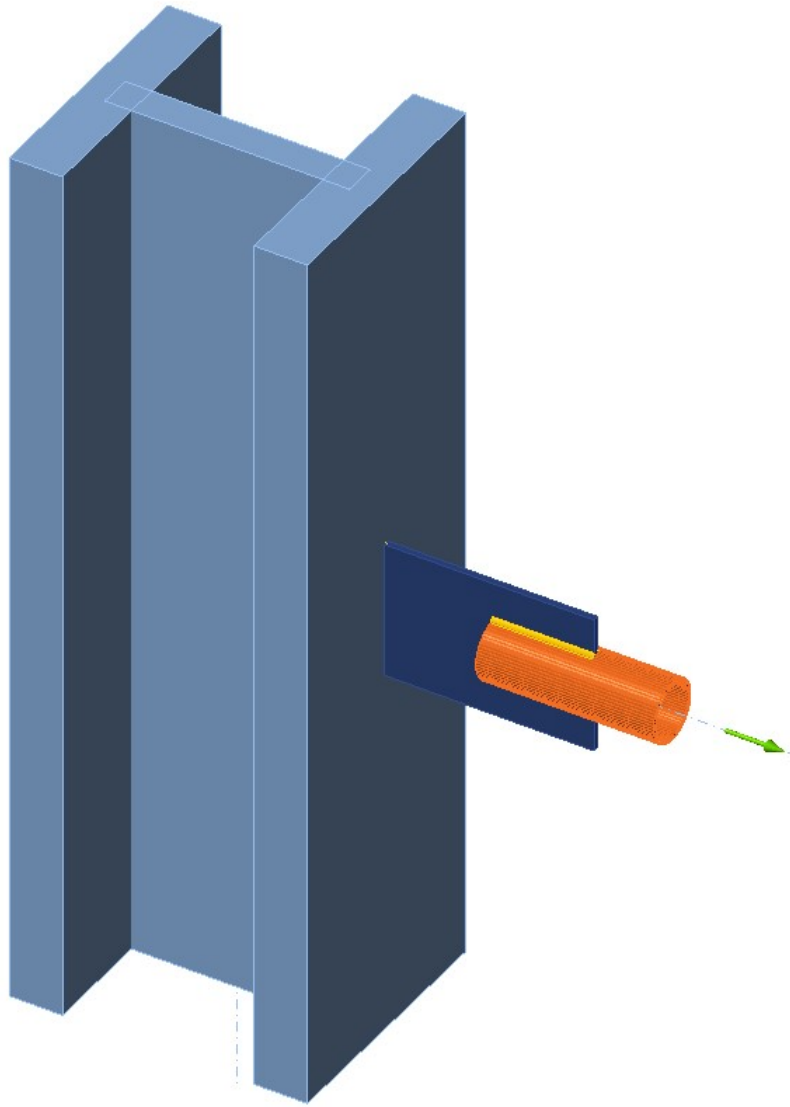


Figure 4.4: Typical Round HSS Model

- a. Type set to “Rib”
 - b. Location set to “Rear”
 - c. X-position set to 0 in. (0 mm)
 - d. Rotation set to 90°
 - e. Pitch set to 0.0°
 - f. Welds set to “Butt welds”
 - i. This weld is for connecting the plate to the rigid wide flange member
4. Create Gusset Plate operation
- a. Member is set to the HSS member
 - b. Connected to is set to “Existing plate”
 - c. Plate is set to the stiffening plate created in the previous step
 - d. Gap is set the distance between the column and the HSS member (assumed to be 3.937 in. (100 mm) if not given)
 - e. Alignment is set to “Center”
 - f. Aligned plate is set to “No plate”
 - g. Notched set to:
 - i. “None” for all specimens except for indices 3 and 4
 - ii. “Rectangle” for specimens with indices 3 and 4
 - h. Connection type is set to “Welded”
 - i. Welds are set to:
 - i. “No weld” for all specimens except for specimens with indices 3 and 4
 - ii. “Double Fillet Welds” with appropriate weld strength and size for Indices 3 and 4
5. Create Cut of Member operation (necessary for all specimens except for those with indices 3 and 4)
- a. Member is set to the HSS member
 - b. Cut by is set to the stiffening plate created in step 3

- c. Cutting method is set to “Surface- all around”
- d. Offset is set to 0
- e. Welds are set to “Fillet Weld- Front Side” with the appropriate weld size and strength for each specimen

4.2.2 Results

The results of the experimental set strength calculations per the AISC *Specification* (2016, 2022a) are provided in Table 4.4. The strengths are calculated based on both the 2016 and 2022 AISC *Specification* equations. For the 2016 code, one weld length is outside the bounds provided for the shear lag factor equations. In this case, the equation is not applicable and is denoted by “N/A”.

A summary of the strength results for the experimental set is provided in Table 4.5. Consistent with the majority of the experiments presented in this study, the failure mode was primarily reported as tensile rupture with some indicating tensile yield. The AISC strength, P_{AISC} , is reported as the minimum of tensile yield and tensile rupture in this table. The reported IDEA StatiCa strength, P_{IDEA} , is for the default mesh settings in the software and the default plastic strain limit (5%). The maximum permitted applied load for IDEA StatiCa, P_{IDEA} , produced generally conservative results for the experimental set compared to the AISC *Specification* strength equations and the experimental results. The most extreme case is found in experimental index specimen 3 with a 65% lower strength than the AISC *Specification* (2022a) equations. When compared to the experimental results, the largest difference was found in experimental index specimen 19 with a 67% difference from P_{IDEA} to P_{EXP} .

The results plotted with the corresponding experimental set index are provided in Figure 4.5. The strengths, P_{IDEA} , $P_{RUPTURE}$, and P_{EXP} , are normalized by the predicted tensile yield strength, $F_y A_g$. The AISC strengths in the plots only include the limit state of tensile rupture. This is to provide an equal comparison across all methods since the experimentalists typically allowed significant yielding before failure was considered. For round HSS tension members, these results suggests IDEA StatiCa provides conservative

Table 4.4: Round HSS AISC Calculation Results

Index	P _{YIELD} , kips	AISC 2016			AISC 2022		
		U	Controlling U Case	P _{RUPTURE} , kips	U	Controlling U Case	P _{RUPTURE} , kips
1	276.1	0.723	Case 5	216.6	0.909	Case 5	272.1
2	276.1	0.745	Case 5	222.9	0.929	Case 5	278.0
3	276.1	N/A	N/A	N/A	0.855	Case 5	256.1
4	276.1	0.728	Case 5	217.8	0.913	Case 5	273.3
5	42.2	1.000	Case 5	64.1	0.942	Case 5	60.4
6	54.5	1.000	Case 5	81.3	0.950	Case 5	77.2
7	57.5	0.744	Case 5	69.6	0.949	Case 5	88.8
8	80.5	1.000	Case 5	126.1	0.933	Case 5	117.6
9	106.2	1.000	Case 5	171.4	0.942	Case 5	161.5
10	148.0	0.749	Case 5	160.3	0.936	Case 5	200.2
11	164.0	1.000	Case 5	187.3	0.965	Case 5	180.7
12	164.0	1.000	Case 5	187.3	0.965	Case 5	180.7
13	164.0	1.000	Case 5	187.3	0.965	Case 5	180.7
14	164.0	1.000	Case 5	187.3	0.965	Case 5	180.7
15	114.4	1.000	Case 5	137.6	0.947	Case 5	130.4
16	114.4	1.000	Case 5	137.6	0.947	Case 5	130.4
17	114.4	1.000	Case 5	137.6	0.947	Case 5	130.4
18	381.3	1.000	Case 5	472.3	0.956	Case 5	451.4
19	381.3	0.746	Case 5	352.2	0.911	Case 5	430.2

Table 4.5: Round HSS Results Summary

Index	Experimental		AISC 2016		AISC 2022		IDEA StatiCa	
	P _{EXP} , kips	Failure Mode	P _{AISC} , kips	Controlling Limit State	P _{AISC} , kips	Controlling Limit State	P _{IDEA} , kips	Failure Mode
1	259.4	[2]	216.6	[2]	272.1	[2]	193.9	[3]
2	272.2	[2]	222.9	[2]	276.1	[1]	202.9	[3]
3	248.9	[2]	N/A	N/A	256.1	[2]	90.1	[3]
4	268.9	[2]	217.8	[2]	273.3	[2]	110.0	[3]
5	57.6	[2]	42.2	[1]	42.2	[1]	35.1	[3]
6	73.3	[2]	54.5	[1]	54.5	[1]	47.1	[3]
7	83.4	[2]	57.5	[1]	57.5	[1]	44.7	[3]
8	117.4	[2]	80.5	[1]	80.5	[1]	68.4	[3]
9	146.6	[2]	106.2	[1]	106.2	[1]	86.1	[3]
10	178.7	[2]	148.0	[1]	148.0	[1]	109.2	[3]
11	186.5	[2]	164.0	[1]	164.0	[1]	124.2	[3]
12	195.3	[1]	164.0	[1]	164.0	[1]	124.2	[3]
13	191.0	[1]	164.0	[1]	164.0	[1]	124.2	[3]
14	196.7	[1]	164.0	[1]	164.0	[1]	124.2	[3]
15	144.9	[1]	114.4	[1]	114.4	[1]	71.3	[3]
16	142.5	[1]	114.4	[1]	114.4	[1]	71.3	[3]
17	141.9	[1]	114.4	[1]	114.4	[1]	71.3	[3]
18	485.6	[1]	381.3	[1]	381.3	[1]	248.0	[3]
19	480.8	[2]	352.2	[2]	381.3	[1]	159.9	[3]

[1] tensile yield; [2] tensile rupture; [3] tension member plastic strain limit

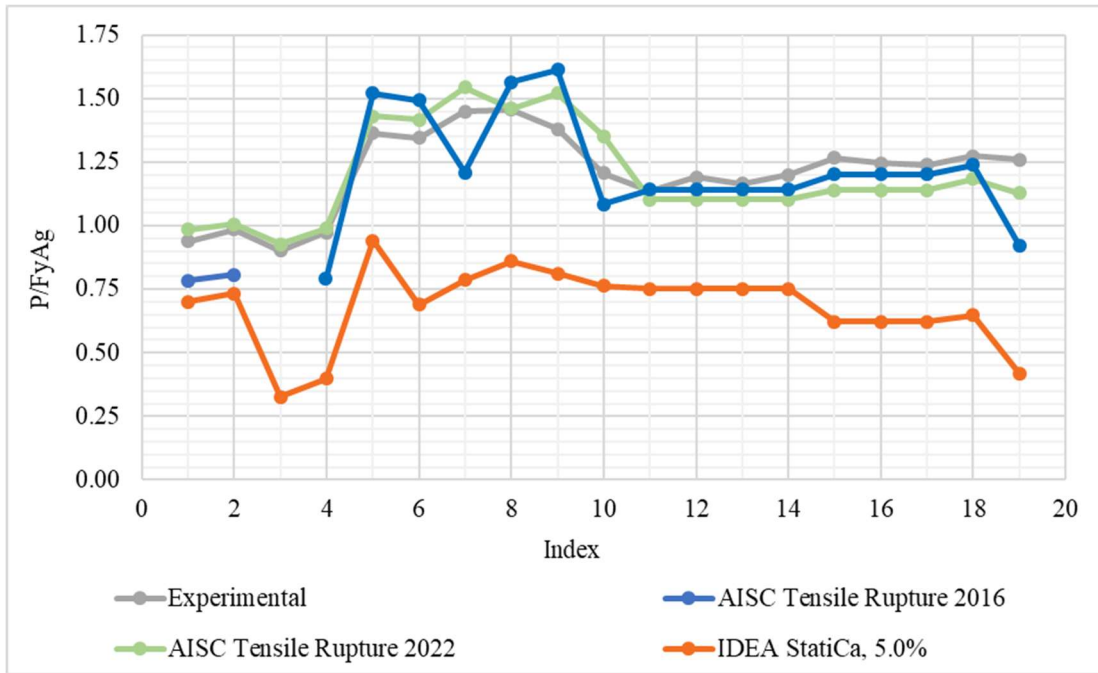


Figure 4.5: Round HSS results: strength ratio vs. index

strengths with respect to experimental tests and AISC *Specification* calculated strengths. Specimens with experimental set indices 3 and 4 show more conservative results than other specimens. An investigation into these specimens is provided later in this section. Despite the clearly conservative results in this plot, these results do not consider uncertainties in material properties, geometric properties, or in the analysis. A rigorous evaluation of reliability is presented in the next section.

IDEA StatiCa utilizes a bilinear stress-strain relationship for modeling connecting elements such as the tube and the plate. The hardening stiffness used is low ($1/1000^{\text{th}}$ of the elastic modulus) and is only intended to avoid numerical issues, not to represent the strain hardening behavior of the steel. Tensile rupture strength is related to the tensile strength, F_u , more than the yield stress, F_y , therefore, it is anticipated that the accuracy of IDEA StatiCa is related to the ratio of the two strengths, F_u/F_y . Figure 4.6 provides a scatterplot of the normalized strength plotted against the ratio of ultimate strength to yield strength. In addition to the scatter points, a trend line was added. For this particular set of specimens, as F_u/F_y increases, the ratio of $P_{\text{AISC}}/P_{\text{IDEA}}$ increases. This is shown better in Figure 4.7 where the strength ratio of IDEA StatiCa to the experimentally observed strength is plotted against the material ratio, F_u/F_y . The plot aims to show the relationship between the strength comparisons and the gap of F_u to F_y . The slope of trendline is basically zero in Figure 4.7 concluding there is not a relationship between these parameters for this particular set of specimens.

As previously mentioned, specimens with indices 3 and 4 suggested noticeably smaller strengths for IDEA StatiCa than the experimental and AISC calculated strengths in Figure 4.5. These two specimens, as indicated by Table 4.2, have notched plates. To investigate these specimens further, Figure 4.8 is provided. This figure contains a plot similar to that in Figure 4.5 except with varying plastic strain limits. A small change in strength between different plastic strain limits suggests a more severe stress concentration within the connection. Additionally, to better understand the impact of varying plastic strain limits, Figure 4.9 a plot with the ratio of IDEA StatiCa strength for varying plastic

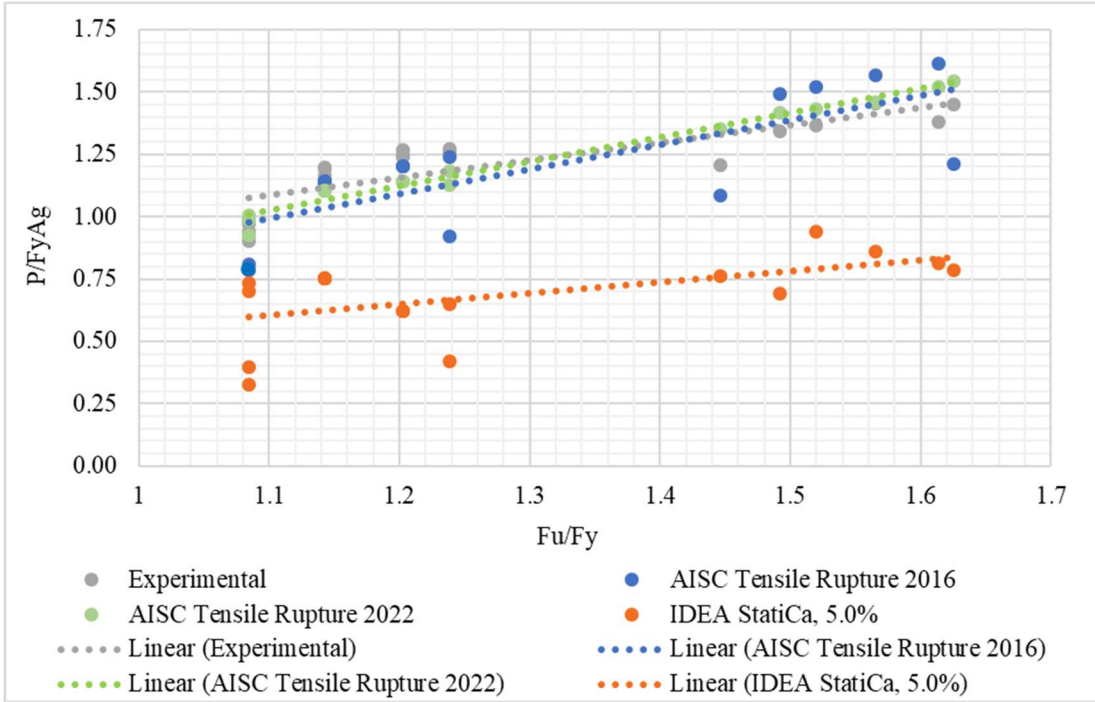


Figure 4.6: Round HSS results: normalized strength as a function of material ratio scatterplot

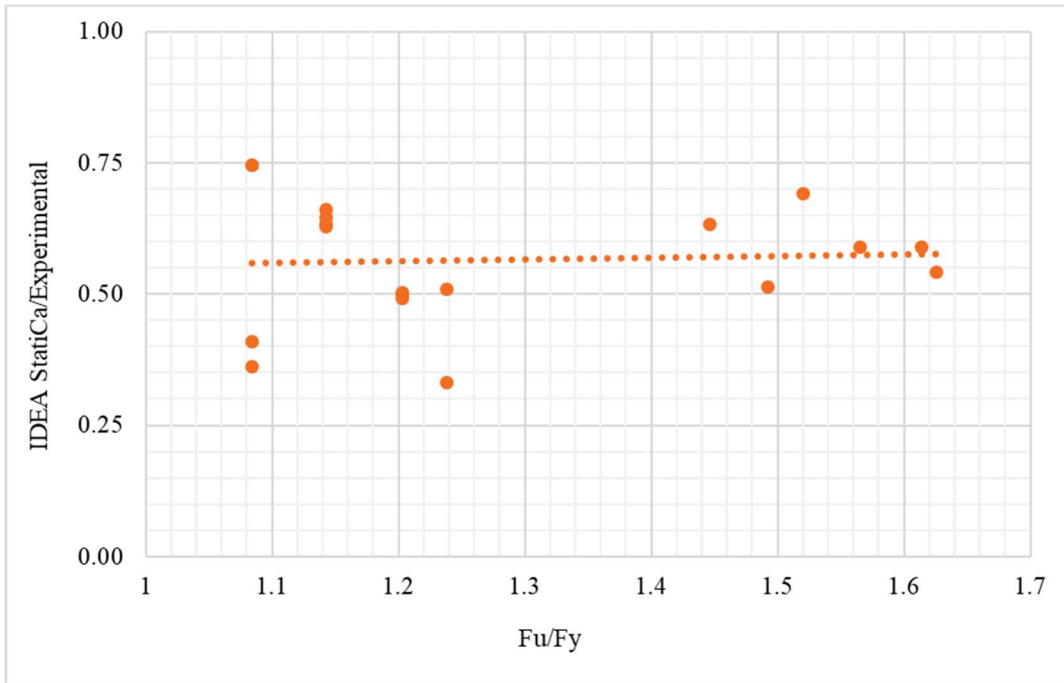


Figure 4.7: Round HSS results: IDEA StatiCa to experimental ratio as function of material ratio scatterplot

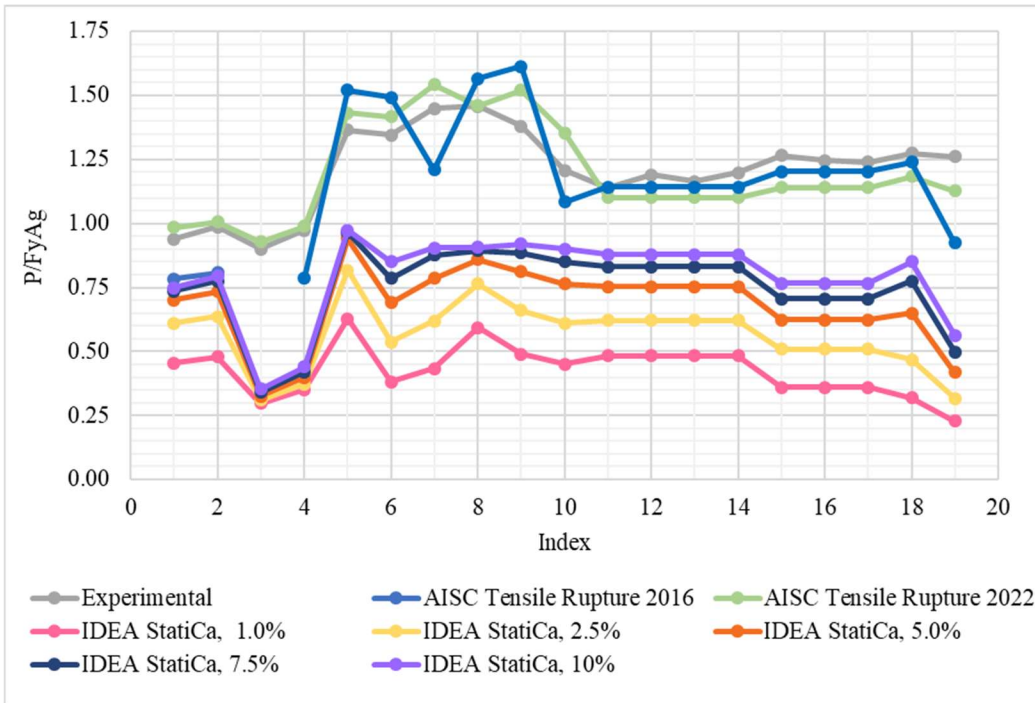


Figure 4.8: Round HSS results: strength ratio vs. index for varying plastic strain limits

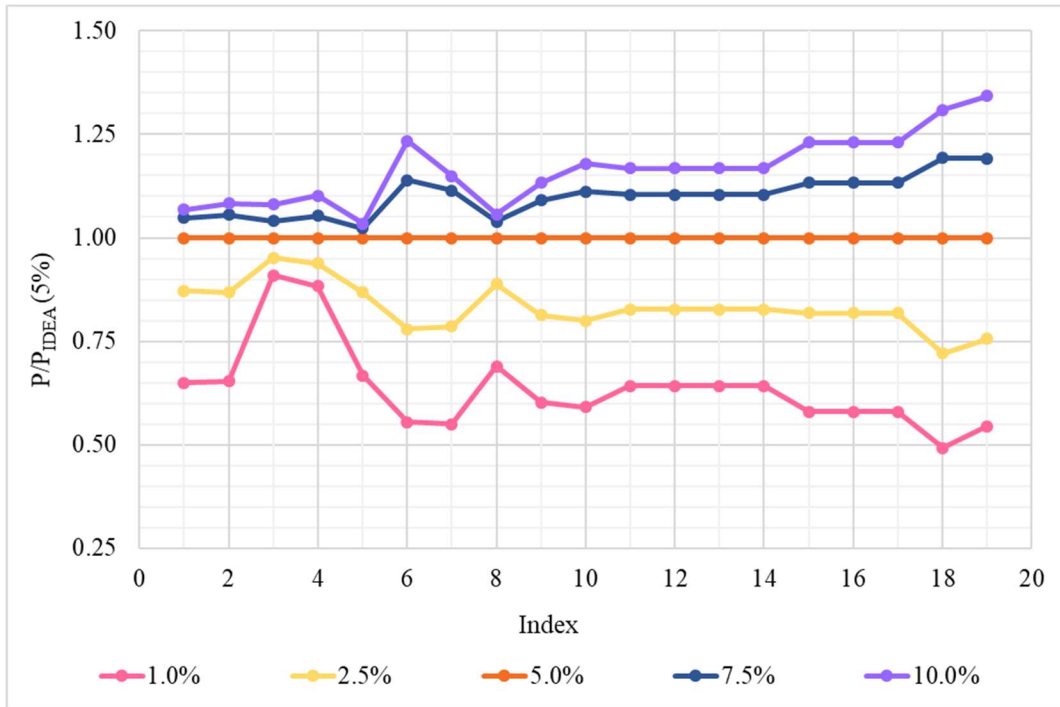


Figure 4.9: Round HSS results: ratio of strength to IDEA StatiCa strength with 5% plastic strain limit plotted with index

strain limits to the IDEA StatiCa strength for 5% plastic strain (default) plotted against the experimental set index. It is worth noting in the specimens with experimental indices 3 and 4, the change from one plastic strain limit to the next is considerably small when compared to the other specimens, potentially due to a more severe stress concentration for these specimens. A visual of the stress concentration from IDEA StatiCa is provided in Figure 4.10. The IDEA StatiCa strength results with respect to the varying plastic strain limits is as expected in general. More specifically, the strength decreases as the plastic strain limit decreases, and the strength increases as the plastic strain limit increases.

An investigation into mesh dependency was conducted as well. The mesh parameter set list is outlined in Table 3.1. All strengths presented in Figure 4.11 are with 5% plastic strain limit. The strengths for each parameter set is normalized by set 'B' to show how the strengths change with respect to the default mesh settings. These particular results are not as expected. Generally, for finite element analysis solutions, the results should follow a consistent pattern with the difference in results decreasing as the mesh is refined. However, this was not observed for this experimental set of specimens. Further investigation is required to determine why this pattern is not observed.

Table 4.6 presents the statistical results for each test-to-predicted ratio of this experimental set. All average ratios are greater than 1.0, implying the AISC strengths and IDEA StatiCa strengths, on average, did not result in strengths larger than those observed in the physical experiments. The results for the test-to-predicted ratio for AISC tensile rupture 2022 is directly used in the reliability analysis for the random variable \tilde{X}_R . The coefficient of variation of this ratio is used as well.

4.3 Reliability Analysis

4.3.1 Description of Reliability Set

As previously discussed, the reliability set is selected based on the desired varying parameters and not based upon experimental specimens found in literature. For the round HSS reliability set, the parameters outlined in Table 4.7 are based upon varying the

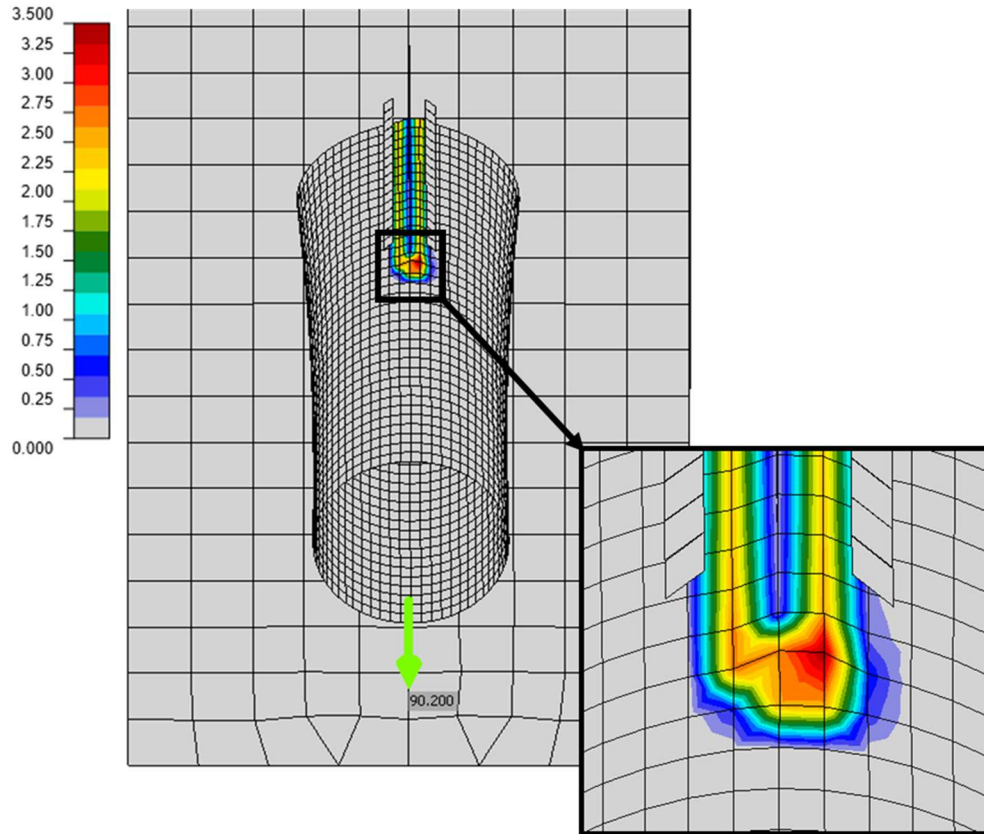


Figure 4.10: Round HSS experimental set index 3 plastic stress concentration, deformation scale: 10

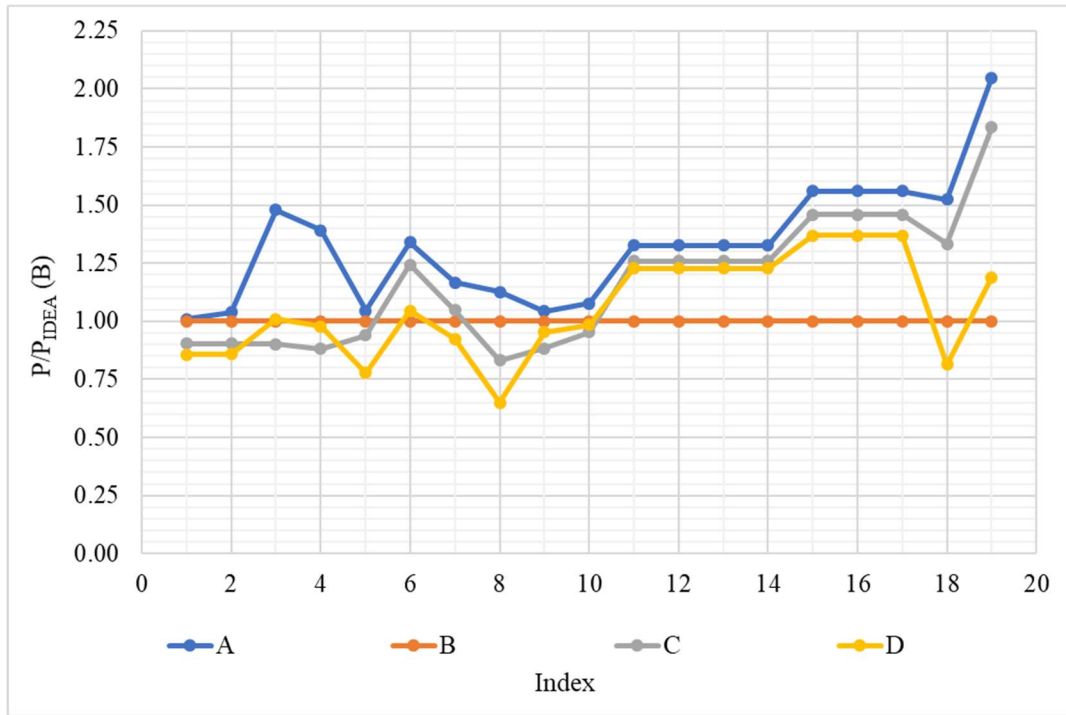


Figure 4.11: Round HSS results: ratio of varying mesh parameters sets to the default mesh settings plotted with index

Table 4.6: Statistical Results for Round HSS

Test-to-Predicted Ratio	Average	Standard Deviation	Coefficient of Variation
$P_{EXP}/P_{RUPTURE}$ (AISC 2016)	1.065	0.135	0.127
$P_{EXP}/P_{RUPTURE}$ (AISC 2022)	1.014	0.073	0.072
P_{EXP}/P_{IDEA}	1.86	0.458	0.246

Table 4.7: Round HSS Reliability Analysis Parameters

Index	Cross-Section Type	D , in.	t , in.	Weld Length, in.	Gusset Plate Thickness, in.	Material Grade	F_y , ksi	F_u , ksi
1	Pipe	6	0.864	6	0.5	A53 Gr. B	35	60
2	Pipe	6	0.432	6	0.5	A53 Gr. B	35	60
3	Pipe	6	0.280	6	0.5	A53 Gr. B	35	60
4	Pipe	6	0.864	12	0.5	A53 Gr. B	35	60
5	Pipe	6	0.432	12	0.5	A53 Gr. B	35	60
6	Pipe	6	0.280	12	0.5	A53 Gr. B	35	60
7	Pipe	6	0.864	6	1.0	A53 Gr. B	35	60
8	Pipe	6	0.432	6	1.0	A53 Gr. B	35	60
9	Pipe	6	0.280	6	1.0	A53 Gr. B	35	60
10	Pipe	6	0.864	12	1.0	A53 Gr. B	35	60
11	Pipe	6	0.432	12	1.0	A53 Gr. B	35	60
12	Pipe	6	0.280	12	1.0	A53 Gr. B	35	60
13	HSS	6	0.500	6	0.5	A500 Gr. C	50	62
14	HSS	6	0.250	6	0.5	A500 Gr. C	50	62
15	HSS	6	0.125	6	0.5	A500 Gr. C	50	62
16	HSS	6	0.500	12	0.5	A500 Gr. C	50	62
17	HSS	6	0.250	12	0.5	A500 Gr. C	50	62
18	HSS	6	0.125	12	0.5	A500 Gr. C	50	62
19	HSS	6	0.500	6	1.0	A500 Gr. C	50	62
20	HSS	6	0.250	6	1.0	A500 Gr. C	50	62
21	HSS	6	0.125	6	1.0	A500 Gr. C	50	62
22	HSS	6	0.500	12	1.0	A500 Gr. C	50	62
23	HSS	6	0.250	12	1.0	A500 Gr. C	50	62
24	HSS	6	0.125	12	1.0	A500 Gr. C	50	62

following parameters: diameter to thickness ratio, weld length to diameter ratio, gusset plate thickness, material grade, and cross-section thickness. It was desired to vary the F_u/F_y ratio; thus, material grades A53 Gr. B and A500 Gr. C were selected. In an effort to stay practical and consistent with current standards, the specimens with A53 Gr. B material were selected to be pipes, and the specimens with A500 Gr. C were selected to be HSS members. It should be noted specimens with specimen indices 1-12 have a different set of varying thicknesses than those with specimen indices 13-24 for the reasons just discussed.

The modeling of the round HSS reliability set was, in general, the same as the experimental set previously described. There were a few differences regarding geometric and material properties. The reliability set is based on nominal properties and modeled as such. As previously mentioned, the round HSS contains ‘Pipe’ and ‘HSS’ cross-section types. The round HSS members selected in IDEA StatiCa were from the ‘PIPE (AISC 15.0 – A53)’ category for the pipe cross-section type and ‘HSS (AISC 15.0 – A500, A502, A618, A847)’ category for the HSS cross-section. The IDEA StatiCa models included reduced design thicknesses. Additionally, the material grade A500 Gr. C has a few options in IDEA StatiCa. The material ‘A500, Gr. C, shaped’ was selected for the reliability set to match current ASTM standards (2018).

4.3.2 Results

The strength results for the reliability set of specimens is provided in Table 4.8. The nominal tensile yield and nominal tensile rupture strengths according to the AISC *Specification* (2022a) are provided, as well as the design strengths for each. The design strengths (including ϕ -factors) were used in the reliability analysis. Additionally, the maximum permitted applied loads from IDEA StatiCa are provided using all default settings (plastic strain limit of 5.0%, mesh parameter set ‘B’, and applicable resistance factors). These strengths were directly used in the reliability analysis for determining the nominal dead and live loads and ultimately the reliability index, β . For this particular reliability set, the maximum permitted applied load in IDEA StatiCa, P_{IDEA} , exceeded the

Table 4.8: Round HSS Reliability Strength Results

Index	AISC 2022				IDEA StatiCa
	P_{YIELD} , kips	$P_{RUPTURE}$, kips	ϕP_{YIELD} , kips	$\phi P_{RUPTURE}$, kips	P_{IDEA} , kips
1	514.5	685.6	463.1	514.2	273.1
2	274.1	366.5	246.6	274.9	151.1
3	182.0	243.7	163.8	182.8	99.8
4	514.5	816.0	463.1	612.0	461.7
5	274.1	436.2	246.6	327.1	248.1
6	182.0	290.0	163.8	217.5	162.2
7	514.5	678.3	463.1	508.8	295.8
8	274.1	364.0	246.6	273.0	157.3
9	182.0	242.4	163.8	181.8	104.4
10	514.5	772.9	463.1	579.7	438.9
11	274.1	414.7	246.6	311.0	236.0
12	182.0	276.2	163.8	207.2	156.6
13	404.5	388.8	364.1	291.6	229.1
14	211.0	203.3	189.9	152.5	117.0
15	107.0	103.2	96.3	77.4	58.7
16	404.5	462.7	364.1	347.0	358.6
17	211.0	241.9	189.9	181.5	186.9
18	107.0	122.8	96.3	92.1	84.9
19	404.5	383.4	364.1	287.6	233.5
20	211.0	201.0	189.9	150.8	122.1
21	107.0	102.2	96.3	76.6	61.3
22	404.5	436.9	364.1	327.6	339.1
23	211.0	229.0	189.9	171.8	176.2
24	107.0	116.4	96.3	87.3	72.8

design strength according to the AISC *Specification* equations only a few times by small margins. The most extreme case only resulted in a 3.5% larger strength of P_{IDEA} than ϕP_n , where ϕP_n is the minimum of ϕP_{YIELD} and $\phi P_{RUPTURE}$. The most conservative case was the specimen with reliability set specimen index 1 resulting in a P_{IDEA} 41% less than the corresponding AISC design strength. Overall, these results compare well with IDEA StatiCa being mostly on the conservative side.

Echoing the reliability strength results presented above, the results from the reliability analysis for the round HSS specimen set is presented in Figure 4.12. For specimens 1, 2, 3, 7, 8, 9, 13, 14, and 15, the reliability index for IDEA StatiCa was returned as a very large number, indicating no failures in 1,000,000 simulations. The minimum β for IDEA StatiCa was 3.50. The AISC *Specification* (2022a) equations resulted in a β range of 3.63 to 4.42. These results indicate that, for this particular set of specimens and parameters, IDEA StatiCa provides a comparable or sometimes higher level of reliability when compared to the AISC *Specification*.

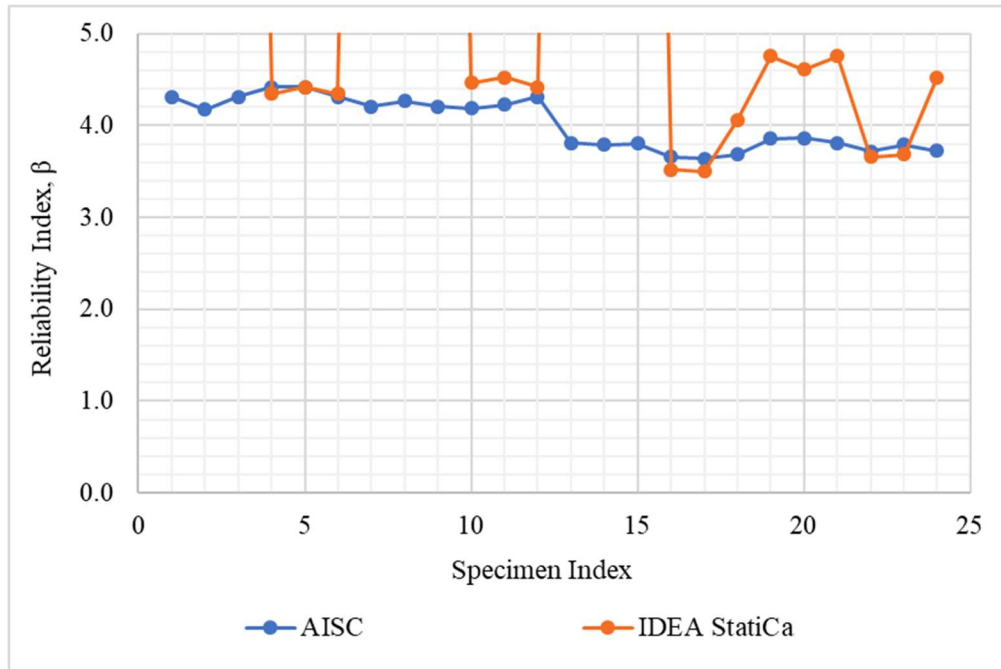


Figure 4.12: Round HSS: Reliability index for IDEA StatiCa and AISC 2022

CHAPTER 5

WELDED RECTANGULAR HSS

5.1 Description of Connection

Square and rectangular HSS members that are welded to a gusset plate are evaluated in this chapter. A typical schematic with relevant terminology is provided in Figure 5.1. The typical connection includes a slotted rectangular HSS member welded to a gusset plate. For simplicity, square HSS are referred to as rectangular HSS. The dimension ‘H’ is always parallel to the gusset plate with the dimension ‘B’ being perpendicular to the plate.

Similar to round HSS, the shear lag factor varies significantly from the AISC *Specification* 2016 edition to the 2022 edition, based on the work of Dowswell (2021) for the 2022 edition. Therefore, the AISC equation calculations are provided for both editions and labeled accordingly. The 2016 shear lag factor calculations include the use of Case 6 from Table D3.1 of the AISC *Specification* shown in Figure 3.3. There are two subcategories for Case 6: rectangular HSS with a single concentric gusset plate and rectangular HSS with two side gusset plates. All rectangular HSS specimens included in this study consist of only a single concentric gusset plate. The case with two side gusset plates was not evaluated in this work. The applicable equations are as follows:

$$l \geq H, \quad U = 1 - \frac{\bar{x}}{l} \quad (5-1)$$

$$\bar{x} = \frac{B^2 + 2BH}{4(B + H)} \quad (5-2)$$

where l is the length of the weld, \bar{x} is the eccentricity of the connection, and geometric dimensions B and H are consistent with Figure 5.1. Note that no equation for the shear lag factor is provided for when $l < H$.

As for the AISC *Specification* 2022 edition, the applicable case is number 5. This case contains two subcategories: round HSS and rectangular HSS. The equation for a

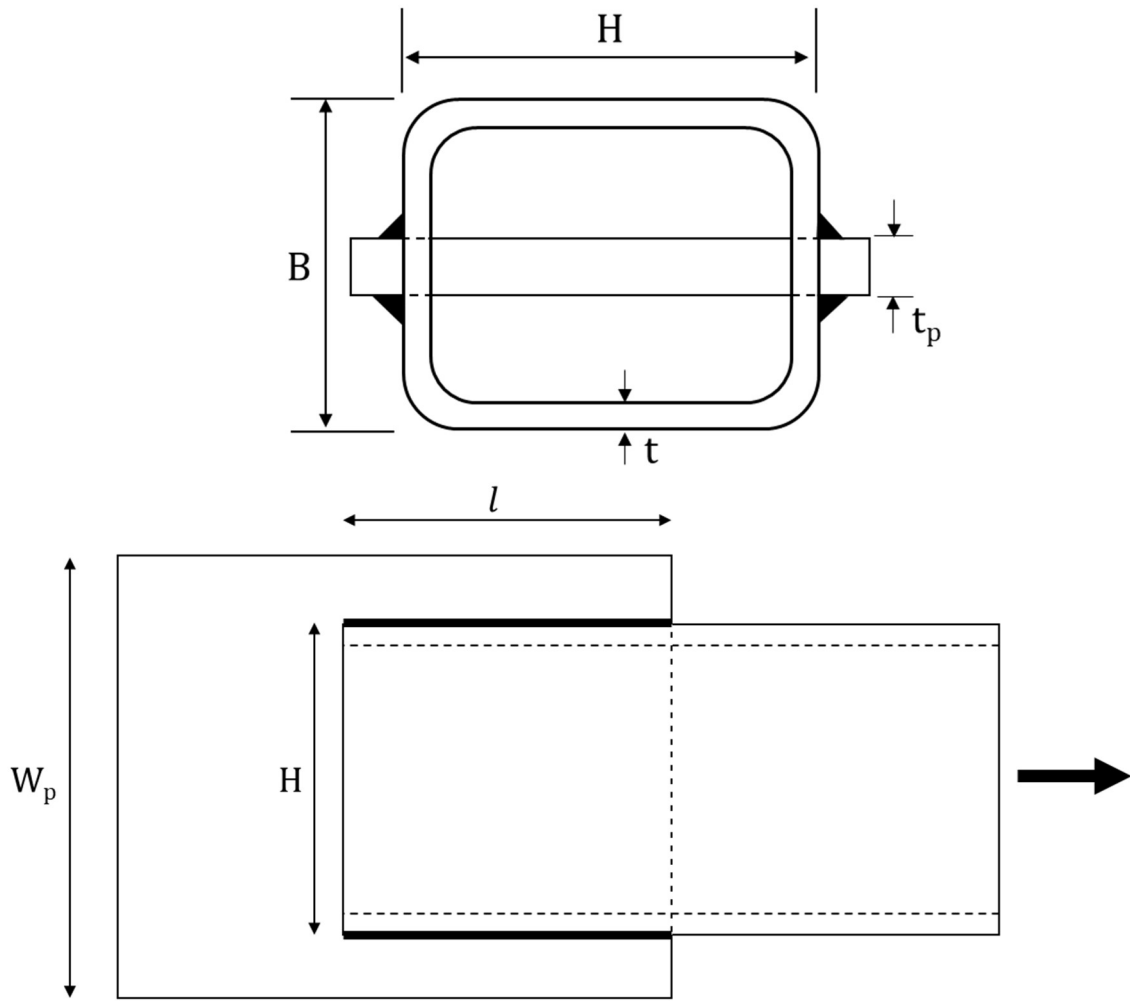


Figure 5.1: Welded Rectangular HSS Schematic

concentrically loaded rectangular HSS is as follows:

$$U = 1 - \frac{\bar{x}}{l} \quad (5-3)$$

$$\bar{x} = b - \frac{2b^2 + tH - 2t^2}{2H + 4b - 4t} \quad (5-4)$$

where l is the weld length, \bar{x} is the eccentricity of the connection, and geometric dimensions b , H , and t are defined in Figure 5.2. It should be noted, the 2016 edition of the code has a limit such that if l is less than H , the equation is not applicable. However, this limit does not exist for the 2022 edition.

Similar to the round HSS specimens, there are some connections with a weld return. The net area of specimens with a weld return was taken as the gross area. Whereas, the net area of specimens without the extra weld was taken as the gross area minus the removed area for the slot on both sides.

5.2 Comparison to Experimental Results

5.2.1 Description of Experimental Specimens

There were 46 total rectangular HSS specimens used for this study. The specimen count for each reference is provided in Table 5.1. It should be noted 20 specimens were removed across all three references. Zhao et al. (2008) reported 30 specimens, but specimen R3 was removed due to weld failure. Yeomans (1993) reported 18 rectangular HSS specimens, however 6 specimens failed in the gusset plate (S-SEP-1, R-SEP-1, R-SEP-2, R-SEP-4, R-SEP-11, R-SEP-12), one specimen experienced bolt failure in the test setup (R-SEP-6), and one test did not complete (R-SEP-7). All of these specimens from Yeomans (1993) were removed from the current study. Korol (1996) reported a total of 18 specimens, however specimens 4A, 4B, 5B, 6A, 6B, 7A, 7B, 8A, 8B, 9A, and 9B were removed due to the experimental failure mode being tearout.

A detailed description of each specimen is provided in Table 5.2. The specimens presented in Korol (1996) did not provide measured yield and ultimate strengths. However, it was reported CSA 350W steel was used. For this study, a yield strength of

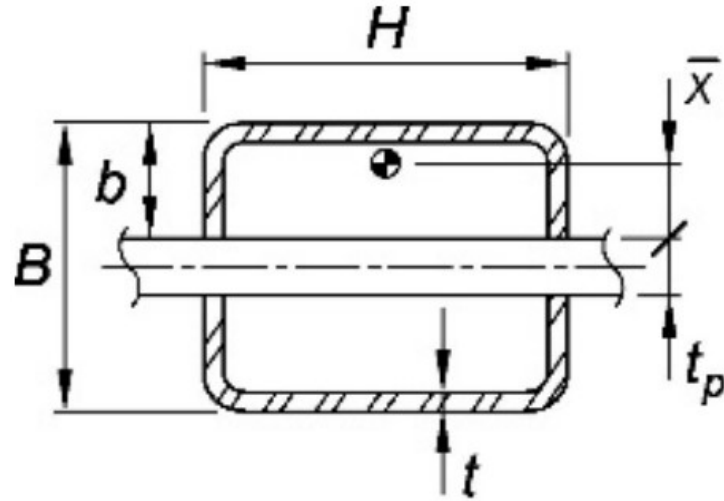


Figure 5.2: Figure from AISC *Specification* (2022) defining rectangular HSS parameters

Table 5.1: Rectangular HSS Specimen Enumeration

Reference	Specimen Count
Zhao et al. (2008)	29
Korol (1996)	7
Yeomans (1993)	10
Total	46

Table 5.2: Rectangular HSS Specimen Detail

Index	Reference	Specimen	* F_y , ksi	* F_u , ksi	* B , in.	* H , in.	* t , in.	Weld Size, in.	l , in.	Weld Return
1	Zhao (2008)	RL5G05P16	55.1	65.0	5.005	2.030	0.176	0.315	7.689	No
2	Zhao (2008)	RS5G05P16	55.1	65.0	2.024	5.014	0.176	0.315	7.677	No
3	Zhao (2008)	SM5G05P16	58.6	70.3	3.411	3.535	0.174	0.315	7.673	No
4	Zhao (2008)	SM5G05P16R	58.6	70.3	3.521	3.527	0.174	0.315	7.752	No
5	Zhao (2008)	RL4G05P16	55.1	65.0	5.011	2.032	0.176	0.315	6.122	No
6	Zhao (2008)	RS4G05P16	55.1	65.0	2.029	5.010	0.177	0.315	6.126	No
7	Zhao (2008)	SM4G05P16	58.6	70.3	3.520	3.533	0.173	0.315	6.146	No
8	Zhao (2008)	SM4G05P16R	58.6	70.3	3.527	3.522	0.174	0.315	6.185	No
9	Zhao (2008)	RL3G05P16	55.1	65.0	4.999	2.023	0.176	0.315	4.547	No
10	Zhao (2008)	RS3G05P16	55.1	65.0	2.022	5.009	0.178	0.315	4.626	No
11	Zhao (2008)	SM3G05P16	58.6	70.3	3.532	3.531	0.174	0.315	4.543	No
12	Zhao (2008)	SM3G05P16R	58.6	70.3	3.524	3.523	0.174	0.315	4.559	No
13	Zhao (2008)	SM3G05P12	58.6	70.3	3.519	3.524	0.174	0.315	4.697	No
14	Zhao (2008)	SM3G05P12R	58.6	70.3	3.523	3.525	0.174	0.315	4.638	No
15	Zhao (2008)	SM5G05P12	58.6	70.3	3.527	3.523	0.174	0.315	7.929	No
16	Zhao (2008)	SM5G05P12R	58.6	70.3	3.537	3.526	0.174	0.315	7.933	No
17	Zhao (2008)	SM3G05P20	58.6	70.3	3.497	3.502	0.174	0.315	4.500	No
18	Zhao (2008)	SM3G05P20R	58.6	70.3	3.519	3.548	0.175	0.315	4.480	No
19	Zhao (2008)	SM5G05P20	58.6	70.3	3.528	3.531	0.174	0.315	7.504	No
20	Zhao (2008)	SM5G05P20R	58.6	70.3	3.517	3.527	0.174	0.315	7.484	No
21	Zhao (2008)	SM3G25P16	58.6	70.3	3.519	3.528	0.174	0.315	4.618	No
22	Zhao (2008)	SM3G25P16R	58.6	70.3	3.516	3.537	0.174	0.315	4.598	No
23	Zhao (2008)	SM3G50P16	58.6	70.3	3.511	3.530	0.174	0.315	4.587	No
24	Zhao (2008)	SM3G50P16R	58.6	70.3	3.509	3.527	0.174	0.315	4.559	No
25	Zhao (2008)	SM5G50P16	58.6	70.3	3.516	3.531	0.174	0.315	7.717	No
26	Zhao (2008)	SM5G50P16R	58.6	70.3	3.515	3.532	0.173	0.315	7.689	No
27	Zhao (2008)	S4	53.7	63.8	3.517	3.491	0.174	0.433	6.272	Yes
28	Zhao (2008)	S4R	53.7	63.8	3.510	3.495	0.174	0.413	6.335	Yes
29	Zhao (2008)	S3	53.7	63.8	3.510	3.496	0.175	0.433	4.413	Yes
30	Korol (1996)	1A	NP	NP	1.969	4.921	0.252	0.315	6.299	No
31	Korol (1996)	1B	NP	NP	1.969	4.921	0.244	0.315	6.181	No
32	Korol (1996)	2A	NP	NP	3.465	3.465	0.242	0.315	6.181	No
33	Korol (1996)	2B	NP	NP	3.465	3.465	0.252	0.315	6.378	No
34	Korol (1996)	3A	NP	NP	4.961	1.969	0.242	0.315	6.142	No
35	Korol (1996)	3B	NP	NP	4.961	1.969	0.246	0.315	6.339	No

Table 5.2 continued

Index	Reference	Specimen	* F_y , ksi	* F_{ts} , ksi	* B , in.	* H , in.	* t , in.	Weld Size, in.	l , in.	Weld Return
35	Korol (1996)	3B	NP	NP	4.961	1.969	0.246	0.315	6.339	No
36	Korol (1996)	5A	NP	NP	3.504	3.504	0.236	0.315	3.858	No
37	Yeomans (1993)	S-SEP-2	54.1	66.7	1.969	1.969	0.134	NP	3.150	Yes
38	Yeomans (1993)	S-SEP-3	52.5	69.9	1.969	1.969	0.244	NP	2.953	Yes
39	Yeomans (1993)	S-SEP-4	44.7	63.7	3.543	3.543	0.146	NP	5.906	Yes
40	Yeomans (1993)	S-SEP-5	59.0	72.8	3.543	3.543	0.205	NP	5.906	Yes
41	Yeomans (1993)	S-SEP-6	51.1	74.0	3.543	3.543	0.241	NP	5.709	Yes
42	Yeomans (1993)	R-SEP-3	54.8	67.3	2.362	1.575	0.262	NP	2.953	Yes
43	Yeomans (1993)	R-SEP-5	63.2	76.9	1.575	2.362	0.160	NP	3.150	Yes
44	Yeomans (1993)	R-SEP-8	61.1	77.4	4.724	2.362	0.215	NP	5.709	Yes
45	Yeomans (1993)	R-SEP-9	54.1	70.8	4.724	2.362	0.253	NP	5.709	Yes
46	Yeomans (1993)	R-SEP-10	52.2	65.8	2.362	4.724	0.140	NP	5.906	Yes

* indicates measured value; NP: not provided

$F_y = 50$ ksi and ultimate strength of $F_u = 65$ ksi was used. Zhao et al. (2008) reported the use of ASTM A500 Gr. C material, and the measured material properties were reported. Yeomans (1993) did not report the material used, but reported measured material strengths. Additionally, Yeomans did not report a weld size, but it was noted the welds were designed not to fail. For the rectangular HSS study, butt welds were used in IDEA StatiCa for Yeomans specimens to eliminate the impacts of weld size (butt welds are not modeled in IDEA StatiCa, rather the connecting elements are tied to each other directly). Zhao et al. (2008) reported the use of E480XX (metric) weld strength. E70XX was determined to be the English equivalent and thus, used in the analyses. The remaining two studies did not indicate a specific weld strength, therefore E70XX was used. Consistent with the previous chapter and Figure 4.3, the ‘Weld Return’ column is the indication of a weld across the thickness of the gusset plate. The gross area of the rectangular HSS specimens was calculated based on measured geometric properties. Additionally, the inner radius of the specimens was taken as the thickness, unless otherwise reported.

In general, the modeling of the rectangular HSS tension members was identical to the modeling of the round HSS. As mentioned in the previous chapter, a rigid wide-flange member was created for this analysis and the gusset plate was welded to this member and connected to the HSS on the other side of the gusset plate as appropriate. An example for a typical rectangular HSS model is shown in Figure 5.3. The modeling of the specimens includes the following process:

1. Process outlined in Chapter 3.3
 - a. Create members:
 - i. Member 1: Rigid wide flange member
 - ii. Geometrical Type set to “Continuous”
 - iii. Pitch of 90°
 - b. Member 2: Round HSS tension member
 - i. Geometrical Type set to “Ended”
 - ii. β set to 180°

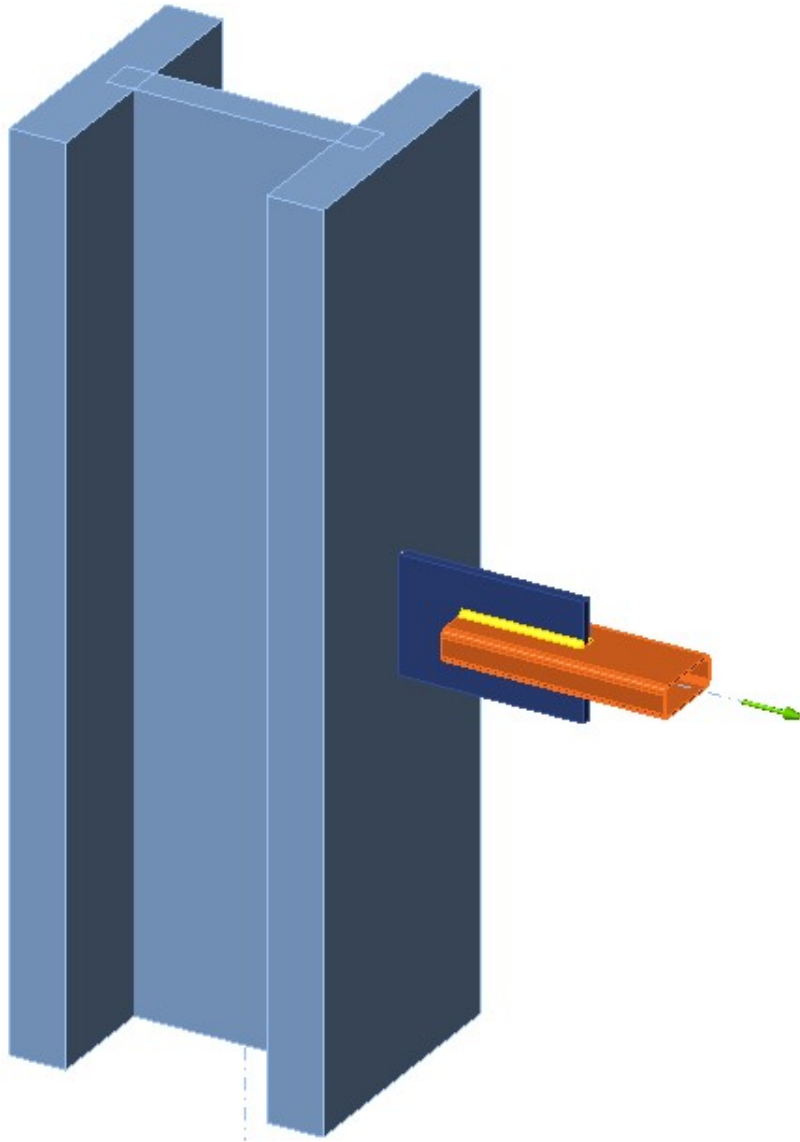


Figure 5.3: Typical Rectangular HSS Model

2. Create Stiffening Plate operation
 - a. Select material based on specimen parameters
 - b. Select thickness based on specimen parameters
 - c. Input B1-width and B2-width based on specimen specific plate width
 - i. B1, B2 are equal to half the plate width
 - d. Input H1-height
 - i. Unless otherwise specific in the text, the distance between the column and the HSS was always taken as 3.937” (100 mm). Note: Korol (1996) indicated a gap of 2.756” (70 mm) between test setup (bolts) and HSS member. Therefore, 2.756” was used as the gap for all Korol (1996) specimens.
 - ii. H1 is calculated as (distance between the column and the HSS) + the weld length, l
 - e. Origin is set to member with the member being the rigid wide flange (member 1)
 - f. Plate set to “Top Flange 1”
 - g. Type set to “Rib”
 - h. Location set to “Rear”
 - i. X-position set to 0.0 in. (0 mm)
 - j. Rotation set to 90°
 - k. Pitch set to 0.0°
 - l. Welds set to “Butt welds”
 - i. This weld is for connecting the plate to the rigid wide flange member
3. Create Gusset Plate operation
 - m. Member is set to the HSS member
 - n. Connected to is set to “Existing plate”
 - o. Plate is set to the stiffening plate created in the previous step

- p. Gap is set the distance between the column and the HSS member (assumed to be 3.937 in. (100 mm) if not given)
 - q. Alignment is set to “Center”
 - r. Aligned plate is set to “No plate”
 - s. Notched set to: “None”
 - t. Connection type is set to “Welded”
 - u. Welds are set to: “No weld”
4. Create Cut of Member operation
- v. Member is set to the HSS member
 - w. Cut by is set to the stiffening plate created in step 3
 - x. Cutting method is set to “Surface- all around”
 - y. Offset is set to 0
 - z. Welds are set to “Fillet Weld- Front Side” with the appropriate weld size and strength for each specimen

5.2.2 Results

The results of the strengths for the rectangular HSS experimental set of specimens according to the AISC *Specification* (2016, 2022a) equations are provided in Table 5.3. The strengths are calculated based on both the 2016 and 2022 editions of the AISC *Specification*. For the 2016 edition equations, specimen with experimental set index 10 is outside of the weld length bounds and is denoted by ‘N/A’.

A summary of the strength results for the experimental set is presented in Table 5.4. Three specimens were reported as failing in tensile yield in the experiments, with the remainder failing in tensile rupture. The AISC *Specification* (2016, 2022a) strengths are presented here as P_{AISC} indicating this is the smaller of the tensile rupture strength and tensile yield strength. The IDEA StatiCa strengths reported are from the mesh parameter group ‘B’ and plastic strain limit of 5%. The failure mode for the IDEA StatiCa strengths did sometimes indicate weld failures, however the specimen was always loaded until

Table 5.3: Rectangular HSS AISC Calculation Results

Index	P_{YIELD} , kips	AISC 2016			AISC 2022		
		U	Controlling U Case	$P_{RUPTURE}$, kips	U	Controlling U Case	$P_{RUPTURE}$, kips
1	129.6	0.790	Case 6	108.5	0.823	Case 5	113.1
2	129.4	0.887	Case 6	120.4	0.934	Case 5	126.8
3	134.8	0.832	Case 6	120.4	0.870	Case 5	125.9
4	136.6	0.830	Case 6	122.1	0.866	Case 5	127.5
5	129.8	0.736	Case 6	101.6	0.777	Case 5	107.2
6	130.3	0.858	Case 6	118.0	0.915	Case 5	125.8
7	135.9	0.785	Case 6	115.1	0.831	Case 5	121.8
8	136.4	0.786	Case 6	114.5	0.835	Case 5	121.6
9	129.1	0.646	Case 6	88.4	0.701	Case 5	96.0
10	130.7	N/A	N/A	N/A	0.889	Case 5	122.3
11	136.6	0.708	Case 6	104.3	0.771	Case 5	113.5
12	136.6	0.710	Case 6	104.7	0.772	Case 5	113.8
13	136.5	0.719	Case 6	108.3	0.770	Case 5	115.9
14	136.6	0.715	Case 6	107.9	0.766	Case 5	115.5
15	137.0	0.833	Case 6	125.4	0.864	Case 5	130.0
16	136.7	0.833	Case 6	125.4	0.863	Case 5	130.0
17	135.6	0.709	Case 6	101.2	0.781	Case 5	111.6
18	137.9	0.705	Case 6	102.6	0.778	Case 5	113.2
19	136.9	0.824	Case 6	118.6	0.868	Case 5	124.9
20	136.9	0.824	Case 6	118.8	0.867	Case 5	125.1
21	136.6	0.714	Case 6	105.1	0.776	Case 5	114.2
22	136.7	0.713	Case 6	105.2	0.774	Case 5	114.2
23	136.5	0.713	Case 6	105.9	0.770	Case 5	114.4
24	136.7	0.711	Case 6	105.3	0.771	Case 5	114.2
25	136.3	0.829	Case 6	121.6	0.866	Case 5	127.1
26	136.0	0.828	Case 6	121.8	0.865	Case 5	127.1
27	124.4	0.790	Case 6	116.8	0.833	Case 5	123.2
28	124.6	0.792	Case 6	117.4	0.835	Case 5	123.8
29	124.9	0.702	Case 6	104.3	0.764	Case 5	113.4
30	160.9	0.866	Case 6	162.2	0.924	Case 5	173.0
31	156.3	0.863	Case 6	157.1	0.922	Case 5	167.7
32	156.1	0.790	Case 6	143.6	0.839	Case 5	152.5
33	161.9	0.796	Case 6	150.2	0.844	Case 5	159.2
34	156.1	0.741	Case 6	134.7	0.785	Case 5	142.8
35	158.4	0.749	Case 6	138.2	0.792	Case 5	146.2

Table 5.3 continued

Index	P_{YIELD} , kips	AISC 2016			AISC 2022		
		U	Controlling U Case	$P_{RUPTURE}$, kips	U	Controlling U Case	$P_{RUPTURE}$, kips
36	154.4	0.659	Case 6	118.8	0.737	Case 5	132.8
37	53.1	0.766	Case 6	50.2	0.843	Case 5	55.3
38	88.4	0.750	Case 6	88.3	0.867	Case 5	102.1
39	88.4	0.775	Case 6	97.7	0.827	Case 5	104.2
40	161.4	0.775	Case 6	154.3	0.842	Case 5	167.7
41	162.7	0.767	Case 6	180.9	0.849	Case 5	200.1
42	98.0	0.720	Case 6	86.6	0.831	Case 5	100.0
43	73.1	0.800	Case 6	71.1	0.888	Case 5	78.9
44	174.4	0.724	Case 6	160.2	0.795	Case 5	176.0
45	180.0	0.724	Case 6	170.5	0.819	Case 5	192.9
46	99.3	0.833	Case 6	104.4	0.881	Case 5	110.3

Table 5.4: Rectangular HSS Results Summary

Index	Experimental		AISC 2016		AISC 2022		IDEA StatiCa	
	P_{EXP} , kips	Failure Mode	P_{AISC} , kips	Controlling Limit State	P_{AISC} , kips	Controlling Limit State	P_{IDEA} , kips	Failure Mode
1	151.7	[2]	108.5	[2]	113.1	[2]	120.9	[3]
2	151.5	[2]	120.4	[2]	126.8	[2]	122.6	[3]
3	152.9	[2]	120.4	[2]	125.9	[2]	124.8	[3]
4	151.3	[2]	122.1	[2]	127.5	[2]	126.2	[3]
5	152.2	[2]	101.6	[2]	107.2	[2]	120.3	[3]
6	146.8	[2]	118.0	[2]	125.8	[2]	122.8	[3]
7	152.4	[2]	115.1	[2]	121.8	[2]	125.4	[3]
8	151.5	[2]	114.5	[2]	121.6	[2]	126.7	[3]
9	138.5	[2]	88.4	[2]	96.0	[2]	100.3	[3]
10	144.3	[2]	N/A	N/A	122.3	[2]	103.4	[3]
11	146.4	[2]	104.3	[2]	113.5	[2]	103.8	[3]
12	146.8	[2]	104.7	[2]	113.8	[2]	104.5	[3]
13	152.0	[2]	108.3	[2]	115.9	[2]	108.9	[3]
14	150.4	[2]	107.9	[2]	115.5	[2]	106.4	[3]
15	156.5	[2]	125.4	[2]	130.0	[2]	130.0	[3]
16	155.3	[2]	125.4	[2]	130.0	[2]	129.8	[3]
17	139.6	[2]	101.2	[2]	111.6	[2]	104.7	[3]
18	142.8	[2]	102.6	[2]	113.2	[2]	105.2	[3]
19	149.9	[2]	118.6	[2]	124.9	[2]	124.4	[3]
20	151.5	[2]	118.8	[2]	125.1	[2]	124.3	[3]
21	149.3	[2]	105.1	[2]	114.2	[2]	106.9	[3]
22	150.2	[2]	105.2	[2]	114.2	[2]	105.0	[3]
23	149.7	[2]	105.9	[2]	114.4	[2]	105.0	[3]
24	146.1	[2]	105.3	[2]	114.2	[2]	104.7	[3]
25	150.6	[2]	121.6	[2]	127.1	[2]	126.2	[3]
26	150.6	[2]	121.8	[2]	127.1	[2]	125.9	[3]
27	150.2	[1]	116.8	[2]	123.2	[2]	116.8	[3]
28	148.4	[1]	117.4	[2]	123.8	[2]	116.8	[3]
29	149.9	[1]	104.3	[2]	113.4	[2]	95.9	[3]
30	182.3	[2]	160.9	[1]	160.9	[1]	151.8	[3]
31	188.0	[2]	156.3	[1]	156.3	[1]	146.7	[3]
32	149.3	[2]	143.6	[2]	152.5	[2]	148.6	[3]
33	163.0	[2]	150.2	[2]	159.2	[2]	153.6	[3]

Table 5.4 continued

Index	Experimental		AISC 2016		AISC 2022		IDEA StatiCa	
	P_{EXP} , kips	Failure Mode	P_{AISC} , kips	Controlling Limit State	P_{AISC} , kips	Controlling Limit State	P_{IDEA} , kips	Failure Mode
34	190.0	[2]	134.7	[2]	142.8	[2]	149.4	[3]
35	192.0	[2]	138.2	[2]	146.2	[2]	151.3	[3]
36	137.6	[2]	118.8	[2]	132.8	[2]	105.6	[3]
37	61.6	[2]	50.2	[2]	53.1	[1]	50.6	[3]
38	113.5	[2]	88.3	[2]	88.4	[1]	77.8	[3]
39	107.5	[2]	88.4	[1]	88.4	[1]	85.3	[3]
40	187.3	[2]	154.3	[2]	161.4	[1]	151.2	[3]
41	213.4	[2]	162.7	[1]	162.7	[1]	145.5	[3]
42	106.8	[2]	86.6	[2]	98.0	[1]	86.4	[3]
43	86.3	[2]	71.1	[2]	73.1	[1]	70.4	[3]
44	159.8	[2]	160.2	[2]	174.4	[1]	156.7	[3]
45	205.3	[2]	170.5	[2]	180.0	[1]	148.8	[3]
46	125.9	[2]	99.3	[1]	99.3	[1]	96.8	[3]

[1] tensile yield; [2] tensile rupture; [3] member strain

the plastic strain limit was reached. To be clear, the model was loaded until a plastic strain limit of $\sim 5.0\%$ was reached, regardless of weld utilization. Since the welds did not fail in the experiments the weld utilization was ignored. There are a few instances where P_{IDEA} exceeds the controlling strength according to the 2022 AISC *Specification* strength results. The maximum difference appears with experimental index specimen 5, with a 12% difference. As for the most conservative case, P_{IDEA} provides a strength $\sim 20\%$ less than P_{AISC} in experimental specimen index 36. There did not exist any specimens in the rectangular HSS experimental set where P_{IDEA} exceeded the experimental strength, P_{EXP} . However, the largest difference occurred in the specimen with experimental set index 29. This specimen indicated roughly a 36% difference from IDEA StatiCa's strength to the experimentally observed strength. Typically IDEA StatiCa provided conservatism between 20-22% when compared to the experimental results.

The strength results for the rectangular HSS experimental set plotted with the experimental set index is provided in Figure 5.4. The strengths, P , are normalized by the predicted tensile yield strength, $F_y A_g$. Additionally, the AISC strengths only include the limit state of tensile rupture. IDEA StatiCa compares well with both editions of the AISC *Specification* (2016, 2022a). There are some instances where IDEA StatiCa suggests a stronger connection compared to the AISC equations as previously mentioned and expressed further in the figure.

The tensile rupture limit state is related to the ultimate tensile strength, F_u . IDEA StatiCa does not utilize F_u in these analyses, it primarily takes advantage of F_y . The plots provided in Figure 5.5 show the impact of the material ratio, F_u/F_y , on the strength trends. All normalized strengths trend in a positive direction. However, strengths corresponding to the smaller F_u/F_y (from around 1.18 to 1.22) provide interesting insight. The IDEA StatiCa normalized strength trend line is on par with the AISC 2022 equation results and resulted in a larger strength trend than the AISC 2016 trendline for F_u/F_y equal to ~ 1.18 . As F_u/F_y increases, both AISC strengths trend to larger values of $P/F_y A_g$ than the IDEA

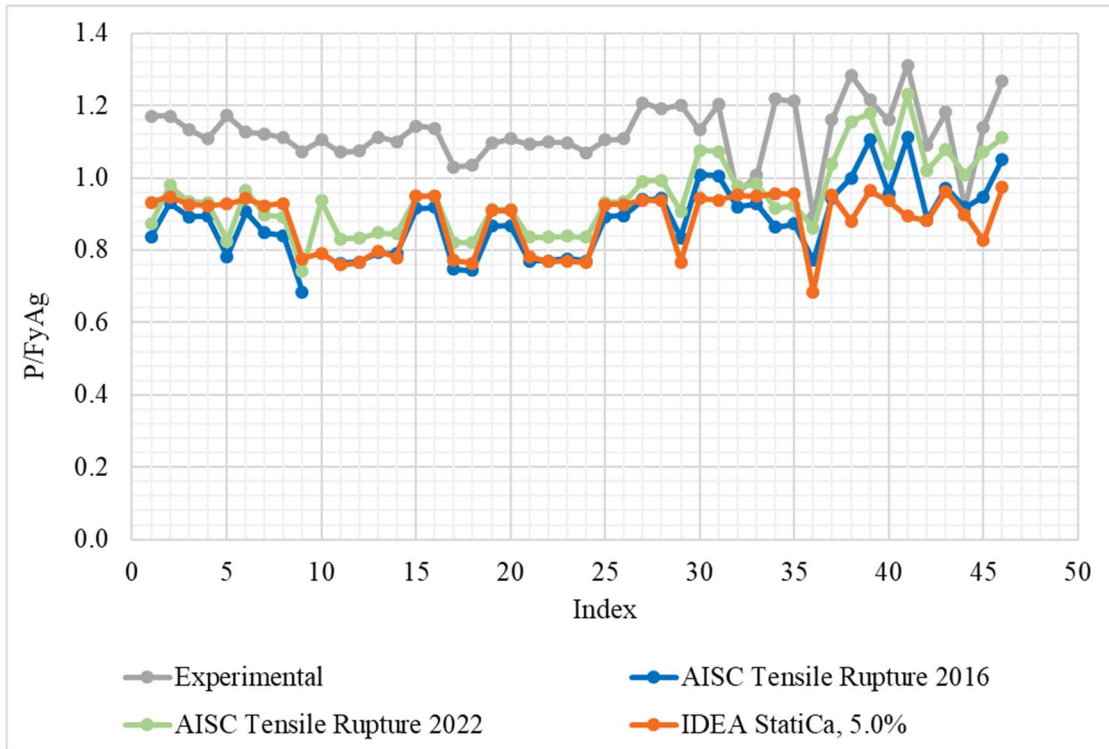


Figure 5.4: Rectangular HSS results: strength ratio vs. index

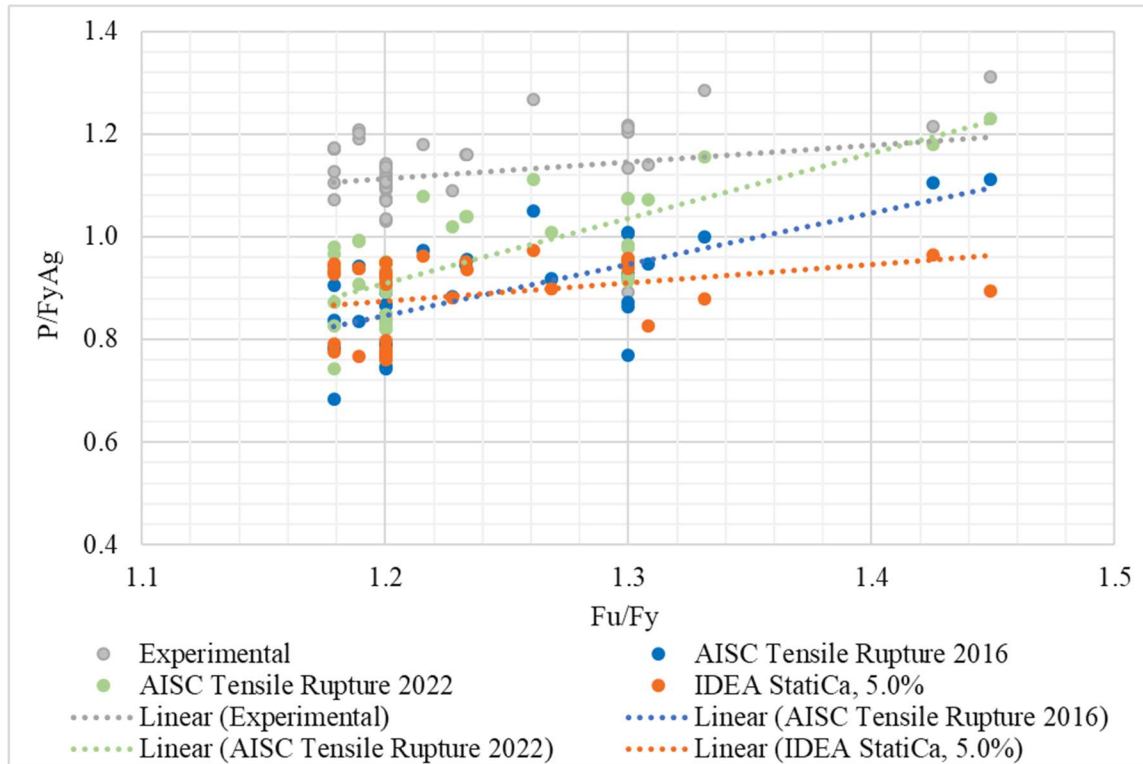


Figure 5.5: Rectangular HSS: normalized strength as a function of material ratio scatterplot

StatiCa results. This is relatively less apparent when comparing the maximum applied load according to IDEA StatiCa, P_{IDEA} , to the strength observed in experiments, P_{EXP} . Figure 5.6 provides the ratio of P_{IDEA} to P_{EXP} plotted with the material ratio, F_u/F_y . The overall trend for this plot is positive, however it does not show a significant relationship.

The IDEA StatiCa strength results are also investigated for varying plastic strain limits. The results of this analysis are provided in Figure 5.7 and Figure 5.8. Some lines in Figure 5.7 overlap with other plastic strain limits since there is little change, however the strengths are visible in Figure 5.8. The latter figure provides the varying plastic strain limit as a ratio with respect to the strength of the 5% plastic strain limit analysis. Overall, the results are as expected such that the larger plastic strain limits indicate larger strengths, and vice versa. The 1.0% plastic strain limit was much more sensitive than the other limits.

As previously mentioned, a mesh study was also conducted. The mesh study for this connection proved to be relatively as expected. Figure 5.9 provides the results of each mesh parameter set (defined in Table 3.1). The strengths for each mesh set is normalized by the strength using the default mesh set (mesh set 'B') and plotted with the experimental set index. Each strength is presented with a plastic strain limit of 5%. It was expected the increments between 'C' and 'D' would be less than the increments between 'B' and 'C', however this was not observed.

Table 5.5 provides test-to-predicted statistics for the rectangular HSS experimental set. The $P_{EXP}/P_{RUPTURE}$ (AISC 2022a) mean and coefficient of variation were directly used in the reliability simulations for the random variable \tilde{X}_R . It is worth noting, the average test-to-predicted ratios for the AISC *Specification* (AISC 2016) equations according to the 2016 edition is very close to that of IDEA StatiCa. Additionally, the newer specification equations provide an average test-to-predicted ratio closer to one, implying the equations are predicting the behavior of the rectangular HSS tension members relatively better than the previous code equations.

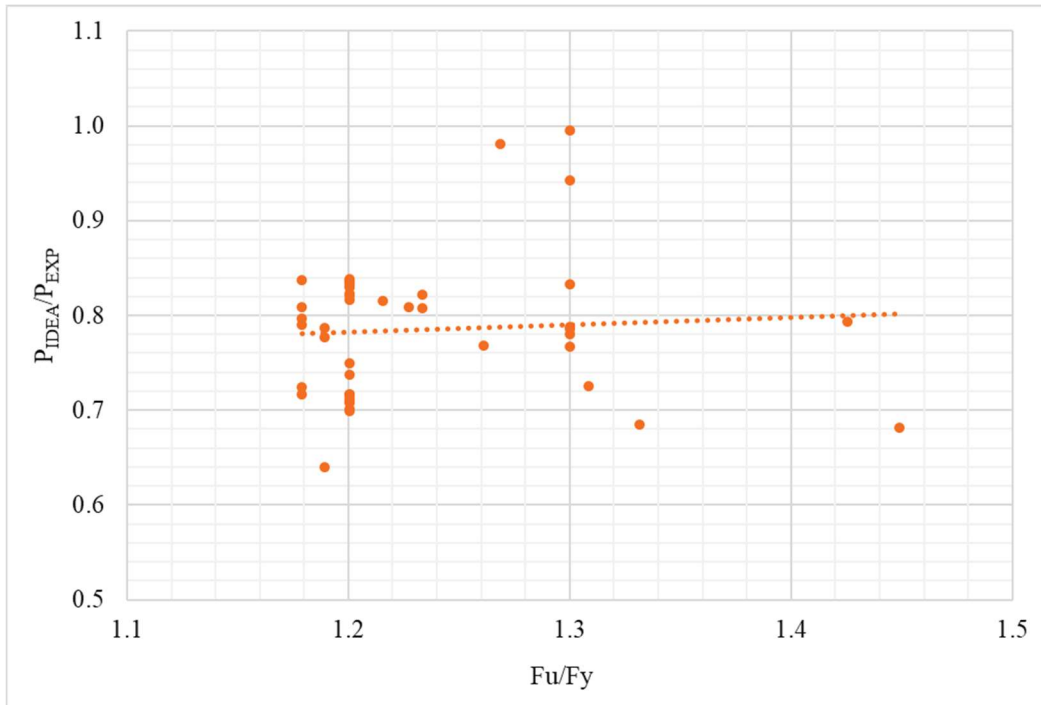


Figure 5.6: Rectangular HSS: IDEA StatiCa to experimental ratio as function of material ratio scatterplot

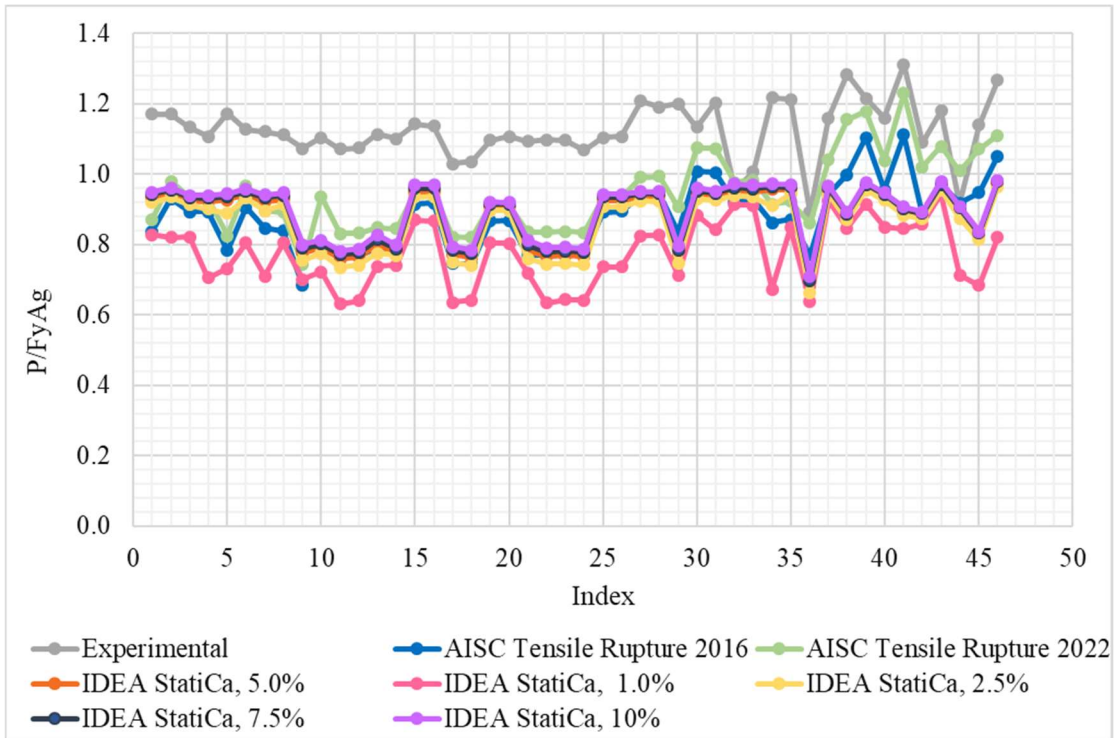


Figure 5.7: Rectangular HSS results: strength ratio vs. index for varying plastic strain limits

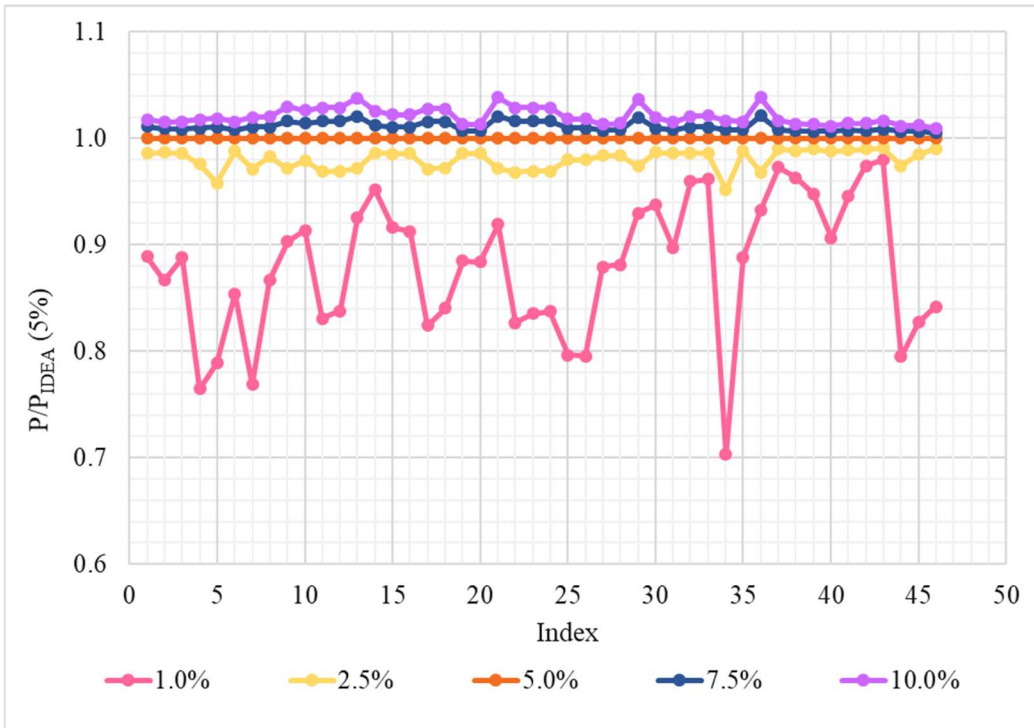


Figure 5.8: Rectangular HSS results: ratio of strength to IDEA StatiCa strength with 5% plastic strain limit plotted with index

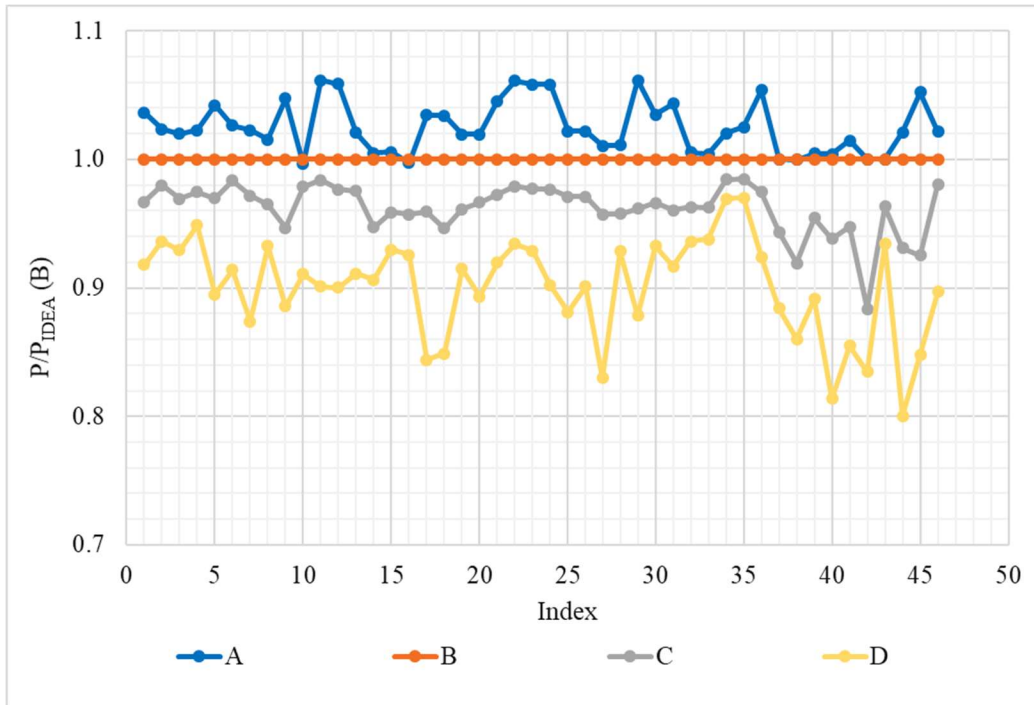


Figure 5.9: Rectangular HSS results: ratio of varying mesh parameters sets to the default mesh settings plotted with index

Table 5.5: Statistical Results for Rectangular HSS

Test-to-Predicted Ratio	Average	Standard Deviation	Coefficient of Variation
$P_{EXP}/P_{RUPTURE}$ (AISC 2016)	1.287	0.122	0.095
$P_{EXP}/P_{RUPTURE}$ (AISC 2022a)	1.197	0.116	0.097
P_{EXP}/P_{IDEA}	1.284	0.116	0.090

5.3 Reliability Analysis

5.3.1 Description of Reliability Set

For the rectangular HSS reliability set, the parameters were selected by varying the following: H/B ratios, weld lengths, rectangular HSS thicknesses, and gusset plate thicknesses. As a reminder, the dimension ‘H’ is parallel to the gusset plate, and the dimension ‘B’ is perpendicular to the gusset plate. The selected set is outlined in Table 5.6.

The connections were modeled identically to the previously described rectangular HSS experimental specimens with just a few adjustments. The reliability set is based on nominal properties and modeled as such. The rectangular HSS members selected in IDEA StatiCa were from the ‘HSS (AISC 15.0 – A500, A502, A618, A847)’ section of the cross-section categories. These members contain reduced thicknesses consistent with practice. Additionally, the material grade A500 Gr. C has a few options in IDEA StatiCa. The material ‘A500, Gr. C, *shaped*’ was selected for the reliability set, as it is consistent with the current ASTM standard (2018).

5.3.2 Results

The strength results for the reliability set of rectangular HSS specimens is provided in Table 5.7. The AISC strength calculations are based on the 2022 edition of the code (AISC 2022a). The nominal and design strengths are provided; however, the controlling design strength was used for the purpose of this reliability analysis (ϕP_{AISC} is the minimum of ϕP_{YIELD} and $\phi P_{RUPTURE}$). The IDEA StatiCa strength results, P_{IDEA} , are based upon all default settings (including LRFD resistance factors). When comparing P_{IDEA} to ϕP_{AISC} , IDEA StatiCa typically resulted in larger strengths than the AISC code equations. The most extreme cases resulted in a 25% higher strength in IDEA StatiCa than the AISC *Specification* equations. On average, P_{IDEA} exceeds ϕP_{AISC} by about 13%.

Table 5.6: Rectangular HSS Reliability Analysis Parameters

Index	H , in.	B , in.	t , in.	Gusset Plate Thickness, in.	Weld Length, in.	Material Grade	F_y , ksi	F_u , ksi
1	8	8	0.500	0.5	8	A500 Gr. C	50	62
2	8	8	0.250	0.5	8	A500 Gr. C	50	62
3	8	8	0.125	0.5	8	A500 Gr. C	50	62
4	8	8	0.500	0.5	16	A500 Gr. C	50	62
5	8	8	0.250	0.5	16	A500 Gr. C	50	62
6	8	8	0.125	0.5	16	A500 Gr. C	50	62
7	8	8	0.500	1.0	8	A500 Gr. C	50	62
8	8	8	0.250	1.0	8	A500 Gr. C	50	62
9	8	8	0.125	1.0	8	A500 Gr. C	50	62
10	8	8	0.500	1.0	16	A500 Gr. C	50	62
11	8	8	0.250	1.0	16	A500 Gr. C	50	62
12	8	8	0.125	1.0	16	A500 Gr. C	50	62
13	8	4	0.500	0.5	8	A500 Gr. C	50	62
14	8	4	0.250	0.5	8	A500 Gr. C	50	62
15	8	4	0.125	0.5	8	A500 Gr. C	50	62
16	8	4	0.500	0.5	16	A500 Gr. C	50	62
17	8	4	0.250	0.5	16	A500 Gr. C	50	62
18	8	4	0.125	0.5	16	A500 Gr. C	50	62
19	8	4	0.500	1.0	8	A500 Gr. C	50	62
20	8	4	0.250	1.0	8	A500 Gr. C	50	62
21	8	4	0.125	1.0	8	A500 Gr. C	50	62
22	8	4	0.500	1.0	16	A500 Gr. C	50	62
23	8	4	0.250	1.0	16	A500 Gr. C	50	62
24	8	4	0.125	1.0	16	A500 Gr. C	50	62
25	4	8	0.500	0.5	8	A500 Gr. C	50	62
26	4	8	0.250	0.5	8	A500 Gr. C	50	62
27	4	8	0.125	0.5	8	A500 Gr. C	50	62
28	4	8	0.500	0.5	16	A500 Gr. C	50	62
29	4	8	0.250	0.5	16	A500 Gr. C	50	62
30	4	8	0.125	0.5	16	A500 Gr. C	50	62
31	4	8	0.500	1.0	8	A500 Gr. C	50	62
32	4	8	0.250	1.0	8	A500 Gr. C	50	62
33	4	8	0.125	1.0	8	A500 Gr. C	50	62
34	4	8	0.500	1.0	16	A500 Gr. C	50	62
35	4	8	0.250	1.0	16	A500 Gr. C	50	62
36	4	8	0.125	1.0	16	A500 Gr. C	50	62

Table 5.7: Rectangular HSS Reliability Strength Results

Index	AISC 2022				IDEA StatiCa
	P_{YIELD} , kips	$P_{RUPTURE}$, kips	ϕP_{YIELD} , kips	$\phi P_{RUPTURE}$, kips	P_{IDEA} , kips
1	675.0	538.2	607.5	403.7	373.5
2	355.0	279.1	319.5	209.3	192.6
3	181.0	141.2	162.9	105.9	101.8
4	675.0	673.2	607.5	504.9	608.2
5	355.0	352.4	319.5	264.3	324.3
6	181.0	179.2	162.9	134.4	165.9
7	675.0	534.6	607.5	400.9	378.9
8	355.0	277.8	319.5	208.3	195.4
9	181.0	140.7	162.9	105.6	99.9
10	675.0	657.0	607.5	492.7	590.7
11	355.0	344.6	319.5	258.4	315.9
12	181.0	175.4	162.9	131.5	161.2
13	487.0	481.3	438.3	360.9	384.7
14	262.0	256.4	235.8	192.3	197.4
15	135.0	131.4	121.5	98.6	104.4
16	487.0	528.2	438.3	396.1	441.4
17	262.0	283.4	235.8	212.6	239.7
18	135.0	145.8	121.5	109.4	123.8
19	487.0	470.2	438.3	352.7	400.0
20	262.0	251.5	235.8	188.6	203.4
21	135.0	129.1	121.5	96.8	102.7
22	487.0	508.2	438.3	381.2	431.5
23	262.0	273.7	235.8	205.3	234.1
24	135.0	141.1	121.5	105.8	120.6
25	487.0	406.0	438.3	304.5	368.4
26	262.0	215.8	235.8	161.9	191.3
27	135.0	110.5	121.5	82.9	100.9
28	487.0	490.5	438.3	367.9	440.6
29	262.0	263.1	235.8	197.3	240.3
30	135.0	135.3	121.5	101.5	123.9
31	487.0	395.1	438.3	296.4	371.8
32	262.0	211.0	235.8	158.2	194.0
33	135.0	108.2	121.5	81.2	99.1
34	487.0	470.7	438.3	353.0	422.0
35	262.0	253.5	235.8	190.1	232.1
36	135.0	130.6	121.5	98.0	120.1

It is possible the AISC tensile rupture ϕ -factor is a significant reason for these differences since large differences were not observed in the rectangular HSS experimental set (where LRFD resistance factors were not used). Reliability index specimens 1, 2, and 3 indicated around a 9% lower strength for IDEA StatiCa than the AISC *Specification* equations.

The reliability index, β , results are presented in Figure 5.10. The β -values for AISC fell within the range of 3.88 to 4.38. For IDEA StatiCa, the range was from 3.31 to 4.61. Specimen indices 1 through 24 appear to be more sensitive to longer welds for IDEA StatiCa than the AISC β -value results. Specimen indices 4, 5, 6, 10, 11, 12, 16, 17, 18, 22, 23, and 24 all have welds of 16 in. (longest weld in reliability set) and result in lower reliability for IDEA StatiCa. However, specimen indices 25 through 36 appear to be less influenced by weld length. These specimens have an H/B of 0.5, which results in a larger eccentricity.

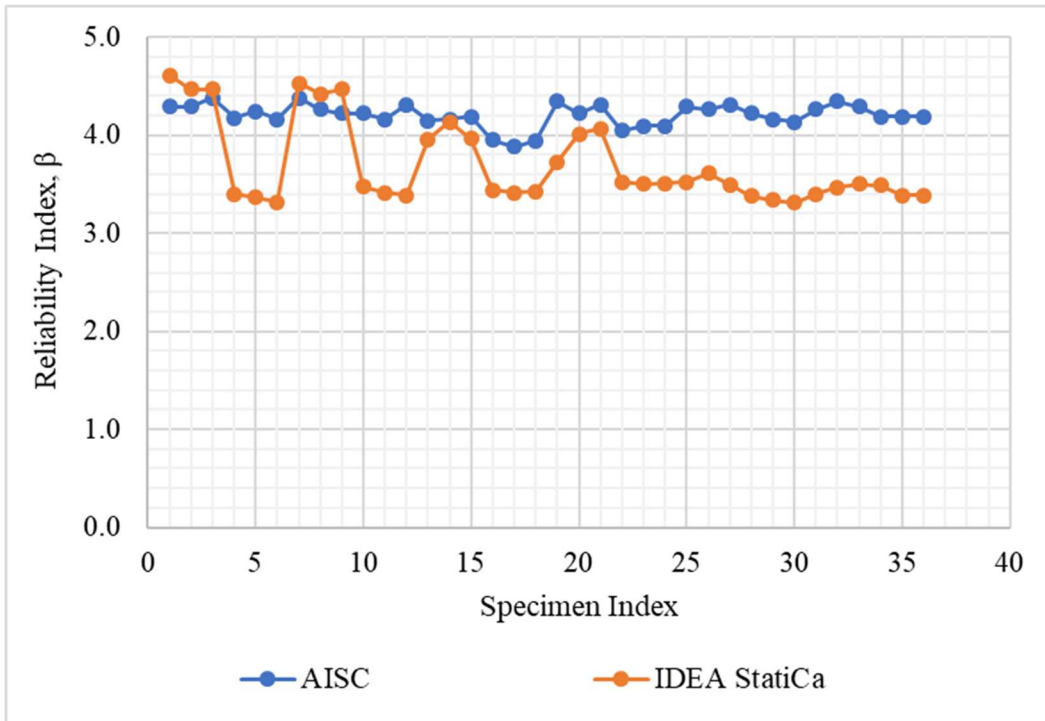


Figure 5.10: Rectangular HSS: Reliability index for IDEA StatiCa and AISC 2022

CHAPTER 6

WELDED ANGLES

6.1 Description of Connection

Single and double angle tension members that are welded to a gusset plate are evaluated in this chapter. The weld configurations investigated in this chapter include longitudinal welds only and longitudinal welds combined with transverse welds. A typical schematic is provided in Figure 6.1 with the terminology consistent throughout this chapter.

For the AISC *Specification* (2016) hand calculations, the gross area and centroid were calculated based on measured dimensions ignoring fillets. The applicable shear lag factor cases for the evaluation of tensile rupture for welded angles were cases 2, 3, and 4 from Table D3.1 of the AISC *Specification* (also provided in Figure 3.3). Case 2 includes the use of the following equation:

$$U = 1 - \frac{\bar{x}}{l} \quad (6-1)$$

where \bar{x} is the eccentricity of the connection (i.e., the distance between the centroid of the angle and the faying surface) and l is defined in Figure 6.2. When weld lengths are unequal, l is the average of the two lengths. The case is only applicable when the load is transmitted to some, but not all cross-sectional elements by longitudinal welds in combination with transverse welds. Case 3 is applicable when the load is transmitted to some but not all elements only by transverse welds. For the specimens in this study, this case was never applicable. Case 4 includes the use of the following equation:

$$U = \frac{3l^2}{3l^2 + w^2} \left(1 - \frac{\bar{x}}{l} \right) \quad (6-2)$$

where \bar{x} is the eccentricity of the connection; l and w are defined in Figure 6.2. When weld lengths are unequal, l is the average of the two longitudinal welds. Case 4 is only applicable when the load is transmitted by longitudinal welds only. Additionally, Section D3 of the AISC *Specification* sets a lower bound for shear lag factors that is applicable to

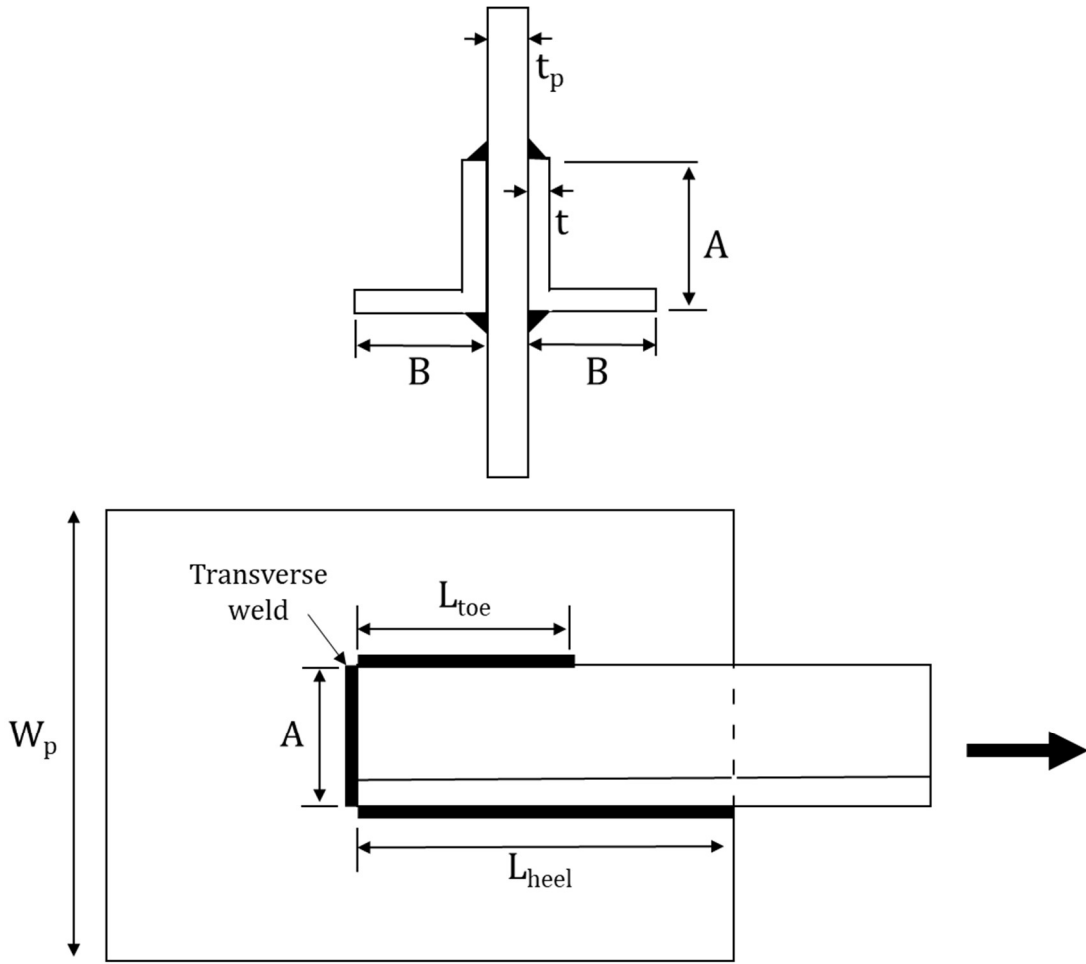


Figure 6.1: Weld Angle Schematic

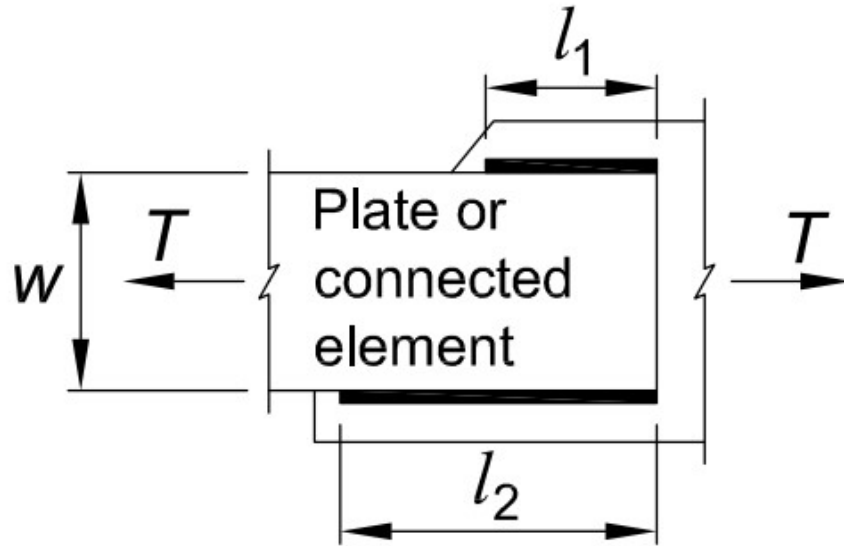


Figure 6.2: Example and dimensions for case 2 and 4 of Table D3.2 from the AISC
Specification

single and double angles. The section states that the shear lag factor does not need to be less than the ratio of the gross of the connected elements to the gross area of the member. This lower bound was evaluated, but never controlled for welded angle members.

6.2 Comparison to Experimental Results

6.2.1 Description of Experimental Specimens

A total of 127 specimens were examined in this chapter. The enumeration of specimens from each paper is shown in Table 6.1. Gonzalez (1989), also in Easterling and Gonzalez Giroux (1993), reported nine welded angle specimens, but specimens L-B-1b and L-T-1 were removed due to weld failures. Zhu et al. (2009) reported 13 specimens, however four specimens were removed due to insufficient weld strength (specimens A1-300UL, A1-250US, A2-200BS, and A2-200UL). Mannem (2002) actually reported 22 experimental specimens, and specimens DEA3, DEA4, DEA5, DUEA1, UEA4, and UEA7 were removed from the current study due to weld failures. Pettretta, 1999 included 18 specimens, however 11 specimens were removed for a variety of reason. Specimens A4-ii-s, C11-L-l, C12-L-ii, T21, T18, T20, T22, PS6-23, and PS6-MP24 were all removed due to the experimental failure mode being something other than tensile yield or rupture. Specimens X14-bx and X15-x were removed because the configuration of the angles is outside the scope of this chapter. Gibson and Wake (1942) actually reported 24 specimens. There were 14 specimens removed due to weld failures (single angles 1, 2, 4, 6, 8, 11, 12, 13, and 14; double angles 1, 8, 10, 11, 13), five specimens had configurations outside the scope of this section (single angles 5, 7, 9, and 15; double angles 5), and the machine reached full capacity before failure on double angle specimen 2. Dhanuskar and Gupta (2021a; b) has two separate publications, one in May and one in April. Some specimens were included in both papers, but unique specimens were presented in both as well. For the May 2021 paper, four specimens were excluded due to non-regular configurations (specimens 9 through 12). As for the April 2021 paper, five specimens excluded were because they were already accounted for in the

Table 6.1: Welded Angle Specimen Enumeration

Reference	Specimen Count
Gonzalez (1989)	7
Zhu et al. (2009)	9
Ke et al. (2018)	9
Fang et al. (2013)	12
Regan and Salter (1984)	17
Mannem (2002)	16
Petretta (2000)	7
Bauer and Benaddi (2002)	6
Gibson and Wake (1942)	4
Dhanuskar and Gupta (2021b)	8
Dhanuskar and Gupta (2021a)	18
Uzoegbo (1998)	14
Total	127

May 2021 paper (specimens 16, 17, 18, 26, and 27). Specimens 5 through 8 failed in the welds, and thus removed as well.

The details for each experimental set specimen are provided in Table 6.2. As shown in the table, 25 specimens were double angles with the remainder being single angles. The dimensions ‘A’ and ‘B’ are consistent with Figure 6.1 where ‘A’ is the connected leg length and ‘B’ is the unconnected leg length. Due to the large volume of information pertaining to the weld angles, the weld details are provided in a separate table, Table 6.3. Unless otherwise reported, a weld strength of E70XX was assumed. If a different weld strength was reported, it was modeled as such. In regards to transverse welds, if the table does not show a value in the transverse weld columns, then transverse welds were not included on the specimen. If the length of the transverse weld was not provided, the weld was assumed to be continued along the entire length of the connected leg. There was not a reported case where the transverse weld was shorted than the connected leg. It should be noted, the names given to the specimens in Gibson and Wake (1942) consisted of two sets of numbers, one for single angles and one for double angles. There were duplicate specimen names between the two sets. For clarity, an ‘s’ or ‘d’ was provided at the beginning of the specimens’ name for the current study.

The modeling of the welded angles was different from that outlined in the previous two chapters, but similar to the remainder of the connection types. These specimens were modeled using two or three members, depending if the specimen consisted of one or two angles. The gusset plate was modeled as a member in addition to the angle specimen. The specimens were then attached using a variety of weld operations. An example of a modeled specimen with two angles is provided in Figure 6.3. The modeling process included the following:

1. Process outlined in Chapter 3.3
2. Create members:
 - a. Member 1: Gusset plate
 - i. Geometrical type set to “Ended”
 - ii. B set to 180°

Table 6.2: Welded Angles Specimen Details

Index	Reference	Specimen	# of angles	* F_y , ksi	* F_u , ksi	A, in.	B, in.
1	Gonzalez (1989)	L-L-1	2	54.1	81.1	2.011	1.991
2	Gonzalez (1989)	L-L-2	2	54.1	81.1	2.011	1.992
3	Gonzalez (1989)	L-L-3	2	54.1	81.1	2.009	1.989
4	Gonzalez (1989)	L-B-1a	2	47.8	71.3	3.972	2.978
5	Gonzalez (1989)	L-B-1c	2	54.1	81.1	2.01	1.992
6	Gonzalez (1989)	L-B-2	2	54.1	81.1	2.01	1.992
7	Gonzalez (1989)	L-B-3	2	54.1	81.1	2.01	1.994
8	Zhu et. al (2009)	A1-200BL	1	38.9	60.6	4.937	2.953
9	Zhu et. al (2009)	A1-200BS	1	38.9	60.6	2.953	4.937
10	Zhu et. al (2009)	A1-200UL	1	38.9	60.6	4.937	2.953
11	Zhu et. al (2009)	A1-250UL	1	38.9	60.6	4.937	2.953
12	Zhu et. al (2009)	A1-200US	1	38.9	60.6	2.953	4.937
13	Zhu et. al (2009)	A1-300US	1	38.9	60.6	2.953	4.937
14	Zhu et. al (2009)	A2-200BL	1	38.0	62.7	5.902	2.957
15	Zhu et. al (2009)	A2-200BS-d	1	38.0	62.7	2.957	5.902
16	Zhu et. al (2009)	A2-200US	1	38.0	62.7	2.957	5.902
17	Ke et al. (2018)	C1-220L	1	110.4	115.7	3.15	2.362
18	Ke et al. (2018)	C1-300L	1	110.4	115.7	3.15	2.362
19	Ke et al. (2018)	C1-380L	1	110.4	115.7	3.15	2.362
20	Ke et al. (2018)	C1-300S	1	110.4	115.7	2.362	3.150
21	Ke et al. (2018)	C2-220S	1	110.4	115.7	2.544	3.984
22	Ke et al. (2018)	C2-300S	1	110.4	115.7	2.559	3.937
23	Ke et al. (2018)	C2-380S	1	110.4	115.7	2.559	3.937
24	Ke et al. (2018)	D1-300L	1	42.4	65.7	3.101	2.395
25	Ke et al. (2018)	D2-300S	1	42.4	65.7	2.591	3.983
26	Fang et al. (2013)	A1-170B	1	39.7	59.8	1.181	2.362
27	Fang et al. (2013)	A1-170U	1	39.7	59.8	1.181	2.362
28	Fang et al. (2013)	A2-200B	1	70.2	100.5	1.969	2.953
29	Fang et al. (2013)	A2-200U	1	70.2	100.5	1.969	2.953
30	Fang et al. (2013)	A3-215B	1	41.6	60.2	1.969	2.362
31	Fang et al. (2013)	A3-215U	1	41.6	60.2	1.969	2.362
32	Fang et al. (2013)	A4-305B	1	32.8	54.4	2.953	4.921
33	Fang et al. (2013)	A4-305U	1	32.8	54.4	2.953	4.921
34	Fang et al. (2013)	A5-335B	1	40.3	51.5	2.953	5.906
35	Fang et al. (2013)	A5-335U	1	40.3	51.5	2.953	5.906
36	Fang et al. (2013)	A5-380B	1	40.3	51.5	2.953	5.906
37	Fang et al. (2013)	A5-380U	1	40.3	51.5	2.953	5.906
38	Regan and Salter (1984)	A1	1	43.9	68.0	0.984	0.984

Table 6.2 continued

Index	Reference	Specimen	# of angles	* F_y , ksi	* F_u , ksi	A, in.	B, in.
39	Regan and Salter (1984)	B1	1	45.0	65.7	1.969	1.969
40	Regan and Salter (1984)	B2	1	46.7	67.2	1.969	1.969
41	Regan and Salter (1984)	B3	1	46.7	67.2	1.969	1.969
42	Regan and Salter (1984)	B4	1	47.6	68.6	1.969	1.969
43	Regan and Salter (1984)	C1	1	47.1	73.0	3.937	3.937
44	Regan and Salter (1984)	C2	1	49.0	74.7	3.937	3.937
45	Regan and Salter (1984)	D1	1	47.9	70.3	1.181	2.362
46	Regan and Salter (1984)	D2	1	46.7	68.3	1.181	2.362
47	Regan and Salter (1984)	D3	1	45.7	66.7	2.362	1.181
48	Regan and Salter (1984)	D4	1	46.7	68.3	2.362	1.181
49	Regan and Salter (1984)	D5	1	46.7	68.3	1.181	2.362
50	Regan and Salter (1984)	D6	1	46.4	67.6	1.181	2.362
51	Regan and Salter (1984)	E1	1	39.4	66.4	1.969	2.559
52	Regan and Salter (1984)	E2	1	38.4	68.5	2.559	1.969
53	Regan and Salter (1984)	F1	1	47.1	69.9	2.953	4.921
54	Regan and Salter (1984)	F2	1	48.3	71.5	4.921	2.953
55	Mannem (2002)	DEA1	2	52.1	74.1	4.004	3.992
56	Mannem (2002)	DEA2	2	52.1	74.1	4.004	3.992
57	Mannem (2002)	EA1	1	51.4	73.2	3.992	4.000
58	Mannem (2002)	EA2	1	51.4	73.2	3.992	4.000
59	Mannem (2002)	EA3	1	52.2	76.1	5.969	5.961
60	Mannem (2002)	EA4	1	52.2	76.1	5.969	5.961
61	Mannem (2002)	EAm1	1	51.4	73.2	3.992	4.000
62	Mannem (2002)	EAm2	1	51.4	73.2	3.992	4.000
63	Mannem (2002)	DUEA2	2	51.2	69.6	2.953	4.921
64	Mannem (2002)	UEA1	1	51.7	69.8	4.965	2.980
65	Mannem (2002)	UEA2	1	51.7	69.8	2.980	4.965
66	Mannem (2002)	UEA3	1	51.7	69.8	4.965	2.980
67	Mannem (2002)	UEA5	1	51.2	69.6	2.953	4.921
68	Mannem (2002)	UEA6	1	51.2	69.6	2.953	4.921
69	Mannem (2002)	UEA8	1	53.2	70.4	6.000	4.020
70	Mannem (2002)	UEA9	1	53.2	70.4	6.000	4.020
71	Petretta (2000)	A1-i	2	58.9	79.9	2.502	2.510
72	Petretta (2000)	A3-ii	2	58.9	79.9	2.504	2.510
73	Petretta (2000)	A6-iii	2	58.9	79.9	2.506	2.506
74	Petretta (2000)	B8-i-t	2	58.9	79.9	2.506	2.506
75	Petretta (2000)	B10-iii-t	2	58.9	79.9	2.504	2.514
76	Petretta (2000)	C12-L-ii-retest	2	51.5	76.0	2.437	3.482
77	Petretta (2000)	T19	2	50.8	73.1	2.516	2.518

Table 6.2 continued

Index	Reference	Specimen	# of angles	* F_y , ksi	* F_u , ksi	A, in.	B, in.
78	Bauer and Benaddi (2002)	No. 1	2	57.0	77.0	1.496	1.496
79	Bauer and Benaddi (2002)	No. 2	2	50.6	71.4	2.008	2.008
80	Bauer and Benaddi (2002)	No. 3	2	46.1	66.9	2.008	2.520
81	Bauer and Benaddi (2002)	No. 4	2	50.0	72.4	2.520	2.520
82	Bauer and Benaddi (2002)	No. 5	2	49.2	70.6	2.008	2.992
83	Bauer and Benaddi (2002)	No. 6	2	50.5	76.4	2.992	2.992
84	Gibson and Wake (1942)	s3	1	38.8	64.4	2.500	2.500
85	Gibson and Wake (1942)	s10	1	38.8	64.4	2.500	2.500
86	Gibson and Wake (1942)	d3	2	38.8	64.4	2.500	2.500
87	Gibson and Wake (1942)	d4	2	38.8	64.4	2.500	2.500
88	Dhanuskar and Gupta (2021b)	S1-250/90-B	1	52.5	70.9	3.961	3.961
89	Dhanuskar and Gupta (2021b)	S1-250/90-B	1	52.5	70.9	3.961	3.961
90	Dhanuskar and Gupta (2021b)	S1-250/90-B	1	52.5	70.9	3.961	3.961
91	Dhanuskar and Gupta (2021b)	S1-195/195-U	1	52.5	70.9	3.961	3.961
92	Dhanuskar and Gupta (2021b)	S1-195/195-U	1	52.5	70.9	3.961	3.961
93	Dhanuskar and Gupta (2021b)	S2-125/125-U	1	49.3	70.6	3.941	3.941
94	Dhanuskar and Gupta (2021b)	S2-125/125-U	1	49.3	70.6	3.941	3.941
95	Dhanuskar and Gupta (2021b)	S2-125/125-U	1	49.3	70.6	3.941	3.941
96	Dhanuskar and Gupta (2021a)	S1-150/100-U	1	59.8	82.4	2.539	2.524
97	Dhanuskar and Gupta (2021a)	S1-150/100-U	1	59.8	82.4	2.539	2.524
98	Dhanuskar and Gupta (2021a)	S1-150/100-U	1	59.8	82.4	2.539	2.524
99	Dhanuskar and Gupta (2021a)	S1-100/65-U	1	59.8	82.4	2.539	2.524
100	Dhanuskar and Gupta (2021a)	S2-225/85-B	1	48.9	63.5	2.594	2.547
101	Dhanuskar and Gupta (2021a)	S2-225/85-B	1	48.9	63.5	2.594	2.547
102	Dhanuskar and Gupta (2021a)	S2-225/85-B	1	48.9	63.5	2.594	2.547
103	Dhanuskar and Gupta (2021a)	S3-255/95-B	1	48.6	64.2	2.969	3.004
104	Dhanuskar and Gupta (2021a)	S3-255/95-B	1	48.6	64.2	2.969	3.004
105	Dhanuskar and Gupta (2021a)	S3-255/95-B	1	48.6	64.2	2.969	3.004
106	Dhanuskar and Gupta (2021a)	S3-225/135-U	1	48.6	64.2	2.969	3.004
107	Dhanuskar and Gupta (2021a)	S2-155/155-U	1	48.9	63.5	2.594	2.547
108	Dhanuskar and Gupta (2021a)	S2-155/155-U	1	48.9	63.5	2.594	2.547
109	Dhanuskar and Gupta (2021a)	S2-155/155-U	1	48.9	63.5	2.594	2.547
110	Dhanuskar and Gupta (2021a)	S3-255/135-U	1	48.6	64.2	2.969	3.004
111	Dhanuskar and Gupta (2021a)	S3-175/175-U	1	48.6	64.2	2.969	3.004
112	Dhanuskar and Gupta (2021a)	S3-175/175-U	1	48.6	64.2	2.969	3.004
113	Dhanuskar and Gupta (2021a)	S3-175/175-U	1	48.6	64.2	2.969	3.004
114	Uzoegbo (1998)	E1	1	46.4	75.4	2.953	4.921
115	Uzoegbo (1998)	E2	1	46.4	75.4	1.969	2.953
116	Uzoegbo (1998)	E3	1	46.4	75.4	1.969	2.559

Table 6.2 continued

Index	Reference	Specimen	# of angles	* F_y , ksi	* F_u , ksi	A , in.	B , in.
117	Uzoegbo (1998)	E4	1	46.4	75.4	2.756	2.756
118	Uzoegbo (1998)	E5	1	46.4	75.4	4.921	2.953
119	Uzoegbo (1998)	E6	1	46.4	75.4	2.953	1.969
120	Uzoegbo (1998)	E7	1	46.4	75.4	2.560	1.969
121	Uzoegbo (1998)	U1	1	46.4	75.4	2.953	4.921
122	Uzoegbo (1998)	U2	1	46.4	75.4	1.969	2.953
123	Uzoegbo (1998)	U3	1	46.4	75.4	1.966	2.559
124	Uzoegbo (1998)	U4	1	46.4	75.4	2.756	2.756
125	Uzoegbo (1998)	U5	1	46.4	75.4	4.921	2.953
126	Uzoegbo (1998)	U6	1	46.4	75.4	2.953	1.969
127	Uzoegbo (1998)	U7	1	46.4	75.4	2.560	1.969

* indicates measured value

Table 6.3: Welded Angle Weld Details

Index	Weld Material	Toe Weld Size, in.	L _{TOE} , in.	Heel Weld Size, in.	L _{HEEL} , in.	Transverse Weld Size, in.	L _{TRANS.} , in.
1	E70XX	0.188	4.500	0.375	4.500	-	-
2	E70XX	0.188	4.500	0.375	4.500	-	-
3	E70XX	0.188	4.500	0.375	4.500	-	-
4	E70XX	0.250	3.500	0.250	3.500	0.250	4.000
5	E70XX	0.188	3.000	0.438	3.000	0.188	2.000
6	E70XX	0.188	3.000	0.438	3.000	0.188	2.000
7	E70XX	0.188	3.000	0.438	3.000	0.188	2.000
8	E70XX	0.315	4.724	0.315	11.024	0.315	4.937
9	E70XX	0.315	3.150	0.315	12.598	0.315	2.953
10	E70XX	0.315	7.874	0.315	7.874	0.315	4.937
11	E70XX	0.315	9.843	0.315	9.843	0.315	4.937
12	E70XX	0.315	7.874	0.315	7.874	0.315	2.953
13	E70XX	0.315	11.811	0.315	11.811	0.315	2.953
14	E70XX	0.315	4.724	0.315	11.024	0.315	5.902
15	E70XX	0.315	2.756	0.315	12.992	0.315	2.957
16	E70XX	0.315	7.874	0.315	7.874	0.315	2.957
17	NP	0.276	8.661	0.276	8.661	0.276	3.150
18	NP	0.276	11.811	0.276	11.811	0.276	3.150
19	NP	0.276	14.961	0.276	14.961	0.276	3.150
20	NP	0.276	11.811	0.276	11.811	0.276	2.362
21	NP	0.276	8.661	0.276	8.661	0.276	2.559
22	NP	0.276	11.811	0.276	11.811	0.276	2.559
23	NP	0.276	14.961	0.276	14.961	0.276	2.559
24	NP	0.276	11.811	0.276	11.811	0.276	3.150
25	NP	0.276	11.811	0.276	11.811	0.276	2.559
26	NP	0.236	2.756	0.236	10.630	0.236	1.181
27	NP	0.236	6.693	0.236	6.693	0.236	1.181
28	NP	0.236	3.543	0.236	12.205	0.236	1.969
29	NP	0.236	7.874	0.236	7.874	0.236	1.969
30	NP	0.236	3.937	0.236	12.992	0.236	1.969
31	NP	0.236	8.465	0.236	8.465	0.236	1.969
32	NP	0.394	4.724	0.394	19.291	0.394	2.953
33	NP	0.394	12.008	0.394	12.008	0.394	2.953
34	NP	0.394	5.118	0.394	21.260	0.394	2.953
35	NP	0.394	13.189	0.394	13.189	0.394	2.953
36	NP	0.394	6.693	0.394	23.228	0.394	NP

Table 6.3 continued

Index	Weld Material	Toe Weld Size, in.	L _{TOE} , in.	Heel Weld Size, in.	L _{HEEL} , in.	Transverse Weld Size, in.	L _{TRANS.} , in.
37	NP	0.394	14.961	0.394	14.961	0.394	NP
38	NP	0.157	7.874	0.157	7.874	0.157	0.984
39	NP	0.157	7.874	0.157	7.874	0.157	1.969
40	NP	0.157	7.874	0.157	7.874	0.157	1.969
41	NP	0.157	7.874	0.157	7.874	0.157	1.969
42	NP	0.157	7.874	0.157	7.874	0.157	1.969
43	NP	0.236	15.748	0.236	15.748	0.236	3.937
44	NP	0.236	15.748	0.236	15.748	0.236	3.937
45	NP	0.157	6.890	0.157	6.890	0.157	1.181
46	NP	0.157	6.890	0.157	6.890	0.157	1.181
47	NP	0.157	5.906	0.157	5.906	0.157	2.362
48	NP	0.157	5.906	0.157	5.906	0.157	2.362
49	NP	0.157	6.890	0.157	6.890	0.157	1.181
50	NP	0.157	6.890	0.157	6.890	0.157	1.181
51	NP	0.236	9.843	0.236	9.843	0.236	1.969
52	NP	0.236	8.858	0.236	8.858	0.236	2.559
53	NP	0.236	15.748	0.236	15.748	0.236	2.953
54	NP	0.236	14.764	0.236	14.764	0.236	4.921
55	E760XX#	0.264	3.937	0.709	3.937	0.264	4.004
56	E760XX#	0.264	15.748	0.709	15.748	-	-
57	E760XX#	0.268	5.512	0.472	5.512	0.268	3.992
58	E760XX#	0.268	5.315	0.630	5.315	-	-
59	E760XX#	0.382	8.268	0.709	8.268	0.382	5.969
60	E760XX#	0.382	8.465	0.709	8.465	-	-
61	E760XX#	0.268	5.906	0.551	5.906	0.268	3.992
62	E760XX#	0.268	5.906	0.551	5.906	0.268	3.992
63	E760XX#	0.256	4.921	0.551	4.921	0.256	2.980
64	E760XX#	0.256	4.921	0.551	4.921	0.256	4.965
65	E760XX#	0.256	5.315	0.551	5.315	0.335	2.980
66	E760XX#	0.256	6.102	0.551	6.102	-	-
67	E760XX#	0.260	9.843	0.630	9.843	-	-
68	E760XX#	0.260	7.480	0.630	7.480	-	-
69	E760XX#	0.319	9.055	0.630	9.055	-	-
70	E760XX#	0.319	11.811	0.630	11.811	-	-
71	ER480S	0.236	3.543	0.394	3.543	-	-
72	ER480S	0.236	4.724	0.236	4.724	-	-

Table 6.3 continued

Index	Weld Material	Toe Weld Size, in.	L _{TOE} , in.	Heel Weld Size, in.	L _{HEEL} , in.	Transverse Weld Size, in.	L _{TRANS.} , in.
73	ER480S	0.236	6.299	0.236	6.299	-	-
74	ER480S	0.236	3.543	0.394	3.543	0.236	2.506
75	ER480S	0.236	6.299	0.236	6.299	0.236	2.504
76	ER480S	0.236	4.724	0.394	4.724	-	-
77	ER480S	0.236	7.480	0.236	3.937	-	-
78	NP	0.197	3.425	0.197	3.425	-	-
79	NP	0.197	4.409	0.197	4.409	-	-
80	NP	0.197	4.803	0.197	4.803	-	-
81	NP	0.197	5.354	0.197	5.354	-	-
82	NP	0.197	5.433	0.197	5.433	-	-
83	NP	0.197	6.654	0.197	6.654	-	-
84	E-6012	0.250	2.875	0.375	4.375	-	-
85	E-6012	0.250	4.875	0.250	2.375	0.250	2.500
86	E-6012	0.250	2.875	0.375	4.375	-	-
87	E-6012	0.250	2.875	0.500	3.500	-	-
88	NP	0.236	3.642	0.236	9.961	-	-
89	NP	0.236	3.720	0.236	9.843	-	-
90	NP	0.236	3.642	0.236	9.823	-	-
91	NP	0.236	7.677	0.236	7.677	-	-
92	NP	0.236	7.677	0.236	7.677	-	-
93	NP	0.236	4.961	0.236	4.961	-	-
94	NP	0.236	4.941	0.236	4.941	-	-
95	NP	0.236	4.921	0.236	4.921	-	-
96	NP	0.236	3.937	0.236	5.925	-	-
97	NP	0.236	4.035	0.236	6.024	-	-
98	NP	0.236	3.976	0.236	5.945	-	-
99	NP	0.236	2.579	0.236	3.957	-	-
100	NP	0.236	3.386	0.236	8.839	-	-
101	NP	0.236	3.366	0.236	8.917	-	-
102	NP	0.236	3.425	0.236	8.819	-	-
103	NP	0.197	3.799	0.197	10.059	-	-
104	NP	0.197	3.780	0.197	10.039	-	-
105	NP	0.197	3.780	0.197	10.098	-	-
106	NP	0.197	5.295	0.197	10.039	-	-
107	NP	0.236	6.102	0.236	6.102	-	-
108	NP	0.236	6.102	0.236	6.102	-	-

Table 6.3 continued

Index	Weld Material	Toe Weld Size, in.	L _{TOE} , in.	Heel Weld Size, in.	L _{HEEL} , in.	Transverse Weld Size, in.	L _{TRANS.} , in.
109	NP	0.236	6.102	0.236	6.102	-	-
110	NP	0.197	6.890	0.197	6.890	-	-
111	NP	0.197	6.890	0.197	6.890	-	-
112	NP	0.197	6.890	0.197	6.890	-	-
113	NP	0.197	6.890	0.197	6.890	-	-
114	E480XX#	0.197	9.843	0.197	9.843	0.197	2.953
115	E480XX#	0.197	5.906	0.197	5.906	0.197	1.969
116	E480XX#	0.197	5.906	0.197	5.906	0.197	1.969
117	E480XX#	0.197	5.906	0.197	5.906	0.197	2.756
118	E480XX#	0.197	9.843	0.197	9.843	0.197	4.921
119	E480XX#	0.197	5.906	0.197	5.906	0.197	2.953
120	E480XX#	0.197	5.906	0.197	5.906	0.197	2.559
121	E480XX#	0.197	6.693	0.197	13.386	0.197	2.953
122	E480XX#	0.197	3.937	0.197	7.874	0.197	1.969
123	E480XX#	0.197	3.937	0.197	7.874	0.197	1.969
124	E480XX#	0.197	3.937	0.197	7.874	0.197	2.756
125	E480XX#	0.197	6.693	0.197	13.386	0.197	4.921
126	E480XX#	0.197	3.937	0.197	7.874	0.197	2.953
127	E480XX#	0.197	3.937	0.197	7.874	0.197	2.559

NP is not provided; # indicates metric units

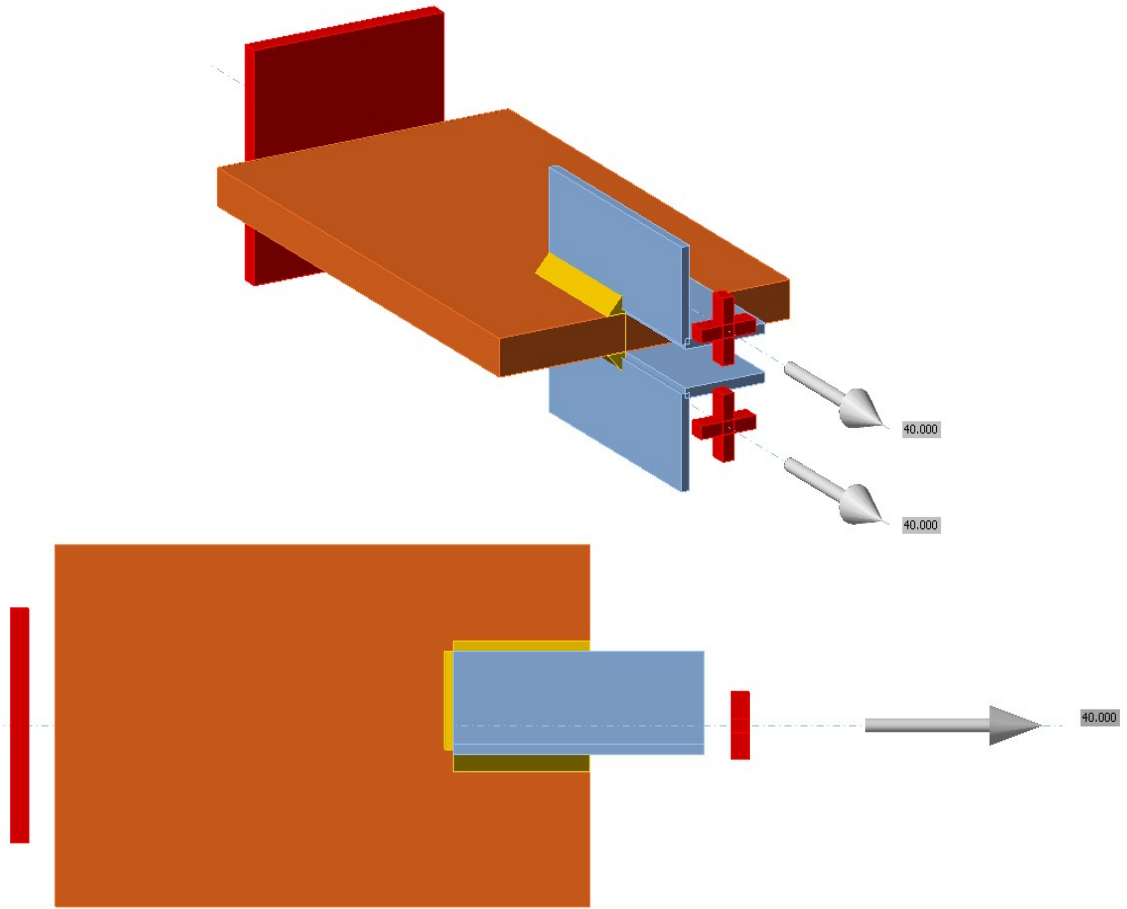


Figure 6.3: Typical Welded Angle Model

- iii. Offset ex set to the negative of the connection length (longest longitudinal weld length)
 - b. Member 2, 3 (if applicable)
 - i. Geometrical type set to “Ended”
 - ii. Align set to “To member plate”
 - iii. Aligned plate set to “[member name] | Bottom flange 1”
 - iv. Related plate set to “[gusset plate member name] Bottom flange 1”
 - v. Model type set to “N-Vy-Vz”
- 3. Create weld operations:
 - a. Continuous welds:
 - i. Placement set to “Edge to surface”
 - ii. Type set to “Weld”
 - iii. First plate: Member or plate set to “[angle member name] | Bottom flange 1”
 - iv. Select correct edge index
 - v. Second plate: Plate set to “[gusset plate name] | Bottom flange 1”
 - vi. Input desired weld size and type (fillet- front side for all specimens)
 - vii. Weld type set to “Continuous”
 - b. Partial welds:
 - i. Placement set to “Edge to surface”
 - ii. Type set to “Weld”
 - iii. First plate: Member or plate set to “[angle member name] | Bottom flange 1”
 - iv. Select correct edge index
 - v. Second plate: Plate set to “[gusset plate name] | Bottom flange 1”
 - vi. Input desired weld size and type (fillet- front side for all specimens)
 - vii. Weld type set to “Partial”

- viii. Weld offset 2 set to the absolute value of the offset in Step 2 minus the partial weld length
4. Repeat as necessary until all welds are modeled

6.2.2 Results

The strength results of the welded angle experimental set according to the AISC *Specification* (2016) equations are provided in Table 6.4. Shear lag factor case 2 was applicable for about 60% of the specimens, with the remainder being controlled by case 4. A summary of the strength results for the welded angle experimental set is provided in Table 6.5. The AISC strength, P_{AISC} , is the minimum of P_{YIELD} and $P_{RUPTURE}$. The maximum permitted applied load according to IDEA StatiCa, P_{IDEA} , presented here are for the default mesh settings and 5% plastic strain limit. The failure mode for IDEA StatiCa was occasionally in the welds. This failure was ignored, and the strength was reported when the plastic strain reached 5.0%. For this experimental set, P_{IDEA} compares well with the corresponding strength according to the AISC *Specification* equations, with differences primarily on the conservative side. The most conservative case results from experimental set specimen 45 with about a 45% difference from P_{AISC} . For the experimental set specimens where P_{IDEA} exceeds P_{AISC} , the difference was less than 10%. In comparison to the experimental strengths, P_{EXP} , the strength according to IDEA StatiCa never exceeded the experimental strength.

The results plotted with the corresponding experimental set index are provided in Figure 6.4. The strengths for each experimental set specimen are normalized by the predicted tensile yield strength, $F_y A_g$. The tensile rupture strength, $P_{RUPTURE}$, is plotted for the AISC *Specification* strength results, rather than P_{AISC} . In general, this plot indicates IDEA StatiCa provides strength results lower or comparable to the AISC *Specification* and always provides strengths more conservative than that observed in experiments. However, a reliability analysis that includes the consideration of uncertainties is provided in the next section. Such considerations include uncertainties in material and geometric properties and even uncertainties in the analysis.

Table 6.4: Welded Angle AISC Calculation Results

Index	P _{YIELD} , kips	U	Controlling U Case	P _{RUPTURE} , kips
1	82.3	0.819	Case 4	101.0
2	82.3	0.819	Case 4	101.0
3	81.8	0.819	Case 4	100.5
4	160.7	0.791	Case 2	189.7
5	83.4	0.810	Case 2	101.3
6	82.7	0.810	Case 2	100.4
7	81.1	0.810	Case 2	98.6
8	115.9	0.911	Case 2	164.7
9	115.9	0.785	Case 2	141.9
10	115.9	0.911	Case 2	164.7
11	115.9	0.929	Case 2	167.9
12	115.9	0.785	Case 2	141.9
13	115.9	0.857	Case 2	154.8
14	132.7	0.917	Case 2	200.6
15	132.7	0.730	Case 2	159.7
16	132.7	0.730	Case 2	159.7
17	182.8	0.928	Case 2	177.9
18	181.8	0.947	Case 2	180.5
19	181.2	0.958	Case 2	182.1
20	181.8	0.914	Case 2	174.2
21	217.3	0.846	Case 2	192.8
22	214.9	0.889	Case 2	200.3
23	215.5	0.912	Case 2	206.2
24	68.9	0.946	Case 2	101.1
25	80.2	0.888	Case 2	110.5
26	31.0	0.869	Case 2	40.5
27	31.0	0.869	Case 2	40.5
28	101.9	0.873	Case 2	127.3
29	101.9	0.873	Case 2	127.3
30	40.2	0.914	Case 2	53.1
31	40.2	0.914	Case 2	53.1
32	96.6	0.860	Case 2	137.8
33	96.6	0.860	Case 2	137.8
34	159.6	0.837	Case 2	170.6

Table 6.4 continued

Index	P _{YIELD} , kips	U	Controlling U Case	P _{RUPTURE} , kips
35	159.6	0.837	Case 2	170.6
36	159.6	0.856	Case 2	174.5
37	159.6	0.856	Case 2	174.5
38	15.3	0.960	Case 2	22.8
39	33.1	0.928	Case 2	44.9
40	34.4	0.928	Case 2	45.9
41	34.4	0.928	Case 2	45.9
42	35.1	0.928	Case 2	46.9
43	112.2	0.930	Case 2	161.6
44	116.7	0.930	Case 2	165.4
45	37.4	0.873	Case 2	47.9
46	36.5	0.873	Case 2	46.5
47	35.7	0.951	Case 2	49.5
48	36.4	0.951	Case 2	50.7
49	36.5	0.873	Case 2	46.5
50	36.2	0.873	Case 2	46.0
51	52.4	0.915	Case 2	80.6
52	51.0	0.939	Case 2	85.3
53	112.2	0.895	Case 2	148.9
54	115.0	0.954	Case 2	162.5
55	215.1	0.722	Case 2	220.7
56	215.1	0.911	Case 4	278.5
57	106.5	0.800	Case 2	121.4
58	106.5	0.667	Case 4	101.2
59	231.2	0.803	Case 2	270.6
60	231.2	0.692	Case 4	233.5
61	106.5	0.814	Case 2	123.4
62	106.5	0.814	Case 2	123.4
63	203.2	0.667	Case 2	184.4
64	102.9	0.866	Case 2	120.3
65	103.0	0.690	Case 2	95.8
66	102.9	0.731	Case 4	101.5
67	101.6	0.809	Case 4	111.8
68	101.6	0.743	Case 4	102.6
69	166.0	0.783	Case 4	172.2
70	166.0	0.848	Case 4	186.6

Table 6.4 continued

Index	P _{YIELD} , kips	U	Controlling U Case	P _{RUPTURE} , kips
71	141.2	0.683	Case 4	130.9
72	140.8	0.775	Case 4	148.1
73	141.8	0.841	Case 4	161.9
74	142.8	0.797	Case 2	154.4
75	143.5	0.885	Case 2	172.4
76	150.3	0.701	Case 4	155.5
77	121.4	0.820	Case 4	143.4
78	60.4	0.819	Case 4	58.6
79	73.2	0.814	Case 4	73.5
80	75.6	0.793	Case 4	73.2
81	91.7	0.810	Case 4	93.5
82	89.4	0.786	Case 4	83.0
83	110.5	0.822	Case 4	120.7
84	56.8	0.687	Case 4	64.8
85	56.8	0.796	Case 2	75.1
86	113.7	0.687	Case 4	129.6
87	113.7	0.637	Case 4	120.2
88	107.6	0.755	Case 4	109.7
89	107.6	0.754	Case 4	109.5
90	107.6	0.751	Case 4	109.2
91	107.6	0.788	Case 4	114.5
92	107.6	0.788	Case 4	114.5
93	93.4	0.647	Case 4	86.5
94	93.4	0.645	Case 4	86.3
95	93.4	0.644	Case 4	86.1
96	64.8	0.786	Case 4	70.2
97	64.8	0.791	Case 4	70.7
98	64.8	0.788	Case 4	70.3
99	64.8	0.651	Case 4	58.1
100	53.8	0.833	Case 4	58.3
101	53.8	0.834	Case 4	58.4
102	53.8	0.834	Case 4	58.3
103	55.3	0.830	Case 4	60.7
104	55.3	0.829	Case 4	60.6
105	55.3	0.830	Case 4	60.7
106	55.3	0.849	Case 4	62.1

Table 6.4 continued

Index	P _{YIELD} , kips	U	Controlling U Case	P _{RUPTURE} , kips
107	53.8	0.833	Case 4	58.3
108	53.8	0.833	Case 4	58.3
109	53.8	0.833	Case 4	58.3
110	55.3	0.828	Case 4	60.6
111	55.3	0.828	Case 4	60.6
112	55.3	0.828	Case 4	60.6
113	55.3	0.828	Case 4	60.6
114	110.5	0.832	Case 2	149.3
115	67.3	0.830	Case 2	90.8
116	61.6	0.858	Case 2	85.8
117	76.0	0.864	Case 2	106.6
118	110.5	0.932	Case 2	167.3
119	67.3	0.913	Case 2	100.0
120	61.6	0.908	Case 2	90.9
121	110.5	0.835	Case 2	149.9
122	67.3	0.830	Case 2	90.8
123	61.6	0.858	Case 2	85.8
124	76.0	0.864	Case 2	106.6
125	110.5	0.933	Case 2	167.5
126	67.3	0.913	Case 2	100.0
127	61.6	0.908	Case 2	90.9

Table 6.5: Welded Angle Results Summary

Index	Experimental		AISC		IDEA StatiCa	
	P_{EXP} , kips	Failure Mode	P_{AISC} , kips	Controlling Limit State	P_{IDEA} , kips	Failure Mode
1	100.0	[2]	82.3	[1]	84.3	[3]
2	101.0	[2]	82.3	[1]	84.4	[3]
3	100.8	[2]	81.8	[1]	83.9	[3]
4	197.4	[2]	160.7	[1]	142.5	[3]
5	100.0	[2]	83.4	[1]	81.1	[3]
6	92.4	[2]	82.7	[1]	80.3	[3]
7	97.6	[2]	81.1	[1]	78.8	[3]
8	176.7	[2]	115.9	[1]	80.7	[3]
9	175.8	[2]	115.9	[1]	67.9	[3]
10	170.9	[2]	115.9	[1]	78.9	[3]
11	175.8	[2]	115.9	[1]	78.9	[3]
12	149.5	[2]	115.9	[1]	67.6	[3]
13	170.0	[2]	115.9	[1]	67.7	[3]
14	222.6	[2]	132.7	[1]	95.0	[3]
15	210.4	[2]	132.7	[1]	85.3	[3]
16	179.0	[2]	132.7	[1]	75.5	[3]
17	178.9	[2]	177.9	[2]	112.9	[3]
18	188.6	[1]	180.5	[2]	112.3	[3]
19	191.1	[2]	181.2	[1]	112.0	[3]
20	168.2	[2]	174.2	[2]	103.5	[3]
21	187.9	[2]	192.8	[2]	122.8	[3]
22	185.0	[2]	200.3	[2]	121.6	[3]
23	207.9	[2]	206.2	[2]	122.0	[3]
24	109.7	[1]	68.9	[1]	45.8	[3]
25	114.9	[2]	80.2	[1]	48.2	[3]
26	46.1	[1]	31.0	[1]	20.2	[3]
27	45.4	[2]	31.0	[1]	19.7	[3]
28	109.9	[2]	101.9	[1]	59.1	[3]
29	104.1	[2]	101.9	[1]	58.2	[3]
30	55.1	[2]	40.2	[1]	27.2	[3]
31	56.2	[1]	40.2	[1]	26.3	[3]
32	159.4	[2]	96.6	[1]	57.2	[3]

Table 6.5 continued

Index	Experimental		AISC		IDEA StatiCa	
	P_{EXP} , kips	Failure Mode	P_{AISC} , kips	Controlling Limit State	P_{IDEA} , kips	Failure Mode
33	147.3	[2]	96.6	[1]	57.0	[3]
34	189.3	[2]	159.6	[1]	89.7	[3]
35	170.2	[2]	159.6	[1]	89.6	[3]
36	187.3	[2]	159.6	[1]	89.7	[3]
37	182.8	[2]	159.6	[1]	89.7	[3]
38	23.2	[2]	15.3	[1]	9.0	[3]
39	45.0	[2]	33.1	[1]	21.1	[3]
40	47.4	[2]	34.4	[1]	21.9	[3]
41	45.0	[2]	34.4	[1]	26.0	[3]
42	50.8	[2]	35.1	[1]	22.3	[3]
43	163.4	[2]	112.2	[1]	72.8	[3]
44	172.4	[2]	116.7	[1]	75.6	[3]
45	49.9	[2]	37.4	[1]	20.5	[3]
46	50.4	[2]	36.5	[1]	20.1	[3]
47	51.7	[2]	35.7	[1]	22.9	[3]
48	51.3	[2]	36.4	[1]	23.4	[3]
49	52.2	[2]	36.5	[1]	25.0	[3]
50	50.6	[2]	36.2	[1]	19.9	[3]
51	83.2	[2]	52.4	[1]	30.7	[3]
52	82.7	[2]	51.0	[1]	32.0	[3]
53	150.0	[2]	112.2	[1]	66.7	[3]
54	160.1	[2]	115.0	[1]	79.4	[3]
55	223.7	[2]	215.1	[1]	174.3	[3]
56	265.5	[2]	215.1	[1]	219.5	[3]
57	129.7	[2]	106.5	[1]	68.8	[3]
58	123.0	[2]	101.2	[2]	68.8	[3]
59	281.0	[2]	231.2	[1]	149.1	[3]
60	275.4	[2]	231.2	[1]	149.1	[3]
61	129.7	[2]	106.5	[1]	68.8	[3]
62	125.0	[2]	106.5	[1]	68.8	[3]
63	208.0	[2]	184.4	[2]	153.4	[3]
64	126.3	[2]	102.9	[1]	74.7	[3]
65	109.0	[2]	95.8	[2]	61.8	[3]
66	125.4	[2]	101.5	[2]	74.6	[3]

Table 6.5 continued

Index	Experimental		AISC		IDEA StatiCa	
	P_{EXP} , kips	Failure Mode	P_{AISC} , kips	Controlling Limit State	P_{EXP} , kips	Failure Mode
67	125.0	[2]	101.6	[1]	61.0	[3]
68	116.9	[2]	101.6	[1]	61.0	[3]
69	206.8	[2]	166.0	[1]	114.5	[3]
70	202.6	[2]	166.0	[1]	114.4	[3]
71	180.3	[2]	130.9	[2]	133.5	[3]
72	185.7	[2]	140.8	[1]	143.2	[3]
73	180.1	[2]	141.8	[1]	144.7	[3]
74	185.5	[2]	142.8	[1]	132.4	[3]
75	188.8	[2]	143.5	[1]	146.5	[3]
76	196.7	[2]	150.3	[1]	131.9	[3]
77	175.8	[2]	121.4	[1]	123.1	[3]
78	79.4	[1]	58.6	[2]	62.1	[3]
79	93.1	[2]	73.2	[1]	75.0	[3]
80	110.2	[2]	73.2	[2]	77.4	[3]
81	127.2	[2]	91.7	[1]	93.8	[3]
82	126.1	[2]	83.0	[2]	91.0	[3]
83	160.3	[2]	110.5	[1]	112.9	[3]
84	77.3	[2]	56.8	[1]	35.3	[3]
85	75.8	[2]	56.8	[1]	35.1	[3]
86	170.7	[2]	113.7	[1]	116.3	[3]
87	172.8	[2]	113.7	[1]	107.0	[3]
88	107.6	[2]	107.6	[1]	70.4	[3]
89	106.4	[2]	107.6	[1]	70.4	[3]
90	103.7	[2]	107.6	[1]	70.4	[3]
91	106.9	[2]	107.6	[1]	69.7	[3]
92	104.8	[2]	107.6	[1]	69.7	[3]
93	81.4	[2]	86.5	[2]	60.4	[3]
94	79.8	[2]	86.3	[2]	60.4	[3]
95	78.8	[2]	86.1	[2]	60.4	[3]
96	76.5	[2]	64.8	[1]	41.8	[3]
97	80.4	[2]	64.8	[1]	41.8	[3]
98	77.6	[2]	64.8	[1]	41.8	[3]
99	76.5	[2]	58.1	[2]	41.7	[3]
100	63.8	[2]	53.8	[1]	35.5	[3]
101	64.8	[2]	53.8	[1]	35.5	[3]

Table 6.5 continued

Index	Experimental		AISC		IDEA StatiCa	
	P_{EXP} , kips	Failure Mode	P_{AISC} , kips	Controlling Limit State	P_{EXP} , kips	Failure Mode
102	64.7	[2]	53.8	[1]	35.5	[3]
103	68.4	[2]	55.3	[1]	36.7	[3]
104	65.7	[2]	55.3	[1]	36.8	[3]
105	66.6	[2]	55.3	[1]	36.7	[3]
106	67.1	[2]	55.3	[1]	36.7	[3]
107	61.0	[2]	53.8	[1]	34.6	[3]
108	59.0	[2]	53.8	[1]	34.6	[3]
109	64.9	[2]	53.8	[1]	34.6	[3]
110	65.8	[2]	55.3	[1]	36.0	[3]
111	62.3	[2]	55.3	[1]	36.0	[3]
112	67.2	[2]	55.3	[1]	36.0	[3]
113	64.1	[2]	55.3	[1]	36.0	[3]
114	123.9	[2]	110.5	[1]	71.9	[3]
115	80.9	[2]	67.3	[1]	50.9	[3]
116	80.0	[2]	61.6	[1]	48.4	[3]
117	98.9	[2]	76.0	[1]	57.3	[3]
118	139.4	[2]	110.5	[1]	90.8	[3]
119	105.7	[2]	67.3	[1]	60.7	[3]
120	91.1	[2]	61.6	[1]	54.7	[3]
121	122.3	[2]	110.5	[1]	74.8	[3]
122	78.7	[2]	67.3	[1]	53.5	[3]
123	71.9	[2]	61.6	[1]	51.8	[3]
124	81.6	[2]	76.0	[1]	61.9	[3]
125	138.9	[2]	110.5	[1]	96.3	[3]
126	84.5	[2]	67.3	[1]	63.8	[3]
127	77.3	[2]	61.6	[1]	58.1	[3]

[1] tensile yield; [2] tensile rupture; [3] member strain

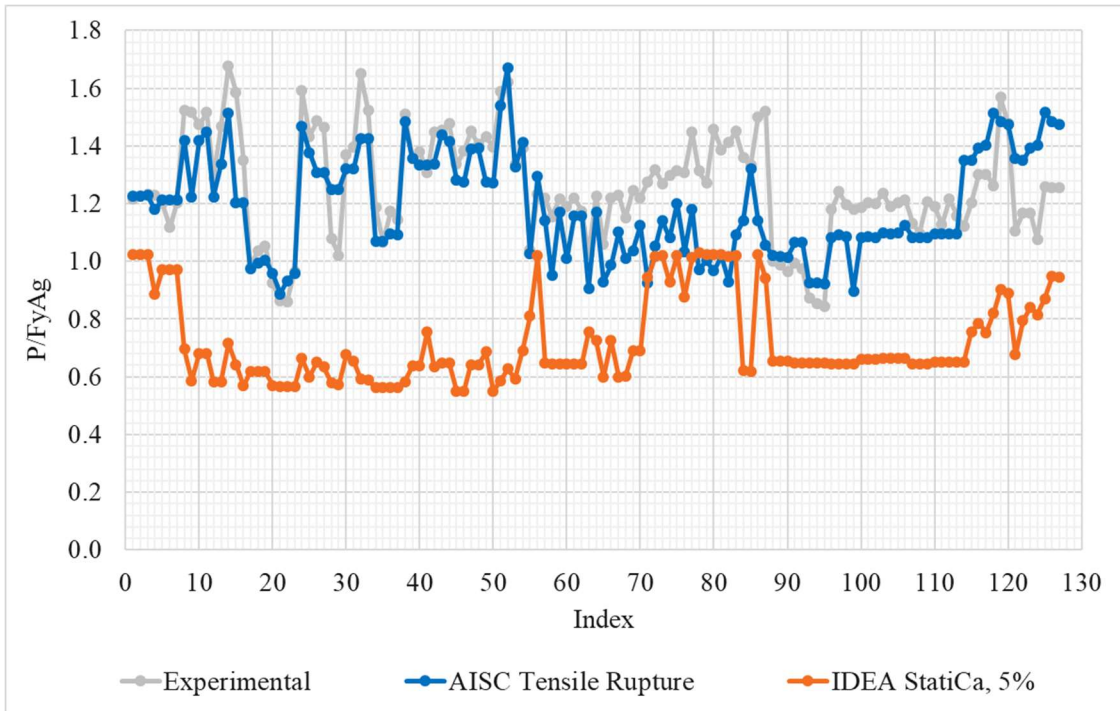


Figure 6.4: Welded angle results: strength ratio vs. index

Due to the basis of IDEA StatiCa's material behavior model being based off the tensile yield strength and not incorporating the ultimate tensile strength, an investigation into the impact of the ratio of F_u/F_y was conducted. Figure 6.5 is a scatterplot with strengths, P , normalized by $F_y A_g$ and plotted with the material ratio F_u/F_y . Trendlines were added, and all strengths trend with a positive slope as the material ratio, F_u/F_y , increases. Figure 6.6 provides a scatterplot representing the correlation of P_{IDEA}/P_{EXP} to F_u/F_y . The trendline contains a negative slope meaning as the difference of F_u to F_y increases, the difference of P_{IDEA} to P_{EXP} increases.

An investigation into the impact of plastic strain limits was conducted for this experimental set of specimens. The results are presented in two separate ways in the following figures. Figure 6.7 provides a plot similar to Figure 6.4 previously described, except with the addition of IDEA StatiCa strengths for varying plastic strain limits. Figure 6.8 provides the strengths for each plastic strain limit normalized by the strength obtained with the default plastic strain limit (5%). It should be noted, there are some gaps in the data where the Python code did not complete the determination of the maximum permitted applied load. The plots depict the impact of changing the plastic strain limit such that as the plastic strain limit increases, the maximum permitted applied load increases. Similarly, as the plastic strain limit decreases, the maximum permitted applied load decreases. It is interesting to note, the plot in Figure 6.8 appears to be very symmetrical about the line representing the strength with the 5% plastic strain limit. Some specimens resulted in a smaller difference from one strain limit to the next. This could indicate a more severe stress concentration on that particular specimen.

An examination of mesh dependency was conducted for the set of experimental specimens as well. The results are provided in Figure 6.9 as the strengths for each mesh parameter set is normalized by the corresponding strength of the default mesh. For the majority of this experimental specimen set, there is very little change in strength from one mesh parameter set to the next, indicating convergence of the mesh. However, there are a few cases where the change from mesh set 'C' to the stricter mesh set 'D' is quite

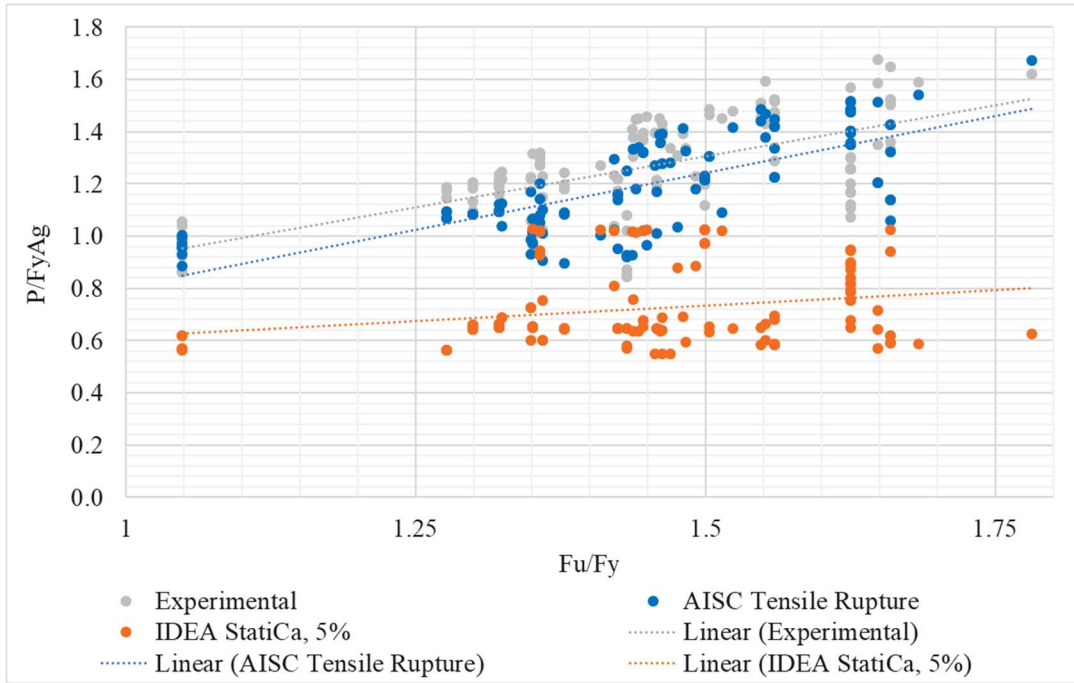


Figure 6.5: Welded angle results: normalized strength as a function of material ratio scatterplot

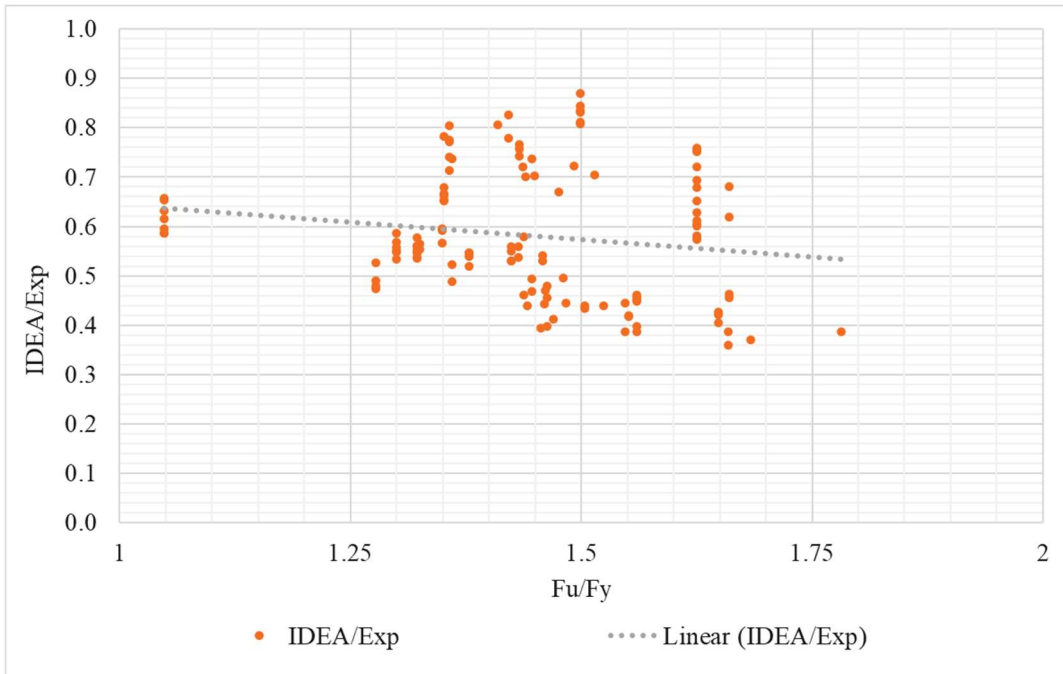


Figure 6.6: Welded angle results: IDEA StatiCa to experimental ratio as function of material ratio scatterplot

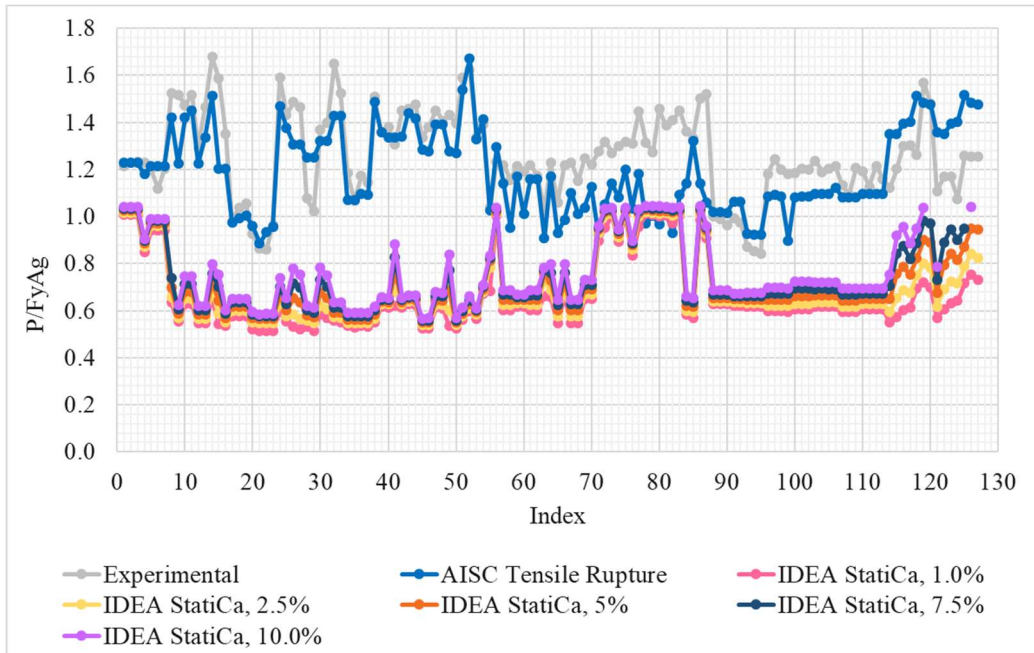


Figure 6.7: Welded angle results: strength ratio vs. index for varying plastic strain limits

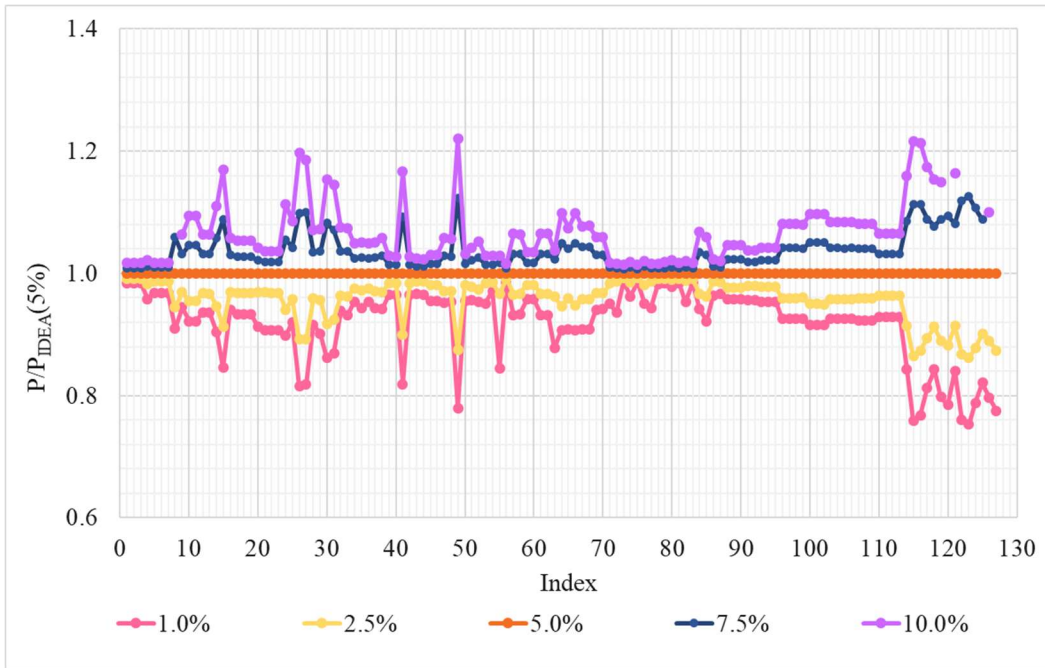


Figure 6.8: Welded angle results: ratio of strength to IDEA StatiCa strength with 5% plastic strain limit plotted with index

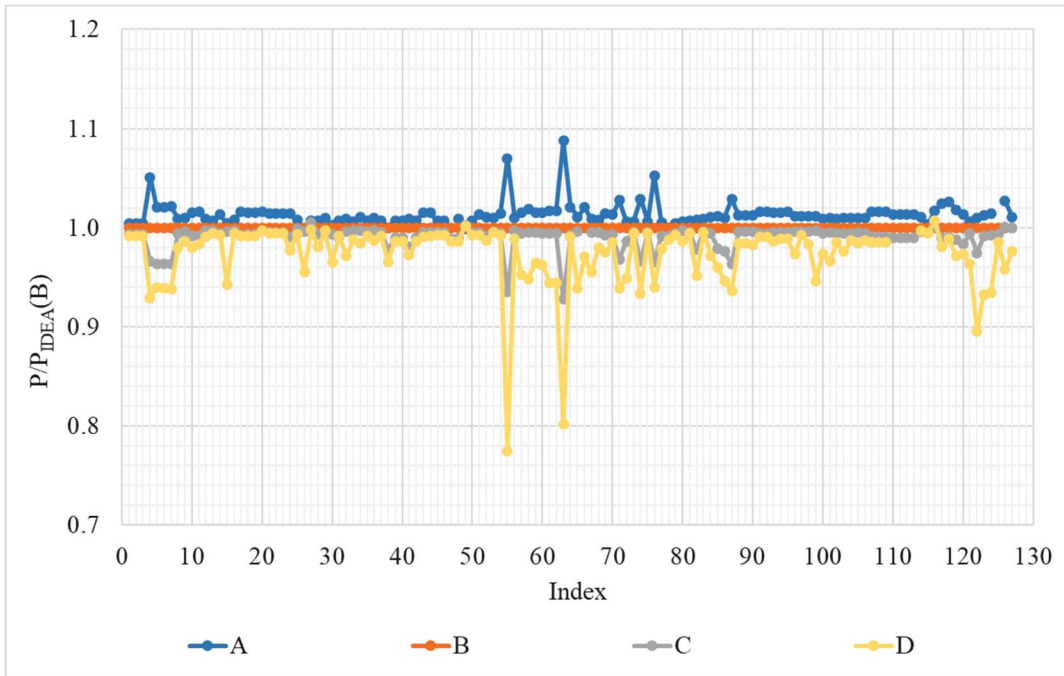


Figure 6.9: Welded angle results: ratio of varying mesh parameters sets to the default mesh settings plotted with index

significant. For example, this is seen in specimens with experimental indices 55, 63 and 122.

Table 6.6 contains the statistical data from the experimental strength comparisons for the welded angle experimental specimen set. The average test-to-predicted ratio for the tensile rupture strength according to the AISC *Specification* (2016) is just slightly above one, indicating the specification equations are predicting the strength very well on average. The average test-to-predicted ratio for IDEA StatiCa is well above 1.0. On average for this particular set of data, IDEA StatiCa is conservative at predicting the strength of this set of specimens. This data generated was used in the reliability analysis, which is outlined in the next section for welded angles. The reliability analysis only uses the average and coefficient of variation of the test-to-predicted ratio $P_{EXP/PRUPTURE}$ for the generation of random variable \tilde{X}_R .

6.3 Reliability Analysis

6.3.1 Description of Reliability Set

The reliability set consists of selected connections based on varying desired parameters. For the welded angle set it was desired to vary the following: A/B ratio (connected leg length to unconnected leg length), thickness, and weld configuration. There were three weld configurations that were selected for these specimens, 2 longitudinal 4 in. welds, 2 longitudinal 8 in. welds, and a balanced weld configuration. The reliability set specimen parameters are outlined in Table 6.7.

6.3.2 Results

The strength results for the reliability set of welded angle specimens is provided in Table 6.8. The nominal and design strengths for the AISC *Specification* (2016) is provided; however, only the controlling design strength was used in the reliability analysis. As for the IDEA StatiCa strength results, P_{IDEA} was based on the use of all default settings (mesh parameter set 'B', 5.0% plastic strain limit, and all resistance

Table 6.6: Statistical Results for Welded Angles

Test-to-Predicted Ratio	Average	Standard Deviation	Coefficient of Variation
$P_{EXP}/P_{RUPTURE}$ (AISC)	1.065	0.138	0.130
P_{EXP}/P_{IDEA}	1.804	0.400	0.222

Table 6.7: Welded Angle Reliability Analysis Parameters

Index	A , in.	B , in.	t , in.	Material Grade	F_y , ksi	F_u , ksi	L_{toe} , in.	L_{heel} , in.	Weld Size, in.	Balanced/ Unbalanced
1	4.0	6.0	0.375	A36 (Angle)	36	58	4.00	4.00	0.313	Unbalanced
2	4.0	6.0	0.500	A36 (Angle)	36	58	4.00	4.00	0.313	Unbalanced
3	4.0	6.0	0.375	A36 (Angle)	36	58	8.00	8.00	0.313	Unbalanced
4	4.0	6.0	0.500	A36 (Angle)	36	58	8.00	8.00	0.313	Unbalanced
5	4.0	6.0	0.375	A36 (Angle)	36	58	2.50	8.25	0.313	Balanced
6	4.0	6.0	0.500	A36 (Angle)	36	58	3.50	10.75	0.313	Balanced
7	6.0	4.0	0.375	A36 (Angle)	36	58	4.00	4.00	0.313	Unbalanced
8	6.0	4.0	0.500	A36 (Angle)	36	58	4.00	4.00	0.313	Unbalanced
9	6.0	4.0	0.375	A36 (Angle)	36	58	8.00	8.00	0.313	Unbalanced
10	6.0	4.0	0.500	A36 (Angle)	36	58	8.00	8.00	0.313	Unbalanced
11	6.0	4.0	0.375	A36 (Angle)	36	58	3.50	7.25	0.313	Balanced
12	6.0	4.0	0.500	A36 (Angle)	36	58	4.75	9.50	0.313	Balanced
13	4.0	4.0	0.375	A36 (Angle)	36	58	4.00	4.00	0.313	Unbalanced
14	4.0	4.0	0.500	A36 (Angle)	36	58	4.00	4.00	0.313	Unbalanced
15	4.0	4.0	0.375	A36 (Angle)	36	58	8.00	8.00	0.313	Unbalanced
16	4.0	4.0	0.500	A36 (Angle)	36	58	8.00	8.00	0.313	Unbalanced
17	4.0	4.0	0.375	A36 (Angle)	36	58	2.50	6.25	0.313	Balanced
18	4.0	4.0	0.500	A36 (Angle)	36	58	5.00	11.75	0.313	Balanced

Table 6.8: Welded Angle Reliability Strength Results

Index	AISC				IDEA StatiCa
	P_{YIELD} , kips	$P_{RUPTURE}$, kips	ϕP_{YIELD} , kips	$\phi P_{RUPTURE}$, kips	P_{IDEA} , kips
1	130.0	87.0	117.0	65.3	72.2
2	171.0	116.0	153.9	87.0	92.9
3	130.0	146.6	117.0	110.0	71.8
4	171.0	191.4	153.9	143.5	92.4
5	130.0	113.3	117.0	85.0	72.4
6	171.0	180.0	153.9	135.0	92.8
7	130.0	130.5	117.0	97.9	73.5
8	171.0	174.0	153.9	130.5	93.4
9	130.0	155.8	117.0	116.8	82.1
10	171.0	203.6	153.9	152.7	104.1
11	130.0	130.5	117.0	97.9	83.9
12	171.0	192.1	153.9	144.1	105.9
13	103.0	89.3	92.7	66.9	60.0
14	135.0	116.0	121.5	87.0	76.2
15	103.0	131.5	92.7	98.6	59.9
16	135.0	171.2	121.5	128.4	75.9
17	103.0	96.2	92.7	72.2	61.3
18	135.0	173.7	121.5	130.2	77.0

factors). When comparing P_{IDEA} to the controlling design strength according to the AISC equations (ϕP_{AISC}), P_{IDEA} resulted in a larger strength in only two specimens with a 10% and 7% increased strength for reliability set specimen indices 1 and 2, respectively. For all other specimens, IDEA StatiCa indicated decreased strengths compared to the AISC code equations with an average of 26% decreased strength.

The reliability index, β , results are provided in Figure 6.10. Connections with specimen indices 3, 4, 6, 11, 12, 15, 16, and 18 all returned very large values for β indicating zero failures in 1,000,000 simulations. In general, for this particular set of reliability specimens IDEA StatiCa provided more reliable results than the AISC *Specification* (2016). Connections with specimen indices 1 and 2 were the only specimens where the AISC strength equations resulted in more reliable results than IDEA StatiCa. These specimens have the smaller A/B ratio resulting in a larger eccentricity. These two specimens also have the smallest unbalanced weld length. The larger eccentricity coupled with the smaller unbalanced weld length could be reason for this difference. IDEA StatiCa resulted in a β -value range of 3.36 to a large value. Whereas AISC resulted in a range of 3.63 to 3.77.

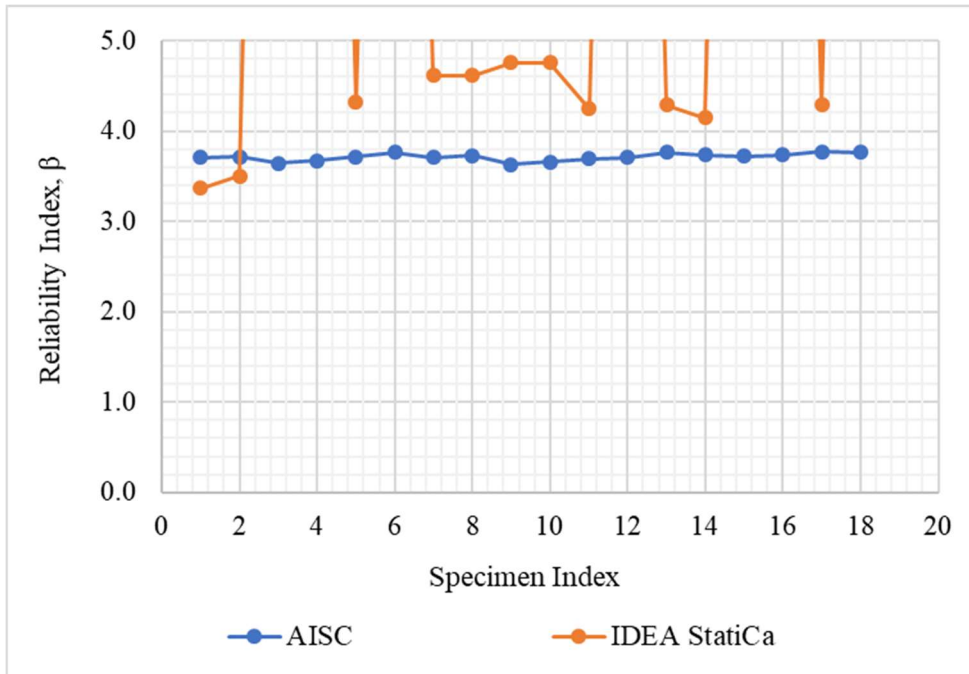


Figure 6.10: Welded angles: Reliability index for IDEA StatiCa and AISC

CHAPTER 7

BOLTED ANGLES

7.1 Description of Connection

Single and double angle tension members that are bolted or riveted to a gusset plate are evaluated in this chapter. A typical schematic with the relevant terminology is shown in Figure 7.1. For the double angle specimens, the angles are identical in cross section and material. Additionally, this chapter is only limited to regular bolt patterns without staggering.

For this set of connections, the applicable shear lag factor cases outlined in Section D3 of the AISC *Specification* (2016) and shown in Figure 3.3 include cases 2 and 8 as well as the lower limit defined in Section D3. The lower limit (the area of connected elements divided by the gross area) was checked, but never controlled. Case 2 is applicable to tension members where the load is transmitted to some but not all of the cross-section elements through fasteners (or welds). The equation for this case is as follows:

$$U = 1 - \frac{\bar{x}}{l} \quad (7-1)$$

where \bar{x} is the eccentricity of the connection (i.e. the distance between the centroid of the angle to the faying surface), and l is the length of the connection (i.e., center of first bolt to center of last bolt along the longitudinal axis of the member). Case 8 is only applicable to specimens with three or more fasteners in the direction of loading. Case 8 suggests specimens with three fasteners per line to take a U of 0.60 and specimens with four or more fasteners in each line to take a U of 0.80. The shear lag factor was taken as the larger of case 2 and case 8. The gross area and centroid were always calculated based on measured dimensions. For all bolt and rivet holes, the additional 1/16 in. for damage in accordance with Section B4.3b of the AISC *Specification* (2016) was used in the calculation of the net area. Note, however, that IDEA StatiCa does not consider the additional 1/16 in.

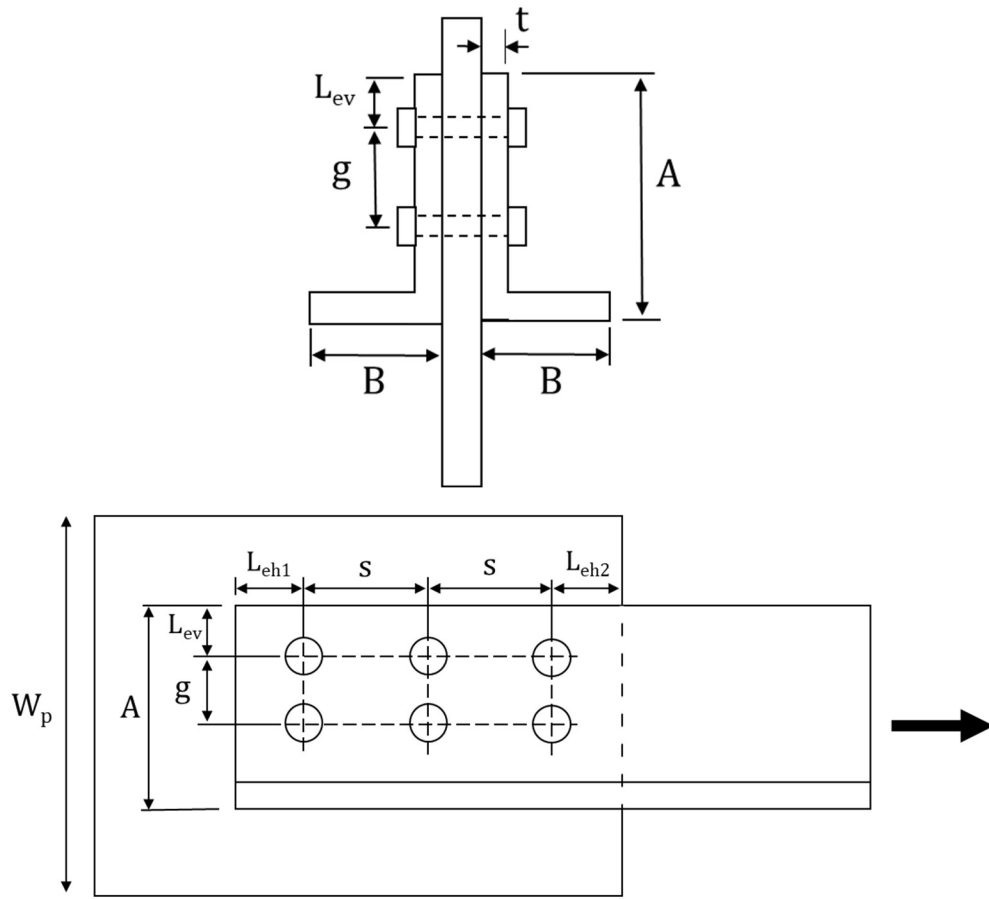


Figure 7.1: Bolted Angle Schematic

7.2 Comparison to Experimental Results

7.2.1 Description of Experimental Specimens

For this particular set of experimental specimens, there were 56 total specimens across five references. A detailed enumeration can be found in Table 7.1. A majority of specimens reported in Epstein (1992) were removed from the experimental set for a variety of reasons. A total of 22 specimens were removed due to failures classified as block shear rupture (specimens 1, 2, 3, 4, 9, 10, 11, 17, 18, 19, 21, 25, 26, 27, 29, 30, 32, 33, 34, 35, 37, and 38) and three specimens failed in a combination of block shear and bolt shear (specimens 6, 14, and 22). Additionally, seven specimens contained non-regular bolt configurations and thus removed (specimens 5, 12, 13, 20, 28, 31, and 36).

McKibben (1907) contained a variety of different bolt and angle configurations, resulting in the removal of 45 total specimens. There were 39 specimens with non-regular angle configurations (4, 5, 6, 10, 11, 12, 16, 17, 18, 19, 20, 21, 25, 26, 27, 28, 29, 30, 31, 32, 33, 34, 35, 36, 37, 38, 39, 40, 41, 42, 43, 44, 45, 52, 53, 54, 58, 59, and 60) and 6 specimens with staggered bolt patterns (46, 47, 48, 49, 50, and 51). Lastly, only two specimens were considered applicable to this study from Greiner (1897). The remaining specimens were removed due to staggered bolt patterns (47 B, 48 B) or due to non-regular angle configurations (45 AX, 46 AX, 49 BX, and 50 BX)

A detailed description of each specimen is provided in Table 7.2 and Table 7.3. The terminology of these tables is consistent with Figure 7.1. The first table provides information only on the angle members whereas the second table provides information solely pertaining to the fasteners. For specimens with only one row of bolts, the bolt gage dimension, g , is not defined and is indicated by 'N/A'. This is likewise for specimens with only bolt per row and the bolt spacing, 's'. If provided, the diameter of the bolt or rivet hole was taken as reported. Otherwise, bolt holes were taken as indicated by Table J3.3 of the AISC *Specification* (2016). For rivets, the diameter of the hole was taken as the rivet diameter unless specifically reported by the experimentalist.

Table 7.1: Bolted Angle Specimen Enumeration

Reference	Specimen Count
Kulak and Wu (1997)	24
Ke et al. (2018)	9
Epstein (1992)	6
McKibben (1907)	15
Greiner (1897)	2
Total	56

Table 7.2: Bolted Angle Specimen Details

Index	Reference	Specimen	# of angles	* F_y , ksi	* F_u , ksi	* A , in.	* B , in.	* t , in.
1	Kulak and Wu (1997)	S1	1	49.3	76.0	4.016	4.016	0.257
2	Kulak and Wu (1997)	S2	1	48.8	76.5	4.016	4.016	0.256
3	Kulak and Wu (1997)	S3	1	48.3	76.0	4.016	3.976	0.257
4	Kulak and Wu (1997)	S4	1	46.7	68.6	2.996	2.945	0.193
5	Kulak and Wu (1997)	S5	1	47.4	69.8	4.055	2.906	0.254
6	Kulak and Wu (1997)	S6	1	47.0	69.2	2.933	4.055	0.252
7	Kulak and Wu (1997)	S7	1	47.1	69.3	4.055	2.937	0.253
8	Kulak and Wu (1997)	S8	1	48.4	70.8	2.988	2.000	0.378
9	Kulak and Wu (1997)	S9	1	49.4	70.7	3.028	1.988	0.187
10	Kulak and Wu (1997)	S10	1	49.3	70.4	3.043	1.984	0.185
11	Kulak and Wu (1997)	S11	1	49.1	70.7	3.031	1.988	0.186
12	Kulak and Wu (1997)	D1-1	2	49.3	76.0	4.016	4.016	0.256
13	Kulak and Wu (1997)	D1-2	2	48.9	76.5	4.016	4.016	0.256
14	Kulak and Wu (1997)	D1-3	2	48.3	76.0	4.016	3.976	0.257
15	Kulak and Wu (1997)	D2	2	46.7	68.6	3.004	2.945	0.194
16	Kulak and Wu (1997)	D3-1	2	47.4	69.8	4.055	2.909	0.254
17	Kulak and Wu (1997)	D3-2	2	47.0	69.2	4.055	2.929	0.253
18	Kulak and Wu (1997)	D4-1	2	47.5	69.8	2.921	4.055	0.255
19	Kulak and Wu (1997)	D4-2	2	47.0	69.2	2.937	4.055	0.253
20	Kulak and Wu (1997)	D5	2	47.2	69.0	4.055	2.933	0.253
21	Kulak and Wu (1997)	D6	2	48.4	70.8	2.984	2.000	0.375

Table 7.2 continued

Index	Reference	Specimen	# of angles	* F_y , ksi	* F_u , ksi	* A , in.	* B , in.	* t , in.
22	Kulak and Wu (1997)	D7	2	49.4	70.7	3.020	1.988	0.185
23	Kulak and Wu (1997)	D8	2	49.3	70.4	3.039	1.992	0.185
24	Kulak and Wu (1997)	D9	2	49.1	70.7	3.035	1.992	0.185
25	Ke et al. (2018)	A1-60L	1	110.4	115.7	3.178	2.391	0.319
26	Ke et al. (2018)	A1-75L	1	110.4	115.7	3.129	2.374	0.317
27	Ke et al. (2018)	A1-90L	1	110.4	115.7	3.172	2.359	0.317
28	Ke et al. (2018)	A1-75S	1	110.4	115.7	2.374	3.129	0.315
29	Ke et al. (2018)	A2-60S	1	110.4	115.7	2.480	3.898	0.318
30	Ke et al. (2018)	A2-75S	1	110.4	115.7	2.559	3.898	0.313
31	Ke et al. (2018)	A2-90S	1	110.4	115.7	2.520	3.898	0.319
32	Ke et al. (2018)	B1-75L	1	42.4	65.7	3.071	2.362	0.235
33	Ke et al. (2018)	B2-75S	1	42.4	65.7	2.559	3.976	0.220
34	Epstein (1992)	7	1	51.6	74.8	6.000	6.000	0.313
35	Epstein (1992)	8	1	52.0	74.6	6.000	6.000	0.313
36	Epstein (1992)	15	1	46.5	64.9	6.000	4.000	0.313
37	Epstein (1992)	16	1	48.1	65.7	6.000	4.000	0.313
38	Epstein (1992)	23	1	45.6	69.3	6.000	3.500	0.313
39	Epstein (1992)	24	1	46.8	69.7	6.000	3.500	0.313
40	McKibben (1907)	1	1	33.2	59.3	3.500	3.000	0.375
41	McKibben (1907)	2	1	33.2	59.3	3.500	3.000	0.375
42	McKibben (1907)	3	1	33.2	59.3	3.500	3.000	0.375
43	McKibben (1907)	7	1	31.6	54.0	4.000	3.000	0.375
44	McKibben (1907)	8	1	31.6	54.0	4.000	3.000	0.375
45	McKibben (1907)	9	1	31.6	54.0	4.000	3.000	0.375
46	McKibben (1907)	13	1	31.6	54.0	4.000	3.000	0.375
47	McKibben (1907)	14	1	31.6	54.0	4.000	3.000	0.375
48	McKibben (1907)	15	1	31.6	54.0	4.000	3.000	0.375
49	McKibben (1907)	22	2	34.8	61.0	3.000	3.000	0.313
50	McKibben (1907)	23	2	34.8	61.0	3.000	3.000	0.313
51	McKibben (1907)	24	2	34.8	61.0	3.000	3.000	0.313
52	McKibben (1907)	55	2	34.8	61.0	3.000	3.000	0.313
53	McKibben (1907)	56	2	34.8	61.0	3.000	3.000	0.313
54	McKibben (1907)	57	2	34.8	61.0	3.000	3.000	0.313
55	Greiner (1897)	43 A	1	38.9	59.4	3.500	3.500	0.375
56	Greiner (1897)	44 A	1	38.9	59.4	3.500	3.500	0.375

* indicates measured value

Table 7.3: Bolted Angle Fastener Details

Index	Bolts/ Rivets	Bolt Material	<i>d</i> , in.	# of rows of fasteners	# of fasteners per row	<i>s</i> , in.	<i>L_{eh}</i> , in.	<i>g</i> , in.	<i>L_{ev}</i> , in.
1	Bolts	A490	0.875	1	6	3.000	1.500	N/A	1.516
2	Bolts	A490	0.875	1	6	3.000	1.500	N/A	1.516
3	Bolts	A490	0.875	1	6	3.000	1.500	N/A	1.516
4	Bolts	A490	0.875	1	6	3.000	1.500	N/A	1.246
5	Bolts	A490	0.875	1	6	3.000	1.500	N/A	1.555
6	Bolts	A490	0.875	1	6	3.000	1.500	N/A	1.183
7	Bolts	A490	0.875	1	6	3.000	1.500	N/A	1.555
8	Bolts	A490	0.875	1	6	3.000	1.500	N/A	1.238
9	Bolts	A490	0.875	1	6	3.000	1.500	N/A	1.278
10	Bolts	A490	0.875	1	4	3.000	1.500	N/A	1.293
11	Bolts	A490	0.875	1	2	3.000	1.500	N/A	1.281
12	Bolts	A490	0.875	1	6	3.000	1.500	N/A	1.516
13	Bolts	A490	0.875	1	6	3.000	1.500	N/A	1.516
14	Bolts	A490	0.875	1	6	3.000	1.500	N/A	1.516
15	Bolts	A490	0.875	1	6	3.000	1.500	N/A	1.254
16	Bolts	A490	0.875	1	6	3.000	1.500	N/A	1.555
17	Bolts	A490	0.875	1	6	3.000	1.500	N/A	1.555
18	Bolts	A490	0.875	1	6	3.000	1.500	N/A	1.171
19	Bolts	A490	0.875	1	6	3.000	1.500	N/A	1.187
20	Bolts	A490	0.875	1	6	3.000	1.500	N/A	1.555
21	Bolts	A490	0.875	1	6	3.000	1.500	N/A	1.234
22	Bolts	A490	0.875	1	6	3.000	1.500	N/A	1.270
23	Bolts	A490	0.875	1	4	3.000	1.500	N/A	1.289
24	Bolts	A490	0.875	1	2	3.000	1.500	N/A	1.285
25	Bolts	Gr. 12.9	0.866	1	5	2.362	2.362	N/A	1.575
26	Bolts	Gr. 12.9	0.866	1	5	2.953	2.362	N/A	1.575
27	Bolts	Gr. 12.9	0.866	1	5	3.543	2.362	N/A	1.575
28	Bolts	Gr. 12.9	0.866	1	5	2.953	2.362	N/A	1.181
29	Bolts	Gr. 12.9	0.866	1	5	2.362	2.362	N/A	1.280
30	Bolts	Gr. 12.9	0.866	1	5	2.953	2.362	N/A	1.280
31	Bolts	Gr. 12.9	0.866	1	5	3.543	2.362	N/A	1.280
32	Bolts	Gr. 12.9	0.866	1	5	2.953	2.362	N/A	1.575
33	Bolts	Gr. 12.9	0.866	1	5	2.953	2.362	N/A	1.280
34	Bolts	A490X	0.750	2	3	3.000	1.500	2.500	1.250

Table 7.3 continued

Index	Bolts/ Rivets	Bolt Material	d , in.	# of rows of fasteners	# of fasteners per row	s , in.	L_{eh} , in.	g , in.	L_{ev} , in.
35	Bolts	A490X	0.750	2	4	3.000	1.500	2.500	1.250
36	Bolts	A490X	0.750	2	3	3.000	1.500	2.500	1.250
37	Bolts	A490X	0.750	2	4	3.000	1.500	2.500	1.250
38	Bolts	A490X	0.750	2	3	3.000	1.500	2.500	1.250
39	Bolts	A490X	0.750	2	4	3.000	1.500	2.500	1.250
40	Rivets	NP	0.875	1	6	2.625	1.500	N/A	1.500
41	Rivets	NP	0.875	1	6	2.625	1.500	N/A	1.500
42	Rivets	NP	0.875	1	6	2.625	1.500	N/A	1.500
43	Rivets	NP	0.875	1	6	2.625	1.500	N/A	1.500
44	Rivets	NP	0.875	1	6	2.625	1.500	N/A	1.500
45	Rivets	NP	0.875	1	6	2.625	1.500	N/A	1.500
46	Rivets	NP	0.875	1	6	2.625	1.500	N/A	1.500
47	Rivets	NP	0.875	1	6	2.625	1.500	N/A	1.500
48	Rivets	NP	0.875	1	6	2.625	1.500	N/A	1.500
49	Rivets	NP	0.875	1	6	3.000	1.500	N/A	1.250
50	Rivets	NP	0.875	1	6	3.000	1.500	N/A	1.250
51	Rivets	NP	0.875	1	6	3.000	1.500	N/A	1.250
52	Rivets	NP	0.875	1	6	3.000	1.500	N/A	1.250
53	Rivets	NP	0.875	1	6	3.000	1.500	N/A	1.250
54	Rivets	NP	0.875	1	6	3.000	1.500	N/A	1.250
55	Rivets	NP	0.875	1	5	2.750	1.500	N/A	1.750
56	Rivets	NP	0.875	1	5	2.750	1.500	N/A	1.750

The modelling process of the bolted angle specimens was similar to the majority of this study. The gusset plates and angles were all modeled as members. The bearing member was always selected as the gusset plate for all bolted angles. An example modeled in IDEA StatiCa is provided in Figure 7.2. The typical process for modelling the bolted angle specimens included the following:

1. Procedure outlined in Chapter 3.3
2. Create members:
 - a. Member 1: Gusset plate
 - i. Geometrical Type set to “Ended”
 - ii. Offset ex set to the negative of the connection length
 1. Connection length is 2 times L_{ch} + (the number of bolts per row minus one) times the bolt spacing
 - b. Member 2, 3 (if applicable): Angle(s)
 - i. β set to 180°
 - ii. Aligned set to “To member plate”
 - iii. Aligned plate set to “[angle name] | bottom flange 1”
 - iv. Related plate set to “[gusset plate name] | bottom flange 1”
 - v. Model type set to “N-Vy-Vz”
3. Create Bolt Grid operation:
 - a. Fastener set to “Bolts”
 - b. Items count set to the 2 for single angles and 3 for double angles
 - c. Item 1, 2, 3, set to each member created in step 1
 - d. Type set to the diameter and bolt type indicated by report
 - i. Bolt type typically selected as A490 bolts due to the removal of bolt failures
 - e. Coord. System set to “Orthogonal”
 - f. Rows, Positions set to dimension indicated by reports
 - g. Grid set to “Regular”
 - h. Shear force transfer set to “Bearing – tension/shear interaction”

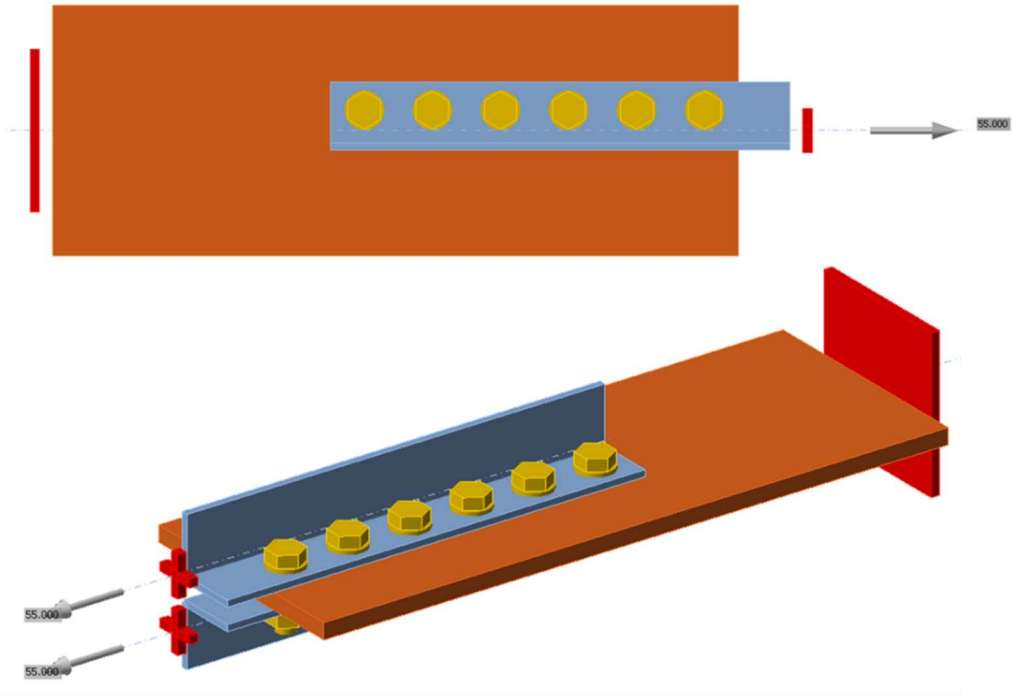


Figure 7.2: Typical Bolted Angle Model

7.2.2 Results

The results according to the AISC *Specification* (2016) equations for the bolted angle experimental set are provided in Table 7.4. As previously mentioned, shear lag factor case 2 was the controlling case for all specimens in this experimental set. The results are provided for the tensile yield strength and tensile rupture strength individually in this table.

A summary of the strength results for the experimental set is provided below in Table 7.5. Consistent with much of this study, the experimentalists reported the experimental failure mode as tensile rupture, potentially ignoring tensile yield. The strength according to the AISC *Specification* (2016) equations, P_{AISC} , is presented as the minimum of tensile yield and tensile rupture, unlike the previous table. The AISC *Specification* equations primarily predict tensile yield as the controlling limit state. The IDEA StatiCa results in this table are reported as the default mesh settings (mesh parameter set 'B') and with a 5% plastic strain limit. The maximum permitted applied load according to IDEA StatiCa, P_{IDEA} , was always more conservative than both P_{AISC} and P_{EXP} . When comparing P_{IDEA} to P_{AISC} , the most conservative case was found with the specimen with the experimental set index 33. This specimen resulted in a maximum permitted applied load in IDEA StatiCa of 50% less than the strength according to the AISC *Specification* equations. On the contrary, the least conservative case indicates only a 10% difference between P_{IDEA} and P_{AISC} .

The strength results for the bolted angle experimental set are plotted in Figure 7.3 with the corresponding experimental index. The strengths are normalized with the predicted yield strength, $F_y A_g$. For this experimental set of specimens, the strengths according to the IDEA StatiCa analyses are conservative for all specimens, which is consistent with the tabulated values previously discussed. The results here do show IDEA StatiCa to be conservative, however these results do not consider uncertainties in material properties, geometric properties, or in the analysis. A reliability analysis is conducted in the next section to address these uncertainties.

Table 7.4: Bolted Angle AISC Calculation Results

Index	P _{YIELD} , kips	U	Controlling U Case	P _{RUPTURE} , kips
1	98.4	0.927	Case 2	122.5
2	97.0	0.927	Case 2	122.6
3	96.4	0.928	Case 2	122.4
4	51.8	0.947	Case 2	59.5
5	80.7	0.953	Case 2	96.5
6	80.1	0.915	Case 2	92.0
7	80.3	0.953	Case 2	95.8
8	84.4	0.964	Case 2	93.3
9	44.7	0.969	Case 2	49.2
10	44.2	0.949	Case 2	47.5
11	44.2	0.845	Case 2	42.6
12	196.3	0.927	Case 2	244.4
13	194.5	0.927	Case 2	245.8
14	192.1	0.928	Case 2	243.9
15	104.1	0.947	Case 2	119.5
16	161.8	0.953	Case 2	193.4
17	160.6	0.953	Case 2	191.9
18	162.6	0.915	Case 2	186.2
19	160.0	0.915	Case 2	183.7
20	161.2	0.953	Case 2	191.3
21	167.2	0.964	Case 2	184.7
22	88.3	0.969	Case 2	97.2
23	88.6	0.948	Case 2	95.3
24	88.1	0.845	Case 2	85.0
25	184.6	0.933	Case 2	146.5
26	181.2	0.947	Case 2	145.5
27	182.4	0.956	Case 2	148.1
28	180.1	0.915	Case 2	139.8
29	212.8	0.861	Case 2	160.7
30	212.5	0.890	Case 2	166.4
31	214.7	0.908	Case 2	171.2
32	51.8	0.949	Case 2	61.8
33	59.0	0.891	Case 2	68.7
34	188.5	0.731	Case 2	169.7

Table 7.4 continued

Index	P _{YIELD} , kips	U	Controlling U Case	P _{RUPTURE} , kips
35	189.9	0.820	Case 2	190.1
36	140.8	0.847	Case 2	136.4
37	145.6	0.898	Case 2	146.4
38	130.9	0.873	Case 2	140.6
39	134.4	0.915	Case 2	148.3
40	76.2	0.937	Case 2	106.8
41	76.2	0.937	Case 2	106.8
42	76.2	0.937	Case 2	106.8
43	78.5	0.940	Case 2	107.1
44	78.5	0.940	Case 2	107.1
45	78.5	0.940	Case 2	107.1
46	78.5	0.940	Case 2	107.1
47	78.5	0.940	Case 2	107.1
48	78.5	0.940	Case 2	107.1
49	123.7	0.942	Case 2	168.4
50	123.7	0.942	Case 2	168.4
51	123.7	0.942	Case 2	168.4
52	123.7	0.942	Case 2	168.4
53	123.7	0.942	Case 2	168.4
54	123.7	0.942	Case 2	168.4
55	96.5	0.908	Case 2	113.7
56	96.5	0.908	Case 2	113.7

Table 7.5: Bolted Angles Results Summary

Index	Experimental		AISC		IDEA StatiCa	
	P_{EXP} , kips	Failure Mode	P_{AISC} , kips	Controlling Limit State	P_{IDEA} , kips	Failure Mode
1	115.3	[2]	98.4	[1]	54.2	[3]
2	117.1	[2]	97.0	[1]	53.5	[3]
3	109.5	[2]	96.4	[1]	53.1	[3]
4	62.2	[2]	51.8	[1]	28.1	[3]
5	100.4	[2]	80.7	[1]	46.2	[3]
6	91.0	[2]	80.1	[1]	40.1	[3]
7	97.3	[2]	80.3	[1]	46.0	[3]
8	93.3	[2]	84.4	[1]	43.1	[3]
9	52.5	[2]	44.7	[1]	26.3	[3]
10	53.9	[2]	44.2	[1]	26.2	[3]
11	44.6	[2]	42.6	[2]	23.9	[3]
12	218.8	[2]	196.3	[1]	163.3	[3]
13	224.2	[2]	194.5	[1]	162.0	[3]
14	222.6	[2]	192.1	[1]	160.5	[3]
15	110.7	[2]	104.1	[1]	92.8	[3]
16	188.4	[2]	161.8	[1]	145.1	[3]
17	191.1	[2]	160.6	[1]	143.5	[3]
18	179.2	[2]	162.6	[1]	143.0	[3]
19	175.8	[2]	160.0	[1]	140.8	[3]
20	192.7	[2]	161.2	[1]	143.9	[3]
21	183.2	[2]	167.2	[1]	145.3	[3]
22	92.8	[2]	88.3	[1]	77.1	[3]
23	96.5	[2]	88.6	[1]	76.2	[3]
24	77.5	[2]	85.0	[2]	52.2	[3]
25	142.1	[2]	146.5	[2]	91.6	[3]
26	147.5	[2]	145.5	[2]	90.1	[3]
27	148.4	[2]	148.1	[2]	90.7	[3]
28	121.8	[2]	139.8	[2]	79.0	[3]
29	132.6	[2]	160.7	[2]	89.9	[3]
30	137.8	[2]	166.4	[2]	91.8	[3]
31	140.5	[2]	171.2	[2]	91.1	[3]
32	88.8	[2]	51.8	[1]	29.0	[3]
33	69.9	[2]	59.0	[1]	29.4	[3]
34	237.1	[2]	169.7	[2]	90.0	[3]

Table 7.5 continued

Index	Experimental		AISC		IDEA StatiCa	
	P_{EXP} , kips	Failure Mode	P_{AISC} , kips	Controlling Limit State	P_{EXP} , kips	Failure Mode
35	297.7	[2]	189.9	[1]	97.6	[3]
36	218.6	[2]	136.4	[2]	76.2	[3]
37	243.5	[2]	145.6	[1]	81.9	[3]
38	236.5	[2]	130.9	[1]	73.3	[3]
39	255.2	[2]	134.4	[1]	77.4	[3]
40	89.5	[2]	76.2	[1]	41.2	[3]
41	96.1	[2]	76.2	[1]	41.2	[3]
42	95.2	[2]	76.2	[1]	41.2	[3]
43	85	[2]	78.5	[1]	43.7	[3]
44	84	[2]	78.5	[1]	43.7	[3]
45	85.6	[2]	78.5	[1]	43.7	[3]
46	88.6	[2]	78.5	[1]	43.7	[3]
47	90.4	[2]	78.5	[1]	43.7	[3]
48	91	[2]	78.5	[1]	43.7	[3]
49	134.1	[2]	123.7	[1]	111.2	[3]
50	136.5	[2]	123.7	[1]	111.2	[3]
51	139.1	[2]	123.7	[1]	111.2	[3]
52	140	[2]	123.7	[1]	111.2	[3]
53	140.7	[2]	123.7	[1]	111.2	[3]
54	140.6	[2]	123.7	[1]	111.2	[3]
55	99	[2]	96.5	[1]	51.0	[3]
56	91	[2]	96.5	[1]	51.0	[3]

[1] tensile yield; [2] tensile rupture; [3] plate strain

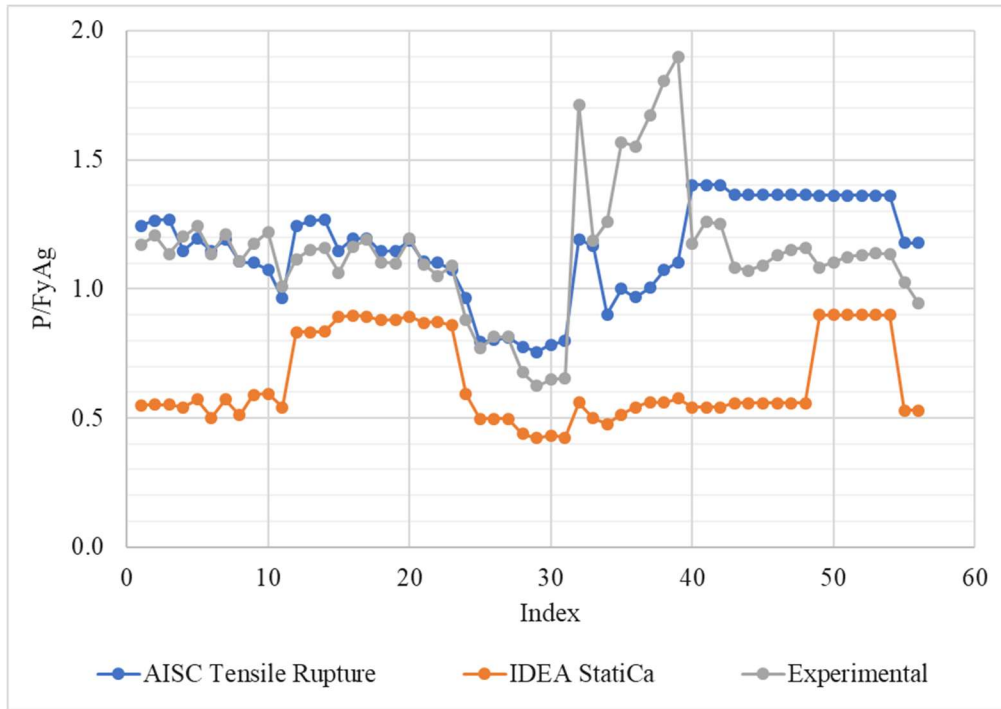


Figure 7.3: Bolted angles results: strength ratio vs. index

Similar to the previous experimental sets, the impact of the ratio F_u/F_y is examined due to the tensile rupture limit state relating more to F_u than F_y and IDEA StatiCa's behavior model incorporating F_y more than F_u . It is anticipated the accuracy of IDEA StatiCa is related to F_u/F_y . Figure 7.4 provides the strengths, P_{IDEA} , $P_{RUPTURE}$, and P_{EXP} , normalized by $F_y A_g$ and plotted against the material strength ratio F_u/F_y . Trendlines were created to see the overall trend of the data for each strength method. All trendlines result in a positive slope. Figure 7.5 provides additional detail to this investigation as the ratio P_{IDEA}/P_{EXP} is plotted with the material strength ratio F_u/F_y . The trendline does not indicate a significant correlation of this particular relationship for this set of experimental specimens.

When comparing the AISC *Specification* strength results to those from IDEA StatiCa, IDEA StatiCa provides very conservative strengths for most cases. If deemed useful, varying the plastic strain limit could be used to provide less conservative results. For this reason, an investigation into the impacts of varying plastic strain limits was conducted for this experimental set of specimens. These results are presented in Figure 7.6, which provides a plot of the normalized strengths plotted with the experimental set indices for $P_{RUPTURE}$, P_{EXP} , and P_{IDEA} for a variety of plastic strain limits. Since this entire experimental set of results indicated conservative results, the larger plastic strain limits are of more interest. When comparing the results from the 10% and 5% plastic strain limit to P_{AISC} , the 10% plastic strain limit only provides a 6% less conservative strength than the 5% plastic strain limit in the most extreme case. Figure 7.7 provides a different perspective on varying plastic strain limits. The figure contains a plot with the ratio of IDEA StatiCa strength for varying plastic strains to the IDEA StatiCa strength with a 5% plastic strain limit (default) plotted against the experimental set index. This plot contains results as expected such that the strength decreases as the plastic strain limit decreases, and the strength increases as the plastic strain limit increases.

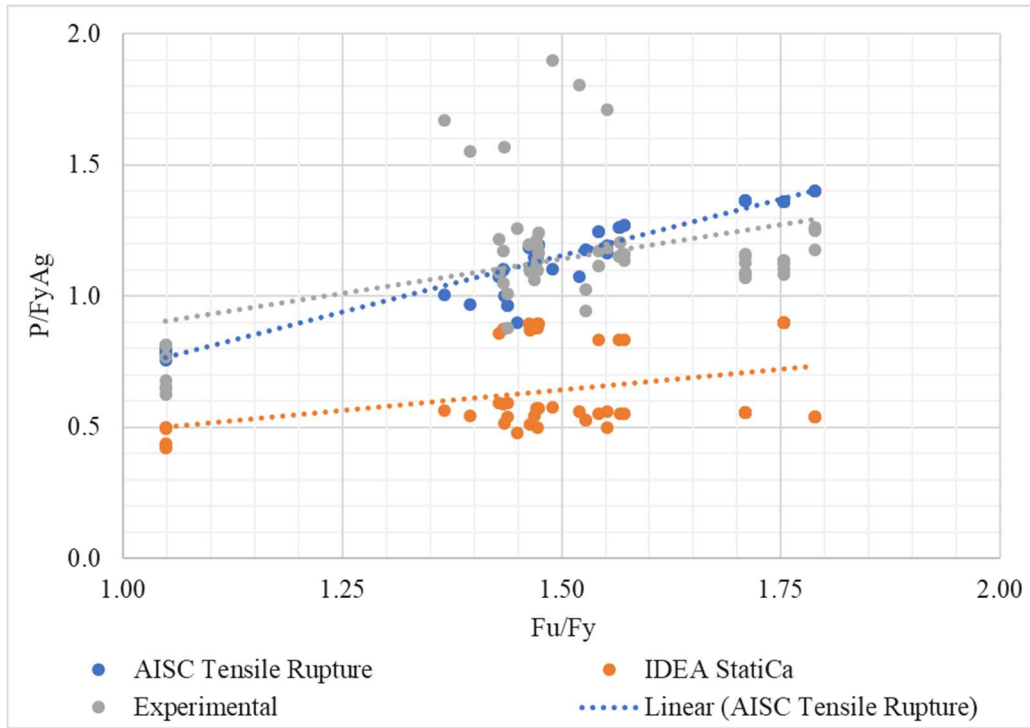


Figure 7.4: Bolted angle results: normalized strength as a function of material ratio scatterplot

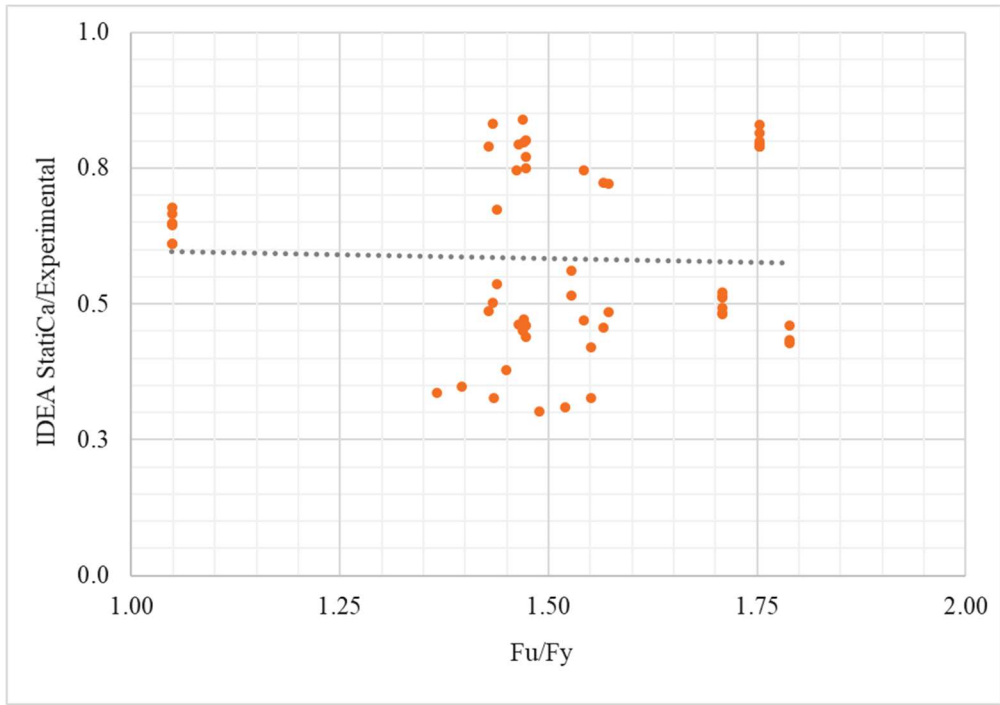


Figure 7.5: Bolted angle results: IDEA StatiCa to experimental ratio as function of material ratio scatterplot

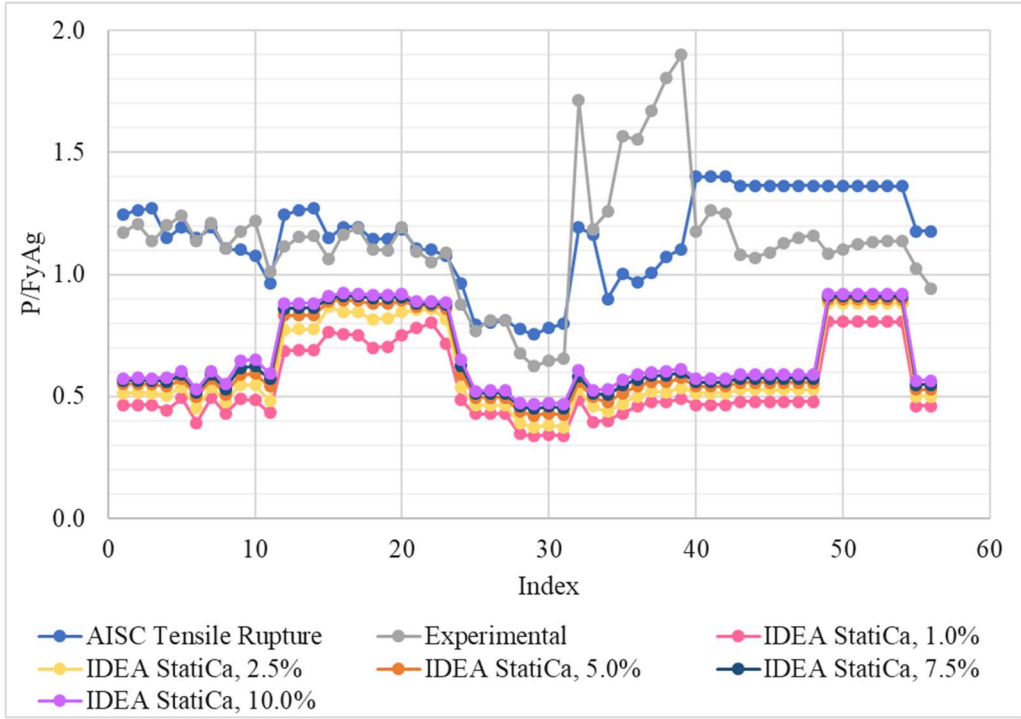


Figure 7.6: Bolted angles results: ratio of strength to IDEA StatiCa strength with 5% plastic strain limit plotted with index

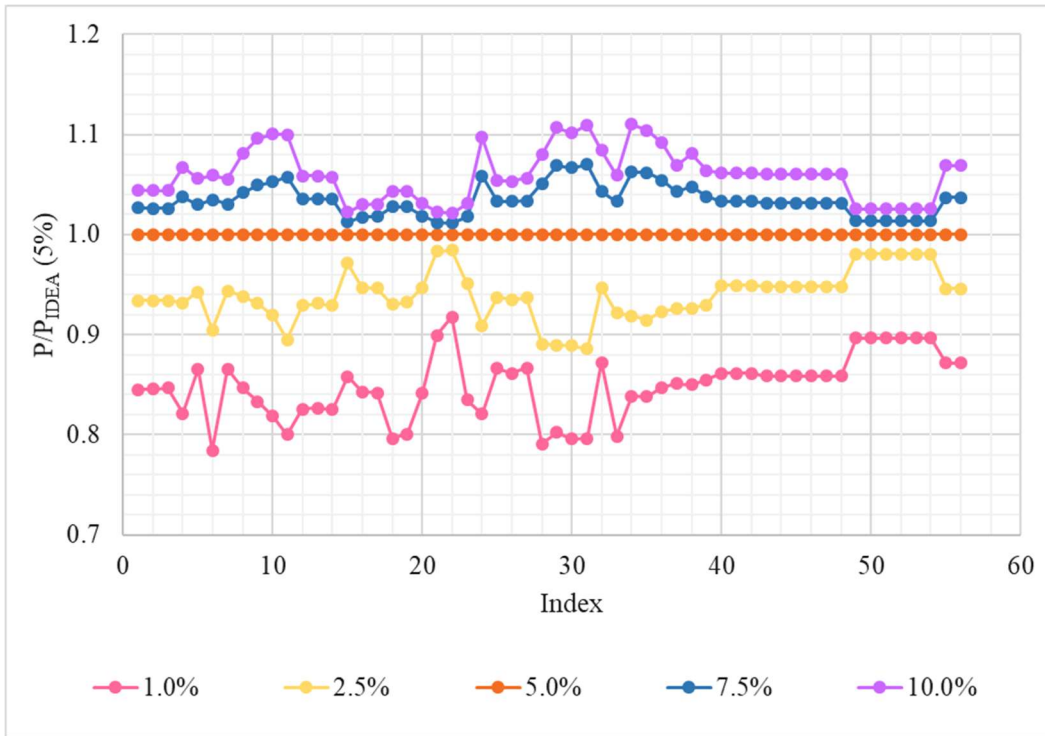


Figure 7.7: Bolted angle results: ratio of strength to IDEA StatiCa strength with 5% plastic strain limit plotted with index

Similarly, there was an investigation into the mesh dependency of the bolted angle experimental set. The results are plotted in Figure 7.8 with the strengths for each mesh parameter set normalized by the strength for the default mesh parameter set (i.e., ‘B’). It should be noted, the mesh around the bolt holes in IDEA StatiCa always remains constant at 8 elements. In general, the change in strength from mesh set to mesh set decreased. However, experimental index specimen 30 proves to be an outlier. The strength for the least refined mesh provides the lowest strength. Further investigation must be conducted to determine the cause of this. For the most part, the results are as expected and suggest some convergence with mesh refinement.

Table 7.6 presents the test-to-predicted ratio statistical results for the bolted angle experimental set. For the AISC (2016) tensile rupture test-to-predicted ratio, the average was 1.002. The results for the test-to-predicted ratio for AISC tensile rupture is directly used in the reliability analysis for the random variable \tilde{X}_R . The coefficient of variation of this ratio is used as well. As for the IDEA StatiCa test-to-predicted ratio, the average was 1.868. This indicates the strengths in the experiments were around 80% higher than that predicted by IDEA StatiCa.

7.3 Reliability Analysis

7.3.1 Description of Reliability Set

The reliability specimen set was created based on a variety of desired parameters. For this particular set, the parameters were selected based upon varying the following: A/B ratio (where A is the connected leg length and B is the non-connected leg length), thickness, bolts per row, and bolt spacing. The spacing was categorized into two groups: minimum and greater than minimum. The spacing was dependent upon the connected leg length and based upon Table 1-7A of the AISC *Steel Construction Manual* (2017) and Section J3 of the AISC *Specification* (2016). The general parameters for each connection are provided in Table 7.7 and the spacing details are provided in Table 7.8.

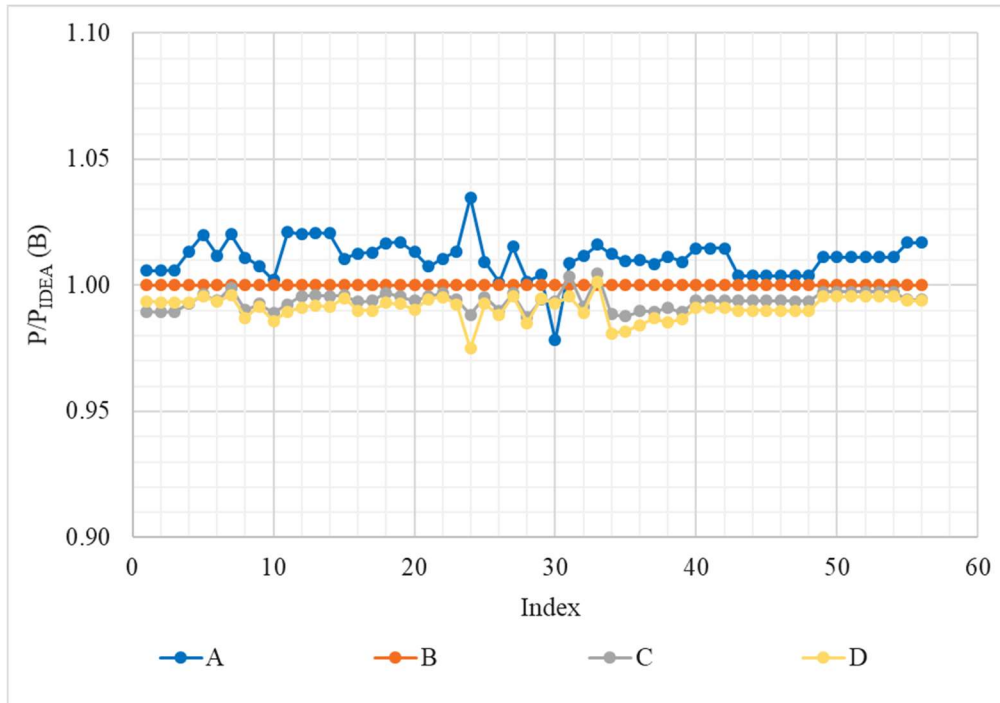


Figure 7.8: Bolted angle results: ratio of varying mesh parameters sets to the default mesh settings plotted with index

Table 7.6: Statistical Results for Bolted Angles

Test-to-Predicted Ratio	Average	Standard Deviation	Coefficient of Variation
$P_{EXP}/P_{RUPTURE}$ (AISC)	1.002	0.240	0.239
P_{EXP}/P_{IDEA}	1.868	0.579	0.310

Table 7.7: Bolted Angle Reliability Analysis Parameters

Index	<i>A</i> , in.	<i>B</i> , in.	<i>t</i> , in.	Material Grade	<i>F_y</i> , ksi	<i>F_u</i> , ksi	Bolt Diameter, in.	Rows of Bolts	Bolts per Row
1	4.0	3.0	0.375	A36 (Angle)	36	58	0.75	1	4
2	4.0	3.0	0.375	A36 (Angle)	36	58	0.75	1	4
3	4.0	3.0	0.500	A36 (Angle)	36	58	0.75	1	4
4	4.0	3.0	0.500	A36 (Angle)	36	58	0.75	1	4
5	4.0	3.0	0.375	A36 (Angle)	36	58	0.75	1	6
6	4.0	3.0	0.375	A36 (Angle)	36	58	0.75	1	6
7	4.0	3.0	0.500	A36 (Angle)	36	58	0.75	1	6
8	4.0	3.0	0.500	A36 (Angle)	36	58	0.75	1	6
9	3.0	4.0	0.375	A36 (Angle)	36	58	0.75	1	4
10	3.0	4.0	0.375	A36 (Angle)	36	58	0.75	1	4
11	3.0	4.0	0.500	A36 (Angle)	36	58	0.75	1	4
12	3.0	4.0	0.500	A36 (Angle)	36	58	0.75	1	4
13	3.0	4.0	0.375	A36 (Angle)	36	58	0.75	1	6
14	3.0	4.0	0.375	A36 (Angle)	36	58	0.75	1	6
15	3.0	4.0	0.500	A36 (Angle)	36	58	0.75	1	6
16	3.0	4.0	0.500	A36 (Angle)	36	58	0.75	1	6
17	4.0	4.0	0.375	A36 (Angle)	36	58	0.75	1	4
18	4.0	4.0	0.375	A36 (Angle)	36	58	0.75	1	4
19	4.0	4.0	0.500	A36 (Angle)	36	58	0.75	1	4
20	4.0	4.0	0.500	A36 (Angle)	36	58	0.75	1	4
21	4.0	4.0	0.375	A36 (Angle)	36	58	0.75	1	6
22	4.0	4.0	0.375	A36 (Angle)	36	58	0.75	1	6
23	4.0	4.0	0.500	A36 (Angle)	36	58	0.75	1	6
24	4.0	4.0	0.500	A36 (Angle)	36	58	0.75	1	6

Table 7.8: Bolted Angle Reliability Analysis Spacing Parameters

Index	s , in.	L_{ev} , in.	L_{eh} , in.
1	2.00	1.50	1.00
2	4.00	1.50	2.00
3	2.00	1.50	1.00
4	4.00	1.50	2.00
5	2.00	1.50	1.00
6	4.00	1.50	2.00
7	2.00	1.50	1.00
8	4.00	1.50	2.00
9	2.00	1.25	1.00
10	4.00	1.25	2.00
11	2.00	1.25	1.00
12	4.00	1.25	2.00
13	2.00	1.25	1.00
14	4.00	1.25	2.00
15	2.00	1.25	1.00
16	4.00	1.25	2.00
17	2.00	1.50	1.00
18	4.00	1.50	2.00
19	2.00	1.50	1.00
20	4.00	1.50	2.00
21	2.00	1.50	1.00
22	4.00	1.50	2.00
23	2.00	1.50	1.00
24	4.00	1.50	2.00

7.3.2 Results

For this reliability set of bolted angles, the strength results are provided in Table 7.9. Consistent with previous chapters, the nominal and design strengths are provided for both tensile yield and tensile rupture in this table. However, for the purpose of the reliability analysis only the controlling design strength was used (ϕP_{AISC} is the minimum of ϕP_{YIELD} and $\phi P_{RUPTURE}$). As for the strength according to IDEA StatiCa, P_{IDEA} , it was determined using all default settings (mesh parameter set 'B', 5% plastic strain limit, and all LRFD resistance factors applied). For this reliability set, IDEA StatiCa never exceeded the strength according to the AISC equations. On average, IDEA StatiCa provided a strength 47% less than the AISC *Specification* equations.

The reliability index, β , results are provided in Figure 7.9. The β -values are plotted against the specimen index for the reliability set. For the IDEA StatiCa results, the analysis indicated no failures in any of the 1,000,000 Monte Carlo trials, thus the β -values for IDEA StatiCa are large (i.e., greater than 4.75) and off the plot in Figure 7.9. The AISC β -values ranged from 3.71 to 3.87. These results are consistent with both the experimental set strength results and strength results of the reliability set for bolted angles. In conclusion, IDEA StatiCa consistently provided more reliable results when compared to the AISC *Specification* equations.

Table 7.9: Bolted Angle Reliability Strength Results

Index	AISC				IDEA StatiCa
	P_{YIELD} , kips	$P_{RUPTURE}$, kips	ϕP_{YIELD} , kips	$\phi P_{RUPTURE}$, kips	P_{IDEA} , kips
1	89.6	109.2	80.7	81.9	44.1
2	89.6	117.3	80.7	88.0	45.0
3	117.0	140.8	105.3	105.6	54.5
4	117.0	152.0	105.3	114.0	55.6
5	89.6	115.7	80.7	86.8	45.1
6	89.6	120.5	80.7	90.4	45.4
7	117.0	149.7	105.3	112.3	55.9
8	117.0	156.4	105.3	117.3	56.3
9	89.6	100.3	80.7	75.2	39.6
10	89.6	112.1	80.7	84.1	40.3
11	117.0	130.5	105.3	97.9	50.1
12	117.0	145.2	105.3	108.9	50.8
13	89.6	109.5	80.7	82.1	40.3
14	89.6	117.4	80.7	88.1	40.6
15	117.0	141.6	105.3	106.2	51.0
16	117.0	152.4	105.3	114.3	51.2
17	103.0	119.2	92.7	89.4	48.2
18	103.0	133.0	92.7	99.8	50.4
19	135.0	154.3	121.5	115.8	60.4
20	135.0	173.2	121.5	129.9	63.2
21	103.0	130.3	92.7	97.7	50.5
22	103.0	138.6	92.7	103.9	50.9
23	135.0	169.5	121.5	127.1	63.7
24	135.0	180.8	121.5	135.6	64.2

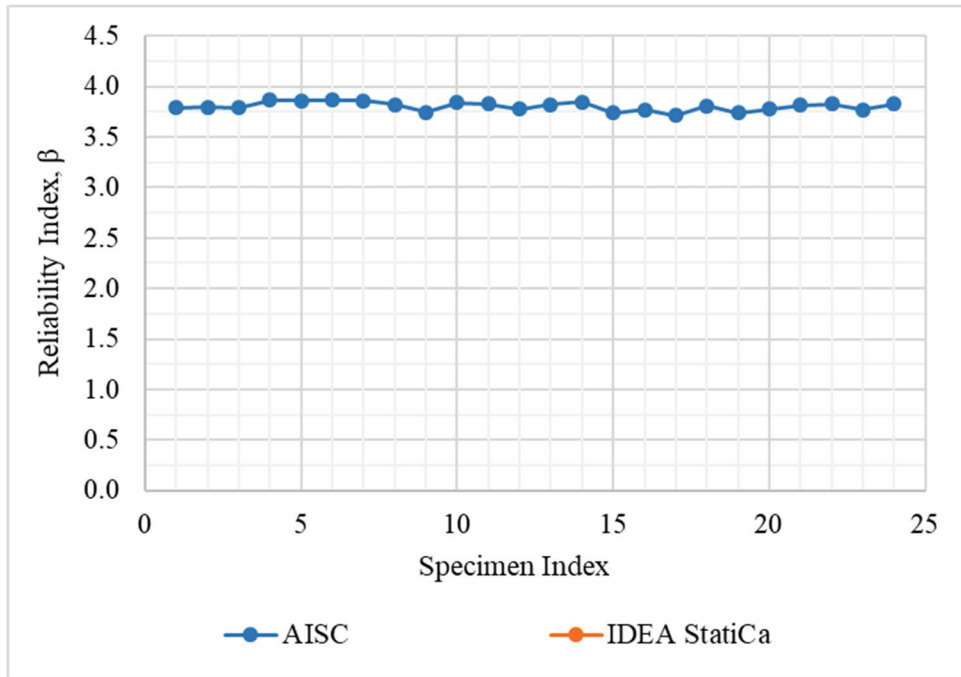


Figure 7.9: Bolted angles: Reliability index for IDEA StatiCa and AISC

CHAPTER 8

WELDED PLATES

8.1 Description of Connection

Single and double plate tension member welded to a gusset plate are evaluated in this chapter. A general schematic of the connection is provided in Figure 8.1. A variety of possible weld configurations are investigated. For clarity, the dimension ‘ t ’ will always represent thickness of the tension member and ‘ t_p ’ will always represent the plate to which the tension member is connected, referred to as the gusset plate. The failure always occurred in the tension member in the physical tests.

For the AISC *Specification* equations, the gross area for these connections were calculated based on measured geometric properties. The shear lag factor cases applicable to this connection are cases 1 and 4. Case 1 is applicable when transverse welds are used. The shear lag factor for case 1 is 1.0. Case 4 is applicable when only longitudinal welds are used. The shear lag factor for case 4 is:

$$U = \frac{3l^2}{3l^2 + w^2} \left(1 - \frac{\bar{x}}{l}\right) \quad (8-1)$$

where l and w are defined in Figure 6.2 and \bar{x} is eccentricity of the connection (one half the tension member thickness, t).

8.2 Comparison to Experimental Results

8.2.1 Description of Experimental Specimens

There were 28 total welded plate specimens in this experimental set. The specimen enumeration of this connection type is included in Table 8.1. These specimens were only taken from two sources: Gonzalez (1989), also reported in Easterling and Gonzalez Giroux (1993), and Mannem (2002). It should be noted Gonzalez reported 11 specimens total, however specimens P-L1-1a and P-B-1a were removed because it reported the testing machine reached its full capacity before failure could occur. As for Mannem, 27

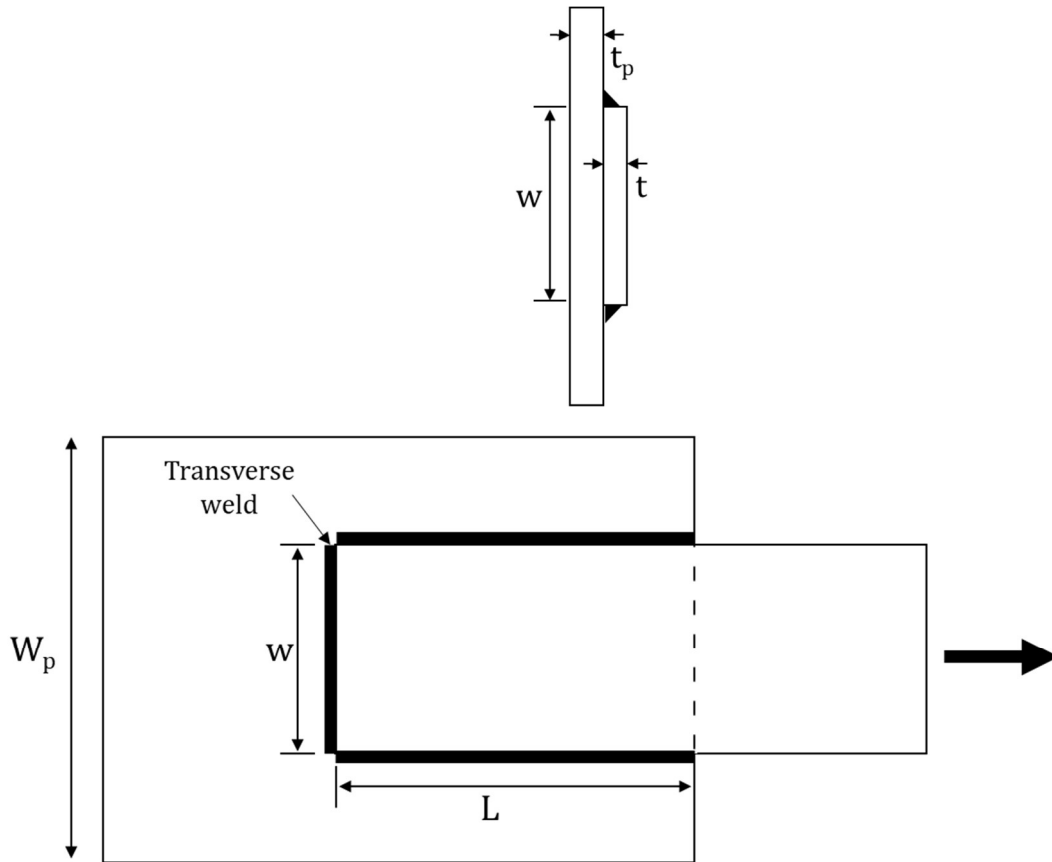


Figure 8.1: Welded Plate Schematic

Table 8.1: Welded Plate Specimen Enumeration

Reference	Specimen Count
Gonzalez (1989)	9
Mannem (2002)	19
Total	28

total specimens were reported, but specimens OP120-S-a and P120-1-b failed in the welds. Specimens OP120-s-b, DP120-s, P120-s, P75-s, P75-s-b, and DP75-s were all removed because they included only one longitudinal weld. These specimens were deemed a special case and removed from the study.

The parameters associated with each specimen is provided in Table 8.2. The measured F_y and F_u of the Mannem (2002) specimens were provided as a result of three coupon tests. The average of the three was taken as the measured F_y and F_u . Table 8.3 provides information specifically on the welds for this set of specimens. Mannem did not indicate a weld size. Mannem did report a metric weld strength of E760XX (E110XX English) and noted the welds were designed not to fail. A weld size of 0.315 in. (8 mm) and strength of E760XX (metric) was used for modelling in IDEA StatiCa. To be clear, ‘NP’ in Table 8.3 indicates that the weld size was not provided in the literature. The dashes, ‘-’, indicate there is not a weld in that particular location.

The modelling of these specimens is typical from the previous chapters. More specifically, the modeling process is identical to the welded angle chapter. The tested plate and gusset plate are both modeled as a member. A typical model is provided in Figure 8.2. For clarity, the tested plate is referred to as ‘plate’ and the non-tested plate is referred to as the ‘gusset plate’. The modeling process is as follows:

1. Process outlined in Chapter 3.3
2. Create members:
 - a. Member 1: Gusset plate
 - i. Geometrical type set to “Ended”
 - ii. B set to 180°
 - iii. Offset ex set to the negative of the connection length (longest longitudinal weld length)
 - b. Member 2, 3 (if applicable)
 - i. Geometrical type set to “Ended”
 - ii. Align set to “To member plate”

Table 8.2: Welded Plate Specimen Details

Index	Reference	Specimen	# of plates	* F_y , ksi	* F_u , ksi	* t , in.	* w , in.
1	Gonzalez (1989)	P-L1-1b	2	51.9	73.0	0.260	3.020
2	Gonzalez (1989)	P-L1-2	2	51.9	73.0	0.259	3.024
3	Gonzalez (1989)	P-L1-3	2	51.9	73.0	0.258	3.025
4	Gonzalez (1989)	P-L2-1	2	51.9	73.0	0.260	3.020
5	Gonzalez (1989)	P-L2-2	2	51.9	73.0	0.259	3.025
6	Gonzalez (1989)	P-L2-3	2	51.9	73.0	0.257	3.023
7	Gonzalez (1989)	P-B-1b	2	51.9	73.0	0.258	3.024
8	Gonzalez (1989)	P-B-2	2	51.9	73.0	0.257	3.024
9	Gonzalez (1989)	P-B-3	2	51.9	73.0	0.259	3.023
10	Mannem (2002)	OP120-1-a	1	30.5	62.6	0.505	4.724
11	Mannem (2002)	OP120-1-b	1	30.5	62.6	0.505	4.720
12	Mannem (2002)	OP120-T	1	30.5	62.6	0.505	4.724
13	Mannem (2002)	P120-1-a	1	53.2	73.5	0.511	4.748
14	Mannem (2002)	P120-1-c	1	53.2	73.5	0.511	4.756
15	Mannem (2002)	P120-1.5	1	53.2	73.5	0.511	4.756
16	Mannem (2002)	DP120-1	2	53.2	73.5	0.511	4.803
17	Mannem (2002)	P120-T-a	1	53.2	73.5	0.511	4.780
18	Mannem (2002)	P120-T-b	1	53.2	73.5	0.511	4.736
19	Mannem (2002)	DP120-2	2	53.2	73.5	0.511	4.732
20	Mannem (2002)	P75-0.87	1	53.2	73.5	0.511	3.000
21	Mannem (2002)	P75-1.0	1	53.2	73.5	0.511	3.051
22	Mannem (2002)	P75-1.6	1	53.2	73.5	0.511	3.063
23	Mannem (2002)	P75-2.0	1	53.2	73.5	0.511	2.992
24	Mannem (2002)	P75-T	1	53.2	73.5	0.511	2.972
25	Mannem (2002)	P75-e3/4	1	53.2	73.5	0.511	2.953
26	Mannem (2002)	P75-e5/4	1	53.2	73.5	0.511	2.972
27	Mannem (2002)	UP75-3/4	1	53.2	73.5	0.511	2.906
28	Mannem (2002)	P250-1	1	53.2	73.5	0.511	9.862

* indicates measured value

Table 8.3: Welded Plate Weld Details

Index	Longitudinal Weld Size, in.	L, in.	Transverse Weld Size, in.	Transverse Weld Length, in.
1	0.250	4.250	-	-
2	0.250	4.250	-	-
3	0.250	4.250	-	-
4	0.250	5.000	-	-
5	0.250	5.000	-	-
6	0.250	5.000	-	-
7	0.250	3.000	0.250	3.000
8	0.250	3.000	0.250	3.000
9	0.250	3.000	0.250	3.000
10	NP	4.528	-	-
11	NP	4.528	-	-
12	NP	2.165	NP	4.724
13	NP	4.724	-	-
14	NP	4.724	-	-
15	NP	7.087	-	-
16	NP	4.724	-	-
17	NP	3.937	NP	4.780
18	NP	1.969	NP	4.736
19	NP	9.252	-	-
20	NP	2.559	-	-
21	NP	2.953	-	-
22	NP	4.724	-	-
23	NP	6.024	-	-
24	NP	1.181	NP	2.953
25	NP	2.953	-	-
26	NP	2.953	-	-
27	NP	3.740	-	-
28	NP	9.843	-	-

NP: not provided

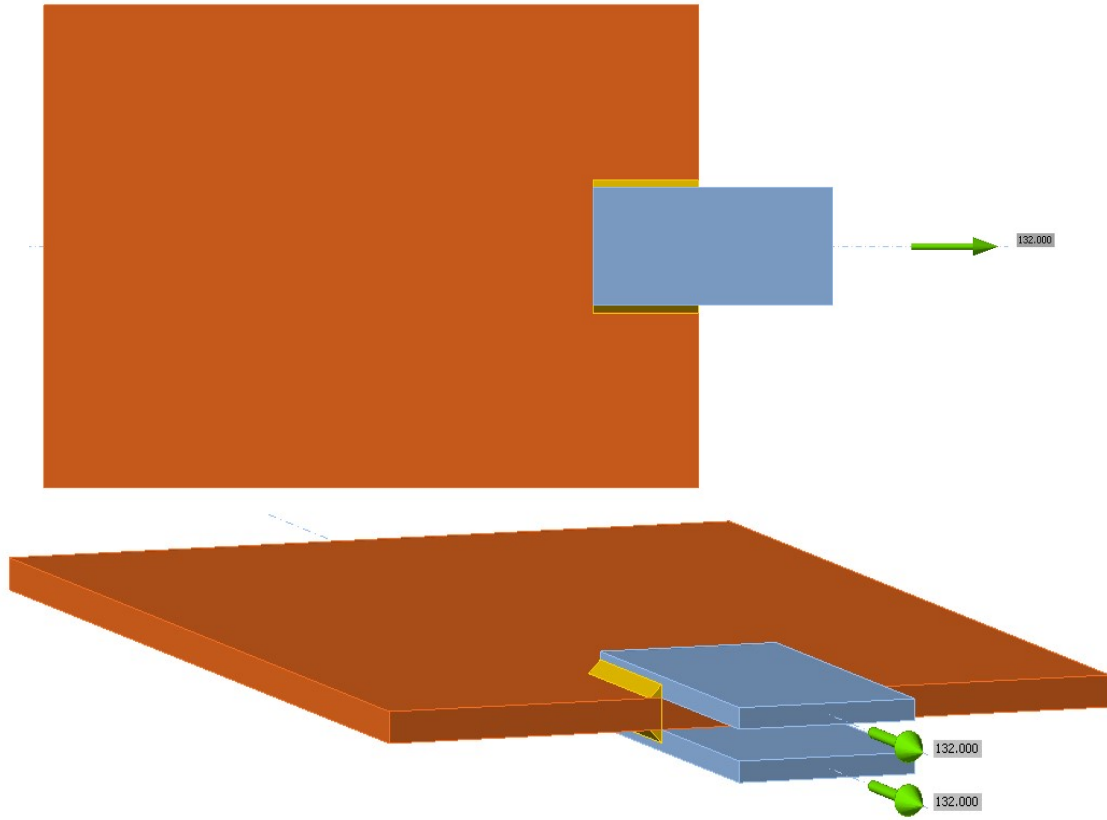


Figure 8.2: Typical Welded Plate Model

- i. Aligned plate set to “[member name] | Bottom flange 1”
 - ii. Related plate set to “[gusset plate member name] Bottom flange 1”
 - iii. Model type set to “N-Vy-Vz”
- 3. Create weld operations:
 - a. Continuous welds:
 - i. Placement set to “Edge to surface”
 - ii. Type set to “Weld”
 - iii. First plate: Member or plate set to “[plate member name] | Bottom flange 1”
 - iv. Select correct edge index
 - v. Second plate: Plate set to “[gusset plate name] | Bottom flange 1”
 - vi. Input desired weld size and type (fillet- front side for all specimens)
 - vii. Weld type set to “Continuous”
 - b. Partial welds:
 - i. Placement set to “Edge to surface”
 - ii. Type set to “Weld”
 - iii. First plate: Member or plate set to “[plate member name] | Bottom flange 1”
 - iv. Select correct edge index
 - v. Second plate: Plate set to “[gusset plate name] | Bottom flange 1”
 - vi. Input desired weld size and type (fillet- front side for all specimens)
 - vii. Weld type set to “Partial”
 - viii. Weld offset 2 set to the absolute value of the offset in Step 2 minus the partial weld length
- 4. Repeat as necessary until all welds are modeled

8.2.2 Results

The experimental set strengths according to the AISC *Specification* equations are provided in Table 8.4. The tensile yield and tensile rupture strengths are presented separately in this table. The shear lag factor case 1 was applicable to only seven specimens, with the rest being governed by case 4, due to the variety of weld configurations.

A summary of the strength results for the welded plate experimental set is provided in Table 8.5 below. The strength reported for AISC, P_{AISC} , is the minimum of the yield and rupture strengths with the controlling limit state labelled accordingly. The strength according to IDEA StatiCa is provided for the default mesh settings and 5% plastic strain limit. Similar to previous chapters, some specimens indicated a weld failure in IDEA StatiCa. The weld utilization was ignored, and the strength was still reported as the maximum load before the plastic strain limit was reached. There were several cases in this experimental set where the maximum permitted applied load in IDEA StatiCa, P_{IDEA} , resulted in a larger value than indicated by the AISC *Specification* equations, P_{AISC} . The most severe case was a result of the specimen with the experimental index 20. The P_{IDEA} for this specimen was around 16% higher than P_{AISC} . The most conservative specimen, experimental set index 14, resulted in an IDEA StatiCa strength of around 23% less than the AISC *Specification* equations suggest. In comparison to the experimental strengths, P_{EXP} , IDEA StatiCa strength never exceeded the experimental for this particular set of experimental specimens.

The strength results for the experimental set of specimens plotted are provided in Figure 8.3. The strengths, P_{IDEA} , $P_{RUPTURE}$, and P_{EXP} , are normalized by the expected tensile yield strength, $F_y A_g$, and plotted with the corresponding experimental set index. The plot indicates IDEA StatiCa provides strengths larger than the strengths according to the AISC *Specification* by a very small margin with tensile yield controlling the AISC strength calculations for most specimens. The specimen with experimental index 20, as

Table 8.4: Welded Plates AISC Calculation Results

Index	P _{YIELD} , kips	U	Controlling U Case	P _{RUPTURE} , kips
1	81.5	0.830	Case 4	95.1
2	81.3	0.830	Case 4	94.8
3	81.1	0.830	Case 4	94.6
4	81.5	0.868	Case 4	99.5
5	81.4	0.868	Case 4	99.4
6	80.7	0.868	Case 4	98.5
7	81.0	1.000	Case 1	113.9
8	80.7	1.000	Case 1	113.4
9	81.3	1.000	Case 1	114.3
10	72.6	0.693	Case 4	103.4
11	72.6	0.693	Case 4	103.4
12	72.6	1.000	Case 1	149.3
13	128.9	0.708	Case 4	126.1
14	129.1	0.707	Case 4	126.2
15	129.1	0.838	Case 4	149.6
16	260.9	0.704	Case 4	253.6
17	129.8	1.000	Case 1	179.3
18	128.6	1.000	Case 1	177.7
19	257.0	0.894	Case 4	317.6
20	81.5	0.617	Case 4	69.5
21	82.9	0.674	Case 4	77.1
22	83.2	0.830	Case 4	95.4
23	81.3	0.885	Case 4	99.3
24	80.7	1.000	Case 1	111.5
25	80.2	0.685	Case 4	75.9
26	80.7	0.683	Case 4	76.2
27	78.9	0.727	Case 4	79.3
28	267.8	0.730	Case 4	270.1

Table 8.5: Welded Plate Results Summary

Index	Experimental		AISC		IDEA StatiCa	
	P _{EXP} , kip	Failure Mode	P _{AISC} , kips	Controlling Limit State	P _{IDEA} , kips	Failure Mode
1	107.4	[2]	81.5	[1]	83.6	[3]
2	112.0	[2]	81.3	[1]	83.4	[3]
3	115.0	[2]	81.1	[1]	83.1	[3]
4	111.8	[2]	81.5	[1]	83.6	[3]
5	111.6	[2]	81.4	[1]	83.4	[3]
6	108.8	[2]	80.7	[1]	82.7	[3]
7	102.4	[2]	81.0	[1]	83.0	[3]
8	112.2	[2]	80.7	[1]	82.7	[3]
9	111.4	[2]	81.3	[1]	83.3	[3]
10	119.4	[2]	72.6	[1]	75.0	[3]
11	114.2	[2]	72.6	[1]	75.0	[3]
12	127.9	[2]	72.6	[1]	75.0	[3]
13	168.6	[2]	126.1	[2]	128.2	[3]
14	164.8	[2]	126.2	[2]	96.7	[3]
15	170.0	[2]	129.1	[1]	128.2	[3]
16	341.9	[2]	253.6	[2]	267.3	[3]
17	171.5	[2]	129.8	[1]	128.9	[3]
18	173.1	[2]	128.6	[1]	127.7	[3]
19	321.7	[2]	257.0	[1]	263.3	[3]
20	107.5	[2]	69.5	[2]	80.9	[3]
21	109.9	[2]	77.1	[2]	82.4	[3]
22	112.4	[1]	83.2	[1]	82.6	[3]
23	109.9	[2]	81.3	[1]	80.7	[3]
24	105.9	[2]	80.7	[1]	77.8	[3]
25	109.9	[2]	75.9	[2]	78.2	[3]
26	107.9	[2]	76.2	[2]	82.1	[3]
27	106.8	[2]	78.9	[1]	78.4	[3]
28	327.3	[2]	267.8	[1]	244.2	[3]

[1] tensile yield; [2] tensile rupture; [3] member strain

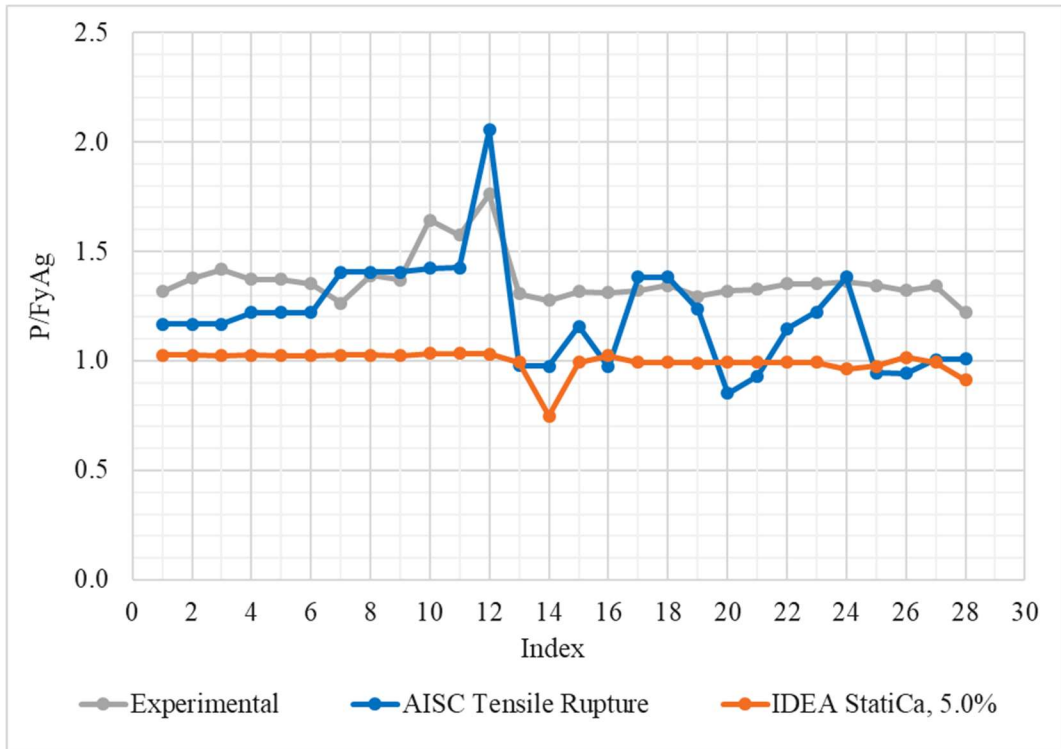


Figure 8.3: Welded plate results: strength ratio vs. index

previously discussed and depicted in Table 8.5, is an example of such a case. The plot also indicates that IDEA StatiCa provides a decent margin of safety when compared to the experimental strengths for this set of experimental specimens. However, as previously addressed, IDEA StatiCa cannot ignore yielding of the plates, whereas the experimentalists typically reported the experimental strength well beyond the point of yield.

As a result of the combination of IDEA StatiCa's heavily reliance of F_y and the limit state of tensile rupture according to the AISC *Specification* (2016) being directly related to F_u , the impact of the material ratio F_u/F_y on the accuracy of P_{IDEA} with respect to P_{AISC} was investigated. Figure 8.4 provides the overall trend of normalized strengths with respect to F_u/F_y . The correlations trend in the positive direction in general, however the strength according to IDEA StatiCa provide little to no correlation with material ratio. Figure 8.5 the ratio of P_{IDEA}/P_{EXP} plotted with the material ratio F_u/F_y . The trendline added to this plot shows a correlation between the strength ratio and material ratio. This indicates as the difference between F_u and F_y increases, the accuracy of IDEA StatiCa decreases with respect to the strength observed in the experimental tests. It should be noted, however, data is limit in this particular experimental set of specimens for those with a lower material ratio F_u/F_y .

Similar to the previous experimental specimen sets, an investigation into the impact of varying plastic strain limits was conducted. The results are presented in Figure 8.6 and Figure 8.7. The varying plastic strain limits does not significantly decrease the conservatism of IDEA StatiCa when comparing to the strengths observed in the experimental tests. The IDEA StatiCa strengths only increased by 1% to 2% when changing the plastic strain limit from 5% to 10%. The results indicate that most specimens are at their tensile yield capacity; therefore, changing the plastic strain limit will not change the strength significantly. As previously mentioned, there was one particular case (specimen with experimental set index 20) that resulted in unconservative strengths when comparing P_{IDEA} to P_{AISC} . As shown in Figure 8.6, using plastic strain limits 1.0% and 2.5% appear to provide values of P_{IDEA} closer to P_{AISC} . For the 2.5%

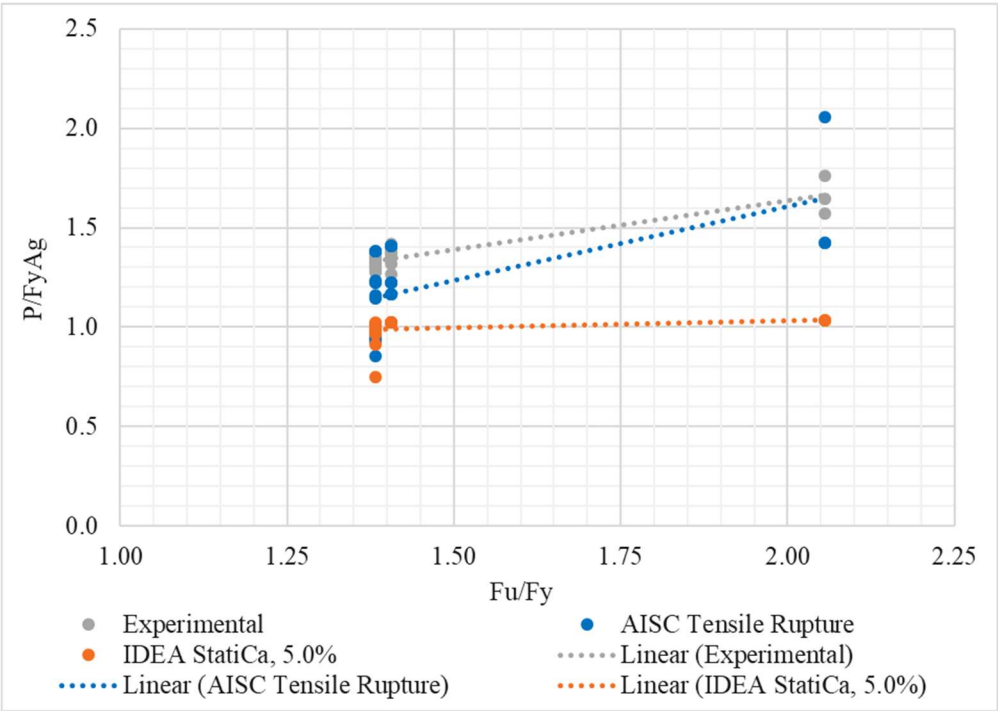


Figure 8.4: Welded plate results: normalized strength as a function of material ratio scatterplot

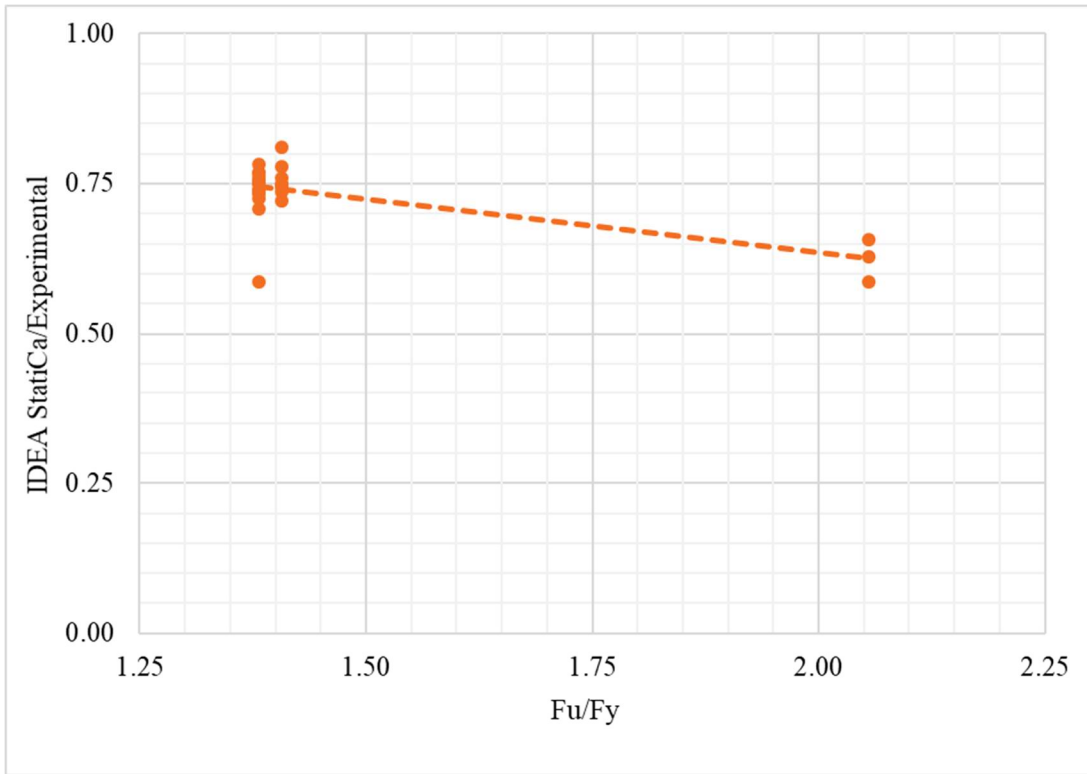


Figure 8.5: Welded plate results: IDEA StatiCa to experimental ratio as function of material ratio scatterplot

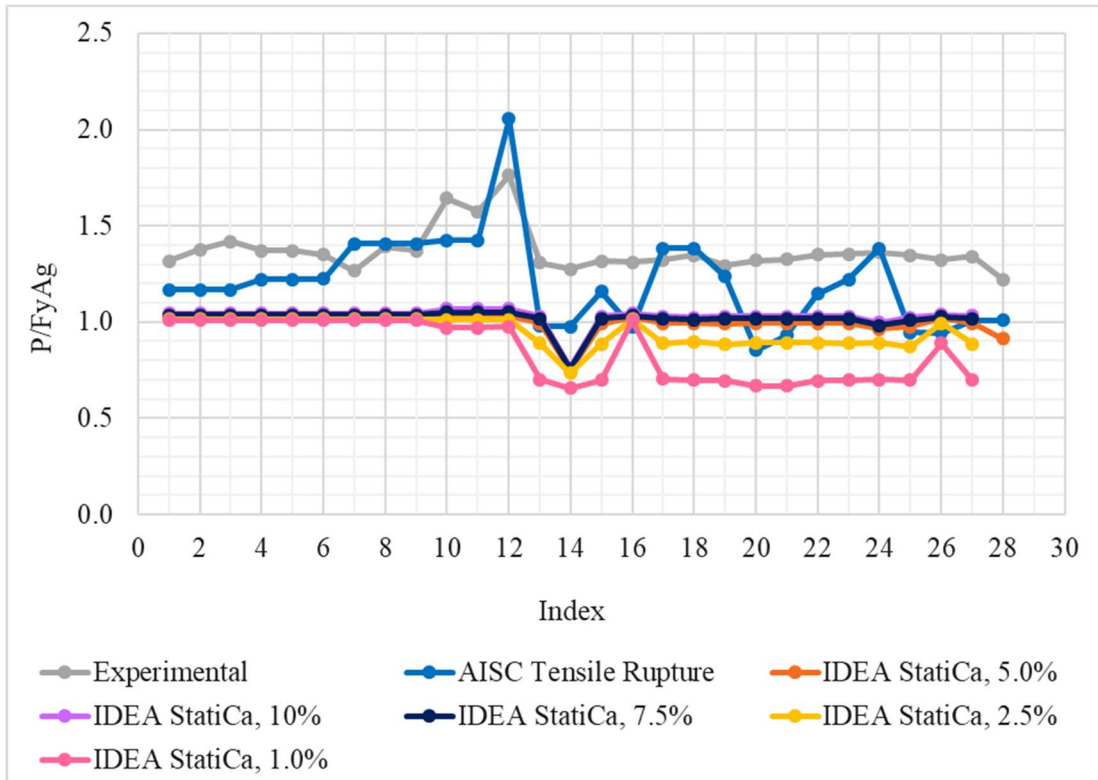


Figure 8.6: Welded plate results: strength ratio vs. index for varying plastic strain limits

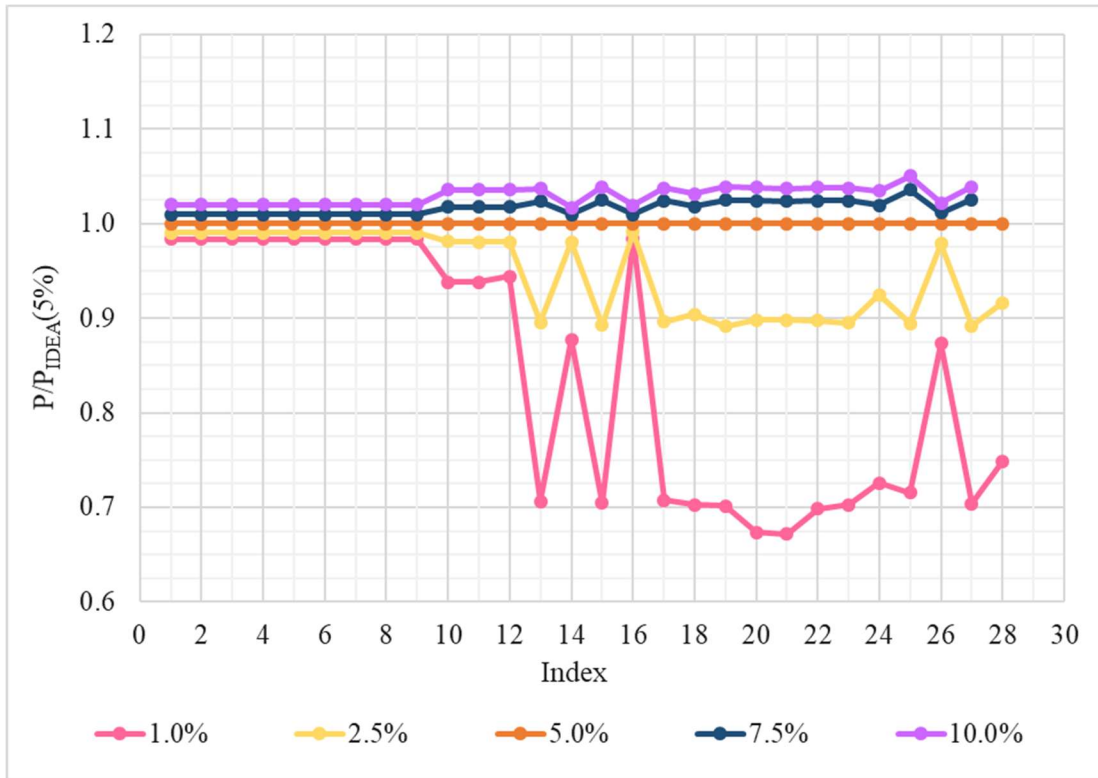


Figure 8.7: Welded plate results: ratio of strength to IDEA StatiCa strength with 5% plastic strain limit plotted with index

plastic strain limit, P_{IDEA} was less than 5.0% larger than P_{AISC} .

In addition to the plastic strain limit investigation, an examination of mesh dependency was conducted as well. Figure 8.8 provides the results of the investigation as the strengths for each parameter set is normalized by the default mesh parameter set (i.e., 'B'). In general, this plot indicates convergence of the mesh. Furthermore, as the mesh parameters became more refined (i.e., smaller elements), the difference in strengths decreases for most specimens. There is little change from mesh setting 'B' to 'C' or 'D' for most cases. This could indicate the mesh settings for this particular set of welded plate experimental specimens are appropriate as the default values. There are some instances where there is not convergence (specimens with indices 12, 18, 20, 21, 24, and 25). For the most severe case with specimen index 25, the largest decrease in strength from one mesh setting to the next was ~11%.

Table 8.6 provides statistics for each test-to-predicted ratio from the results of the experimental set. Data pertaining to the test-to-predicted ratios are provided for the tensile rupture strength according to the *AISC Specification (2016)* and the maximum permitted applied load according to IDEA StatiCa. Both resulting average ratios are above one, indicating both strength methods provide results more conservative than those observed in experimental tests. On average, the ratio P_{EXP}/P_{IDEA} is larger than the ratio $P_{EXP}/P_{RUPTURE}$, indicating IDEA StatiCa was typically more conservative than the strengths according to the *AISC Specification* equations. The average and coefficient of variation results for the test-to-predicted ratio for AISC tensile rupture was directly used in the reliability analysis for the generation of the random variable \tilde{X}_R . The reliability analysis for welded plate tension members is provided in the following section.

8.3 Reliability Analysis

8.3.1 Description of Reliability Set

The reliability set specimens were created based on selected parameters and ratios. The specific parameters are outlined in Table 8.7. It was desired to vary the

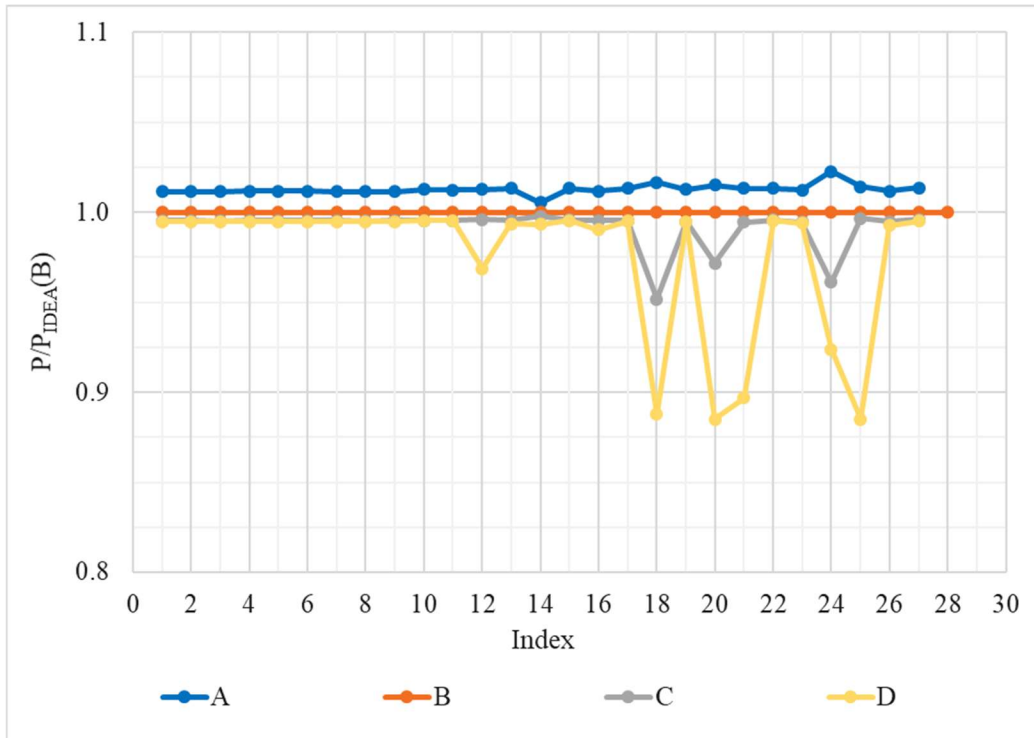


Figure 8.8: Welded plate results: ratio of varying mesh parameters sets to the default mesh settings plotted with index

Table 8.6: Statistical Results for Welded Plates

Test-to-Predicted Ratio	Average	Standard Deviation	Coefficient of Variation
$P_{EXP}/P_{RUPTURE}$ (AISC 2016)	1.163	0.175	0.150
P_{EXP}/P_{IDEA}	1.376	0.115	0.084

Table 8.7: Welded Plate Reliability Analysis Parameters

Index	W , in.	t , in.	Material Grade	F_y , ksi	F_u , ksi	Length of Weld, in.	Transverse weld?
1	5	0.750	A36 (Plate)	36	58	2.5	No
2	5	0.500	A36 (Plate)	36	58	2.5	No
3	5	0.375	A36 (Plate)	36	58	2.5	No
4	5	0.750	A36 (Plate)	36	58	5.0	No
5	5	0.500	A36 (Plate)	36	58	5.0	No
6	5	0.375	A36 (Plate)	36	58	5.0	No
7	5	0.750	A36 (Plate)	36	58	10.0	No
8	5	0.500	A36 (Plate)	36	58	10.0	No
9	5	0.375	A36 (Plate)	36	58	10.0	No
10	5	0.750	A36 (Plate)	36	58	2.5	Yes
11	5	0.500	A36 (Plate)	36	58	2.5	Yes
12	5	0.375	A36 (Plate)	36	58	2.5	Yes
13	5	0.750	A36 (Plate)	36	58	5.0	Yes
14	5	0.500	A36 (Plate)	36	58	5.0	Yes
15	5	0.375	A36 (Plate)	36	58	5.0	Yes
16	5	0.750	A36 (Plate)	36	58	10.0	Yes
17	5	0.500	A36 (Plate)	36	58	10.0	Yes
18	5	0.375	A36 (Plate)	36	58	10.0	Yes
19	5	0.750	A572 Gr. 50 (Plate)	50	65	2.5	No
20	5	0.500	A572 Gr. 50 (Plate)	50	65	2.5	No
21	5	0.375	A572 Gr. 50 (Plate)	50	65	2.5	No
22	5	0.750	A572 Gr. 50 (Plate)	50	65	5.0	No
23	5	0.500	A572 Gr. 50 (Plate)	50	65	5.0	No
24	5	0.375	A572 Gr. 50 (Plate)	50	65	5.0	No
25	5	0.750	A572 Gr. 50 (Plate)	50	65	10.0	No
26	5	0.500	A572 Gr. 50 (Plate)	50	65	10.0	No
27	5	0.375	A572 Gr. 50 (Plate)	50	65	10.0	No
28	5	0.750	A572 Gr. 50 (Plate)	50	65	2.5	Yes
29	5	0.500	A572 Gr. 50 (Plate)	50	65	2.5	Yes
30	5	0.375	A572 Gr. 50 (Plate)	50	65	2.5	Yes
31	5	0.750	A572 Gr. 50 (Plate)	50	65	5.0	Yes
32	5	0.500	A572 Gr. 50 (Plate)	50	65	5.0	Yes
33	5	0.375	A572 Gr. 50 (Plate)	50	65	5.0	Yes
34	5	0.750	A572 Gr. 50 (Plate)	50	65	10.0	Yes
35	5	0.500	A572 Gr. 50 (Plate)	50	65	10.0	Yes
36	5	0.375	A572 Gr. 50 (Plate)	50	65	10.0	Yes

following: width to thickness ratio, material grade, length of longitudinal welds, and the option of a transverse weld. The option of the transverse weld was to vary the shear lag factor case between case 1 and 4 from D3.1 of the *AISC Specification* (2016). The modeling of these specimens in IDEA StatiCa was practically identical to that outlined earlier in this chapter, except that nominal properties were used instead of measured properties. The welds were modeled as 5/16 in. welds with a weld strength of EXX110. This was to reduce the impact of weld failures.

8.3.2 Results

The strength results from the reliability set of specimens is provided in Table 8.8. The strength according to the *AISC Specification* (2016) is provided for tensile yield and tensile rupture. The nominal and design strength are provided for both limit states. The strength according to IDEA StatiCa is provided as well with all default settings. More specifically, all resistance factors were used for this analysis. The strength results according to IDEA StatiCa provided larger strengths than the *AISC Specification* equations for much of this reliability set of specimens. The most significant cases were a result of specimens with specimen indices 19, 20, and 21. These specimens resulted in P_{IDEA} greater than the available strength calculated according to the *AISC Specification* (minimum of ϕP_{YIELD} and $\phi P_{RUPTURE}$) by more than 50%. These specimens have the smallest weld length to plate width ratio of the reliability set with a ratio of 0.5. In comparison to the experimental set, the smallest longitudinal weld length to plate width ratio without a transverse weld was 0.85 for the specimen with experimental index 20. For this case, IDEA StatiCa resulted in a 16% larger strength than the *AISC Specification* equations, which was the largest in the entire welded plate experimental set. However, IDEA StatiCa was still 25% less than the experimentally observed strength for experimental index 20. This could indicate that the *AISC Specification* equations are conservative for shorter weld lengths.

Table 8.8: Welded Plate Reliability Strength Results

Index	AISC				IDEA StatiCa
	P_{YIELD} , kips	$P_{RUPTURE}$, kips	ϕP_{YIELD} , kips	$\phi P_{RUPTURE}$, kips	P_{IDEA} , kips
1	135.0	79.2	121.5	59.4	77.3
2	90.0	55.9	81.0	41.9	53.9
3	67.5	43.1	60.8	32.3	41.7
4	135.0	150.9	121.5	113.2	122.7
5	90.0	103.3	81.0	77.5	83.5
6	67.5	78.5	60.8	58.9	62.8
7	135.0	193.2	121.5	144.9	122.4
8	90.0	130.5	81.0	97.9	83.5
9	67.5	98.5	60.8	73.9	62.8
10	135.0	217.5	121.5	163.1	122.7
11	90.0	145.0	81.0	108.8	83.5
12	67.5	108.8	60.8	81.6	62.8
13	135.0	217.5	121.5	163.1	122.7
14	90.0	145.0	81.0	108.8	83.5
15	67.5	108.8	60.8	81.6	62.8
16	135.0	217.5	121.5	163.1	122.6
17	90.0	145.0	81.0	108.8	83.5
18	67.5	108.8	60.8	81.6	62.8
19	187.5	88.8	168.8	66.6	103.8
20	125.0	62.7	112.5	47.0	72.5
21	93.8	48.3	84.4	36.2	55.8
22	187.5	169.1	168.8	126.8	154.7
23	125.0	115.8	112.5	86.8	114.9
24	93.8	88.0	84.4	66.0	86.5
25	187.5	216.6	168.8	162.4	154.5
26	125.0	146.3	112.5	109.7	114.8
27	93.8	110.4	84.4	82.8	86.5
28	187.5	243.8	168.8	182.8	155.5
29	125.0	162.5	112.5	121.9	114.7
30	93.8	121.9	84.4	91.4	86.5
31	187.5	243.8	168.8	182.8	155.6
32	125.0	162.5	112.5	121.9	114.9
33	93.8	121.9	84.4	91.4	86.5
34	187.5	243.8	168.8	182.8	155.4
35	125.0	162.5	112.5	121.9	114.8
36	93.8	121.9	84.4	91.4	86.5

The results of the reliability analysis are provided in Figure 8.9. For IDEA StatiCa, most of the cases compare very well to the reliability for the AISC *Specification* (2016) equations. However, there are several of cases where IDEA StatiCa provides a lower level of reliability in comparison to AISC. Specimens with index 1, 2, 3, 19, 20, 21, 22, 23, and 24 have a reliability index significantly lower for IDEA StatiCa than the corresponding reliability index for AISC. All of these specimens have a weld length to plate width ratio of 0.5, which is the smallest for this reliability set. These β -value results are consistent with the reliability set strength results discussed previously. The lowest reliability index for IDEA StatiCa was approximately 2.20 and 3.17 for AISC.

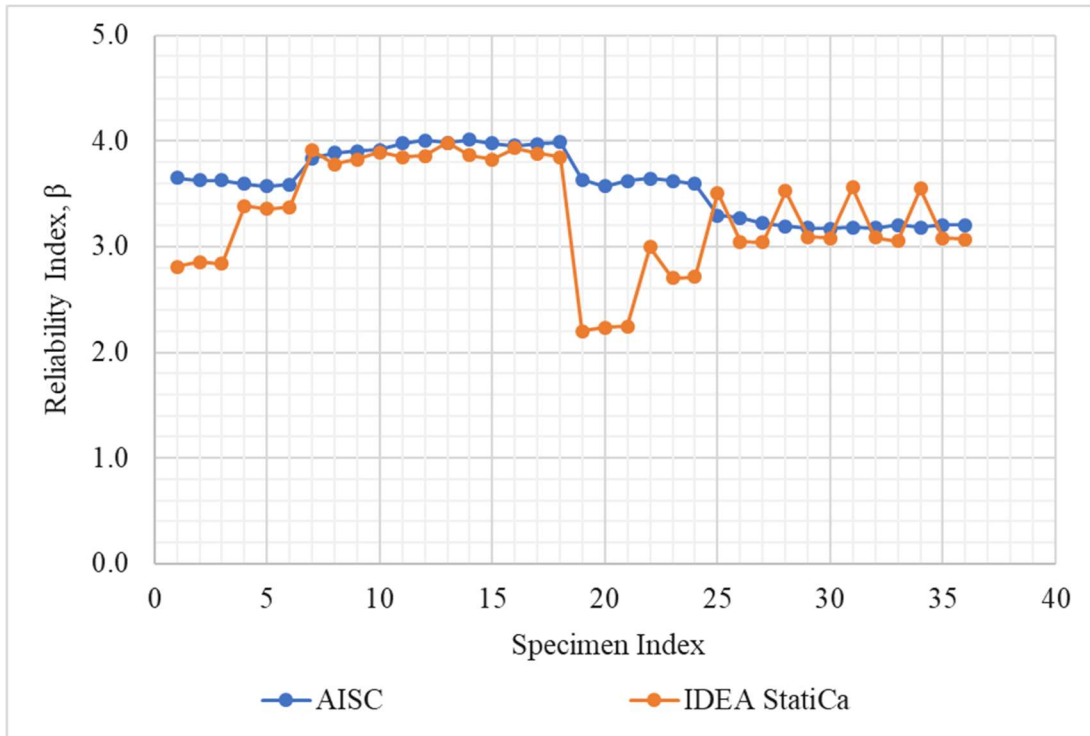


Figure 8.9: Welded plates: Reliability index for IDEA StatiCa and AISC

CHAPTER 9

BOLTED PLATES

9.1 Description of Connection

Single and double plate tension member bolted to a gusset plate are evaluated in this chapter. This chapter is limited to regular bolt patterns without staggering. A typical connection with the relevant terminology consistent throughout this chapter is shown in Figure 9.1.

The calculations according to the AISC *Specification* for bolted plates are less complex than the other connection types. Case 1, defined in the AISC *Specification* and provided in Figure 3.3, is applicable to all specimens within this chapter. The case states the shear lag factor should be taken as 1.0 when the load applied is transmitted directly to each of the cross-sectional elements of the tension member by welds or fasteners except when cases 4, 5, and 6 are applicable. Case 4 is only applicable to welded tension members. Case 5 is only applicable to round HSS tension members, and case 6 is only for rectangular HSS. Therefore, the shear lag factor was taken as unity for all specimens in this chapter.

9.2 Comparison to Experimental Results

9.2.1 Description of Experimental Specimens

There were 109 total specimens applicable to this chapter. The enumeration is shown in Table 9.1. A large number of specimens were removed from this particular chapter for a variety of reasons. Može and Beg (2010) reported 38 total specimens however eight specimens were removed due to bolt failures (B109, B110, B118, B202, B206, B208, B209, and B210) and ten specimens were removed due to ‘splitting failures’ believed to be the equivalent of bolt tearout. These specimens were reported as B102, B103, B111, B112, B116, B117, B119, B120, B121, and B211. Additionally, specimens B108, B115, B124, and B125 contained an eccentric bolt hole pattern and were removed. Munse (1959) reported 131 total riveted specimens tested under tensile loading. A large

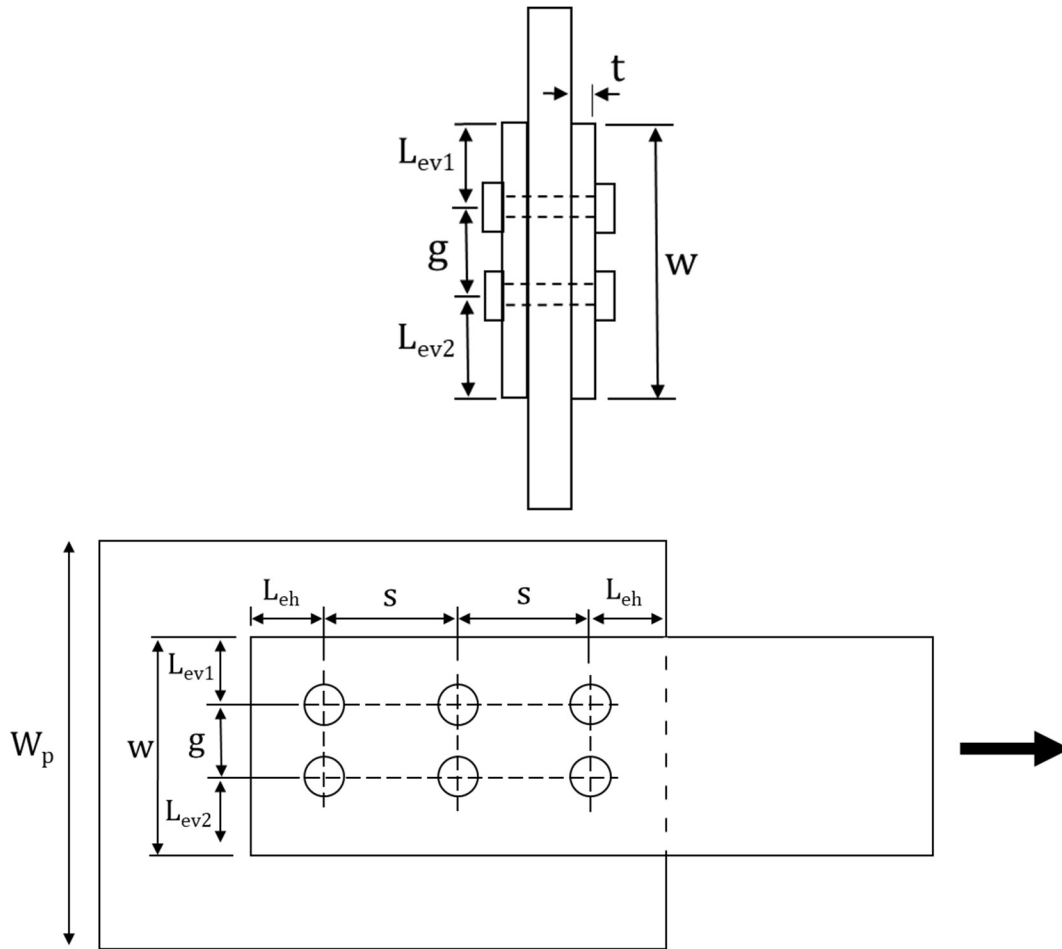


Figure 9.1: Bolted Plate Schematic

Table 9.1: Bolted Plate Specimen Enumeration

Reference	Specimen Count
Može and Beg (2010)	16
Munse (1959)	67
Schutz & Newmark (1952)	22
Total	105

majority of these specimens included a staggered bolt pattern. There were 81 total specimens with a normal fastener configuration. Among these, 14 specimens were removed. Specimens 51-4-1, 51-4-2, 51-4-3, 50-X6-1, 50-X6-2, 50-X6-1A, 50-X6-2A, 50-X6-3A, 50-X7-1, 50-X7-2, and 50-X7-3 experienced rivet failures, and specimens 50-X7-1A, 50-X7-2A, and 50-X7-3A experienced plate tearing. As for Schutz and Newmark (1952), 130 specimens were reported, with only 24 consisting of a regular bolt pattern. Of these 24 specimens, only two were removed. Specimen SE1A was removed for bolt failure, and specimen SE1B was outside the minimum tolerance for edge distance modeling in IDEA StatiCa.

Due to the extent of detail required for these particular specimens, the specimen parameters are split into two tables. Table 9.2 provides general information on the plates and materials. Table 9.3 provides only details pertaining to the fasteners. The terminology of both tables is consistent with Figure 9.1. For specimens with only one row of bolts, the gage dimension, g , is not defined and is indicated by 'N/A'. This is likewise for specimens with only one bolt per row and the bolt spacing, 's'. If provided, the diameter of the bolt or rivet hole was taken as reported. Otherwise, bolt holes were taken as indicated by Table J3.3 of the *AISC Specification*. For rivets, the diameter hole of the was taken as the rivet diameter unless specifically reported by the experimentalist. Additionally, for the *AISC Specification* calculations of the net area, an additional 1/16 in. was added to the hole diameter in accordance with *AISC Specification* Section B4.3b.

The modelling process of the bolted plate specimens was similar to the bolted angles. The gusset plates and tested plates were all modeled as members. The rivets were always modeled as bolts. It should be noted, most plate specimens were tested in the physical experiments as one half of a double-strap, butt-type joint. Of these experiments, some failing specimens were the center plate, and some were the outer plates. The IDEA StatiCa models represented the same test set up. The bearing member was not always selected as the gusset plate in this case due to the unique testing setup in the experiments.

Table 9.2: Bolted Plate Specimen Details

Index	Reference	Specimen	# of plates	* F_y , ksi	* F_u , ksi	* t , in.	* W , in.
1	Može and Beg (2010)	B101	1	122.8	128.4	0.394	2.402
2	Može and Beg (2010)	B104	1	122.8	128.4	0.394	2.823
3	Može and Beg (2010)	B105	1	122.8	128.4	0.394	2.835
4	Može and Beg (2010)	B106	1	122.8	128.4	0.394	3.189
5	Može and Beg (2010)	B107	1	122.8	128.4	0.394	3.169
7	Može and Beg (2010)	B113	1	122.8	128.4	0.394	3.555
8	Može and Beg (2010)	B114	1	122.8	128.4	0.394	3.543
10	Može and Beg (2010)	B122	1	122.8	128.4	0.394	4.677
11	Može and Beg (2010)	B123	1	122.8	128.4	0.394	3.098
14	Može and Beg (2010)	B201	1	122.8	128.4	0.400	3.827
15	Može and Beg (2010)	B203	1	122.8	128.4	0.400	4.563
16	Može and Beg (2010)	B204	1	122.8	128.4	0.400	4.567
17	Može and Beg (2010)	B205	1	122.8	128.4	0.400	4.886
18	Može and Beg (2010)	B207	1	122.8	128.4	0.400	5.394
19	Može and Beg (2010)	B212	1	122.8	128.4	0.400	5.685
20	Može and Beg (2010)	B213	1	122.8	128.4	0.400	4.764
21	Munse (1959)	50-1A	2	37.8	63.4	0.313	8.800
22	Munse (1959)	50-1B	2	37.8	63.4	0.313	8.800
23	Munse (1959)	50-1C	2	37.8	63.4	0.313	8.800
24	Munse (1959)	50-2A	2	37.0	59.7	0.250	10.330
25	Munse (1959)	50-2B	2	37.0	59.7	0.250	10.330
26	Munse (1959)	50-2C	2	37.0	59.7	0.250	10.330
27	Munse (1959)	50-3A	2	35.2	61.2	0.188	13.040
28	Munse (1959)	50-3B	2	35.2	61.2	0.188	13.040
29	Munse (1959)	50-3C	2	35.2	61.2	0.188	13.040
30	Munse (1959)	50-4A	2	36.0	62.0	0.375	10.020
31	Munse (1959)	50-4B	2	36.0	62.0	0.375	10.020
32	Munse (1959)	50-4C	2	36.0	62.0	0.375	10.020
33	Munse (1959)	50-5A	2	37.8	63.4	0.313	11.480
34	Munse (1959)	50-5B	2	37.8	63.4	0.313	11.480
35	Munse (1959)	50-5C	2	37.8	63.4	0.313	11.480
36	Munse (1959)	50-6A	2	39.2	62.3	0.250	13.640
37	Munse (1959)	50-6B	2	39.2	62.3	0.250	13.640
38	Munse (1959)	50-6C	2	39.2	62.3	0.250	13.640

Table 9.2 continued

Index	Reference	Specimen	# of plates	* F_y , ksi	* F_u , ksi	* t , in.	* W , in.
39	Munse (1959)	50-7A	2	35.3	60.1	0.188	17.240
40	Munse (1959)	50-7B	2	35.3	60.1	0.188	17.240
41	Munse (1959)	50-7C	2	35.3	60.1	0.188	17.240
42	Munse (1959)	50-8A	2	35.9	64.9	0.438	11.260
43	Munse (1959)	50-8B	2	35.9	64.9	0.438	11.260
44	Munse (1959)	50-8C	2	35.9	64.9	0.438	11.260
45	Munse (1959)	50-9A	2	36.2	62.7	0.375	12.620
46	Munse (1959)	50-9B	2	36.2	62.7	0.375	12.620
47	Munse (1959)	50-9C	2	36.2	62.7	0.375	12.620
48	Munse (1959)	50-10A	2	37.6	62.9	0.313	14.500
49	Munse (1959)	50-10B	2	37.6	62.9	0.313	14.500
50	Munse (1959)	50-10C	2	37.6	62.9	0.313	14.500
51	Munse (1959)	50-11A	2	37.1	60.1	0.250	17.320
52	Munse (1959)	50-11B	2	37.1	60.1	0.250	17.320
53	Munse (1959)	50-11C	2	37.1	60.1	0.250	17.320
54	Munse (1959)	51-1-1	1	38.7	64.5	0.438	9.480
55	Munse (1959)	51-1-2	1	38.7	64.5	0.438	9.480
56	Munse (1959)	51-1-3	1	38.7	64.5	0.438	9.480
57	Munse (1959)	51-1-1A	1	32.0	63.2	0.438	9.480
58	Munse (1959)	51-1-2A	1	32.6	63.7	0.438	9.480
59	Munse (1959)	51-1-3A	1	31.6	62.9	0.438	9.480
60	Munse (1959)	51-2-1	1	40.2	67.7	0.375	10.340
61	Munse (1959)	51-2-2	1	40.2	67.7	0.375	10.340
62	Munse (1959)	51-2-3	1	40.2	67.7	0.375	10.340
63	Munse (1959)	51-2-1A	1	37.4	64.2	0.375	10.340
64	Munse (1959)	51-2-2A	1	40.5	64.7	0.375	10.340
65	Munse (1959)	51-2-3A	1	37.5	62.9	0.375	10.340
66	Munse (1959)	51-3-1	1	39.7	65.5	0.313	11.500
67	Munse (1959)	51-3-2	1	39.7	65.5	0.313	11.500
68	Munse (1959)	51-3-3	1	39.7	65.5	0.313	11.500
69	Munse (1959)	51-3-1A	1	39.4	67.2	0.313	11.500
70	Munse (1959)	51-3-2A	1	38.4	66.2	0.313	11.500
71	Munse (1959)	51-3-3A	1	38.3	66.9	0.313	11.500
72	Munse (1959)	51-4-1A	1	31.8	66.8	0.563	11.840

Table 9.2 continued

Index	Reference	Specimen	# of plates	* F_y , ksi	* F_u , ksi	* t , in.	* W , in.
73	Munse (1959)	51-4-2A	1	31.4	66.7	0.563	11.840
74	Munse (1959)	51-4-3A	1	32.0	66.1	0.563	11.840
75	Munse (1959)	51-5-1	1	35.4	66.8	0.500	13.440
76	Munse (1959)	51-5-2	1	35.4	66.8	0.500	13.440
77	Munse (1959)	51-5-3	1	35.4	66.8	0.500	13.440
78	Munse (1959)	51-5-1A	1	38.2	62.1	0.500	13.440
79	Munse (1959)	51-5-2A	1	32.5	63.4	0.500	13.440
80	Munse (1959)	51-5-3A	1	31.4	61.8	0.500	13.440
81	Munse (1959)	51-6-1	1	37.6	64.1	0.438	15.720
82	Munse (1959)	51-6-2	1	37.6	64.1	0.438	15.720
83	Munse (1959)	51-6-3	1	37.6	64.1	0.438	15.720
84	Munse (1959)	51-6-1A	1	33.6	60.5	0.438	15.720
85	Munse (1959)	51-6-2A	1	36.0	63.2	0.438	15.720
86	Munse (1959)	51-6-3A	1	32.1	61.6	0.438	15.720
87	Munse (1959)	50-X6-3	2	47.1	64.7	0.250	8.220
88	Schutz and Newmark (1952)	AD1A	1	39.2	65.2	0.313	4.750
89	Schutz and Newmark (1952)	AD1B	1	39.2	65.2	0.313	4.750
90	Schutz and Newmark (1952)	AD2A	1	39.2	65.2	0.313	3.500
91	Schutz and Newmark (1952)	AD2B	1	39.2	65.2	0.313	3.500
92	Schutz and Newmark (1952)	AD3A	1	39.2	65.2	0.313	7.500
93	Schutz and Newmark (1952)	AD3B	1	39.2	65.2	0.313	7.500
94	Schutz and Newmark (1952)	JA1A	1	39.2	65.2	0.313	6.000
95	Schutz and Newmark (1952)	JA1B	1	39.2	65.2	0.313	6.000
96	Schutz and Newmark (1952)	AE1A	1	39.2	65.2	0.313	1.500
97	Schutz and Newmark (1952)	AE1B	1	39.2	65.2	0.313	1.500
98	Schutz and Newmark (1952)	AP1A	1	39.2	65.2	0.313	4.500
99	Schutz and Newmark (1952)	AP1B	1	39.2	65.2	0.313	4.500
100	Schutz and Newmark (1952)	S1A	1	39.2	65.2	0.313	4.500
101	Schutz and Newmark (1952)	S1B	1	39.2	65.2	0.313	4.500
102	Schutz and Newmark (1952)	S2A	1	45.6	63.7	0.250	4.500
103	Schutz and Newmark (1952)	S2B	1	45.6	63.7	0.250	4.500
104	Schutz and Newmark (1952)	S3A	1	37.4	63.6	0.375	4.500
105	Schutz and Newmark (1952)	S3B	1	37.4	63.6	0.375	4.500
106	Schutz and Newmark (1952)	SE2A	1	35.1	65.5	0.500	6.000
107	Schutz and Newmark (1952)	SE2B	1	35.1	65.5	0.500	6.000
108	Schutz and Newmark (1952)	SE3A	1	45.6	63.7	0.250	3.000
109	Schutz and Newmark (1952)	SE3B	1	45.6	63.7	0.250	3.000

* indicates measured value

Table 9.3: Bolted Plate Fastener Details

Index	Bolts/ Rivets	Bolt Material	d , in.	# of fasteners per row	# of rows of fasteners	s , in.	L_{eh} , in.	g , in.	L_{ev1} , in.	L_{ev2} , in.
1	Bolts	12.9	1.063	1	1	N/A	3.555	N/A	1.122	1.280
2	Bolts	12.9	1.063	1	1	N/A	2.374	N/A	1.406	1.417
3	Bolts	12.9	1.063	1	1	N/A	3.520	N/A	1.370	1.465
4	Bolts	12.9	1.063	1	1	N/A	2.976	N/A	1.571	1.618
5	Bolts	12.9	1.063	1	1	N/A	3.567	N/A	1.559	1.610
7	Bolts	12.9	1.063	1	1	N/A	2.941	N/A	1.724	1.831
8	Bolts	12.9	1.063	1	1	N/A	3.543	N/A	1.724	1.819
10	Bolts	12.9	1.063	1	1	N/A	4.181	N/A	2.303	2.374
11	Bolts	10.9	0.866	1	1	N/A	3.987	N/A	1.521	1.577
14	Bolts	10.9	0.866	1	2	N/A	2.806	1.918	0.907	1.002
15	Bolts	10.9	0.866	1	2	N/A	1.899	2.239	1.134	1.190
16	Bolts	10.9	0.866	1	2	N/A	2.825	2.230	1.134	1.203
17	Bolts	10.9	0.866	1	2	N/A	2.797	2.551	1.143	1.191
18	Bolts	10.9	0.866	1	2	N/A	2.863	2.551	1.398	1.444
19	Bolts	10.9	0.866	1	2	N/A	2.872	2.844	1.389	1.452
20	Bolts	10.9	0.866	1	2	N/A	1.899	2.258	1.257	1.249
21	Rivets	A141	0.750	2	3	3.500	1.500	2.650	1.750	1.750
22	Rivets	A141	0.750	2	3	3.500	1.500	2.650	1.750	1.750
23	Rivets	A141	0.750	2	3	3.500	1.500	2.650	1.750	1.750
24	Rivets	A141	0.750	2	3	3.500	1.750	3.440	1.750	1.750
25	Rivets	A141	0.750	2	3	3.500	1.750	3.440	1.750	1.750
26	Rivets	A141	0.750	2	3	3.500	1.750	3.440	1.750	1.750
27	Rivets	A141	0.750	2	3	3.500	2.500	4.770	1.750	1.750
28	Rivets	A141	0.750	2	3	3.500	2.500	4.770	1.750	1.750
29	Rivets	A141	0.750	2	3	3.500	2.500	4.770	1.750	1.750
30	Rivets	A141	0.875	2	3	3.750	1.750	3.130	1.880	1.880
31	Rivets	A141	0.875	2	3	3.750	1.750	3.130	1.880	1.880
32	Rivets	A141	0.875	2	3	3.750	1.750	3.130	1.880	1.880
33	Rivets	A141	0.875	2	3	3.750	2.000	3.860	1.880	1.880
34	Rivets	A141	0.875	2	3	3.750	2.000	3.860	1.880	1.880
35	Rivets	A141	0.875	2	3	3.750	2.000	3.860	1.880	1.880
36	Rivets	A141	0.875	2	3	3.750	2.500	4.940	1.880	1.880
37	Rivets	A141	0.875	2	3	3.750	2.500	4.940	1.880	1.880

Table 9.3 continued

Index	Bolts/ Rivets	Bolt Material	d , in.	# of fasteners per row	# of rows of fasteners	s , in.	L_{eh} , in.	g , in.	L_{ev1} , in.	L_{ev2} , in.
38	Rivets	A141	0.875	2	3	3.750	2.500	4.940	1.880	1.880
39	Rivets	A141	0.875	2	3	3.750	3.250	6.740	1.880	1.880
40	Rivets	A141	0.875	2	3	3.750	3.250	6.740	1.880	1.880
41	Rivets	A141	0.875	2	3	3.750	3.250	6.740	1.880	1.880
42	Rivets	A141	1.000	2	3	4.000	1.750	3.630	2.000	2.000
43	Rivets	A141	1.000	2	3	4.000	1.750	3.630	2.000	2.000
44	Rivets	A141	1.000	2	3	4.000	1.750	3.630	2.000	2.000
45	Rivets	A141	1.000	2	3	4.000	2.000	4.310	2.000	2.000
46	Rivets	A141	1.000	2	3	4.000	2.000	4.310	2.000	2.000
47	Rivets	A141	1.000	2	3	4.000	2.000	4.310	2.000	2.000
48	Rivets	A141	1.000	2	3	4.000	2.500	5.250	2.000	2.000
49	Rivets	A141	1.000	2	3	4.000	2.500	5.250	2.000	2.000
50	Rivets	A141	1.000	2	3	4.000	2.500	5.250	2.000	2.000
51	Rivets	A141	1.000	2	3	4.000	3.000	6.660	2.000	2.000
52	Rivets	A141	1.000	2	3	4.000	3.000	6.660	2.000	2.000
53	Rivets	A141	1.000	2	3	4.000	3.000	6.660	2.000	2.000
54	Rivets	A141	0.750	2	3	3.500	2.000	3.160	1.580	1.580
55	Rivets	A141	0.750	2	3	3.500	2.000	3.160	1.580	1.580
56	Rivets	A141	0.750	2	3	3.500	2.000	3.160	1.580	1.580
57	Rivets	A141	0.750	2	3	3.500	2.000	3.160	1.580	1.580
58	Rivets	A141	0.750	2	3	3.500	2.000	3.160	1.580	1.580
59	Rivets	A141	0.750	2	3	3.500	2.000	3.160	1.580	1.580
60	Rivets	A141	0.750	2	3	3.500	2.000	3.450	1.720	1.720
61	Rivets	A141	0.750	2	3	3.500	2.000	3.450	1.720	1.720
62	Rivets	A141	0.750	2	3	3.500	2.000	3.450	1.720	1.720
63	Rivets	A141	0.750	2	3	3.500	2.000	3.450	1.720	1.720
64	Rivets	A141	0.750	2	3	3.500	2.000	3.450	1.720	1.720
65	Rivets	A141	0.750	2	3	3.500	2.000	3.450	1.720	1.720
66	Rivets	A141	0.750	2	3	3.500	2.000	3.830	1.920	1.920
67	Rivets	A141	0.750	2	3	3.500	2.000	3.830	1.920	1.920
68	Rivets	A141	0.750	2	3	3.500	2.000	3.830	1.920	1.920
69	Rivets	A141	0.750	2	3	3.500	2.000	3.830	1.920	1.920

Table 9.3 continued

Index	Bolts/ Rivets	Bolt Material	d , in.	# of fasteners per row	# of rows of fasteners	s , in.	L_{eh} , in.	g , in.	L_{ev1} , in.	L_{ev2} , in.
70	Rivets	A141	0.750	2	3	3.500	2.000	3.830	1.920	1.920
71	Rivets	A141	0.750	2	3	3.500	2.000	3.830	1.920	1.920
72	Rivets	A141	1.000	2	3	4.000	2.500	3.950	1.970	1.970
73	Rivets	A141	1.000	2	3	4.000	2.500	3.950	1.970	1.970
74	Rivets	A141	1.000	2	3	4.000	2.500	3.950	1.970	1.970
75	Rivets	A141	1.000	2	3	4.000	2.500	4.480	2.240	2.240
76	Rivets	A141	1.000	2	3	4.000	2.500	4.480	2.240	2.240
77	Rivets	A141	1.000	2	3	4.000	2.500	4.480	2.240	2.240
78	Rivets	A141	1.000	2	3	4.000	2.500	4.480	2.240	2.240
79	Rivets	A141	1.000	2	3	4.000	2.500	4.480	2.240	2.240
80	Rivets	A141	1.000	2	3	4.000	2.500	4.480	2.240	2.240
81	Rivets	A141	1.000	2	3	4.000	2.500	5.240	2.620	2.620
82	Rivets	A141	1.000	2	3	4.000	2.500	5.240	2.620	2.620
83	Rivets	A141	1.000	2	3	4.000	2.500	5.240	2.620	2.620
84	Rivets	A141	1.000	2	3	4.000	2.500	5.240	2.620	2.620
85	Rivets	A141	1.000	2	3	4.000	2.500	5.240	2.620	2.620
86	Rivets	A141	1.000	2	3	4.000	2.500	5.240	2.620	2.620
87	Rivets	A141	0.875	1	3	0.000	2.500	2.740	1.370	1.370
88	Rivets	NP	0.375	3	4	1.500	0.750	1.188	0.594	0.594
89	Rivets	NP	0.375	3	4	1.500	0.750	1.188	0.594	0.594
90	Rivets	NP	0.375	3	4	1.500	0.750	0.875	0.438	0.438
91	Rivets	NP	0.375	3	4	1.500	0.750	0.875	0.438	0.438
92	Rivets	NP	0.375	3	4	1.500	0.750	1.875	0.938	0.938
93	Rivets	NP	0.375	3	4	1.500	0.750	1.875	0.938	0.938
94	Rivets	NP	0.375	3	4	1.500	0.750	1.500	0.750	0.750
95	Rivets	NP	0.375	3	4	1.500	0.750	1.500	0.750	0.750
96	Rivets	NP	0.375	3	1	1.500	0.750	N/A	0.750	0.750
97	Rivets	NP	0.375	3	1	1.500	0.750	N/A	0.750	0.750
98	Rivets	NP	0.375	3	3	1.500	0.750	1.500	0.750	0.750
99	Rivets	NP	0.375	3	3	1.500	0.750	1.500	0.750	0.750
100	Rivets	NP	0.375	3	3	1.500	0.750	1.500	0.750	0.750
101	Rivets	NP	0.375	3	3	1.500	0.750	1.500	0.750	0.750
102	Rivets	NP	0.375	3	3	1.500	0.750	1.500	0.750	0.750
103	Rivets	NP	0.375	3	3	1.500	0.750	1.500	0.750	0.750
104	Rivets	NP	0.375	3	3	1.500	0.750	1.500	0.750	0.750

Table 9.3 continued

Index	Bolts/ Rivets	Bolt Material	d , in.	# of fasteners per row	# of rows of fasteners	s , in.	L_{eh} , in.	g , in.	L_{ev1} , in.	L_{ev2} , in.
105	Rivets	NP	0.375	3	3	1.500	0.750	1.500	0.750	0.750
106	Rivets	NP	0.500	3	3	2.000	0.750	2.000	1.000	1.000
107	Rivets	NP	0.500	3	3	2.000	0.750	2.000	1.000	1.000
108	Rivets	NP	0.250	3	3	1.000	0.750	1.000	0.500	0.500
109	Rivets	NP	0.250	3	3	1.000	0.750	1.000	0.500	0.500

NP is not provided

In the cases where the experimentalists used the double-strap, butt-type joint, the center plate was set as the bearing member whether it was the tested or non-tested plate. This is because only one member can be chosen as the bearing member. For all other cases, the bearing member was always taken as the gusset plate. An example model in IDEA StatiCa is provided in Figure 9.2. The procedure described here is for when the failing plate was on the outside. The procedure for when the failing plate was on the outside was similar. The process is as follows:

1. Procedure outlined in Chapter 3.3
2. Create members:
 - a. Member 1: Gusset plate
 - i. Geometrical Type set to “Ended”
 - ii. Offset ex set to the negative of the connection length
 1. Connection length is 2 times L_{ch} + (the number of bolts per row minus one) times the bolt spacing
 - b. Member 2, 3 (if applicable): Tested plate(s)
 - i. β set to 180°
 - ii. Aligned set to “To member plate”
 - iii. Aligned plate set to “[tested plate name] | bottom flange 1”
 - iv. Related plate set to “[gusset plate name] | bottom flange 1”
 - v. Model type set to “N-Vy-Vz”
3. Create Bolt Grid operation:
 - a. Fastener set to “Bolts”
 - b. Items count set to the number of plates (2 or 3)
 - c. Item 1, 2, 3, set to each member created in step 1
 - d. Type set to diameter and type indicated by report
 - e. Coord. System set to “Orthogonal”
 - f. Rows, Positions set to dimension indicated by reports
 - g. Grid set to “Regular”
 - h. Shear force transfer set to “Bearing – tension/shear interaction”

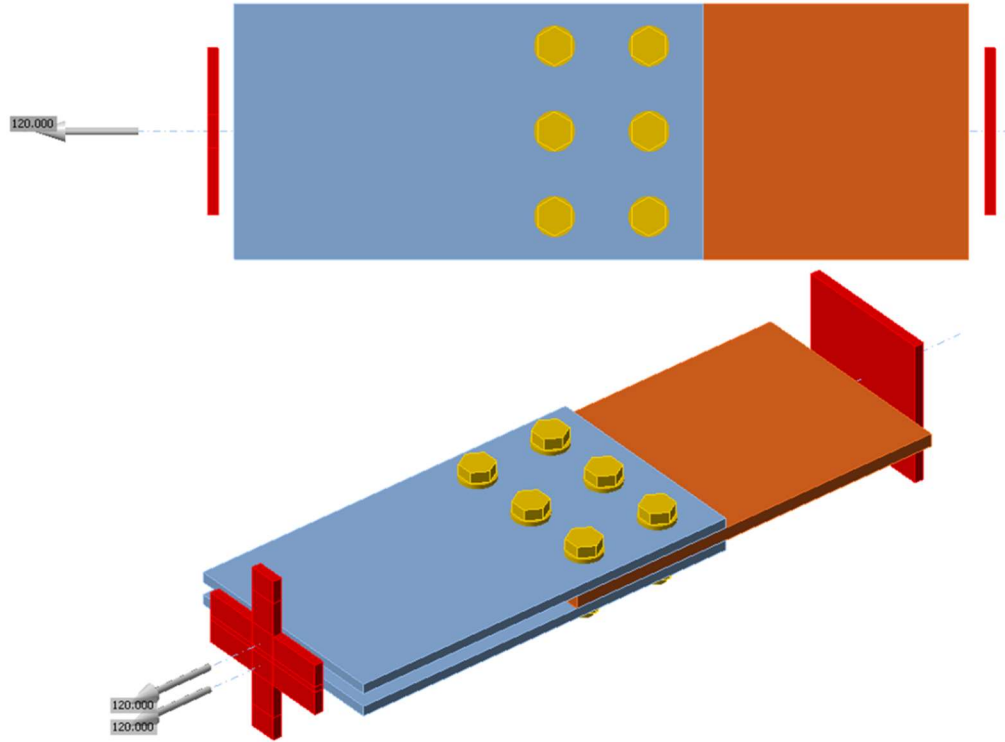


Figure 9.2: Typical Bolted Plate Model

9.2.2 Results

The results calculated based on the AISC *Specification* are provided in Table 9.4. A summary of the strength results for all methods of the experimental set of specimens is provided in Table 9.5. Unlike the previous table, the table provides the AISC predicted strength as the minimum of the tensile yield and tensile rupture strength. For specimens with experimental indices 88 through 109, the experimental failure mode was only indicated as ‘Plate Failure’, without indication of plate failure type. The IDEA StatiCa strength is presented with the default mesh settings and the 5% plastic strain limit. It should be noted; the bolts may have been the controlling failure mode in IDEA StatiCa. However, the bolt utilization was ignored, and the strength is provided as the maximum applied load before the plastic strain in the plates reached 5%. For this experimental set of specimens, there were some instances where IDEA StatiCa provided strengths larger than the strength calculated according to the AISC *Specification* equations and strengths observed in the experimental tests. The most severe case resulted in roughly a 22% greater strength in IDEA StatiCa to both AISC and the experimentally observed strength. Outside of these specimens, P_{IDEA} consistently provided strengths around 10% less than P_{AISC} .

The strengths normalized and plotted with the corresponding experimental set index is provided in Figure 9.3. Outside of specimens with indices 1 through 20, the strength according to IDEA StatiCa provided a pretty consistent level of conservatism compared to both the experimentally observed strengths and the strengths according to the AISC *Specification* equations.

Specimens 1 through 20 are all from Može and Beg (2010); 9 of these specimens provided a larger strength in IDEA StatiCa than the experimentally observed strength. These 9 specimens were the only specimens in the entire study where the IDEA StatiCa strength exceeded that from the experiment. It is worth noting for the 20 specimens tested by Može and Beg (2010), tensile rupture controlled the AISC *Specification* strength

Table 9.4: Bolted Plate AISC Calculation Results

Index	P _{YIELD} , kips	U	Controlling U Case	P _{RUPTURE} , kips
1	116.1	1.00	Case 1	58.5
2	136.5	1.00	Case 1	79.8
3	137.0	1.00	Case 1	80.4
4	154.2	1.00	Case 1	98.3
5	153.2	1.00	Case 1	97.3
7	171.9	1.00	Case 1	116.8
8	171.3	1.00	Case 1	116.3
10	226.1	1.00	Case 1	173.6
11	149.8	1.00	Case 1	105.7
14	187.8	1.00	Case 1	93.0
15	223.9	1.00	Case 1	130.7
16	224.1	1.00	Case 1	131.0
17	239.8	1.00	Case 1	147.3
18	264.7	1.00	Case 1	173.4
19	279.0	1.00	Case 1	188.3
20	233.8	1.00	Case 1	141.1
21	207.9	1.00	Case 1	252.1
22	207.9	1.00	Case 1	252.1
23	207.9	1.00	Case 1	252.1
24	191.1	1.00	Case 1	235.6
25	191.1	1.00	Case 1	235.6
26	191.1	1.00	Case 1	235.6
27	172.1	1.00	Case 1	243.3
28	172.1	1.00	Case 1	243.3
29	172.1	1.00	Case 1	243.3
30	270.5	1.00	Case 1	335.1
31	270.5	1.00	Case 1	335.1
32	270.5	1.00	Case 1	335.1
33	271.2	1.00	Case 1	343.4
34	271.2	1.00	Case 1	343.4
35	271.2	1.00	Case 1	343.4
36	267.3	1.00	Case 1	337.3
37	267.3	1.00	Case 1	337.3
38	267.3	1.00	Case 1	337.3
39	228.2	1.00	Case 1	325.2
40	228.2	1.00	Case 1	325.2

Table 9.4 continued

Index	PYIELD, kips	U	Controlling U Case	PRUPTURE, kips
41	228.2	1.00	Case 1	325.2
42	353.7	1.00	Case 1	458.4
43	353.7	1.00	Case 1	458.4
44	353.7	1.00	Case 1	458.4
45	342.6	1.00	Case 1	443.6
46	342.6	1.00	Case 1	443.6
47	342.6	1.00	Case 1	443.6
48	340.8	1.00	Case 1	444.7
49	340.8	1.00	Case 1	444.7
50	340.8	1.00	Case 1	444.7
51	321.3	1.00	Case 1	424.7
52	321.3	1.00	Case 1	424.7
53	321.3	1.00	Case 1	424.7
54	321.0	1.00	Case 1	397.5
55	321.0	1.00	Case 1	397.5
56	321.0	1.00	Case 1	397.5
57	265.4	1.00	Case 1	389.5
58	270.4	1.00	Case 1	392.5
59	262.1	1.00	Case 1	387.6
60	311.8	1.00	Case 1	401.2
61	311.8	1.00	Case 1	401.2
62	311.8	1.00	Case 1	401.2
63	290.0	1.00	Case 1	380.5
64	314.1	1.00	Case 1	383.5
65	290.8	1.00	Case 1	372.8
66	285.3	1.00	Case 1	371.0
67	285.3	1.00	Case 1	371.0
68	285.3	1.00	Case 1	371.0
69	283.2	1.00	Case 1	380.6
70	276.0	1.00	Case 1	375.0
71	275.3	1.00	Case 1	378.9
72	423.6	1.00	Case 1	650.2
73	418.2	1.00	Case 1	649.3
74	426.2	1.00	Case 1	643.4
75	475.8	1.00	Case 1	684.9
76	475.8	1.00	Case 1	684.9

Table 9.4 continued

Index	P _{YIELD} , kips	U	Controlling U Case	P _{RUPTURE} , kips
77	475.8	1.00	Case 1	684.9
78	513.4	1.00	Case 1	636.7
79	436.8	1.00	Case 1	650.0
80	422.0	1.00	Case 1	633.6
81	517.2	1.00	Case 1	702.9
82	517.2	1.00	Case 1	702.9
83	517.2	1.00	Case 1	702.9
84	462.2	1.00	Case 1	663.4
85	495.2	1.00	Case 1	693.0
86	441.5	1.00	Case 1	675.5
87	193.6	1.00	Case 1	174.9
88	58.1	1.00	Case 1	61.2
89	58.1	1.00	Case 1	61.2
90	42.8	1.00	Case 1	35.7
91	42.8	1.00	Case 1	35.7
92	91.8	1.00	Case 1	117.2
93	91.8	1.00	Case 1	117.2
94	73.4	1.00	Case 1	86.6
95	73.4	1.00	Case 1	86.6
96	18.4	1.00	Case 1	21.7
97	18.4	1.00	Case 1	21.7
98	55.1	1.00	Case 1	65.0
99	55.1	1.00	Case 1	65.0
100	55.1	1.00	Case 1	65.0
101	55.1	1.00	Case 1	65.0
102	51.3	1.00	Case 1	50.8
103	51.3	1.00	Case 1	50.8
104	63.0	1.00	Case 1	76.0
105	63.0	1.00	Case 1	76.0
106	105.3	1.00	Case 1	141.2
107	105.3	1.00	Case 1	141.2
108	34.2	1.00	Case 1	32.9
109	34.2	1.00	Case 1	32.9

Table 9.5: Bolted Plate Results Summary

Index	Experimental		AISC		IDEA StatiCa	
	P_{EXP} , kips	Failure Mode	P_{AISC} , kips	Controlling limit state	P_{IDEA} , kips	Failure Mode
1	58.9	[2]	58.5	[2]	71.5	[3]
2	80.9	[2]	79.8	[2]	88.3	[3]
3	79.8	[2]	80.4	[2]	88.9	[3]
4	100.0	[2]	98.3	[2]	99.4	[3]
5	98.9	[2]	97.3	[2]	99.3	[3]
7	116.0	[2]	116.8	[2]	105.1	[3]
8	114.7	[2]	116.3	[2]	104.9	[3]
10	177.1	[2]	173.6	[2]	107.6	[3]
11	108.6	[2]	105.7	[2]	85.2	[3]
14	102.7	[2]	93.0	[2]	116.9	[3]
15	144.6	[2]	130.7	[2]	146.8	[3]
16	143.4	[2]	131.0	[2]	148.4	[3]
17	154.9	[2]	147.3	[2]	159.3	[3]
18	177.4	[2]	173.4	[2]	169.7	[3]
19	191.3	[2]	188.3	[2]	172.2	[3]
20	152.4	[2]	141.1	[2]	154.2	[3]
21	271.1	[2]	207.9	[1]	181.0	[3]
22	269.2	[2]	207.9	[1]	181.0	[3]
23	270.3	[2]	207.9	[1]	181.0	[3]
24	246.6	[2]	191.1	[1]	171.8	[3]
25	244.0	[2]	191.1	[1]	171.8	[3]
26	245.5	[2]	191.1	[1]	171.8	[3]
27	225.6	[2]	172.1	[1]	160.5	[3]
28	240.9	[2]	172.1	[1]	160.5	[3]
29	232.8	[2]	172.1	[1]	160.5	[3]
30	358.3	[2]	270.5	[1]	235.3	[3]
31	355.8	[2]	270.5	[1]	235.3	[3]
32	360.3	[2]	270.5	[1]	235.3	[3]
33	358.3	[2]	271.2	[1]	244.1	[3]
34	358.6	[2]	271.2	[1]	244.1	[3]
35	361.5	[2]	271.2	[1]	244.1	[3]
36	347.0	[2]	267.3	[1]	250.2	[3]
37	351.9	[2]	267.3	[1]	250.2	[3]
38	337.6	[2]	267.3	[1]	250.2	[3]
39	288.8	[2]	228.2	[1]	196.0	[3]

Table 9.5 continued

Index	Experimental		AISC		IDEA StatiCa	
	P_{EXP} , kips	Failure Mode	P_{AISC} , kips	Controlling limit state	P_{IDEA} , kips	Failure Mode
40	295.3	[2]	228.2	[1]	196.0	[3]
41	285.2	[2]	228.2	[1]	196.0	[3]
42	442.7	[2]	353.7	[1]	305.2	[3]
43	444.5	[2]	353.7	[1]	305.2	[3]
44	442.2	[2]	353.7	[1]	305.2	[3]
45	436.7	[2]	342.6	[1]	303.1	[3]
46	448.9	[2]	342.6	[1]	303.1	[3]
47	454.8	[2]	342.6	[1]	303.1	[3]
48	465.2	[2]	340.8	[1]	314.0	[3]
49	471.5	[2]	340.8	[1]	314.0	[3]
50	460.8	[2]	340.8	[1]	314.0	[3]
51	393.3	[2]	321.3	[1]	301.0	[3]
52	392.2	[2]	321.3	[1]	301.0	[3]
53	399.5	[2]	321.3	[1]	301.0	[3]
54	267.9	[2]	321.0	[1]	275.5	[3]
55	245.0	[2]	321.0	[1]	275.5	[3]
56	244.6	[2]	321.0	[1]	275.5	[3]
57	228.8	[2]	265.4	[1]	238.7	[3]
58	248.9	[2]	270.4	[1]	242.9	[3]
59	238.9	[2]	262.1	[1]	235.9	[3]
60	279.2	[2]	311.8	[1]	274.4	[3]
61	280.0	[2]	311.8	[1]	274.4	[3]
62	247.2	[2]	311.8	[1]	274.4	[3]
63	261.9	[2]	290.0	[1]	265.0	[3]
64	231.3	[2]	314.1	[1]	275.6	[3]
65	241.8	[2]	290.8	[1]	265.4	[3]
66	266.6	[2]	285.3	[1]	261.2	[3]
67	267.9	[2]	285.3	[1]	261.2	[3]
68	244.2	[2]	285.3	[1]	261.2	[3]
69	229.0	[2]	283.2	[1]	259.8	[3]
70	242.6	[2]	276.0	[1]	253.5	[3]
71	251.0	[2]	275.3	[1]	253.1	[3]
72	457.2	[2]	423.6	[1]	370.8	[3]
73	425.3	[2]	418.2	[1]	366.4	[3]
74	409.0	[2]	426.2	[1]	372.8	[3]

Table 9.5 continued

Index	Experimental		AISC		IDEA StatiCa	
	P_{EXP} , kips	Failure Mode	P_{AISC} , kips	Controlling limit state	P_{IDEA} , kips	Failure Mode
75	469.6	[2]	475.8	[1]	426.8	[3]
76	461.1	[2]	475.8	[1]	426.8	[3]
77	409.5	[2]	475.8	[1]	426.8	[3]
78	400.0	[2]	513.4	[1]	456.6	[3]
79	369.8	[2]	436.8	[1]	393.6	[3]
80	376.0	[2]	422.0	[1]	380.9	[3]
81	386.7	[2]	517.2	[1]	479.2	[3]
82	385.6	[2]	517.2	[1]	479.2	[3]
83	389.0	[2]	517.2	[1]	479.2	[3]
84	369.3	[2]	462.2	[1]	431.7	[3]
85	375.4	[2]	495.2	[1]	460.9	[3]
86	367.8	[2]	441.5	[1]	414.1	[3]
87	168.0	[2]	174.9	[2]	141.0	[3]
88	78.1	Plate Failure	58.1	[1]	48.0	[3]
89	79.1	Plate Failure	58.1	[1]	48.0	[3]
90	48.0	Plate Failure	35.7	[2]	30.8	[3]
91	48.5	Plate Failure	35.7	[2]	30.8	[3]
92	135.7	Plate Failure	91.8	[1]	89.3	[3]
93	133.0	Plate Failure	91.8	[1]	89.3	[3]
94	104.6	Plate Failure	73.4	[1]	65.6	[3]
95	103.2	Plate Failure	73.4	[1]	65.6	[3]
96	25.7	Plate Failure	18.4	[1]	15.5	[3]
97	25.7	Plate Failure	18.4	[1]	15.5	[3]
98	69.1	Plate Failure	55.1	[1]	48.7	[3]
99	69.0	Plate Failure	55.1	[1]	48.7	[3]
100	79.0	Plate Failure	55.1	[1]	48.7	[3]
101	80.2	Plate Failure	55.1	[1]	48.7	[3]
102	45.3	Plate Failure	50.8	[2]	45.0	[3]
103	46.3	Plate Failure	50.8	[2]	45.0	[3]
104	88.8	Plate Failure	63.0	[1]	55.8	[3]
105	89.2	Plate Failure	63.0	[1]	55.8	[3]
106	165.6	Plate Failure	105.3	[1]	93.9	[3]
107	160.7	Plate Failure	105.3	[1]	93.9	[3]
108	38.2	Plate Failure	32.9	[2]	29.5	[3]
109	38.6	Plate Failure	32.9	[2]	29.5	[3]

[1] tensile yield; [2] tensile rupture; [3] member strain

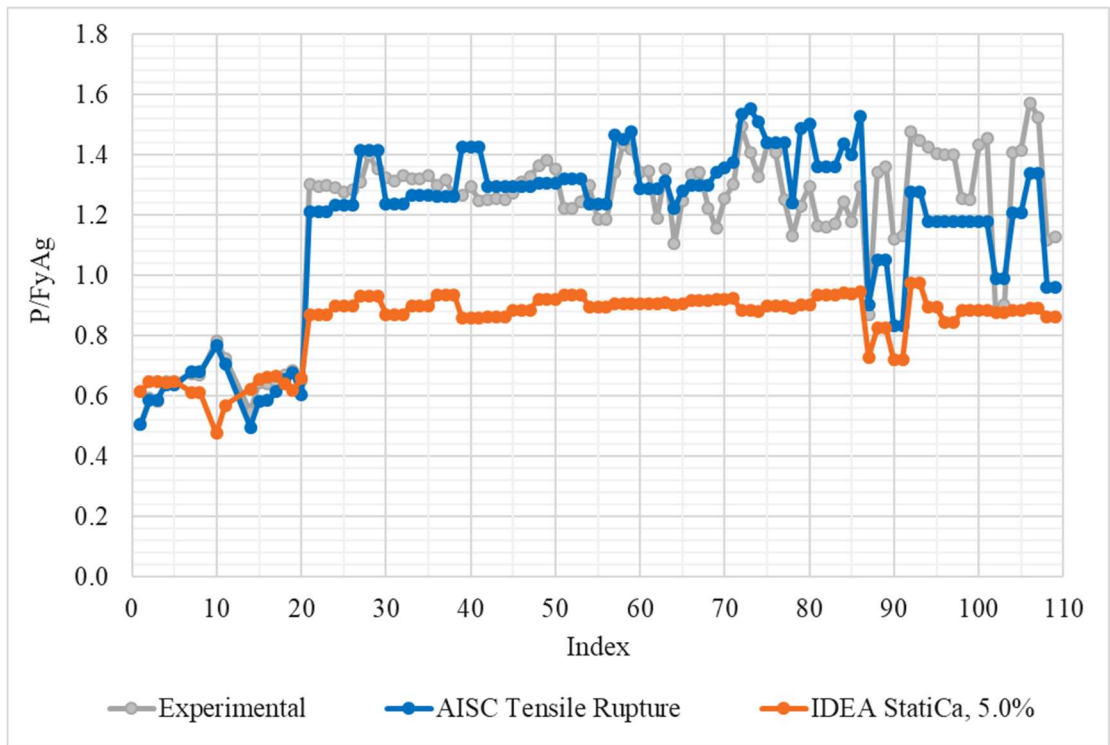


Figure 9.3: Bolted plate results: strength ratio vs. index

calculations and the experimental results by a significant margin. Whereas, almost all other specimens had tensile yield occurring before rupture. This is shown in Figure 9.3 where specimens with indices 1 through 20 have normalized strengths typically well below 1.0. These are cases where IDEA StatiCa is identifying tensile rupture, and not tensile yield.

As mentioned in previous chapters, IDEA StatiCa's material behavior model utilizes a bilinear stress-strain relationship for modeling connecting elements, such as plates in this case. The hardening stiffness is only 1/1000th of the elastic modulus. Therefore, IDEA StatiCa does not utilize F_u , whereas the AISC strength calculations for tensile rupture does. To capture this difference, Figure 9.4 is provided as the strengths, P , normalized by $F_y A_g$ are plotted with the material ratio F_u/F_y . All strength methods trend in the positive direction as F_u/F_y increases, with IDEA StatiCa providing a noticeably smaller slope than the other strength methods. Furthermore, this indicates as F_u increases, the strength according to IDEA StatiCa increases as well, but not as significantly as other methods. In order to specifically compare IDEA StatiCa with the experimental results, Figure 9.5 is provided. The strength ratio of P_{IDEA} to P_{EXP} is plotted against the material F_u/F_y . This plot depicts a strong negative correlation between these two ratios. As F_u with respect to F_y increases, IDEA StatiCa provides more conservative results.

As provided in previous chapters, the plastic strain sensitivity was investigated for this experimental set. The results are presented in Figure 9.6 and Figure 9.7. The first plot provides the comparison of the normalized strength plotted with the corresponding experimental set index. A similar plot is provided in Figure 9.7 where the strengths, P , are normalized by the default plastic strain limit (5%). The overall trend of the plot is as expected, such that as the plastic strain limit increases, the maximum permitted load increases as well and vice versa.

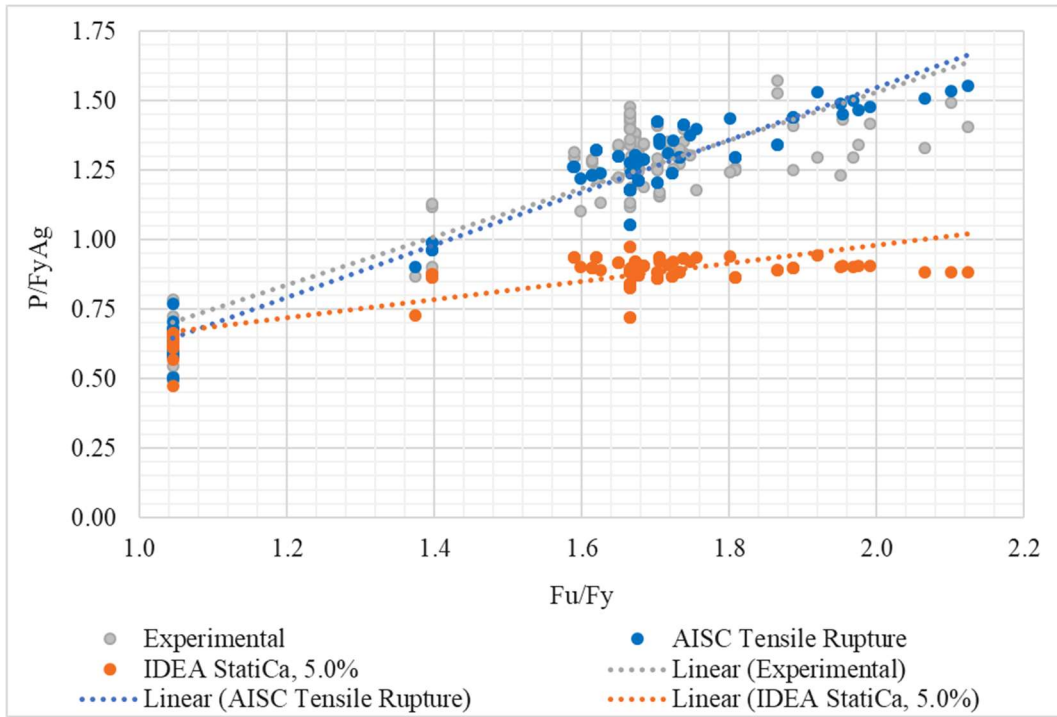


Figure 9.4: Bolted plate results: normalized strength as a function of material ratio scatterplot

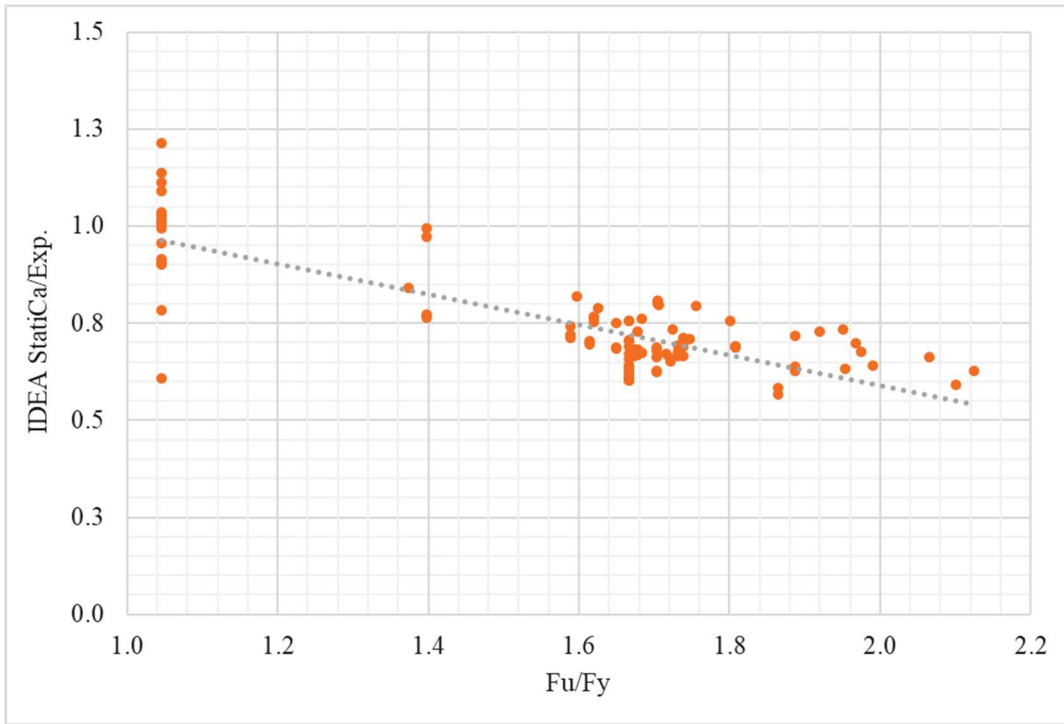


Figure 9.5: Bolted plate results: IDEA StatiCa to experimental ratio as function of material ratio scatterplot

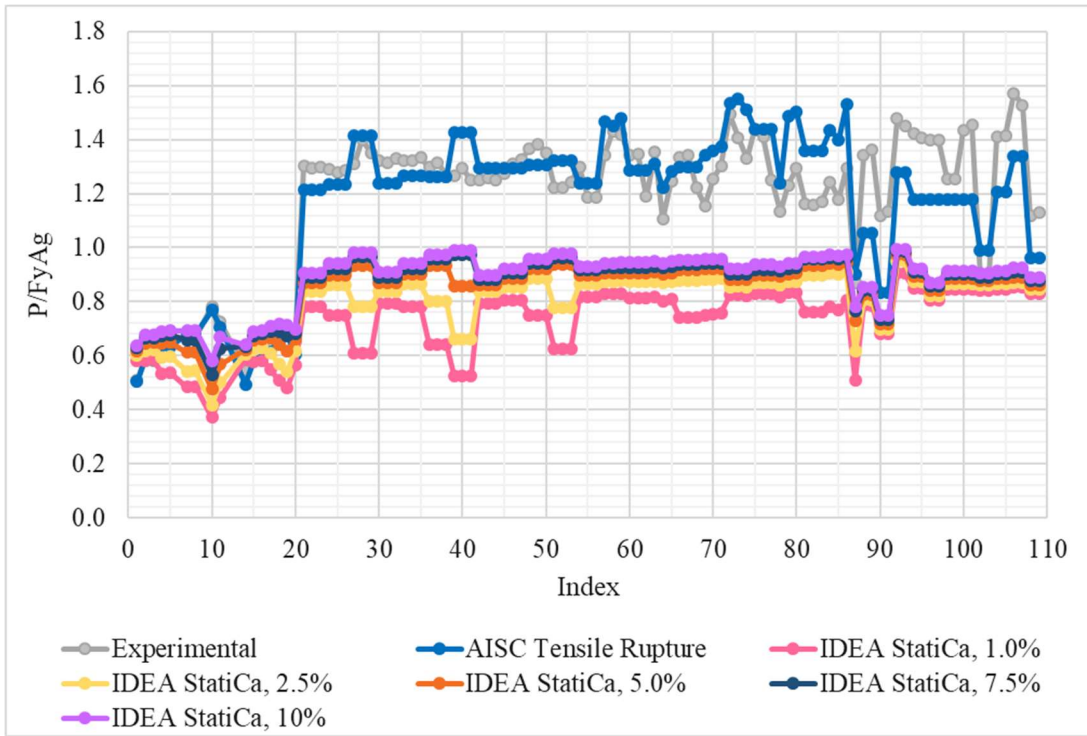


Figure 9.6: Bolted plate results: strength ratio vs. index for varying plastic strain limits

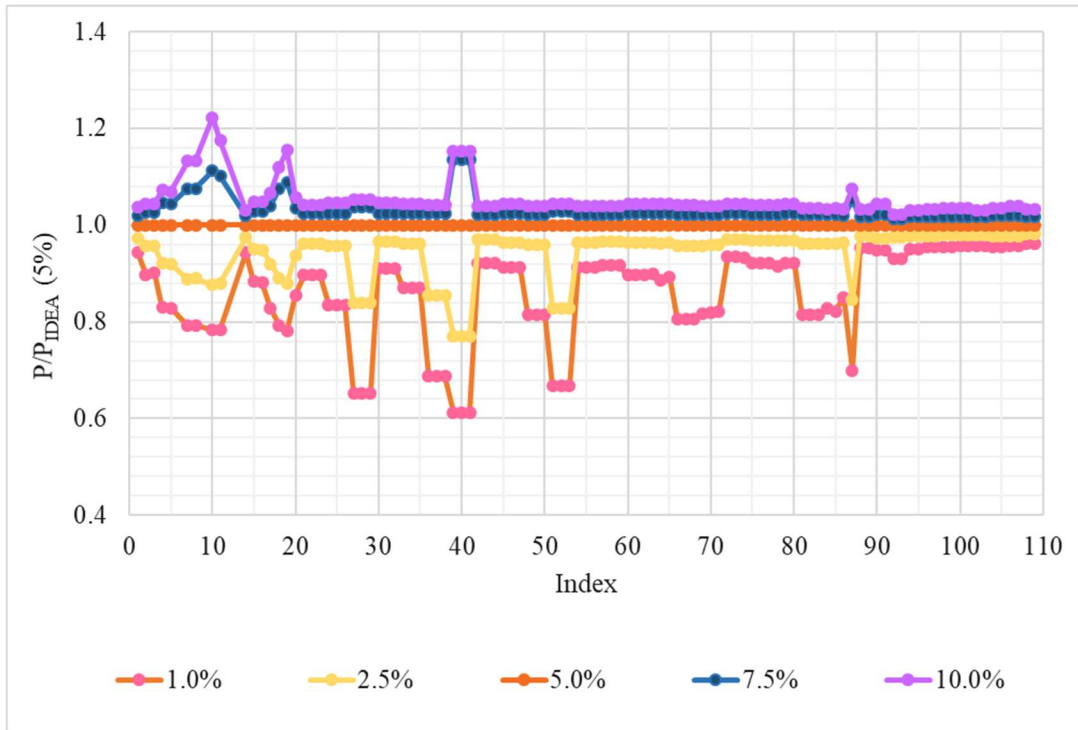


Figure 9.7: Bolted plate results: ratio of strength to IDEA StatiCa strength with 5% plastic strain limit plotted with index

In addition to the plastic strain limit investigation, an examination of mesh dependency was conducted as well. Figure 9.8 provides the results for this study. It should be noted, the mesh around the bolt holes in IDEA StatiCa always remains constant at 8 elements. In general, as the meshes are refined, the strengths change very little. There are a few instances, specimens with experimental set indices 39, 40, and 41, where a less refined mesh provides larger strengths than the next more refined mesh.

Table 9.6 presents the test-to-predicted ratio statistical results. For the AISC (2016) tensile rupture test-to-predicted ratio, the average resulted in a value of 1.021. The results for the test-to-predicted ratio for AISC tensile rupture is directly used in the reliability analysis for the random variable \tilde{X}_R . The coefficient of variation of this ratio was used as well. As for the IDEA StatiCa test-to-predicted ratio, the average was 1.386. This indicates the strengths in the experiments were around 39% higher than that predicted by IDEA StatiCa.

9.3 Reliability Analysis

9.3.1 Description of Reliability Set

For the bolted plate reliability set, it was desired to vary the following parameters: material grade, bolt diameter, and bolt configuration. The width of the plate was directly dependent upon the selected bolt gage and L_{ev} . The bolt spacings were arranged into two categories, a ‘minimum’ and ‘greater than minimum’ spacing type. The bolt spacings for the ‘minimum’ spacing type were selected following the minimum spacing requirements in Section J3 of the AISC *Specification* (2016). The bolt spacings for the ‘greater than minimum’ spacing type were selected based upon spacings typically used in practice. All bolt hole diameters were selected based upon Section J3 of the AISC *Specification* as well. The parameters for this reliability set are provided in two separate tables. Table 9.7 provides general parameters, whereas Table 9.8 provides information specifically on the bolt spacings. The terminology is consistent with that expressed earlier in this chapter.

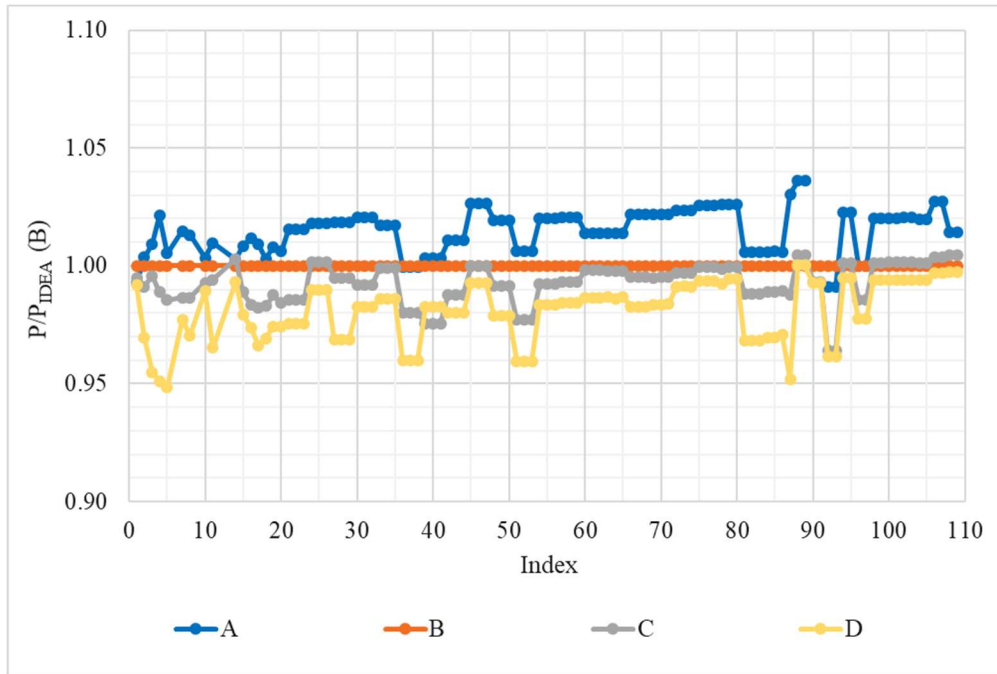


Figure 9.8: Bolted plate results: ratio of varying mesh parameters sets to the default mesh settings plotted with index

Table 9.6: Statistical Results for Bolted Plates

Test-to-Predicted Ratio	Average	Standard Deviation	Coefficient of Variation
$P_{EXP}/P_{RUPTURE} (AISC)$	1.021	0.112	0.110
P_{EXP} / P_{IDEA}	1.386	0.206	0.149

Table 9.7: Bolted Plate Reliability Analysis Parameters

Index	W , in.	t , in.	Material Grade	F_y , ksi	F_u , ksi	Bolt Diameter, in.	Rows of Bolts	Bolts per Row
1	2.000	0.5	A36 (PL)	36	58	0.750	1	2
2	2.000	0.5	A36 (PL)	36	58	0.750	1	4
3	4.000	0.5	A36 (PL)	36	58	0.750	2	2
4	4.000	0.5	A36 (PL)	36	58	0.750	2	4
5	4.000	0.5	A36 (PL)	36	58	0.750	1	2
6	4.000	0.5	A36 (PL)	36	58	0.750	1	4
7	7.000	0.5	A36 (PL)	36	58	0.750	2	2
8	7.000	0.5	A36 (PL)	36	58	0.750	2	4
9	3.000	0.5	A36 (PL)	36	58	1.125	1	2
10	3.000	0.5	A36 (PL)	36	58	1.125	1	4
11	6.000	0.5	A36 (PL)	36	58	1.125	2	2
12	6.000	0.5	A36 (PL)	36	58	1.125	2	4
13	4.000	0.5	A36 (PL)	36	58	1.125	1	2
14	4.000	0.5	A36 (PL)	36	58	1.125	1	4
15	7.375	0.5	A36 (PL)	36	58	1.125	2	2
16	7.375	0.5	A36 (PL)	36	58	1.125	2	4
17	2.000	0.5	A572 Gr. 50 (PL)	50	65	0.750	1	2
18	2.000	0.5	A572 Gr. 50 (PL)	50	65	0.750	1	4
19	4.000	0.5	A572 Gr. 50 (PL)	50	65	0.750	2	2
20	4.000	0.5	A572 Gr. 50 (PL)	50	65	0.750	2	4
21	4.000	0.5	A572 Gr. 50 (PL)	50	65	0.750	1	2
22	4.000	0.5	A572 Gr. 50 (PL)	50	65	0.750	1	4
23	7.000	0.5	A572 Gr. 50 (PL)	50	65	0.750	2	2
24	7.000	0.5	A572 Gr. 50 (PL)	50	65	0.750	2	4
25	3.000	0.5	A572 Gr. 50 (PL)	50	65	1.125	1	2
26	3.000	0.5	A572 Gr. 50 (PL)	50	65	1.125	1	4
27	6.000	0.5	A572 Gr. 50 (PL)	50	65	1.125	2	2
28	6.000	0.5	A572 Gr. 50 (PL)	50	65	1.125	2	4
29	4.000	0.5	A572 Gr. 50 (PL)	50	65	1.125	1	2
30	4.000	0.5	A572 Gr. 50 (PL)	50	65	1.125	1	4
31	7.375	0.5	A572 Gr. 50 (PL)	50	65	1.125	2	2
32	7.375	0.5	A572 Gr. 50 (PL)	50	65	1.125	2	4

PL: plate

Table 9.8: Bolted Plate Reliability Analysis Bolt Spacing Parameters

Index	s , in.	g , in.	L_{ev} , in.	L_{eh} , in.
1	2.000	2.000	1.000	1.000
2	2.000	2.000	1.000	1.000
3	2.000	2.000	1.000	1.000
4	2.000	2.000	1.000	1.000
5	3.000	3.000	2.000	2.000
6	3.000	3.000	2.000	2.000
7	3.000	3.000	2.000	2.000
8	3.000	3.000	2.000	2.000
9	3.000	3.000	1.500	1.500
10	3.000	3.000	1.500	1.500
11	3.000	3.000	1.500	1.500
12	3.000	3.000	1.500	1.500
13	3.375	3.375	2.000	2.000
14	3.375	3.375	2.000	2.000
15	3.375	3.375	2.000	2.000
16	3.375	3.375	2.000	2.000
17	2.000	2.000	1.000	1.000
18	2.000	2.000	1.000	1.000
19	2.000	2.000	1.000	1.000
20	2.000	2.000	1.000	1.000
21	3.000	3.000	2.000	2.000
22	3.000	3.000	2.000	2.000
23	3.000	3.000	2.000	2.000
24	3.000	3.000	2.000	2.000
25	3.000	3.000	1.500	1.500
26	3.000	3.000	1.500	1.500
27	3.000	3.000	1.500	1.500
28	3.000	3.000	1.500	1.500
29	3.375	3.375	2.000	2.000
30	3.375	3.375	2.000	2.000
31	3.375	3.375	2.000	2.000
32	3.375	3.375	2.000	2.000

The material grades are specifically expressed for plates. The literature signified separate factors for the average and coefficient of variation values of \tilde{X}_{F_y} and \tilde{X}_{F_u} for plates and angles. These values are listed in Table 3.4.

9.3.2 Results

The strength results used in the reliability analysis are provided in Table 9.9. For the strengths according to the *AISC Specification (2016)*, the nominal and design strengths are provided for both tensile yield and tensile rupture; however, only the design strengths were used for the purpose of the reliability analysis. The strengths according to IDEA StatiCa, P_{IDEA} , were the result of analyses utilizing all default settings in the program. More specifically, the resistance factors were used with the default mesh settings (mesh parameter set ‘B’) and a 5% plastic strain limit. For this specific reliability specimen set, there were some specimens in which IDEA StatiCa provided a larger maximum permitted applied load, P_{IDEA} , than the available strength according to the AISC equations, the most extreme case resulted in only a 19% increase in strength compared to P_{AISC} . On the more conservative side, IDEA StatiCa provided a maximum decrease of 17% from P_{AISC} .

The resulting reliability indices, β , are provided for each corresponding specimen in Figure 9.9 for AISC and IDEA StatiCa. The reliability indices compare well from AISC to IDEA StatiCa. IDEA StatiCa does appear to provide a higher level of reliability for the first 16 specimens rather than the second set of 16 (reliability specimens with specimen indices 17-32). The second set of specimens consisted of A572 Gr. 50 material, resulting in a larger F_u/F_y ratio.

Table 9.9: Bolted Plate Reliability Strength Results

Index	AISC				IDEA StatiCa
	P_{YIELD} , kips	$P_{RUPTURE}$, kips	ϕP_{YIELD} , kips	$\phi P_{RUPTURE}$, kips	P_{IDEA} , kips
1	36.0	32.6	32.4	24.5	22.7
2	36.0	32.6	32.4	24.5	22.2
3	72.0	65.3	64.8	48.9	46.2
4	72.0	65.3	64.8	48.9	45.2
5	72.0	90.6	64.8	68.0	54.0
6	72.0	90.6	64.8	68.0	53.7
7	126.0	152.3	113.4	114.2	95.6
8	126.0	152.3	113.4	114.2	95.5
9	54.0	48.9	48.6	36.7	34.9
10	54.0	48.9	48.6	36.7	34.9
11	108.0	97.9	97.2	73.4	72.0
12	108.0	97.9	97.2	73.4	71.8
13	72.0	77.9	64.8	58.5	51.2
14	72.0	77.9	64.8	58.5	51.2
15	132.8	137.8	119.5	103.3	95.1
16	132.8	137.8	119.5	103.3	95.2
17	50.0	36.6	45.0	27.4	30.5
18	50.0	36.6	45.0	27.4	29.5
19	100.0	73.1	90.0	54.8	62.1
20	100.0	73.1	90.0	54.8	60.0
21	100.0	101.6	90.0	76.2	71.7
22	100.0	101.6	90.0	76.2	72.7
23	175.0	170.6	157.5	128.0	126.3
24	175.0	170.6	157.5	128.0	128.7
25	75.0	54.8	67.5	41.1	47.2
26	75.0	54.8	67.5	41.1	47.1
27	150.0	109.7	135.0	82.3	97.6
28	150.0	109.7	135.0	82.3	97.4
29	100.0	87.3	90.0	65.5	69.7
30	100.0	87.3	90.0	65.5	69.5
31	184.4	154.4	165.9	115.8	129.2
32	184.4	154.4	165.9	115.8	129.3

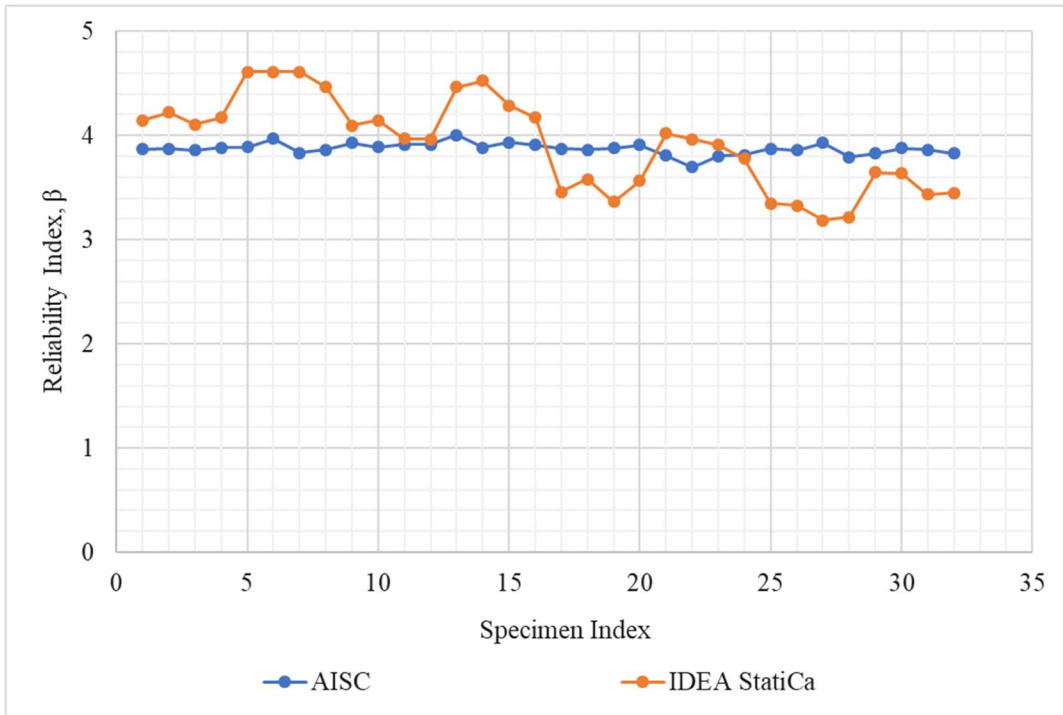


Figure 9.9: Bolted plates: reliability index results

CHAPTER 10

CONCLUSIONS

Inelastic analysis can be a powerful tool for steel connection design that overcomes limitations of traditional hand calculation-based design procedures. However, as with all design methods, validation must be performed to ensure the resulting connections are safe. IDEA StatiCa is a connection design software that employs the component-based finite element method. As part of a larger verification and validation effort, this work compares results from IDEA StatiCa to results from previously published experimental results and to results from design equations for the limit state of net-section tensile rupture. Specifically, this work seeks to answer the following questions: (1) how well does IDEA StatiCa capture net-section tensile rupture? And (2) does IDEA StatiCa provide a comparable or higher level of reliability than the provisions of the AISC *Specification*?

Hundreds of previously published experiments of tension members that failed in either tensile rupture or tensile yield were examined. Each specimen was modeled and analyzed in IDEA StatiCa, and then strengths were compared to the results of design equations in the AISC *Specification* (2016) and experimental results. The sensitivity of the IDEA StatiCa results to mesh density and plastic strain limit was also investigated. Using statistical data from the comparisons to experiments, a reliability analysis was also performed to quantify the probability of failure for connections designed using the various methods.

The results show that IDEA StatiCa captures the limit state of tensile rupture generally well with accurate or conservative expected strength in comparison to experimental results and design equations. Detailed findings of this work include:

1. Using measured material and geometric properties without resistance factors applied, the strength from IDEA StatiCa was less than or equal to the experimentally observed strength for all but a few specimens (9 of 384) and less than or equal to the expected strength computed using design equations for most of the specimens (333 of 384).

2. Using nominal material and geometric properties with resistance factors applied, unconservative errors of up to 56% were observed for IDEA StatiCa in comparison to design strength for plate specimens with relatively short welds, up to 25% for rectangular HSS specimens, and up to 20% in other cases.
3. The AISC *Specification* equations appear well calibrated with reliability indices between 3.17 and 4.42 for the connections investigated.
4. The level of reliability provided by IDEA StatiCa was more variable across the connections investigated and, in some cases, resulted in reliability indices as low as 2.05. The cases of lower reliability were the same as those where IDEA StatiCa exhibited higher strengths than the design strengths. In general, where tensile yield controls, IDEA StatiCa resulted in a greater reliability than the provisions of the AISC *Specification*.
5. Results from IDEA StatiCa often do not converge with mesh refinement as is typically expected with finite element analyses. However, refining the mesh in IDEA StatiCa typically resulted in minor decreases in strength (i.e., less than 5% difference upon halving element size for most specimens). Some cases, particularly the HSS specimens, showed greater mesh dependence.
6. Increasing the plastic strain limit increases the IDEA StatiCa strength and vice versa. The sensitivity of strength to plastic strain limit varied by connection.

Based on these results, use of IDEA StatiCa for capturing tensile rupture in structural steel connection design is typically acceptable. However, cases of unconservative error with respect to the current provisions of the AISC *Specification* identified in this work indicate that modifications to the program may be necessary. Potential modifications could include a different ϕ factor or plastic strain limit. Alternatively, changes to the modeling of welds or bolts may also be necessary. The challenge when implementing these modifications will be to improve results for the unconservative cases while not adding conservatism to the already conservative cases.

Nonetheless, further investigation is needed to verify the true strength of the members which exhibited large differences between IDEA StatiCa and specification equations to determine if the differences are the result of unconservatism in IDEA StatiCa or conservatism in the specification equations and identify the most appropriate course of action. Such studies could include a fundamental characterization and quantification of the interrelationship between stress concentrations, analysis options, plastic strain limits, and fracture. Investigation of other similar limit states, such as block shear rupture, should also be conducted.

LIST OF REFERENCES

- AISC. 2016. *Specification for Structural Steel Buildings*. Chicago, Illinois: American Institute of Steel Construction.
- AISC. 2017. *Steel Construction Manual*. Chicago, Illinois: American Institute of Steel Construction.
- AISC. 2022a. *Public Review Draft of Specification for Structural Steel Buildings*. Chicago, Illinois: American Institute of Steel Construction.
- AISC. 2022b. *Public Review Draft of AISC 341-22 Seismic Provisions for Structural Steel Buildings*. Chicago, Illinois: American Institute of Steel Construction.
- ASTM. 2018. *ASTM A500/A500M-21a: Standard Specification for Cold-Formed Welded and Seamless Carbon Steel Structural Tubing in Rounds and Shapes*. West Conshohocken, PA: American Society of Testing Materials.
- Bauer, D. B., and A. Benaddi. 2002. “Shear lag in double angle truss connections.” *Advances in Steel Structures (ICASS’02)*, 181–188. Elsevier.
- Cheng, J. J. R., G. L. Kulak, and H.-A. Khoo. 1998. “Strength of slotted tubular tension members.” *Canadian Journal of Civil Engineering*, 25 (6): 982–991.
- Denavit, M. D., and K. Truman-Jarrell. 2021. “Single Plate Shear Connections.” Accessed June 25, 2022. <https://www.ideastatica.com/support-center/single-plate-shear-connections-aisc>.
- Dhanuskar, J. R., and L. M. Gupta. 2021a. “Shear Lag Effect in Welded Single Angle Tension Member.” *International Journal of Steel Structures*, 21 (3): 935–949. <https://doi.org/10.1007/s13296-021-00482-1>.
- Dhanuskar, J. R., and L. M. Gupta. 2021b. “Behaviour of a single angle tension member welded at single leg and both legs.” *Asian Journal of Civil Engineering*, 22 (6): 1157–1171. <https://doi.org/10.1007/s42107-021-00372-1>.
- Dowswell, B. 2021. “Analysis of the Shear Lag Factor for Slotted Rectangular HSS Members.” *Engineering Journal, AISC*, 58 (3): 155–164.
- Easterling, W. S., and L. Gonzalez Giroux. 1993. “Shear lag effects in steel tension members.” *Engineering Journal, AISC*, 30 (3): 77–89.

- Ellingwood, B., T. Galambos, J. MacGregor, and C. A. Cornell. 1980. *Development of a probability based load criterion for American National Standard A58: Building code requirements for minimum design loads in buildings and other structures*. NBS Special Publication. 577. Washington, D.C.: National Bureau of Standards.
- Epstein, H. I. 1992. "An experimental study of block shear failure of angles in tension." *Engineering journal*, AISC, 29 (2): 75–84.
- Fang, C., A. C. C. Lam, and M. C. H. Yam. 2013. "Influence of shear lag on ultimate tensile capacity of angles and tees." *Journal of Constructional Steel Research*, 84 (1): 49–61. <https://doi.org/10.1016/j.jcsr.2013.02.006>.
- Fisher, J. M., and L. A. Kloiber. 2006. *Design Guide 1: Base Plate and Anchor Rod Design*. Chicago, Illinois: American Institute of Steel Construction.
- Gibson, G. T., and B. T. Wake. 1942. "An investigation of welded connections for angle tension members." *The Welding Journal*, 21 (1): 44–49.
- Gonzalez, L. 1989. "Investigation of the shear lag coefficient for welded tension members." Master's Thesis. Blacksburg, Virginia: Virginia Tech.
- Greiner, J. E. 1897. "Recent tests of bridge members." *Transactions of the American Society of Civil Engineers*, 38 (2): 41–67.
- Kasapoglu, B., R. A. Giorjao, A. Nassiri, and H. Sezen. 2021. *Verification of the results from IDEA StatiCa for steel connections according to the U.S. design codes*. The Ohio State University.
- Ke, K., Y. H. Xiong, M. C. H. Yam, A. C. C. Lam, and K. F. Chung. 2018. "Shear lag effect on ultimate tensile capacity of high strength steel angles." *Journal of Constructional Steel Research*, 145 (1): 300–314. <https://doi.org/10.1016/j.jcsr.2018.02.015>.
- Korol, R. M. 1996. "Shear lag in slotted HSS tension members." *Can. J. Civ. Eng.*, 23 (6): 1350–1354. <https://doi.org/10.1139/196-943>.
- Kulak, G. L., and E. Y. Wu. 1997. "Shear Lag in Bolted Angle Tension Members." *Journal of Structural Engineering*, ASCE, 123 (9): 1144–1152. [https://doi.org/10.1061/\(ASCE\)0733-9445\(1997\)123:9\(1144\)](https://doi.org/10.1061/(ASCE)0733-9445(1997)123:9(1144)).

- Liu, J., R. Sabelli, R. L. Brockenbrough, and T. P. Fraser. 2007. "Expected Yield Stress and Tensile Strength Ratios for Determination of Expected Member Capacity in the 2005 AISC Seismic Provisions." *Engineering Journal*, AISC, 44 (1): 15–25.
- Mannem, R. 2002. "Shear lag effects on welded steel angles and plates." PhD Thesis. St. John's, NL, Canada: Memorial University of Newfoundland.
- Martinez-Saucedo, G., and J. A. Packer. 2009. "Static Design Recommendations for Slotted End HSS Connections in Tension." *Journal of Structural Engineering*, ASCE, 135 (7): 797–805. [https://doi.org/10.1061/\(ASCE\)ST.1943-541X.0000016](https://doi.org/10.1061/(ASCE)ST.1943-541X.0000016).
- McKibben, F. P. 1907. "Tension tests of steel angles." *Proceedings of the annual meeting*, ASTM, 267–274. Philadelphia, Pennsylvania.
- Može, P., and D. Beg. 2010. "High strength steel tension splices with one or two bolts." *Journal of Constructional Steel Research*, 66 (8–9): 1000–1010. <https://doi.org/10.1016/j.jcsr.2010.03.009>.
- Munse, W. H. 1959. *The effect of bearing pressure on the static strength of riveted connections*. Engineering Experiment Station Bulletin No. 454. Urbana, Illinois: University of Illinois.
- Mustafa, M. 2021. "Chevron Brace Connection in a braced frame." Accessed June 25, 2022. <https://www.ideastatica.com/support-center/chevron-brace-connection-in-a-braced-frame-aisc>.
- Petretta, M. 2000. "An investigation of the shear lag effect in welded angle tensile connections." Master's Thesis. Toronto, Ontario, Canada: University of Toronto.
- Ravindra, M. K., and T. V. Galambos. 1978. "Load and Resistance Factor Design for Steel." *Journal of the Structural Division*, ASCE, 104 (9): 1337–1353.
- Regan, P. E., and P. R. Salter. 1984. "Tests on welded-angle tension members." *The Structural Engineer*, The Institute of Structural Engineers, 62B (2): 25–30.
- Schutz, F. W., and N. M. Newmark. 1952. *The Efficiency of Riveted Structural Joints*. Structural Research Series. 30. Urbana, Illinois: University of Illinois.

- Uzoegbo, H. C. 1998. "Shear lag in steel angles: An investigation of the South African standards." *Journal of Constructional Steel Research*, 1 (46): 162.
- Wald, F., L. Šabatka, M. Bajer, P. Jehlička, J. Kabeláč, M. Kožich, M. Kuříková, and M. Vild. 2020. *Component-Based Finite Element Design of Steel Connections*. Czech Technical University in Prague.
- Willibald, S., J. A. Packer, and G. Martinez-Saucedo. 2006. "Behaviour of gusset plate connections to ends of round and elliptical hollow structural section members." *Can. J. Civ. Eng.*, 33 (4): 373–383. <https://doi.org/10.1139/105-052>.
- Yeomans. 1993. *Slotted End Plate Connection in CHS and RHS*. TS and MD Technical Development Report. P004.S.08-1. Corby, England: British Steel.
- Zhao, R. G., R. F. Huang, H. A. Khoo, and J. J. R. Cheng. 2008. "Experimental study on slotted rectangular and square hollow structural section (HSS) tension connections." *Canadian Journal of Civil Engineering*, 35 (11): 1318–1330. <https://doi.org/10.1139/L08-069>.
- Zhu, H. T., M. C. H. Yam, A. C. C. Lam, and V. P. Iu. 2009. "The shear lag effects on welded steel single angle tension members." *Journal of Constructional Steel Research*, 65 (5): 1171–1186. <https://doi.org/10.1016/j.jcsr.2008.10.004>.

VITA

Kayla Truman-Jarrell was born to Steve and Leigh Truman and raised in Greenbrier, TN. In 2020, she earned her Bachelor of Science in Civil and Environmental Engineering with a focus in structural engineering and a minor in mathematics from the Tennessee Technological University. Upon graduation, she chose to attend the University of Tennessee, Knoxville to pursue a Master of Science in Civil Engineering with a concentration in structural engineering. After graduation, she will start her professional career at Y-12 National Security Complex in Oak Ridge, TN as a structural engineer. She is beyond grateful for the continued support from her parents, boyfriend, and friends.